

Characterizing Seasonal Variations In Pavement Material Properties For Use In A Mechanistic-Empirical Design Procedure

Research

1. Report No. MN/RC - 2000-35		2.		3. Recipients Accession No.	
4. Title and Subtitle CHARACTERIZING SEASONAL VARIATIONS IN PAVEMENT MATERIAL PROPERTIES FOR USE IN A MECHANISTIC-EMPIRICAL DESIGN PROCEDURE				5. Report Date December 2000	
7. Author(s) Jill M. Ovik Bjorn Birgisson David E. Newcomb				6.	
9. Performing Organization Name and Address University of Minnesota – Dept. of Civil Engineering 500 Pillsbury Drive, S.E. Minneapolis, MN 55455				8. Performing Organization Report No.	
12. Sponsoring Organization Name and Address Minnesota Department of Transportation 395 John Ireland Boulevard, Mail Stop 330 St. Paul, Minnesota 55155				10. Project/Task/Work Unit No.	
				11. Contract (C) or Grant (G) No. c) 74358 wo) 197	
15. Supplementary Notes				13. Type of Report and Period Covered Final Report 1996-2000	
				14. Sponsoring Agency Code	
16. Abstract (Limit: 200 words) Recent advances in flexible pavement design have prompted agencies to move toward the development and use of mechanistic-empirical (M-E) design procedures. This report analyzed seasonal trends in flexible pavement layer moduli to calibrate a M-E design procedure specific to Minnesota. Seasonal trends in pavement layer moduli were quantified using data from the Minnesota Road Research Project (Mn/ROAD) and Long Term Pavement Performance Seasonal Monitoring Program (LTPP SMP) sites located in Minnesota. The relationships investigated were between climate factors, subsurface environmental conditions, and pavement material mechanical properties. The results show that pavement layer stiffness is highly respondent to changes in the average daily temperature and available moisture. Five seasons were used to characterize the seasonal variations in pavement layer moduli for design purposes. Seasonal factors were used to quantify the cyclic variations in the pavement layer stiffness for a typical year. The maximum stiffness of the pavement layers is reached when temperatures are cooler. The hot mix asphalt layer moduli is at a minimum in the summer when temperatures are high. The granular base layer moduli is at a minimum during the early spring-thaw period when excess moisture is unable to drain. Finally, the fine-grained subgrade layer moduli is at a minimum late spring and summer due to the low permeability and slow recovery of the material. The Integrated Climate Model (ICM) was used in this study to compared predicted data to actual data from Mn/ROAD. It was found that the ICM data compared favorably, however, it was not able to predict the spring-thaw period.					
17. Document Analysis/Descriptors material properties seasonal changes environmental effects mechanistic-empirical design				18. Availability Statement No restrictions. Document available from: National Technical Information Services, Springfield, Virginia 22161	
19. Security Class (this report) Unclassified		20. Security Class (this page) Unclassified		21. No. of Pages 221	22. Price

**CHARACTERIZING SEASONAL VARIATIONS IN PAVEMENT MATERIAL
PROPERTIES FOR USE IN A MECHANISTIC-EMPIRICAL DESIGN PROCEDURE**

FINAL REPORT

Prepared by

Jill M. Ovik

Minnesota Department of Transportation
Office of Materials and Road Research

Bjorn Birgisson

University of Florida
Department of Civil Engineering

David E. Newcomb

National Asphalt Paving Association
Research and Technology

December 2000

Published by:

Minnesota Department of Transportation
Office of Research Services
395 John Ireland Boulevard, Mail Stop 330
St. Paul, Minnesota 55155

The content of this report reflects the views of the authors who are responsible for the facts and accuracy of the data presented herein. The contents do not necessarily reflect the views or policies of the Minnesota Department of Transportation at the time of publication. This report does not constitute a standard, specification or regulation.

The authors and the Minnesota Department of Transportation do not endorse products or manufacturers. Trade or manufacturers' names appear herein solely because they are considered essential to this report.

ACKNOWLEDGEMENTS

The authors of this report would like to thank the following people for their help in completing this study. A great deal of data was retrieved from the Mn/ROAD database and analyzed with the help of the following Mn/DOT personnel: George Cochran, Glenn Engstrom, Rich Helgerson, Greg Johnson, Roger Olson, Craig Schrader, John Siekmeier, Dave Van Deusen, Ben Worel, Duane Young, several falling weight deflectometer operators and the computer support staff. Also, Dr. Mark Snyder and Dave Timm from the University of Minnesota contributed their expertise.

TABLE OF CONTENTS

	<u>Page</u>
CHAPTER ONE - INTRODUCTION	
Background	1
Objective	4
Scope	5
Minnesota Road Research Project	6
Organization of Report	6
CHAPTER TWO - LITERATURE REVIEW	
Introduction	9
Laboratory Material Properties and Characterization	10
Seasonal Effects on Flexible Pavement Material Properties	10
Poisson's Ratio	11
Basis for Determining the Resilient Modulus of Pavement Materials	13
Elastic Modulus	13
Dynamic Modulus	14
Modulus of Subgrade Reaction	14
Stiffness	14
Resilient Modulus	14
Seasonal Variations in Asphalt Concrete Resilient Modulus	15
Resilient Modulus of Aggregate and Soil Materials	15
Seasonal Effects on Rigid Pavement Material Properties	19
Environmental Distresses Induced in a Rigid Pavement	20
Curling	20
Pumping and Faulting	20
Freeze/Thaw Cycles	21
Measuring In Situ Mechanical Properties	22
Falling Weight Deflectometer Testing	22
Backcalculation of Layer Moduli	25
EVERCALC	27
Quantifying Seasonal Effects of a Pavement Structure Using NDT	29
Washington State	29
Monitoring In Situ Conditions	30
Thermocouples	31
Time Domain Reflectometers	32
Resistivity Probes	35
Watermark Sensors	36
Empirical and Mechanistic Approaches to Pavement Design	38

Empirical Flexible Pavement Design.....	38
Mechanistic-Empirical Flexible Pavement Design.....	39
Washington State Department of Transportation.....	42
Ontario	45
Shell Method, Netherlands.....	45
Idaho.....	48
Texas.....	49
Asphalt Institute.....	50

CHAPTER THREE – METHODOLOGY

Introduction.....	51
Overview.....	51
Typical Seasonal Variations in Pavement Layer Modulus	51
Process Used to Quantify Seasonal Effects on Pavement Layer Moduli.....	53
Materials Description.....	55
Mn/ROAD Test Sections	55
Long Term Pavement Performance (LTPP) Seasonal Monitoring Program (SMP) Sites	59
Relating Climate Factors to Subsurface Environmental Conditions	60
Geographic Climate Data.....	60
Daily Air Temperature and In Situ Temperature Relationships ...	61
Temperature and State of Moisture.....	63
Freezing and Thawing Index.....	63
Freezing Profiles	63
Precipitation and Moisture Content Relationships	64
Relating Subsurface Environmental Conditions to Mechanical Properties	65
HMA Modulus vs. Temperature	65
Base and Subgrade Layer Moduli	66
Applications to Mechanistic Pavement Design	67
Summary.....	68

CHAPTER FOUR - RESULTS AND DISCUSSION OF MN/ROAD DATA

Introduction.....	69
Trends Between Climate Factors and Subsurface Environmental Conditions	70
Climate Data Results.....	70
30-Year Temperature Data.....	71
30-Year Freezing Index and Thawing Index.....	73
Precipitation	76
Daily Air Temperature and In Situ Temperature Results	79

Precipitation and Moisture Content Variations in the Unbound Layers.....	83
Temperature and State of Moisture Results.....	88
Trends Between Subsurface Environmental Conditions and Pavement Layer Stiffness	92
Predicted HMA Modulus.....	92
Predicted Base and Subgrade Layer Moduli.....	98
Applications in Pavement Design.....	102
Seasonal Duration for Use in M-E Design.....	102
Seasonal Variations in Backcalculated HMA Modulus.....	103
Seasonal Variations in Aggregate Base Backcalculated Moduli ..	106
Backcalculated Base Layer Moduli	108
Backcalculation Input Sensitivity Analysis	118
Seasonal Variations in Backcalculated Subgrade Layer Moduli ..	122
Summary	125

CHAPTER FIVE – RESULTS AND DISCUSSION FROM GREATER MN

Introduction.....	127
Geographic Climate Data Results.....	129
Environmental Condition Data Results	132
HMA Layer.....	132
AB and SG Layers	133
Moisture Content	133
State of Moisture Results.....	135
Pavement Layer Stiffness Results.....	139
Backcalculation Input	139
HMA Layer Modulus.....	139
AB and SB Layer Moduli	140
Applications in Pavement Design.....	142
Seasonal Duration in Minnesota	142
Seasonal Layer Moduli and Seasonal Factors.....	143
Summary	145

CHAPTER SIX – INTEGRATED CLIMATE MODEL

Introduction.....	147
The Enhanced Integrated Climate Model	148
Precipitation Model.....	150
Infiltration and Drainage Model	150
Climatic-Materials-Structures Model	151
Frost Heave and Thaw Settlement Model.....	151
Description of Test Sections and Parameters Used	152
Summary of Other Input Parameters	152

Temperature Predictions	157
Moisture Content Predictions	161
Freezing and Thawing Predictions.....	163
Predictions of Layer Moduli	166
Hot Mix Asphalt Layer	166
Aggregate Base Layer	168
Subgrade Layer	170
Other Observations on the Use of the ICM.....	172
Summary	173

CHAPTER SEVEN - CONCLUSIONS AND RECOMMENDATIONS

Summary	175
Conclusions.....	177
Recommendations.....	180

REFERENCES.....	183
------------------------	------------

BIBLIOGRAPHY.....	189
--------------------------	------------

APPENDIX A - MN/ROAD LAYOUT	A-1
--	------------

APPENDIX B - CLIMATE ATLAS PROCEDURE.....	B-1
--	------------

APPENDIX C - COMPUTER CODE.....	C-1
--	------------

LIST OF TABLES

Chapter One

Table 1.1. Seasonal variations of unbound material moduli for Washington state [4].	3
Table 1.2. Seasonal adjustment factors used in Idaho M-E design procedure [7].	4

Chapter Two

Table 2.1. Typical values of Poisson's ratio for various materials [10].	12
Table 2.2. Commonly assumed Poisson's ratio values for HMA [10].	12
Table 2.3. Models used to estimate soil resilient modulus.	18
Table 2.4. FWD sensor spacing for SHRP and Mn/DOT.	24
Table 2.5. Seasonal lengths and their relative modulus of elasticity for pavement design.	40
Table 2.6. Seasonal variations of unbound material moduli for Washington state [4].	42
Table 2.7. Seasonal variation factors used in Idaho M-E design procedure [7].	49
Table 2.8. Traffic ESALs and the corresponding subgrade percentile used by the Asphalt Institute [49].	50

Chapter Three

Table 3.1. Typical relative pavement layer moduli values per season.	52
Table 3.2. Flexible pavement test cells from Mn/ROAD included in study.	57
Table 3.3. Gradation and plasticity specifications for the aggregates at Mn/ROAD [50].	57
Table 3.4. Actual gradation for Mn/ROAD flexible pavement test sections.	58
Table 3.5. LTPP SMP sites used in study.	60
Table 3.6. Characteristics of asphalt concrete layers in LTPP SMP sites.	60
Table 3.7. Traffic information for LTPP SMP sites (1991).	60

Table 3.8. Thermal diffusivity of various materials [53].	62
Table 3.9. Seasonal distribution of a typical year for design purposes.	68
<u>Chapter Four</u>	
Table 4.1. 30-year mean monthly temperature.	72
Table 4.2. Computed maximum FI (°C-days) at the Buffalo weather station.	76
Table 4.3. 30-Year average and Mn/ROAD monthly average precipitation events, mm.	78
Table 4.4. Measured and predicted mean monthly air and surface temperature, °C, 1996.	82
Table 4.5. Unfrozen vol. m.c. distribution in percent for Cl. 3 Sp. base material.	84
Table 4.6. Unfrozen vol. m.c. distribution in percent for Cl. 4 Sp. base material.	85
Table 4.7. Unfrozen vol. m.c. distribution in percent for Cl. 5 Sp. base material.	85
Table 4.8. Unfrozen vol. m.c. distribution in percent for Cl. 6 Sp. base material.	86
Table 4.9. Coefficients of Equation 3.6 (MPa), as a function of temperature (°C).	94
Table 4.10. Seasonal variations in HMA modulus, MPa (COV in %).	104
Table 4.11. HMA seasonal factors.	105
Table 4.12. Condition of materials used in Illinois study [50].	108
Table 4.13. Seasonal distribution of base layer moduli at Mn/ROAD.	109
Table 4.14. Seasonal distribution of bulk stresses in aggregate base layers.	110
Table 4.15. Seasonal factors for the aggregate base layer.	111
Table 4.16. Mean base layer moduli (MPa) for thick and thin pavements.	113
Table 4.17. Volumetric moisture content (%) for cell 22 (thick) with Cl. 6 Sp.	114
Table 4.18. Volumetric moisture content (%) for cell 27 (thin) with Cl. 6 Sp.	114
Table 4.19. Volumetric moisture content (%) for cell 21 (thick) with Cl. 5 Sp.	115

Table 4.20. Volumetric moisture content (%) for cell 28 (thin) with Cl. 5 Sp.	115
Table 4.21. Volumetric moisture content (%) for cell 17 (thick) with Cl. 3 Sp. .	116
Table 4.22. Volumetric moisture content (%) for cell 30 (thin) with Cl. 3 Sp. ..	116
Table 4.23. Mean dry density and moisture content from sand cone test data.	117
Table 4.24. Test section 21 – thick pavement layer moduli.	119
Table 4.25. Test section 28 – thin pavement layer moduli.	120
Table 4.26. Test section 28 – thin pavement moduli with E_{HMA} set at 6,000 MPa.....	121
Table 4.27. Seasonal distributions of the subgrade backcalculated modulus, MPa.....	123
Table 4.28. Mean subgrade modulus, MPa, for all test sections.....	124
Table 4.29. Seasonal distributions of the deviator stress, kPa..	124
Table 4.30. Seasonal factors for subgrade layers.....	125
 <u>Chapter Five</u>	
Table 5.1. Mean and standard deviation of spring load restriction placement dates in Minnesota, 1986 - 2000 [58].	129
Table 5.2. 30-year mean monthly mean temperature (°C) data from weather stations in Minnesota.	130
Table 5.3. Duration and magnitude of winter season for cities in Minnesota, 1965-1995.	130
Table 5.4. Little Falls seasonal volumetric moisture content, %, between 8/24/93 and 6/13/95.....	134
Table 5.5. Detroit Lakes (full depth HMA site) seasonal volumetric moisture content, %,between 10/20/93 and 6/14/95.....	134
Table 5.6. Bemidji seasonal volumetric moisture content, %, between 9/15/93 and 6/15/95.	134

Table 5.7. RP data for the three LTPP SMP sites	138
Table 5.8. Beginning date of seasons based on 30-year average temperature data.	142
Table 5.9. Seasonal variations in the layer moduli at the LTPP SMP sites, MPa (COV in %).	143
Table 5.10. Seasonal factors of the LTPP SMP sites.....	144
Table 5.11. Backcalculated subgrade layer moduli for each district in Minnesota [59].	145
 <u>Chapter Six</u>	
Table 6.1(a). Baseline input for the Integrated Climate Model.	153
Table 6.1(b). Input for the infiltration and drainage calculations.	154
Table 6.2(a). Properties of HMA layer.	155
Table 6.2(b). Properties of aggregate base course layers.....	156
Table 6.2(c). Properties of subgrade layer.	157
 <u>Appendix C</u>	
Table C.1. “Sensor” table column headings.	C-1
Table C.2. “Cells” table column headings.	C-2
Table C.3. “FWD_ Tests” table column headings.....	C-2
Table C.4. “FWD_Backcalc_Results_v50” table column headings.....	C-3
Table C.5. “Weather” table column headings.....	C-3

LIST OF FIGURES

Chapter Two

Figure 2.1. Typical materials used in HMA pavement structures.	11
Figure 2.2. Simplified stress-strain diagram.	13
Figure 2.3. Principal stresses acting on a soil element for a triaxial test condition.	17
Figure 2.4. Typical cross-section of a rigid pavement.	19
Figure 2.5. Curling stresses in a typical PCC slab.	20
Figure 2.6. Planview of location of loading plate and velocity transducers for FWDs.	24
Figure 2.7. Sketch of falling mass systems [27].	25
Figure 2.8. Common elements of backcalculation programs [modified after [28]].	26
Figure 2.9. Simplified flow chart for EVERCALC [12].	28
Figure 2.10. Type-T thermocouple sensor.	31
Figure 2.11. TDR trace where point A is the start and point B is the end of the TDR probe (m ρ /div is millirhos per division).	33
Figure 2.12. Time domain reflectometer at Mn/ROAD.	34
Figure 2.13. Section of a resistivity probe at Mn/ROAD.	36
Figure 2.14. Watermark sensor at Mn/ROAD.	37
Figure 2.15. Flowchart of a basic M-E design process [42].	41
Figure 2.16. WSDOT overlay design flow chart [12].	44
Figure 2.17. Flowchart of Shell overlay design method [47].	47

Chapter Three

Figure 3.1. Process used to quantify the relationships between climate factors and pavement material properties for M-E design.	54
Figure 3.2. Resilient modulus vs. bulk stress for class 5 and 6 samples from Mn/ROAD [50].	59
Figure 3.3. Simplified stress dependency relationships.	66

Chapter Four

Figure 4.1. 30-year monthly mean temperature data for Buffalo (1965-1995).	72
Figure 4.2. 30-year and Mn/ROAD mean monthly temperature.	73
Figure 4.3. Distribution of FI over 30-years.	74
Figure 4.4. Freezing degree day cycles beginning February 1, 1975, Buffalo.	75
Figure 4.5. High, mean and low monthly precipitation events, 1965 - 1995, Buffalo, MN weather station.	77
Figure 4.6. Mean and high monthly snowfall events, 1965 – 1995, Buffalo, MN weather station.	78
Figure 4.7. Precipitation events at Mn/ROAD between 1993 and 1996 compared to 30-year mean data from Buffalo weather station.	79
Figure 4.8. Mean monthly thermal gradient in January 1996 for test sections 19 (AC 20) and 20 (120/150 pen.).	80
Figure 4.9. Mean monthly thermal gradient in July 1996 for test sections 19 (AC 20) and 20 (120/150 pen.).	81
Figure 4.10. Equation 3.1 and TC values from 1996.	83
Figure 4.11. Moisture content of different subgrade materials at similar depths.	87
Figure 4.12. TDR data at mid-depth of Cl. 3 Sp. and Cl. 6 Sp. base materials in OWP.	88
Figure 4.13. TI and TC data in test section 22, Cl. 6 Sp. base, spring 1996.	89
Figure 4.14. TI and WM data in test section 22, Cl. 6 Sp. base, spring 1996.	90

Figure 4.15. TI and TDR data for Cl. 6 Sp. base, spring 1996.	91
Figure 4.16. Equation 3.6 used to estimate HMA modulus from temperature data.	94
Figure 4.17. Predicted HMA modulus with at 25 mm and 195 mm, in 1996.....	95
Figure 4.18. Predicted and backcalculated HMA modulus in 1996.	96
Figure 4.19. A comparison between backcalculated and predicted HMA modulus.	97
Figure 4.20. Cl. 6 Sp. aggregate base and subgrade moduli in 1996 in test section 22.	98
Figure 4.21. Seasonal variations in the base modulus and in the unfrozen volumetric moisture content, test section 22, 1996.....	100
Figure 4.22. Seasonal variations in Cl. 6 Sp. moduli, 1996, test sections 22, 24 and 27.	101
Figure 4.23. Illinois modulus models [50] for Mn/ROAD base materials.	107
Figure 4.24. Linear (A) and non-linear (B) stress-strain relationships.	112
Figure 4.25. Modulus sensitivity for thick pavement, Cl. 5 Sp.	119
Figure 4.26. Modulus sensitivity for thin pavement, Cl. 5 Sp.	120
Figure 4.27. Modulus sensitivity for thin pavement, Cl. 5 Sp., $E_{HMA} = 6000$ MPa.	121
 <u>Chapter Five</u>	
Figure 5.1. Location in Minnesota of the three LTPP SMP sites, Mn/ROAD, and other weather stations used in this study.....	128
Figure 5.2. 30-year mean monthly precipitation events for the LTPP SMP sites in Minnesota.	131
Figure 5.3. 30-year mean monthly snowfall for the LTPP SMP sites in Minnesota.	131
Figure 5.4. Predicted temperature using Equation 3.1 and TM temperature measured at 25 mm in the HMA layer of the Bemidji site (# 27-6251), 1996.	132

Figure 5.5. TI in Bemidji, spring 1995.	136
Figure 5.6. TM data from the Bemidji site (#27-6251), March 1995.	137
Figure 5.7. TDR data from the Bemidji site (#27-6251) beginning January 1, 1995.	137
Figure 5.8. Mn/ROAD test section 17 spring 1995 frost depth data from WM sensors at 330 mm, 480 mm and 635 mm.	138
Figure 5.9. Bemidji site (#27-6251) predicted and backcalculated HMA modulus, 1994, using Equations 3.1 and 3.6.	140
Figure 5.10. Seasonal variations in the AB and SG layer moduli compared to the volumetric moisture content at the Bemidji site.	141
 <u>Chapter Six</u>	
Figure 6.1. Integrated Climate Pavement Model [9].	149
Figure 6.2. Comparison between predicted and measured temperature in the HMA layer in test section 17.	159
Figure 6.3. Comparison of predicted and measured temperatures in the Cl. 3 Sp. base layer in test section 17.	159
Figure 6.4. Comparison of predicted and measured temperatures in the HMA layer in test section 22.	160
Figure 6.5. Comparison of predicted and measured temperatures in the Cl. 6 Sp. base layer in test section 17.	160
Figure 6.6. Comparison between predicted and measured volumetric moisture content in the base layer of test section 17.	162
Figure 6.7. Comparison of measured and predicted volumetric moisture content in the base layer of test section Cell 22.	162
Figure 6.8. Predicted thawing front compared with WM data in test section 17, 1996.	164
Figure 6.9. Predicted thawing front compared with WM data in test section 22, 1996.	165

Figure 6.10. Comparison of predicted and backcalculated HMA moduli in test section 17.....	167
Figure 6.11. Comparison of predicted and backcalculated HMA moduli in test section 22.....	167
Figure 6.12. Comparison of predicted and backcalculated base layer moduli for test section 17.	169
Figure 6.13. Comparison of predicted and backcalculated base layer moduli for test section 22	169
Figure 6.14. Comparison of predicted and backcalculated subgrade layer moduli for test section 17.....	170
Figure 6.15. Comparison of predicted and backcalculated subgrade layer moduli for test section 22.	171

Appendix C

Figure C.1. Example TC query.....	C-4
Figure C.2. Example TDR query.....	C-4
Figure C.3. Example WM query.....	C-5
Figure C.4. Example sensor location query.....	C-5
Figure C.5. Example RP query.....	C-5
Figure C.6. Example weather query.....	C-6
Figure C.7. Example FWD query.....	C-6

EXECUTIVE SUMMARY

Information regarding seasonal variations in pavement layer moduli are critical when designing or evaluating flexible pavement structures. Climate factors such as temperature, temperature history and precipitation will affect the in-situ temperature, moisture content and state of moisture of the pavement layers. In turn, these subsurface environmental conditions will affect the pavement layer moduli, causing seasonal cycles in which the layer moduli fluctuate between maximum and minimum values.

The objective of this study is to quantify the relationships between climate factors, subsurface environmental conditions and pavement material mechanical properties for use in a mechanistic – empirical (M-E) design procedure to reflect conditions specific to Minnesota. The approach used to establish these relationships may suggest possible direction for similar studies. The data used in this study were obtained from the Minnesota Road Research Project (Mn/ROAD), located on Interstate 94 in central Minnesota and three sites from the Long Term Pavement Performance Seasonal Monitoring Program (LTPP SMP). The extensive instrumentation, on-site weather station and deflection testing performed at these sites provided useful environmental and pavement response data.

The methodology in this study is shown in Figure 1. Average daily air temperature were used to estimate HMA temperature at various depths. The relationship between HMA temperature and moduli was modeled exponentially, and thus, field temperature in the HMA layer were used to estimate the modulus. The predicted HMA modulus was slightly higher in the summer than the backcalculated moduli, therefore the prediction may need to be adjusted if used for design in another region to fit the seasonal changes. Average daily air temperature was used

to calculate the thawing index (TI), which was used to predict moisture phase changes in the aggregate base and soil subgrade layers and estimate the critical spring-thaw weakened period in the base layer.

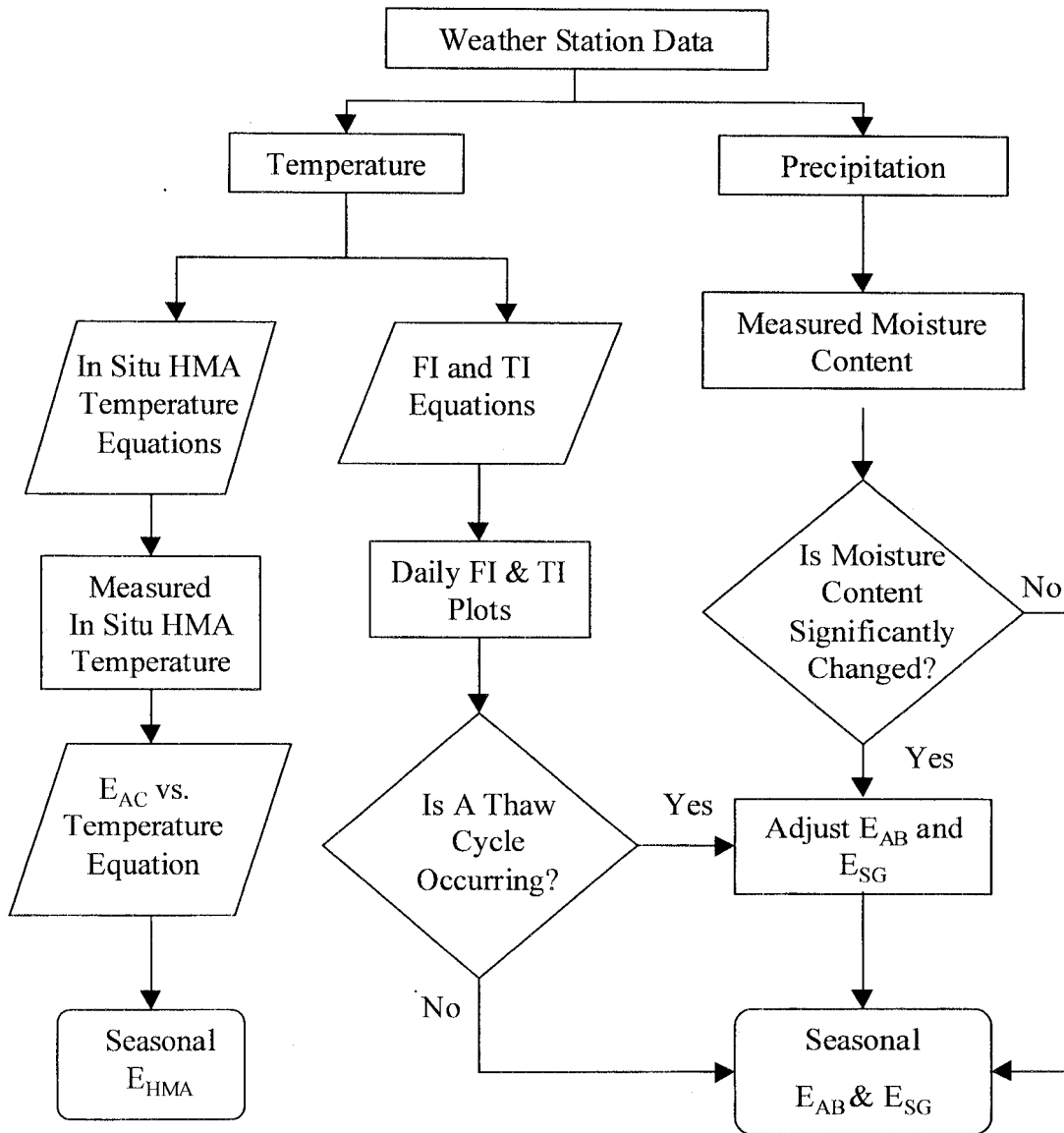


Figure 1. Process used to quantify the relationships between climate factors and pavement material properties for M-E design.

It was found that variations in the pavement layer stiffness occurred at different periods in a typical year for the different layers. The hot mix asphalt (HMA) modulus is at a minimum in the summer when temperatures were at a maximum. The base layer modulus is at a minimum in the early spring when the state of moisture was changing from solid to liquid. The subgrade layer modulus is low in the late spring and summer and slowly recovers in the fall. It was found that five seasons characterized the seasonal variations in pavement layer stiffness better than four seasons for design purposes in Minnesota. The five seasons used in this study are defined in Table 1 for a pavement layer system consisting of a HMA surface layer over an aggregate base layer over a fine-grained soil subgrade layer. These results need to be evaluated for specific sites other than Minnesota since they will vary with latitude and longitude.

Table 1. Seasonal distribution of a typical year for design purposes.

Layer	Season I	Season II	Season III	Season IV	Season V
	Layers are Frozen	Base Thaws	Base Recovers	High T, Low HMA Mod.	Standard Season
Beginning	FI>90°C-days	TI>14°C-days	End of Season II	3-day T _{AVG} > 17°C	3-day T _{AVG} < 17°C
Ending	TI>14°C-days	Approx. 28 days later	3-day T _{AVG} > 17°C	3-day T _{AVG} < 17°C	FI>90°C-days
HMA	High	High	Standard	Low	Standard
Base/ Subbase	High	Low	Low	Standard	Standard
Subgrade	High	High	Low	Low	Standard

The relationships established from the Mn/ROAD data were expanded and verified with data from other sites in Minnesota for use in a M-E pavement design procedure. Factors were used to quantify seasonal variations in material properties. The duration of the seasons were determined with the use of average daily air temperature data. The duration of the seasons varied

throughout Minnesota, typically northern Minnesota had a longer winter season and a shorter summer season than southern Minnesota.

The LTPP database provided useful data to analyze seasonal variations in the stiffness of various pavement structures throughout Minnesota, however there were minimal seasonal LTPP SMP data collected during the critical spring thaw period, in particular the resistivity probe and deflection data. The moisture gradient in the conventional flexible pavement structures investigated were wetter near the bottom of the base, while at the full-depth HMA site near Detroit Lakes, the subgrade was wetter directly under the surface layer.

Another task performed in this study was a comparison between actual Mn/ROAD data and the predicted data from the Integrated Climate Model (ICM) being developed by the Federal Highway Administration. The results indicate that it is possible to predict seasonal variations in flexible pavement layer properties analytically using climate factors. The results showed that the temperature in flexible pavements could be predicted with the ICM. Similarly, the moisture contents in the various pavement layers were captured reasonably well with the ICM, as well as seasonal variations in the HMA layer modulus. In contrast, the progression of freezing and thawing fronts in flexible pavement layers were not captured adequately with the ICM, nor was the transition from frozen to unfrozen moduli for the base and the subgrade for both test sections 17 and 22 located at Mn/ROAD. The ICM offers researchers the ability to use climatic data to predict pavement temperature, moisture content, state of moisture, and variation in layer moduli with time. There is a need for extensive material testing to adequately make use of the ICM, where the level of detail in input may be beyond the information typically available to a highway engineer.

There were many conclusions and recommendations derived from this study. The process used in this study could be used in other states for the design of flexible pavements, especially those affected by seasonal freeze-thaw. For instance, this study related easily attainable climate data to the seasonal variations in the flexible pavement layer stiffness. The climate data is available on-line and the pavement layer stiffness data and is available for various regions and can be retrieved from the LTPP SMP. Together this data can be used with the relationships derived in this study to characterize seasonal variations in pavement layer stiffness for a given region from climate data.

It is recommended that monitoring and data retrieval from the LTPP SMP sites be continued so that further improvements in characterizing seasonal variations in pavement layer mechanical properties and the relationships derived from this study are continually refined. It would be highly advantageous to include more fine-grained subgrade sites in the LTPP SMP sites since these are more frost susceptible.

To adequately use the M-E design procedure, an engineer needs to have a full understanding of the design input values including the pavement material characterization. It is recommended that further research be conducted to create a smooth transition between current flexible pavement design and the M-E design procedures. This may entail the development of correlations between modulus and R-value, CBR or other material properties.

The moisture content measurements showed that an aggregate base or soil subgrade containing less fine-grained material exhibited a lower overall moisture content and smaller fluctuations in the moisture content during the spring thaw period. The seasonal variations in the sand subgrade modulus were similar to the aggregate base in that the layer will thaw sooner than the fine-grained subgrade, the moisture content is lower and the modulus will stay near a

constant value between the spring thaw period and the fall. There was an annual increase of 1% in the TDR measurements between the years of 1994 and 1996. The drift in the TDR measurements could be the result of corrosion of the sensor from moisture or salinity in the moisture due to de-icing agents. Research is needed to determine the cause of this drift to validate the moisture content measurements from TDRs. The existing equations relating measured electrical properties to predicted volumetric moisture are not adequate and further calibration is needed before accurate predictions can be made.

Also, changes in the consolidation of the pavement layers should be investigated to determine the influence on the moisture content or watertable after construction and during the first year of service. This may account for a drift in the moisture content and consequently in the modulus of the unbound layers.

It was found that there were non-linearities in the base and subgrade layers of a flexible pavement structure that were not adequately addressed in a linear elastic analysis tool. The structure of the model, the configuration of the FWD and a variety of assumptions must be considered in order to provide relative estimates. Research is needed to address the issue of non-linear behavior in flexible pavement structures. Linear elastic analysis tools do not consider the non-linearities in the subgrade stiffness or discontinuities in the pavement surface such as cracks. These issues need to be investigated further to accurately calculate flexible pavement behavior for thin and thick pavements.

CHAPTER ONE

INTRODUCTION

Background

To accommodate seasonal changes in pavement material properties, design procedures have been based upon empirical relationships between measurable soil and material parameters and observations of field performance. The 1993 American Association of State Highway and Transportation Officials (AASHTO) Guide [1] for the design of pavement structures presents one such method based upon the results of the AASHO (American Association of State Highway Officials) Road Test conducted in the late 1950s and early 1960s near Ottawa, Illinois. The design roadbed soil resilient modulus (M_R) is the parameter used to describe the subgrade, and it may be measured or estimated on a seasonal basis. It is related to the damage that was incurred by the pavements at the AASHO Road Test facility. The aggregate base and hot mix asphalt (HMA) moduli are typically measured or estimated at only one environmental condition. There are several limitations to this design procedure since the relationships developed are specific to the types of materials used and the climate at the AASHO site. These empirical relationships were adjusted for conditions in other regions by means of satellite studies. In Minnesota, an extensive verification study was completed [2].

A new pavement design procedure is being devised for AASHTO that will use a mechanistic-empirical (M-E) approach. An M-E design procedure uses layer thicknesses, pavement material properties, and loading conditions as input into a numerical or analytical model to calculate stresses, strains and deflections at critical locations in the structure. The empiricism lies in the relationship between the calculated pavement responses and pavement

performance. The application of an M-E design procedure allows for improved reliability in design, the ability to predict specific types of pavement distress, and the ability to reasonably predict performance from limited field and laboratory results.

A realistic approach for characterizing climate effects on pavement material properties is needed in an M-E design procedure. One such approach is to develop engineering relationships between climate factors, subsurface environmental conditions and material mechanical properties with the use of instrumentation and data collection systems that monitor all these parameters.

Many agencies are moving toward M-E approaches for designing pavements and are quantifying climate effects on pavement material properties specific to their region. One study performed in Washington [3] examined seasonal changes in subgrade material stiffness for the purpose of predicting seasonal changes in modulus from measurable field data such as surface deflections, soil moisture content, soil suction and weather information. It was found that soil suction cells were capable of monitoring variations in subgrade moisture content. Subgrade resilient moduli were predicted from soil moisture content and from measured surface deflections to determine seasonal variations with the knowledge of in-situ density and moisture contents.

In another Washington study [4], adjustment factors were incorporated into the design procedure to account for seasonal changes in the pavement layer moduli. The factors were dependent upon the region of the state (eastern or western Washington), type of material (unbound base or subgrade layer), and the condition of the layers (wet/thaw or dry/other), as shown in Table 1.1. These factors were determined from deflection testing performed at various sites in these regions.

Table 1.1. Seasonal Variations of unbound material moduli for Washington State [4].

Region	Base		Subgrade	
	Wet/Thaw	Dry/Other	Wet/Thaw	Dry/Other
Eastern Washington	0.65	1.00	0.95	1.00
Western Washington	0.80	1.00	0.90	1.00

In a Texas study [5] on seasonal variations in pavement deflections, tests were performed at various sites that were subject to freeze/thaw action, a variety of temperature ranges, and different precipitation levels. Over a one-year period, a sine curve was found to be a suitable mathematical model for representing the deflection measured at a test point versus time, with maximum deflection occurring in the summer and minimum deflection occurring in the winter. It was also found that deflection of the pavement structure varied spatially as well as seasonally, and finally that deflection was typically greater in wetter areas.

Similar research was done in Manitoba, Canada [6] using environmental and pavement surface deflection data to calculate variations in the resilient moduli of a flexible pavement. Air, pavement and soil temperatures were compared to seasonal variations of the backcalculated pavement layer moduli and used to develop correlations between backcalculated layer moduli, temperature (for HMA layers) and thawing index (for base and subgrade layers).

Bayomy et al. [7] developed a mechanistic-based flexible overlay design system for the state of Idaho. Six zones and their characteristics were used: 1) to determine the expected moisture changes for the various soil groups within each zone and 2) to define the duration and onset of the seasons and the corresponding subgrade conditions and resilient moduli. In areas experiencing significant subgrade frost penetration, the average year was divided into four periods: summer, freezing transition, winter (frozen) and spring-thaw recovery. Seasonal factors

were created for subgrade soils to adjust for the changes in the resilient modulus during these periods. The factors (Table 1.2) are higher for the frozen period, and lower for the thawing and wet periods, and vary regionally within the state of Idaho.

Table 1.2. Seasonal adjustment factors used in Idaho M-E design procedure [7].

Climate Zone	Material	Seasonal Variation Factor			
		Frozen	Thaw	Summer	Fall
Zone 1	Base/Subbase	1.00	0.65	1	1
	Subgrade	11.20	0.43	1	1
Zone 2	Base/Subbase	1.00	0.65	1	1
	Subgrade	11.20	0.43	1	1
Zone 3	Base/Subbase	0.65	0.85	1	1
	Subgrade	0.35-0.81	0.68-0.90	1	1
Zone 4	Base/Subbase	1.00	0.65	1	1
	Subgrade	11.20	0.43	1	1
Zone 5	Base/Subbase	1.00	0.65	1	1
	Subgrade	11.20	0.43	1	1
Zone 6	Base/Subbase	0.65	0.85	1	1
	Subgrade	0.27-0.73	0.63-0.87	1	1

Objective

The objective of this study is to quantify the relationships between climate factors, subsurface environmental parameters, and material mechanical properties for use in pavement design. These relationships will serve to calibrate a M-E design procedure to reflect conditions specific to Minnesota. The approach used to establish these relationships may suggest possible directions for similar studies.

Scope

The data for this study were acquired from the Long Term Pavement Performance Seasonal Monitoring Program (LTPP SMP) database and the Minnesota Road Research Project (Mn/ROAD) database. The four Minnesota sites are in Little Falls on U.S. Highway 10, in Detroit Lakes on U.S. Hwy 10, in Bemidji on U.S. Hwy 2, and Mn/ROAD located on Interstate 94 near Monticello. The site in Little Falls was evaluated for data prior to the date it was overlaid (1995). In general, most of the data available for the sites were from 1994 to 1996.

The type of data collected consisted of climate data, surface and subsurface condition data and deflection data. Thirty years of temperature and precipitation data from nearby weather stations were used to obtain climate history data. The climate history provides a useful backdrop to the more recently collected weather data collected at the sites. The condition of the pavement was determined with the use of five environmental sensors. The thermistors (TM) and thermocouples (TC) provided temperature data, time domain reflectometers (TDR) provided unfrozen volumetric moisture content data, while resistivity probes (RP) and Watermarks (WM) were used to indicate the occurrence and depth of freezing and thawing in the unbound layers. Finally, deflection data were available for the LTPP SMP sites for the years 1994 and 1995. The Mn/ROAD database contains deflection data from 1994 to the present. Estimation of the in-situ pavement moduli was accomplished using EVERCALC version 5.01, created by the University of Washington [4, 8].

Minnesota Road Research Project

Mn/ROAD is a 9.6-km pavement testing facility located parallel on Interstate Highway 94 near Monticello. It is composed of more than forty test cells divided between two test tracks. One is a 5.6-km mainline (ML) roadway that is subject to live interstate traffic, the other is a 4-km low-volume road (LVR) closed loop that is subject to traffic of a known weight and volume to simulate conditions on rural roads in Minnesota.

The flexible pavement test cells at Mn/ROAD, each 150 m in length, were used in this study. They were constructed with either AC20 asphalt cement or 120/150 penetration graded asphalt cement (the softer of the two binders). The base and subbase materials are composed of different gradations of aggregate and granular materials commonly used in the construction of Minnesota roadways. The two types of subgrade material have an R-value of 12 for the fine-grained material, and 70 for the sand material. Descriptions of these materials are given in Chapter Three.

Organization of Report

This report is organized into seven main chapters: Introduction, Literature Review, Methodology, Results and Discussion of Mn/ROAD, Results and Discussion from Greater Minnesota, Integrated Climate Model, and Conclusions and Recommendations. Chapter One introduces the topic and establishes the hypothesis, which states that it is possible to quantify the relationships between climate factors, subsurface environmental conditions, and material mechanical properties for use in a M-E pavement design process. Chapter Two is a literature review that was completed on previous methods for incorporating temporal changes in pavement material properties in design processes. Chapter Three documents the methodology used in this

study to quantify relationships between climate factors, subsurface environmental conditions and material mechanical properties in a pavement structure. Chapter Four presents the results from Mn/ROAD and Chapter Five presents the results from other flexible pavement sections located in Minnesota. Chapter Six shows the comparison between the trends in the Mn/ROAD data and the Integrated Climate Model developed by the Texas Transportation Institute and sponsored by the Federal Highway Administration [9]. Finally, Chapter Seven contains the conclusions and recommendations.

Appendices are included that detail the Mn/ROAD site and the processes critical to the completion of this report. Appendix A shows the layout of the Mn/ROAD test sections. Appendix B documents the process used to create a climate atlas. Appendix C contains computer code used to query data from the Mn/ROAD database, including thermocouple, time domain reflectometer, resistivity probe, Watermark, on-site weather station, and backcalculated resilient modulus data for the pavement structures.

CHAPTER TWO

LITERATURE REVIEW

Introduction

Estimates of pavement material mechanical properties allow for simulation of how a pavement structure will respond to different loading and environmental conditions and are used as input in most design methods. Laboratory and in-situ testing are common methods used to estimate material properties for individual materials in a pavement structure. Typically, laboratory testing damages or restructures the sample, so it is difficult to relate laboratory material response to the in situ response. Nondestructive testing (NDT) devices do not harm the pavement and allow the materials to be tested in their in situ condition, thus making it more of a system analysis than a component analysis. With the addition of sensors to monitor the pavement subsurface environmental conditions, it is possible to estimate pavement response to varying climate conditions and to quantify these relationships for use in a M-E design process.

In general, seasonal variations in flexible pavement material properties are more critical than in rigid pavement structures. This is primarily due to the fact that HMA is a viscoelastic material for which the properties depend on the rate of loading and temperature. Temporal variations in portland cement concrete (PCC) modulus are not as great.

Several topics are discussed in the next sections concerning pavement layer response to climate conditions and their influence on design approaches including: pavement material laboratory tests, nondestructive testing methods, pavement layer backcalculation methods, empirical and M-E pavement design approaches and the incorporation of seasonal variations in pavement material properties in these methods.

Laboratory Material Properties and Characterization

Seasonal Effects on Flexible Pavement Material Properties

Flexible pavements in Minnesota generally consist of HMA underlain by an unbound aggregate base layer. The system serves two primary purposes: 1) to provide sufficient total pavement thickness to prevent permanent deformation to the subgrade, and 2) to provide a thick enough HMA layer to prevent fatigue cracking. Figure 2.1 shows common materials in a flexible pavement layered system.

When designing a flexible pavement, expected traffic loads are used to determine the types of materials used, their thicknesses, and relative positions within the pavement structure. To ensure that a flexible pavement will be able to distribute traffic loads effectively and withstand various climate conditions, material properties need to be determined by either laboratory or in-situ tests. The material properties typically used for mechanistic analysis that utilize layered elastic theory are the elastic modulus and Poisson's ratio. Laboratory resilient modulus testing is primarily used in mechanistic design procedures as a means to determine the elastic modulus.

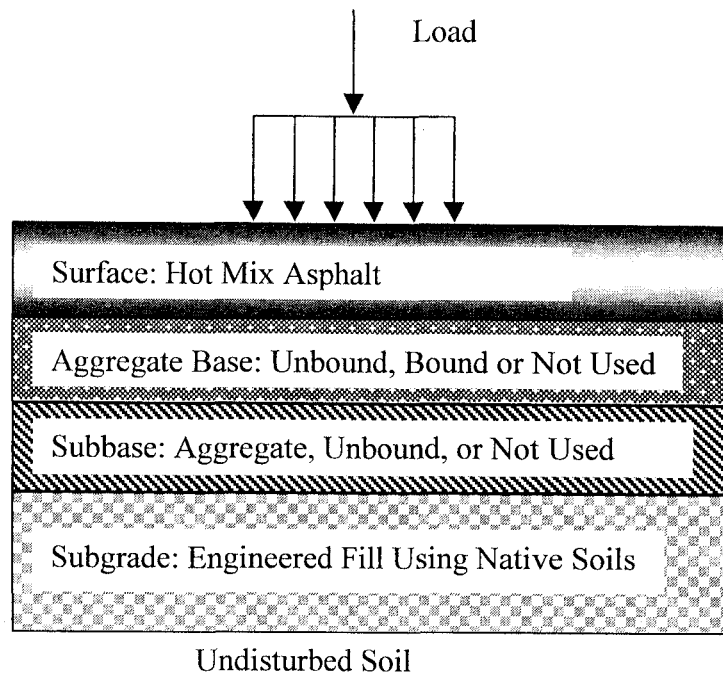


Figure 2.1. Typical materials used in HMA pavement structures.

Poisson's Ratio

Poisson's ratio is a material property that is used in elastic design procedures. Poisson's ratio (ν) is defined as the ratio of lateral strain (ϵ_l) to axial strain (ϵ_a) caused by a load parallel to the axis. These strains can be measured during a triaxial resilient modulus test and used to compute Poisson's ratio, Equation 2.1.

$$\nu \cong \frac{1}{2} \left(1 - \frac{1}{\epsilon_a} \frac{\Delta V}{V_0} \right) \quad (2.1)$$

where

V_0 = original volume, and

ΔV = change in volume.

Poisson's ratio, for a sensible range of 0.0 to 0.5, was shown to have little effect on a pavement's response [10]; therefore, it is customary to assume a reasonable value for Poisson's ratio (see Table 2.1).

Table 2.1. Typical values of Poisson's ratio for various materials [10].

Material	Range	Typical Values
Hot-Mix Asphalt	0.3-0.4	0.35
PCC	0.15-0.20	0.15
Untreated Granular Material	0.3-0.4	0.35
Cement-Treated Granular Material	0.1-0.2	0.15
Cement-Treated Fine-Grained Material	0.15-0.35	0.25
Lime-Stabilized Material	0.1-0.25	0.2
Lime-Flyash Mixture	0.1-0.15	0.15
Loose Sand or Silty Sand	0.2-0.4	0.3
Dense Sand	0.3-0.45	0.35
Fine-Grained Soils	0.3-0.5	0.4
Saturated Soft Clays	0.4-0.5	0.45

Poisson's ratio for a HMA sample is usually assumed because it is a difficult property to measure and has little effect on deflections calculated using a layered elastic model. It varies for a HMA sample according to the temperature (see Table 2.2).

Table 2.2. Commonly assumed Poisson's ratio values for HMA [10].

Temperature		Poisson's ratio
°C	°F	
-18	0	0.2
1	34	0.2
25	77	0.35
40	104	0.5

Basis for Determining the Modulus of Pavement Materials

It is useful to define certain terms related to “modulus” for the following discussion, including the elastic and dynamic modulus, modulus of subgrade reaction, resilient modulus, and stiffness [11].

Elastic Modulus

The modulus of elasticity is essentially the applied axial stress divided by the resulting axial strain, within the linear range of stress-strain behavior of a material [11] (Equation 2.2 and Figure 2.2). This property is important when characterizing the ability of a material to return to its original shape and size immediately after deformation. Strain is proportional to stress in the linear region, and this allows the prediction of the behavior of the material.

$$E = \frac{\sigma}{\epsilon} \quad (2.2)$$

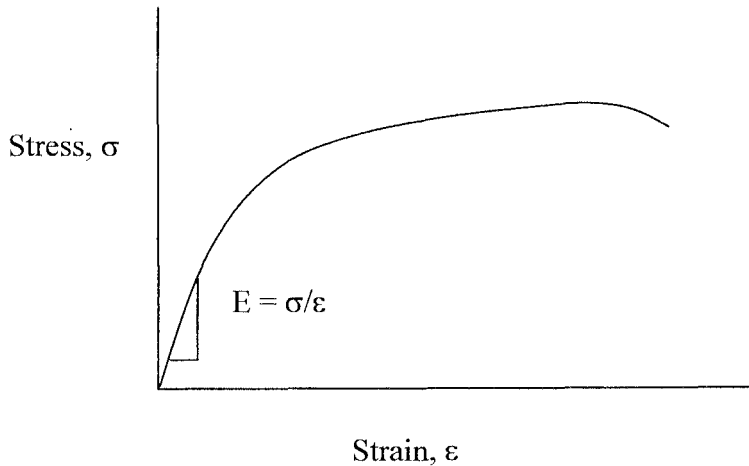


Figure 2.2. Simplified stress-strain diagram.

Dynamic Modulus

The dynamic modulus is the maximum axial stress applied to a material in sinusoidal loading, divided by the maximum axial strain occurring during that loading.

Modulus of Subgrade Reaction

The applied stress imposed by a loaded plate of a specified dimension acting on a soil mass divided by the displacement of the plate within the linear portion of the stress-deformation curve.

Stiffness

Stiffness is a term used in this report to qualitatively describe a general resistance to elastic deformation. It is used interchangeably with the elastic modulus, modulus of subgrade reaction and resilient modulus.

Resilient Modulus

Resilient modulus is the standard value recommended by AASHTO [1] for the modulus of elasticity for pavement materials and is based on stress and strain measurements from rapidly applied loads, similar to those experienced from wheel loads. The resilient modulus is the stress generated by an impulse load divided by the resulting recoverable strain after a loading cycle. This property is used in layered elastic analysis to predict a pavement structure's response to a given load. Modulus values are abbreviated in this report as E_{HMA} for HMA, or E_{AB} and E_{SG} for aggregate base and subgrade materials, respectively.

Typical values of the resilient modulus of HMA are 150 MPa (at 49°C), 3,500 MPa (at 21°C) and 14,000 MPa (at 0°C) [12]. Crushed stone modulus values range between 150 and 300 MPa, silty soil modulus values range between 35 and 150 MPa, and clayey soil modulus values range between 35 and 100 MPa [12].

Seasonal Variations in HMA Resilient Modulus

HMA resilient modulus varies with temperature. While aggregate in the mixture contributes internal friction to the matrix, the asphalt cement provides cohesion. Since the stiffness of asphalt cement is dependent upon temperature, the HMA stiffness is also dependent upon temperature. The change in E_{HMA} is significant and depends on temperature fluctuations in a given climate and therefore it should be included in design. The effect is a lower modulus when temperatures are high in the summer and a higher modulus when temperatures are low in the winter.

There are various laboratory test procedures that may be used to determine the resilient modulus of a HMA sample including: the diametral resilient modulus test procedure (ASTM D 4123) and the Strategic Highway Research Program (SHRP) method (Protocol P07).

Resilient Modulus of Aggregate and Soil Materials

The resilient modulus of aggregate and soil materials is dependent upon the material type, sample preparation, deviator stress (σ_1) confining pressure (σ_3) and the moisture content used in the test. The resilient modulus of a granular material will typically increase with increasing density and confining pressure, decreasing saturation level and increasing angularity of the granular particles. The resilient modulus of a fine-grained soil typically decreases with

increasing deviator stress but also depends upon the soil type, moisture content and density. As Li [13] explains, the resilient modulus of a fine-grained subgrade soil can change from 14 to 140 MPa due to changes in stress state and moisture content.

Similar to HMA, cohesion is a primary factor in determining the resilient modulus of an aggregate-water matrix. The moisture content and particle content of the mixture supplies the cohesion. Excessive moisture contents will lead to a decrease in the modulus value. To properly design a flexible pavement it is critical to test the samples at the moisture content and density expected in the field.

Several models have been developed to estimate the resilient modulus of aggregate base and subgrade soils, Table 2.3. The basis for the granular and fine-grained resilient modulus models are Equations 2.3 and 2.4, respectively. Various test methods are used to determine the modulus of unbound materials including AASHTO T 274 and SHRP Protocol P46. SHRP Protocol P33 is used for asphalt treated base and subbase materials. The principal stresses used in these equations that are acting on the soil elements are shown in Figure 2.3.

$$M_R = K_1 \theta^{K_2} \quad (2.3)$$

$$M_R = K_3 \sigma_d^{K_4} \quad (2.4)$$

where

$$\theta = \text{bulk stress} = \sigma_1 + 2\sigma_3,$$

$$\sigma_d = \text{deviator stress} = \sigma_1 - \sigma_3,$$

$$\sigma_1 = \text{vertical pressure},$$

$$\sigma_3 = \text{confining pressure, and}$$

$$K_1, K_2, K_3, \text{ and } K_4 = \text{constants dependent on material}$$

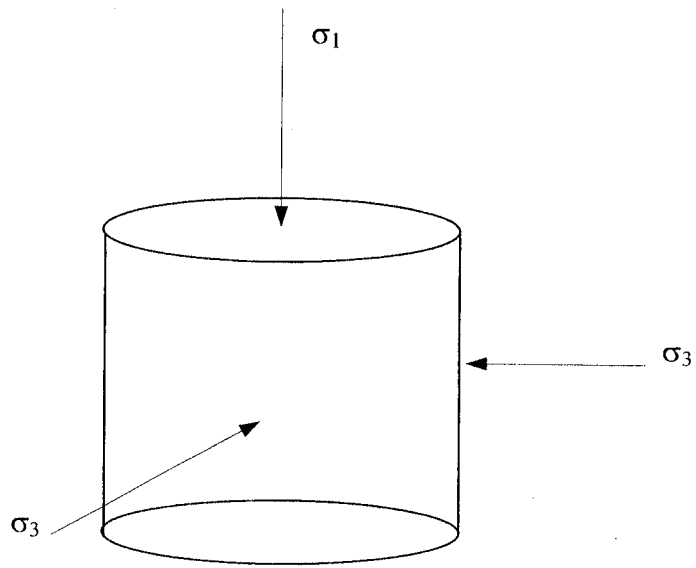


Figure 2.3. Principal stresses acting on a soil element for a triaxial test condition.

Table 2.3. Models used to estimate soil resilient modulus.

Models	Type of Soil	Source
$M_R = k_1 P_a \left[\frac{\theta}{P_a} \right]^{k_2}$ <p>$k_1, k_2 =$ material and physical parameters $P_a =$ atmospheric pressure</p>	Granular	[14], [15]
$M_R = K_1 k_1 \theta^{k_2}$ <p>$K_1 =$ function of pavement structure, test load and developed shear strain $k_1, k_2 =$ constants</p>	Granular	[16]
$M_R = k_1 P_a \left[\frac{\theta}{P_a} \right]^{k_2} \left[\frac{\sigma_d}{P_a} \right]^{k_3}$ <p>$k_1, k_2, k_3 =$ material and physical parameters</p>	Granular	[17]
$\Delta M_R = K_1 K_2 \theta^{K_2 - 1} (\Delta \theta_T + \Delta \theta_S)$ <p>K_1 and $K_2 =$ material and physical property parameters $\Delta \theta_T =$ changes of bulk stress due to temperature $\Delta \theta_S =$ changes of bulk stress due to soil suction</p>	Fine-Grained	[18]
$M_R = K_2 + K_3 [K_1 - (\sigma_d)] \text{ for } K_1 > (\sigma_d)$ $M_R = K_2 + K_4 [(\sigma_d) - K_1] \text{ for } K_1 > (\sigma_d)$ <p>$K_1, K_2, K_3, K_4 =$ material and physical parameters</p>	Fine-Grained	[19, 20]
$M_R = k \left(\frac{\sigma_d}{\sigma'_3} \right)^n$ <p>$n =$ parameter dependent on soil type and physical state</p>	Fine-Grained	[21]
$M_R = 10^{(k - n\sigma_d)}$	Fine-Grained	[22]
$M_R = \frac{k + n\sigma_d}{\sigma_d}$	Fine-Grained	[23]
$M_R = k \left(\frac{\sigma_{oct}^n}{\tau_{oct}^m} \right)$ <p>$\sigma_{oct} =$ octahedral normal stress $\tau_{oct} =$ shear stress</p>	Fine-Grained	[24]

Seasonal Effects on Rigid Pavement Material Properties

A rigid pavement is typically composed of a portland cement concrete (PCC) surface layer, over a base and/or subbase material, over engineered fill, over engineered subgrade, as shown in Figure 2.4. The layers under the PCC layer can consist of various material combinations such as granular material or a stabilized material (such as a permeable asphalt stabilized base) depending on the project.

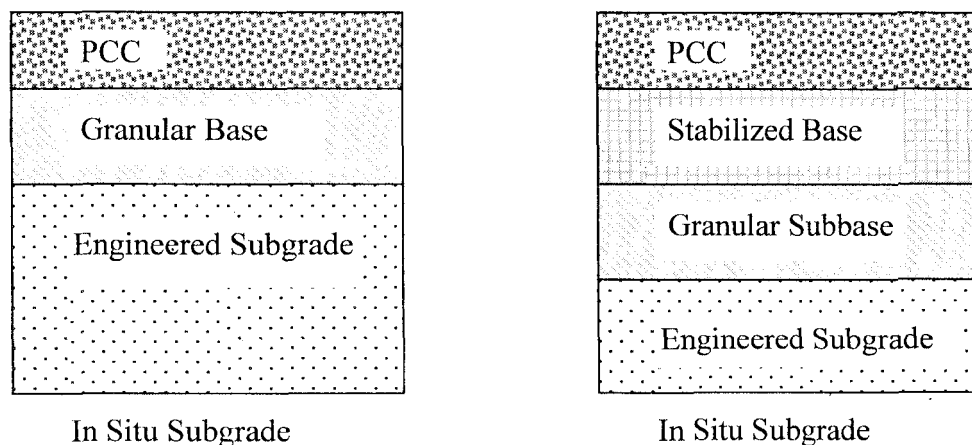


Figure 2.4. Typical cross-section of a rigid pavement.

Environmental factors, such as temperature changes and precipitation events can cause certain distresses in a rigid pavement, and can affect the modulus of subgrade reaction (k-value), which is a measure of the stiffness of the soil. It is the stress that will cause a unit deflection in the underlying soil. If one were to assume that k was constant throughout a range of stress, then the subgrade would be linear elastic. The modulus of subgrade reaction behaves similar to the resilient modulus in regards to soil type and test conditions. However because it is a composite support value, other factors such as seasonal effects, type and thickness of the subbase material used, erosion of subbase, and the presence of bedrock also influence the k-value (AASHTO

1993). Plate bearing tests are used to determine k in the field and the test method is designated as AASHTO T222.

Environmental Distresses Induced in a Rigid Pavement

Curling

Temperature gradients cause curling stresses in the PCC slab due to differential temperatures between the slab surface and bottom. The cooler side contracts while the warmer side expands, thus curling the slab, as shown in Figure 2.5. When traffic on the pavement drives over a slab that is curled up, corner breaks, mid-panel cracking and other distresses in the pavement are possible.

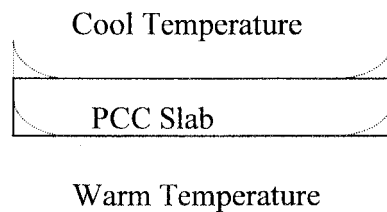


Figure 2.5. Curling stresses in a typical PCC slab.

Pumping and Faulting

The underlying layers in a rigid pavement must be stable and allow for the drainage of excess water. The moisture that accumulates between the layers can be detrimental to the pavement structure by weakening the layers and causing premature failure. Aggregates used for drainage layers should be sound, clean, and open graded materials. They should have a high permeability to allow for excess moisture to drain freely from the pavement structure without clogging.

A common cause of pavement distress is the pumping of excess water from under the concrete slab, which can cause faulting and/or corner breaks. The first step in the mechanics of faulting is the creation of a void space under the concrete slab that water is able to enter. This void may be created from pumping, curling and warping, cracks or other methods. Since the concrete is a rigid structure, it does not deform to fill the void created by this loss of material. When water is introduced into the void and does not drain, it may cause a loss of cohesion in the soil and create a mud-like mixture of water and soil. Traffic loading will cause more deflections in the concrete leave slab and cause the underlying materials and the water to be ejected out through the joints, cracks or the edge of the slab, or butt up under the approach slab. This loss of supporting material under the concrete slab will eventually lead to faulting and corner cracking of the slab. It is particularly noticeable during or just after a precipitation event [10].

Freeze/Thaw Cycles

The primary environmental factor affecting portland cement concrete is exposure to freeze-thaw temperature cycles. The most common damage from frost penetration in concrete is cracking and spalling, caused by progressive expansion of the cement paste matrix from repeated freeze-thaw cycles. Scaling is another type of damage, which is caused by exposing concrete surfaces to freezing and thawing with moisture and deicing chemicals present, or by overworking the concrete when paving. This causes the concrete finished surface to flake or peel off. Another type of damage is D-cracking, which occurs when cracks form around the corners and parallel to the cracks and joints of the slab due to aggregate expansion and degradation [25].

Resistance to frost damage in PCC relies on the interaction of several factors including the location of escape boundaries for water, pore structure of the system, degree of saturation,

rate of cooling, and the tensile strength of the material that must be exceeded to cause rupture. Air entrainment can provide avenues of escape in the cement paste matrix, and proper mix proportions and curing can modify the pore structure [25].

Measuring In Situ Mechanical Properties

Measuring in situ mechanical properties are synthesized in a recent report [11]. Many state highway agencies are moving toward use of falling weight deflectometers (FWD) as the primary means of evaluating the structural condition of pavements. Thus, FWDs are the focus of the following discussion.

Falling Weight Deflectometer Testing

FWDs apply an impact load to the pavement surface and measure the deflection. From the deflection basin, the applied load, and known layer thicknesses, it is possible to calculate pavement layer properties using a backcalculation technique. The process of deflection testing and backcalculating material properties is discussed in the following sections.

The standard test method is ASTM 4694-87 titled “Standard Test Method for Deflections with a Falling Weight Type Impulse Load Device.” A related test method is ASTM D4695-87 titled “Standard Guide for General Pavement Deflection Measurement.” The ASTM D4694-87 test method specifies a falling weight as the means to apply force to the pavement. The force pulse approximates a haversine wave with a specified peak force and duration. Standard loading plates with diameters of 300 mm (11.8 in) and 450 mm (17.7 in) are used. Seismometers and velocity transducers or accelerometers are used to measure the maximum vertical movement of the pavement.

FWDs are used worldwide because measurements are obtained rapidly, the impact load is varied easily, they simulate actual wheel load well and can measure deflection basins accurately. Two disadvantages of these devices are their high initial cost and that they must be stationary during the test, therefore, traffic control is required.

The Strategic Highway Research Program (SHRP) and the current FHWA Long-Term Pavement Performance (LTPP) study use the Dynatest Model 8000E and applied loads of 27 kN (6,000 lb.), 40 kN (9,000 lb.), 53 kN (12,000 lb.), and 71 kN (16,000 lb.). These weights are dropped onto a rubber buffer system resulting in a load duration of 0.025 to 0.030 seconds. The peak deflections are recorded for all four drops and a complete history of deflection and load versus time is recorded for the last drop at each of the four load levels. Figure 2.6 shows the typical locations of the loading plate and seven velocity transducers. The LTPP program uses sensors spaced as shown in Table 2.4 and Figure 2.6, with a 300-mm (11.8-in) load plate [26]. Figure 2.7 illustrates a falling-mass system used in FWD testing to apply an impulse force.

Precision and bias need to be determined for the test results in order to understand the sources of variability. When a device is operated by a single operator in repetitive tests at the same location, the test results are questionable if the difference in the measured deflection between two consecutive tests at the same drop height is greater than 5 percent (ASTM D 4694-87).

Table 2.4. FWD sensor spacing for SHRP and Mn/DOT.

SHRP, mm (in)	Mn/DOT, mm (in)
0	0
203 (8)	203 (8)
305 (12)	305 (12)
457 (18)	457 (18)
610 (24)	610 (24)
914 (36)	914 (36)
1524 (60)	1219 (48)
	1524 (60)
	1829 (72)

Mn/DOT currently uses two Dynatest FWDs at Mn/ROAD. Prior to 1996, there were seven sensors used in agreement with SHRP protocol (Figure 2.6). Beginning in 1996, Mn/DOT added two more sensors at 1219 mm and 1829 mm [8].

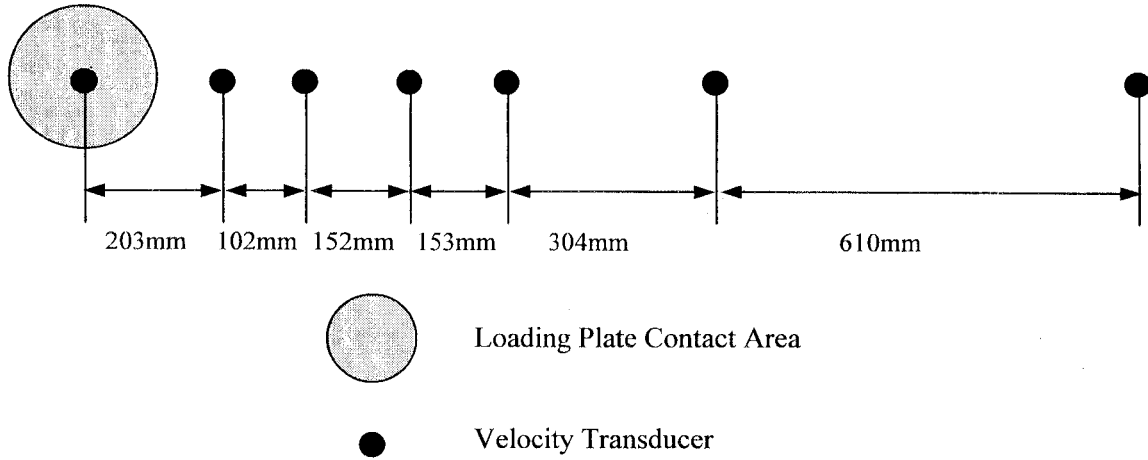


Figure 2.6. Planview of location of loading plate and velocity transducers for FWDs.

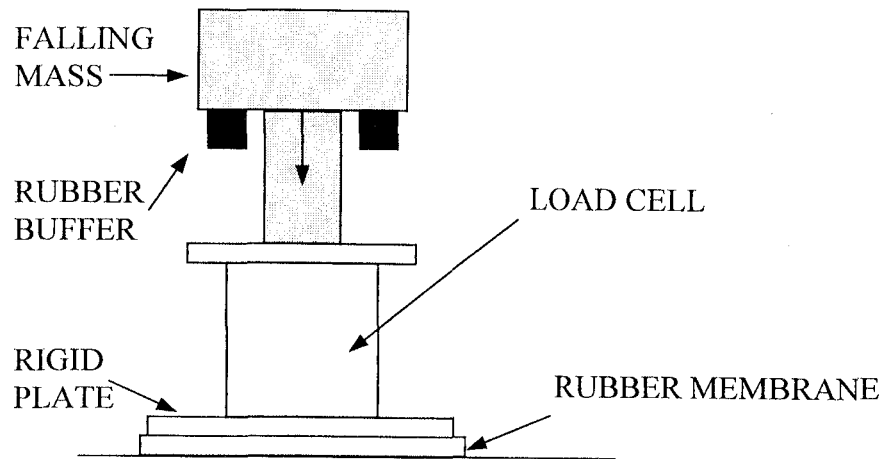


Figure 2.7. Sketch of a falling mass system [27].

Backcalculation of Layer Moduli

Falling weight deflectometer testing produces a deflection basin for each applied load, from which it is possible to backcalculate pavement layer moduli. There are many backcalculation computer programs that can be used for this purpose. These computer programs include measures of convergence, convergence techniques, and subgrade “rigid” layers [12]. A typical flowchart for moduli backcalculation is shown in Figure 2.8. This flowchart is patterned after one by Lytton [28] which includes the following elements:

- Measured deflections, including the measured pavement surface deflections and associated distances from the load.
- Layer thicknesses and loads, including all layer thicknesses and load levels for a specific test location.
- Seed moduli, which are the initial moduli used in the computer program to calculate surface deflections are usually estimated by the user.
- Deflection calculation, using layered elastic computer programs such as WESLEA [29] to calculate a deflection basin.
- An error check that compares the measured and calculated basins.
- Methods that converge on a set of layer moduli, which minimize the error between the measured and calculated deflection basins.
- Controls on the range of moduli, providing a maximum and a minimum moduli to prevent convergence to unreasonable moduli.

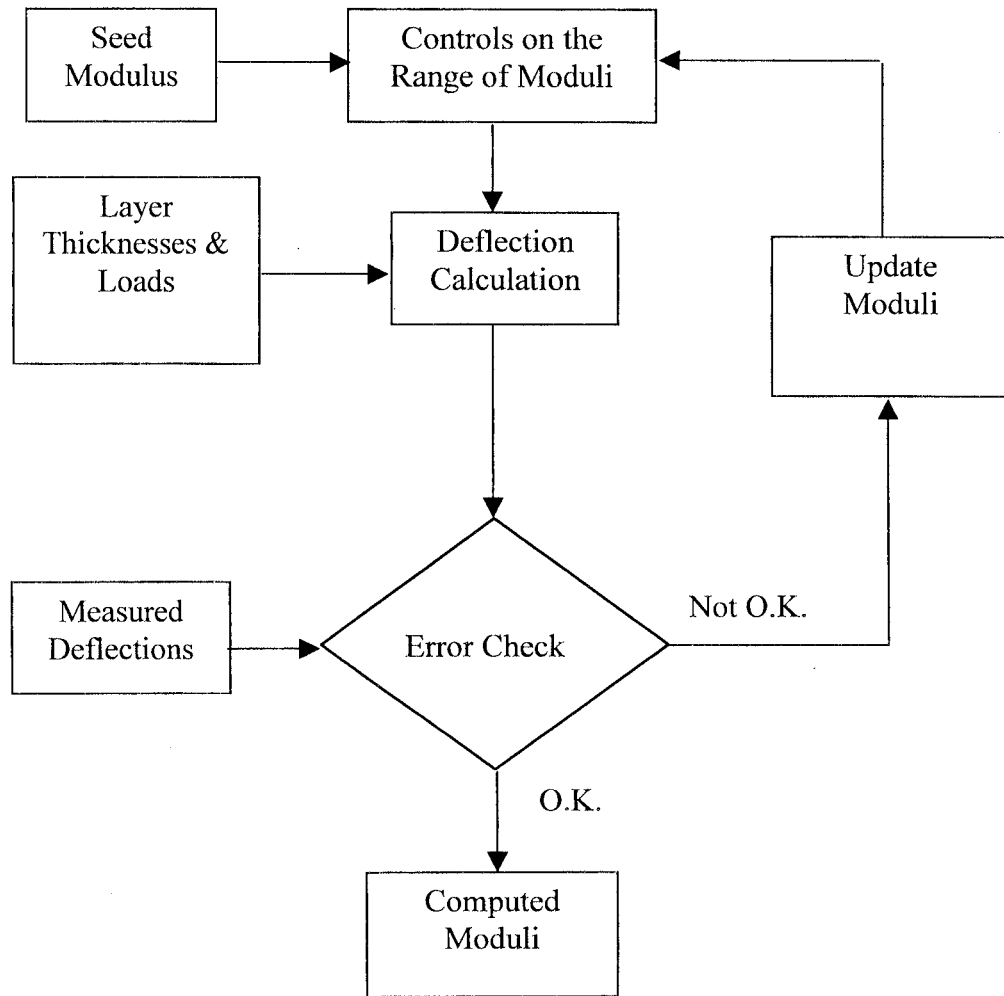


Figure 2.8. Common elements of backcalculation programs [modified after [28]].

EVERCALC

EVERCALC is a backcalculation program created at the University of Washington for the Washington State Department of Transportation [30]. It employs an iterative approach to vary the moduli in a layered elastic solution until a near match is obtained between theoretical and measured deflections. Figure 2.9 shows a simplified flowchart for EVERCALC [12].

EVERCALC uses WESLEA [29] to compute the theoretical deflections. Initial deflections are computed from the seed moduli supplied by the user or the default values in EVERCALC. The moduli are then updated until deflections are within the tolerance specified or until the maximum number of iterations has been reached.

EVERCALC allows the user to enter the deflection data manually or retrieve it from an FWD data file created in the field. The output includes information regarding the backcalculation results from each FWD drop. The coefficients for stress sensitivity of the base and subgrade are computed automatically by the program. Finally, the moduli are normalized to a 40 kN (9000 lb) FWD load, and the modulus of the HMA can be normalized to a temperature of 25°C (77°F).

EVERCALC was selected as the computer program used to backcalculate pavement layer moduli at Mn/ROAD [8]. Research has shown that it is important to consider several limitations when backcalculating pavement layer moduli [8]. Backcalculating moduli for pavement sections with less than 100 mm HMA thickness was not recommended since the layer is too thin. During the spring thaw period, shallow frozen/unfrozen zones in the pavement interfere with the backcalculated moduli because the thickness of these layers is unknown.

In the Mn/ROAD database, two models have been used. Model A does not use a stiff layer and model B estimates the depth to a stiff layer with a modulus equal to 345 MPa. The depth to the stiff layer is computed in EVERCALC using an empirical relationship developed for

shallow bedrock conditions. Input includes the use of uniform weighting factors of the sensors, a maximum of 20 iterations, an RMS tolerance of 0.1%, and modulus tolerance of 0.1%. A temperature correction is used after the moduli are backcalculated to normalize the HMA modulus to 25°C.

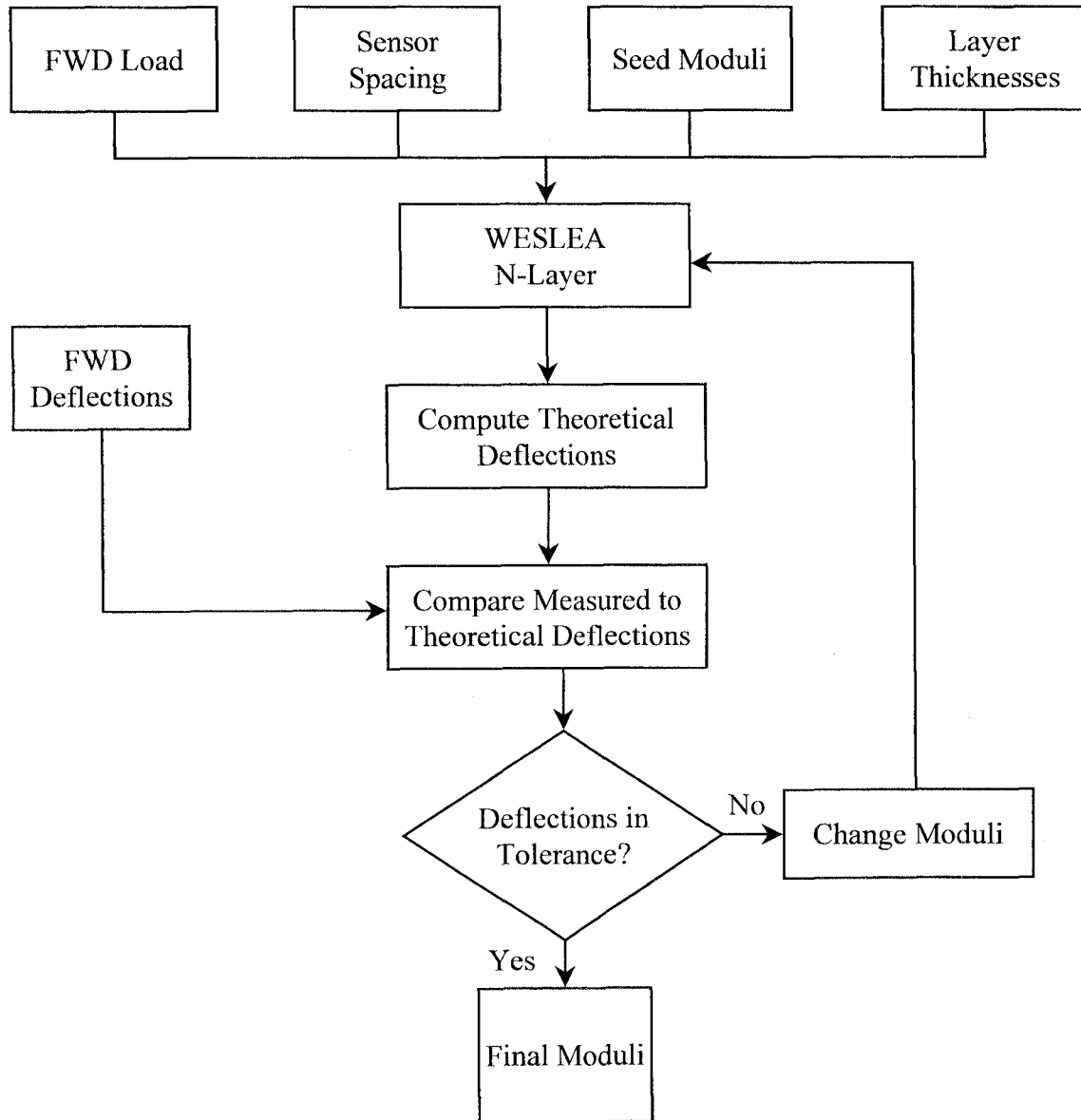


Figure 2.9. Simplified flow chart for EVERCALC [12].

Quantifying Seasonal Effects on a Pavement Structure Using NDT

Washington State

An evaluation of the effect of seasonal variations on pavement stiffness and strength was made to predict seasonal changes in modulus from field data [3]. Four United States Forest Service (USFS) roads were monitored over an 18-month period. Surface deflections were measured by a Dynaflect and Benkelman beam and the subgrade moisture content was measured using Soiltest moisture-temperature cells. Weather data were collected from nearby weather stations, and soil samples and pavement cores were obtained and subjected to resilient modulus testing. Moduli were calculated at 2 week to 2 month intervals to determine the seasonal variation in pavement layer strength at the four test sites.

Two major relationships were explored. First, the prediction of subgrade resilient modulus from soil moisture content. Second, the prediction of subgrade resilient modulus from measured surface deflections. Regression equations were developed [3] from the laboratory resilient modulus testing to predict the subgrade modulus from soil moisture content. These equations are a function of soil type, moisture content, dry density, and bulk or deviator stress. Subgrade modulus values were predicted from measured deflections using two computer programs and a third hand-calculation method.

It was found that the regression equations developed from laboratory resilient modulus data can be used to reasonably predict subgrade and base course resilient modulus [3]. Also, fine-grained subgrade soils exhibit larger variations in resilient modulus throughout the year than do the more granular subgrade soils studied. Finally, when frost penetration was minimal, the subgrade modulus was primarily a function of rainfall, and the minimum modulus for the year was not necessarily in the spring.

Another approach for predicting seasonal variations in pavement layer properties is to perform nondestructive testing on a pavement section with a known composition that contains environmental sensors [6]. This approach allows for the estimation of how pavement layer moduli vary according to different climate conditions that are typical for a given location. The next section discusses four main environmental sensors used at Mn/ROAD to measure field temperature, moisture content and state of moisture.

Monitoring In Situ Conditions

Sensors can be used to characterize subsurface environmental conditions in a pavement structure affecting the mechanistic properties of a pavement layer. For this study, in-situ temperature, moisture content and moisture state are of primary importance for characterizing seasonal variations in the stiffness of pavement layers. To quantify these changes, information from Mn/ROAD was used. These characteristics are measured by thermocouples, time-domain reflectometers, resistivity probes and Watermarks.

In addition to Mn/ROAD, the Strategic Highway Research Program (SHRP) conducted research on Seasonal Monitoring Programs (SMP) as a part of the Long-Term Pavement Performance (LTPP) studies [31]. The goal was to monitor changes in the temperature and moisture content of pavement structures located at approximately 3000 sites in North America for three purposes [31]:

- Develop a means of relating pavement response to design parameters.
- Validate models that relate environmental conditions to in situ mechanistic properties.
- Determine the magnitude and impact of seasonal changes on in situ mechanistic properties.

Instrumentation at these sites includes thermistors, time domain reflectometers and resistivity probes. The three HMA - LTPP SMP sites in Minnesota are located in Bemidji, Detroit Lakes and Little Falls [32, 33, 34].

Thermocouples

Thermocouples (TC) are the most widely used temperature sensor [35]. The basis of their operation [36] is that when two dissimilar metals are in contact with each other a small voltage is induced, which is a function of the temperature at their junction. The voltage occurs since each metal has a different number of free electrons at varying temperatures. The voltage is compared to the reference voltage established in an ice bath.

Mn/ROAD has over 1,000 Type-T thermocouples (Figure 2.10) that are composed of copper and constantan [37]. These TCs are suitable for use in the range of -40°C to 60°C and have an accuracy of $\pm 1^{\circ}\text{C}$ [36]. From the initial construction in 1993 until June 15, 1996, only 2% of the TCs at Mn/ROAD had failed [37]. The TCs are placed at known intervals to determine thermal gradients in the pavement layers.

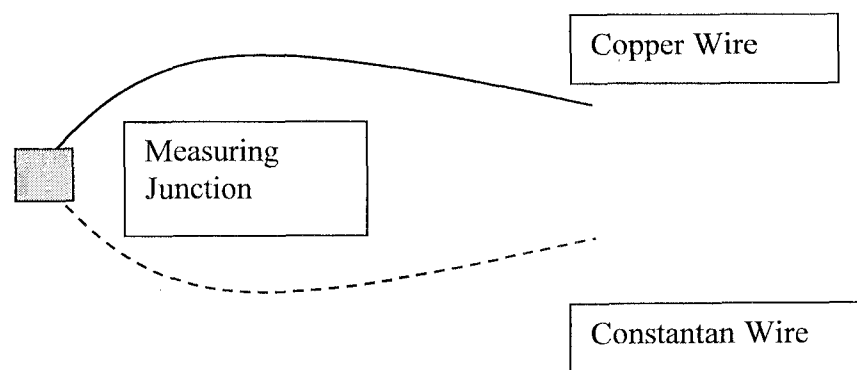


Figure 2.10. Type-T thermocouple sensor.

Time Domain Reflectometry Waveguides

Time domain reflectometry waveguides (TDRs) are used at Mn/ROAD to measure the liquid moisture content [38]. Values are appear in the database as percent volumetric moisture content. Moisture content data from TDRs will be presented as volumetric moisture content unless otherwise noted. To convert between volumetric moisture content (θ) and gravimetric moisture content, multiply θ by the bulk density of the soil [39].

$$\theta (\%) = \frac{V_w}{V_t} = w \frac{\rho_b}{\rho_w} \quad (2.5)$$

where: θ = volumetric moisture content, %,

V_w = volume of water,

V_s = weight of soil solids,

w = gravimetric moisture content,

ρ_b = bulk density, kg/m^3 , and

ρ_w = density of water (1000 kg/m^3 at standard temperature and pressure).

The basis for operation of a TDR is that when an electromagnetic wave is transmitted through a medium, any obstruction or change in impedance will reflect a portion of the original wave back to the source [31]. The TDR readout device displays travel time and amplitude of the signal which is used to calculate the dielectric constant of the material.

The dielectric constant of a material is an indication of its insulating properties. Soil, water and air have dielectric values of 3 to 5, 80 and 1, respectively [38]. Liquid water content has the greatest effect on the dielectric constant of a soil-water-air matrix because the capacitance of water is 16 to 80 times greater than soil and air. This is why TDRs are used for

estimating soil moisture content. Factors that may influence the ability to measure the dielectric constant and thus the TDR response include the solid mineral dielectric constant variability of the soil and the water dielectric constant variability (i.e. temperature effects and salinity). The dielectric constant for this soil-water-air combination can be calculated as follows:

$$K_a = \left(\frac{L_a}{LV_p} \right)^2 \quad (2.6)$$

where

K_a = dielectric constant,

L_a = apparent length of probe,

L = actual length of probe, and

V_p = propagation velocity.

Figure 2.11 shows a typical TDR trace readout. L_a is the distance between the start and end of the TDR probe, points A and B, respectively.

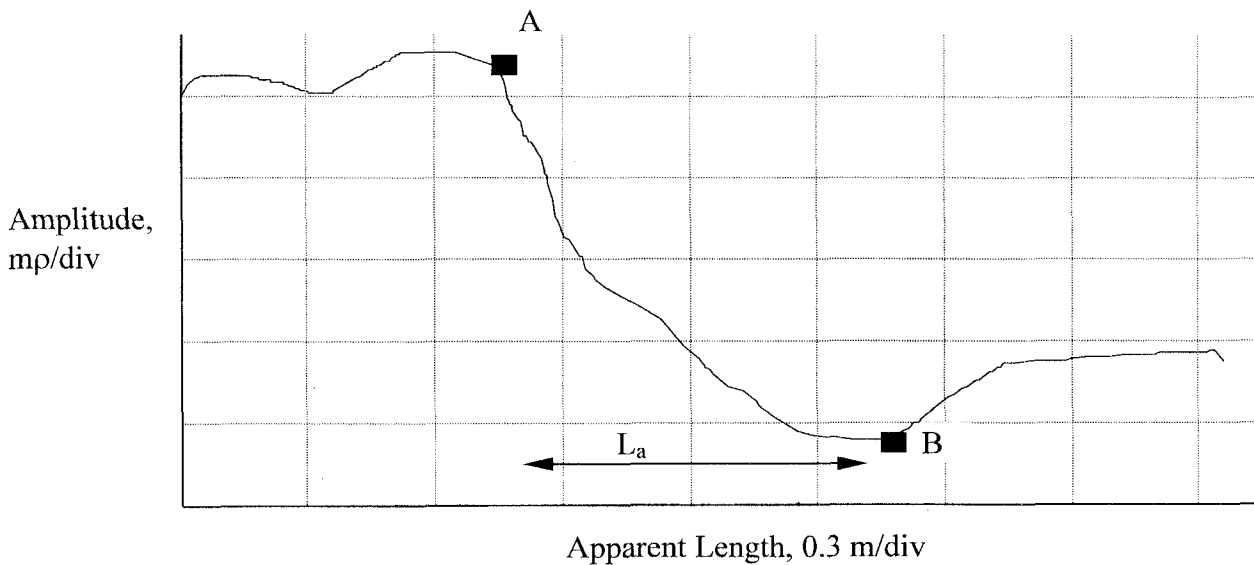


Figure 2.11. TDR trace where point A is the start and point B is the end of the TDR probe (mp/div is millirhos per division).

Over 700 TDRs were installed at Mn/ROAD and a schematic of the TDR sensor is shown in Figure 2.12. Approximately 19% of these sensors had failed between the initial installation in 1993 and June 15, 1996 [37]. Failures were most common for the sensors located at depths between 0.9 to 1.5 meters. These TDRs may have failed due to a physical separation of the cable from the probe as a result of frost action of the soil interacting with the cables [37].

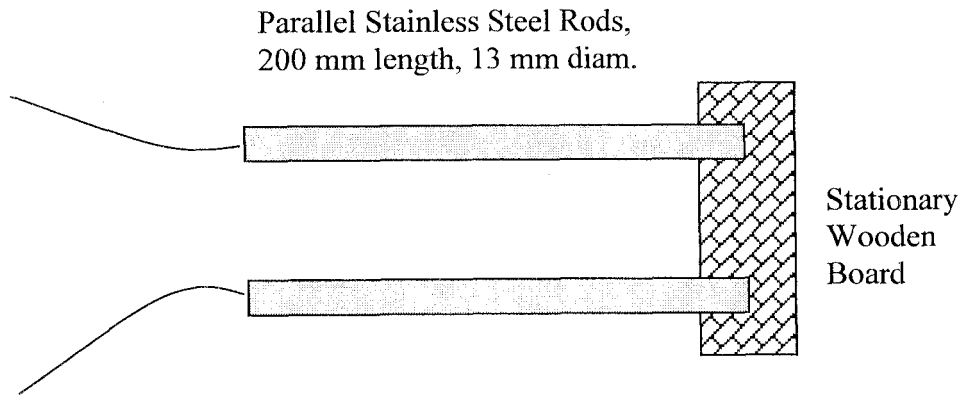


Figure 2.12. Time domain reflectometer at Mn/ROAD.

Resistivity Probes

Resistivity probes (RP) are used to estimate the zone of frozen soil in the aggregate base and subgrade. There are over 100 RPs installed at Mn/ROAD and approximately 1% had failed between construction and June 15, 1996 [37]. Figure 2.13 is a sketch of a typical resistivity probe at Mn/ROAD. They are installed vertically between 0.3 and 2.3 m below the surface. A non-conducting rod, typically polyvinyl chloride (PVC), is mounted with equally spaced electrodes (copper wires) at 50-mm intervals. An individual lead wire is connected to each electrode and the current flow and voltage between two adjacent electrodes is measured with an ohmmeter.

The operating principle for RPs is that electrical resistance varies between the soil, frozen and unfrozen water. For practical purposes, the electrical resistance of soil minerals are nearly infinite and therefore virtually all electrical current flow through soil is carried by free ions in the pore water [31]. Thus the electrical resistivity of soil-water-air mixture depends primarily on the porosity, degree of pore water saturation, electrical resistivity of the pore water, and the state of the pore water. The formation of ice in pores causes an increase in the electrical resistivity due to the electrical resistance of ice being far greater than the unfrozen pore water. Frost areas are identified by a large increases in resistance profiles.

Krantz [40] researched the validity of using resistance to identify frozen soil areas. Several SMP sites located in Manitoba were used to investigate the usefulness of RPs as a means to measure frost/thaw depth. It was found that RPs were useful when used with moisture content (TDR) and temperature (thermistor) probes. RPs did indicate frozen and unfrozen layers if the temperatures were below freezing, however a sudden increase in resistance did not automatically indicate a completely frozen layer since it was difficult to discern between thawed, partially frozen and frozen areas [40].

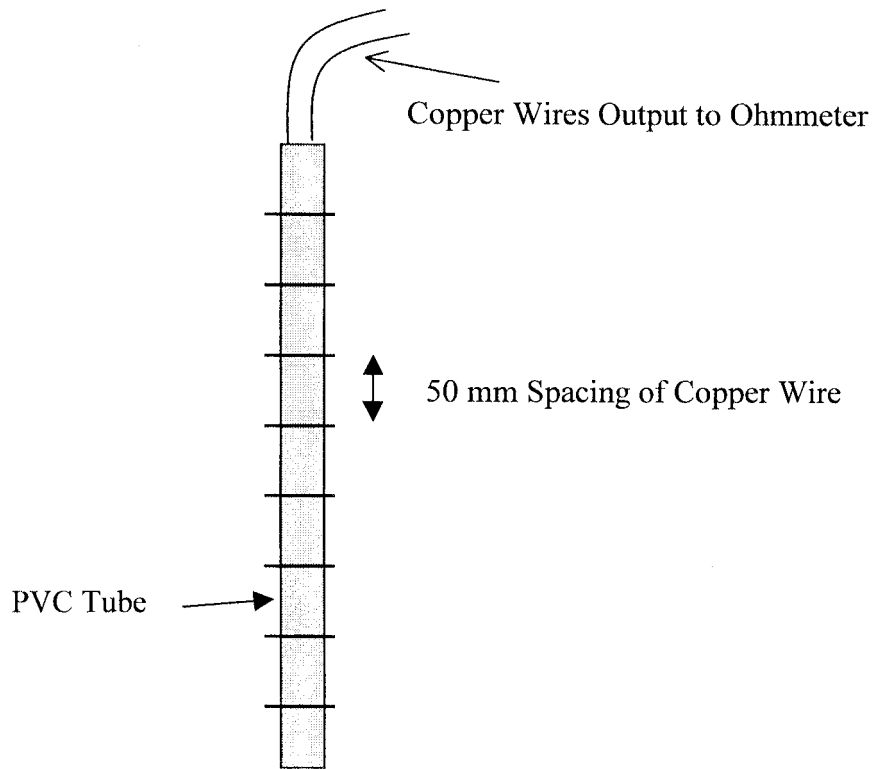


Figure 2.13. Section of a resistivity probe at Mn/ROAD.

Watermark Sensors

Watermark sensors (WM) measure moisture content. They consist of two concentric electrodes that are in a special reference matrix material (usually silica sand) that is held in place by a synthetic membrane, Figure 2.14. While the probe is in operation, soil moisture is constantly being absorbed and released from the sensor. The amount of moisture in the matrix is measured by the electrical resistance between the two electrodes [41]. The resistance is converted to soil pore water pressure measurements through calibration curves derived from laboratory testing and are unique to the type of soil tested.

The data from the WMs appear in the database in units of centibars. For unfrozen soil, the readings fluctuate about some baseline value that is independent for each sensor. When the water in the soil-water-air matrix freezes, the readings exceed the baseline value and return after

thawing. Typical baseline values are between 1 and 3 cbar and frozen values are an order of magnitude larger. WMs can therefore be used as a freeze/thaw indicators [37].

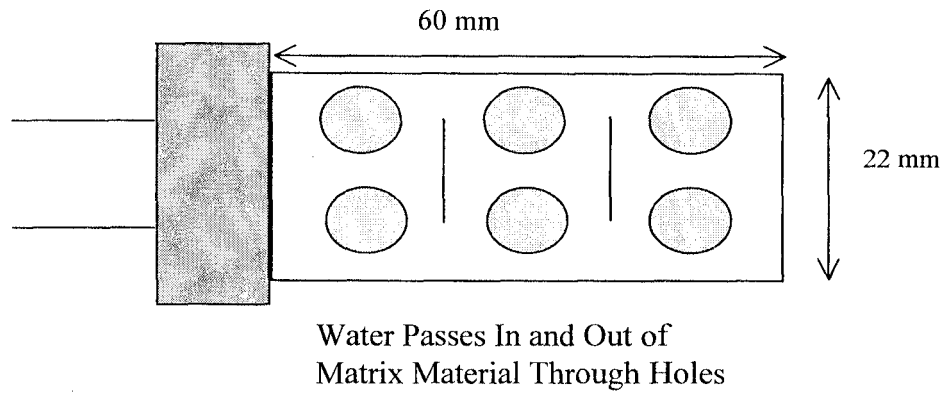


Figure 2.14. Watermark sensor at Mn/ROAD.

The systematic monitoring of environmental conditions in a pavement structure, coupled with the field monitoring of seasonal variations in pavement layer moduli, provides a means to quantify seasonal variations in pavement material properties. This approach gives a realistic account of the seasonal variations to which a pavement structure is subject for a given location and can be used most efficiently in a mechanistic design process. Empirical and M-E pavement design processes are discussed in the next sections.

Empirical and Mechanistic Approaches to Pavement Design

Empirical design approaches are most commonly used to design pavements today by highway agencies [11]. In general, they are based on empirical knowledge of how pavement layers behave and they employ average or “worst-case” seasonal values for material properties to determine pavement layer thicknesses. The M-E design method is a process that is gaining acceptance. It uses the applied stresses to calculate strains which are empirically related to damage and used to determine the appropriate thickness of pavement layers. The failure criteria for both design methods are based on traffic, materials, layer configurations, and environment [12].

Empirical Flexible Pavement Design

Most current flexible pavement design methods are empirical, because in the past it was more practical to use experience or the results of experiments (such as the AASHO Road Test) to design pavements, rather than employ a mechanistic approach, which requires a great amount of computational effort that has only recently become available at the desk top.

The 1993 AASHTO guide [1] empirically accounts for seasonal variations in the subgrade. It is based on the results of tests conducted at the AASHO Road Test facility near Ottawa, Illinois and the damage incurred in the roadbed soil at the site. Several limitations apply to the relationships derived at that facility, such as Equation 2.6, since the relationships apply to specific site and climatic conditions.

The AASHTO procedure involves determining the estimated roadbed soil resilient modulus on a monthly or semi-monthly basis, depending on the expected variations in the modulus. Equation 2.6 is used to relate the soil modulus to a damage factor, μ_r , for each period.

The average damage factor is then used to calculate an effective soil modulus that is used for design.

$$\mu_f = 1.18 \times 10^8 * M_R^{-2.32} \quad (2.6)$$

HMA modulus at 20°C, and base layer moduli are given appropriate design values and are used with the subgrade effective modulus to determine the appropriate layer thicknesses. This is a limitation of the 1993 AASHTO design procedure since the layer thicknesses are determined for average moduli rather than seasonally.

The relationships developed from the AASHO Road Test were expanded to other regions by means of satellite studies. In Minnesota, the procedure is documented in Investigation 183 [2]. In this study, plate bearing tests were taken throughout the year to determine seasonal changes in the plate bearing stiffness of the flexible pavements. The values were normalized by the fall value to determine the seasonal trend in the pavement stiffness with a minimum value occurring in the spring and recovering somewhat linearly through the summer and fall.

Mechanistic-Empirical Flexible Pavement Design

The M-E approach is based on the application of mechanics to determine the reaction of pavement structures to traffic loading [42]. The stresses, strains and displacements are calculated using analytical or numerical mathematical models. The empirical portion of the design process relates these reactions to the performance of the pavement structure. For instance, if strain is related to pavement life, then an empirical relationship could be established between the calculated strain of the pavement and its expected performance. The advantages of M-E design are [1]:

- the accommodation of changing load types,
- a better utilization of available materials,
- the ability to accommodate new materials,
- an improvement in the reliability of performance predictions,
- a better definition of the role of construction,
- material mechanical properties which better predict actual pavement behavior and performance,
- an improved definition of existing pavement layer properties, and
- the accommodation of environmental and aging effects on materials.

The design method for a M-E approach is an iterative process that can include the steps shown in Figure 2.15 [42]. For a given geographic area it is important to establish the length of its seasons. For example, an area could have the seasonal breakdown shown in Table 2.5.

Table 2.5. Seasonal lengths and their relative modulus of elasticity for pavement design.

Season (Length)	Relative Modulus of Elasticity		
	HMA	Base	Subgrade
Winter (3 months)	High	High	High
Spring (2 months)	Intermediate	Low	Low
Summer (4 months)	Low	Intermediate	Intermediate
Fall (3 months)	Intermediate	Intermediate	Intermediate

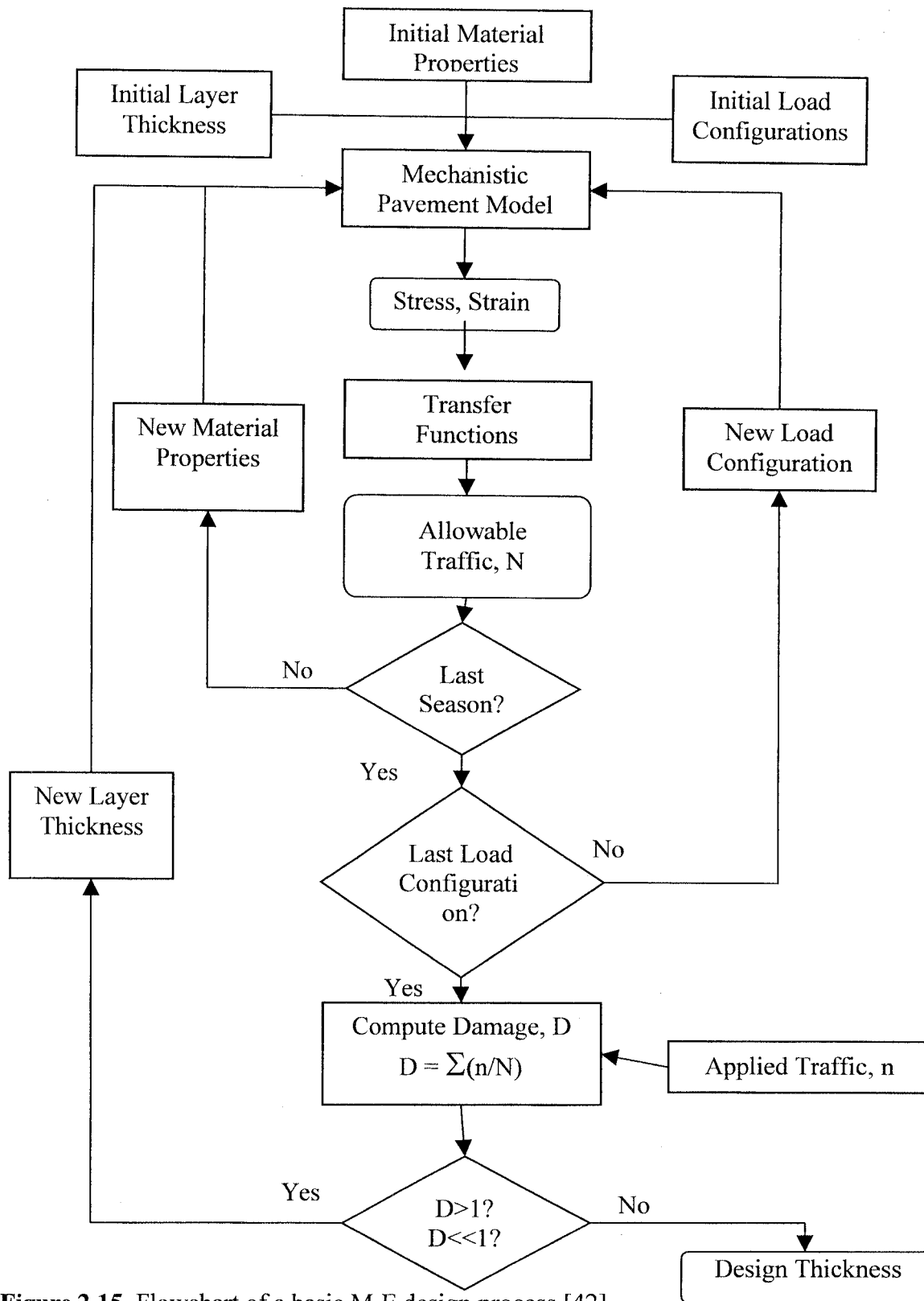


Figure 2.15. Flowchart of a basic M-E design process [42].

Washington State Department of Transportation

The Washington State Department of Transportation developed a procedure called EVERPAVE [12]. It is a M-E design procedure for use in overlay design based on backcalculated material properties, fatigue and rutting. The process is shown in Figure 2.16. The HMA modulus is adjusted for temperature according to data for typical Washington mixtures [12]. An iterative process is then used to calculate the overlay thickness for each deflection test point.

In their study, the environmental effects of temperature and precipitation were incorporated into the design method. Seasonal adjustments for asphalt-bound materials were developed from the relationship between the modulus and temperature. However, the process for unbound materials was complex because of the interaction between unbound materials and the environment.

The soil moisture content and the state of moisture are the primary reasons for seasonal variations of soil moduli. Soil moisture depends on precipitation, temperature, soil gradation and permeability, surface distress level and drainage conditions [43]. The data on the seasonal variations were based on the backcalculated moduli from three years of FWD data and climatic data. The ratio of the moduli of different seasons were determined and are presented in Table 2.6 [4].

Table 2.6. Seasonal variations of unbound material moduli ratios for Washington state [4].

Region	Base		Subgrade	
	Wet/Thaw	Dry/Other	Wet/Thaw	Dry/Other
Eastern Washington	0.65	1.00	0.95	1.00
Western Washington	0.80	1.00	0.90	1.00

Washington State used an equivalent stiffness concept of pavement modeling for overlay design. Although the subgrade may have consisted of various layers, it was assumed to be homogeneous and semi-infinite in depth for the pavement modeling. The backcalculated subgrade modulus was the equivalent modulus of the whole layer depth [4].

Care should be taken in applying seasonal variation adjustments because the climate conditions tend to vary with location and time [4]. Also the surface condition of the pavement should be taken into account.

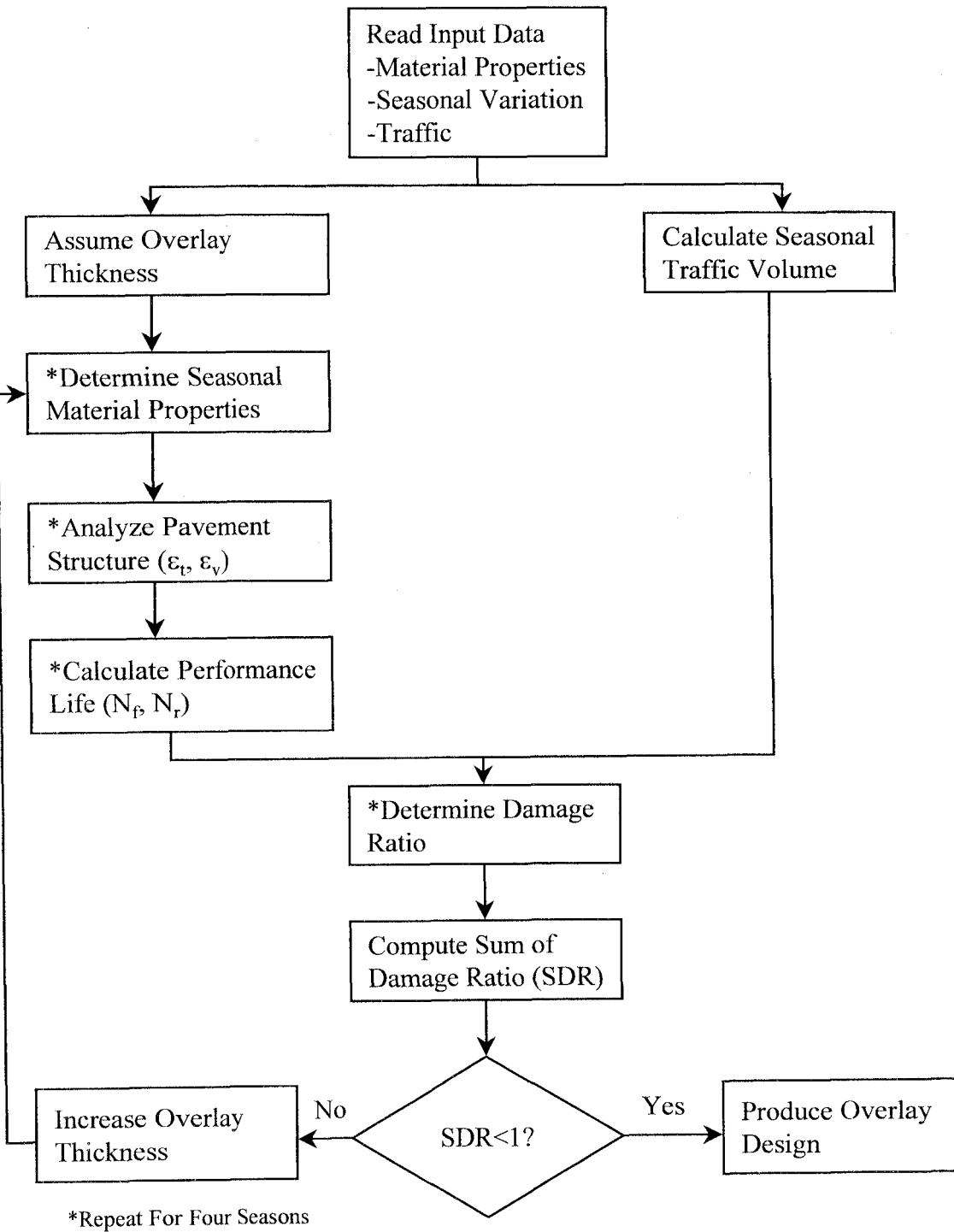


Figure 2.16. WSDOT overlay design flow chart [12].

Ontario

Hein and Jung [44] researched the seasonal variations in pavement strength for the province of Ontario, which is subjected to severe frost and spring thaw periods. They found that a reduction in subgrade strength is expected in the spring and that the magnitude of pavement damage varies with the amount of thawing, type of subgrade and loads applied.

Hein and Jung calculated pavement layer response indicators such as normalized dynamic deflection, subgrade modulus, subgrade deflection, and vertical compressive strain. A "spring factor" was used to account for the decrease in the stiffness of the subgrade during the spring thaw and was based on spring, summer and fall deflection tests. The decrease in moduli between the fall and the early spring testing varied from 20 to 80 percent for the clay and silty clay subgrades.

Shell Method, Netherlands

The Shell method of design is based on results of FWD testing [45]. Deflection measurements are used with past traffic and environmental conditions to estimate the remaining life as shown in Figure 2.17. Failure criteria are based on fatigue. The interpretation of the FWD results is not done by backcalculation, but instead by the following:

- maximum deflection,
- a deflection ratio between the deflection at 600 mm from the load to the maximum,
- assumed Poisson's ratios,
- thickness of the aggregate base,
- assumed ratio of base to subgrade modulus, and
- the HMA stiffness.

The Poisson's ratio is assumed because it has a small range of values and is difficult to measure accurately [45].

This method considers the influence of ambient temperatures. The procedure relates the mean annual or monthly air temperature to an effective asphalt temperature depending on the thickness of the HMA.

Edwards and Valkering's [46] procedure allows for differences in the temperature that occur in different climates. From relationships between mean monthly air temperature and HMA temperature at various depths, HMA moduli are determined and maximum subgrade and HMA strains are calculated for each of the temperature gradients. An effective strain (ϵ_{eff}) is calculated for n different temperature gradients from the following equation:

$$\left(\epsilon_{\text{eff}}\right)^4 = \frac{1}{n} \sum_{i=1}^n \left(\epsilon_i\right)^4 \quad (2.7)$$

In this procedure, the effect of temperature on the permissible strain values and on the relative damage was ignored [45]. Another procedure was used to introduce the effect of temperature on the thickness design based on the HMA strain criterion. Using the BISAR program, the HMA strains at the bottom, at one-third and at two-thirds of the HMA layer thickness were calculated for these gradients. For each gradient and depth, the design life (N_i) associated with the prevailing strain and modulus was determined using the fatigue data of the relevant mix. Then the effective design life for a series of n gradients was calculated for each structure and depth.

$$N_{\text{eff}} = \frac{1}{\frac{1}{n} \sum_{i=1}^n (1/N_i)} \quad (2.8)$$

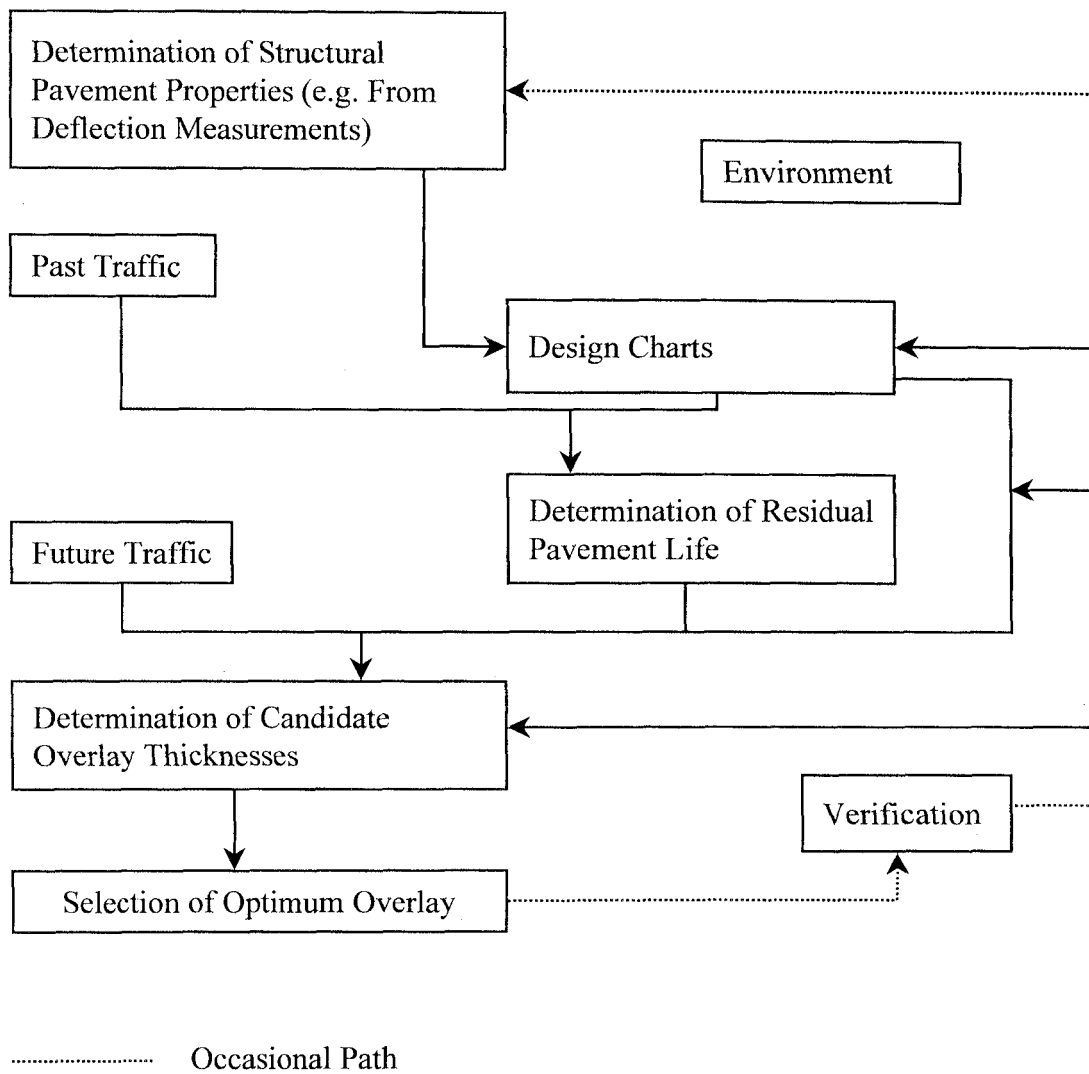


Figure 2.17. Flowchart of Shell overlay design method [47].

Idaho

Bayomy et al. [7] developed a mechanistic-based flexible overlay design system for the state of Idaho. The materials considered were subgrade soils, stabilized and unstabilized bases and subbases and HMA. The pavement was regarded as a multi-layered elastic system. Poisson's ratio was assumed and layer moduli were determined from nondestructive testing using a FWD.

For the study, Idaho was segmented into six pavement climate zones based on the geographic area. The six zones and their characteristics were used to determine the expected moisture changes for the various soil groups at each location, and to define the duration and onset of the seasons and their corresponding subgrade conditions and resilient moduli.

In the areas that experience significant subgrade frost penetration, the average year was divided into four periods: summer, freezing transition, winter (frozen) and spring-thaw recovery. Then seasonal adjustment factors were created for the subgrade soils to adjust the resilient modulus during these periods [7]. These factors are R_f , R_t , and R_w for the frozen period, thaw period, and wet periods, respectively, and were dependent on the zone's location in Idaho. Typical adjustment factors are given in Table 2.7. They were inserted into the following equation to obtain the appropriate resilient modulus (M_f , M_t , and M_w).

$$M_i = M_{\text{Summer}} \times R_i \quad (2.17)$$

The resilient modulus of the base and subbase are treated similarly. Based on Hardcastle's study [48], it was assumed that the effect of freezing was negligible for the base and subbase, thus the resilient modulus of a winter aggregate layer was the same as its summer resilient modulus. The freeze-thaw period resilient modulus was reduced for aggregate materials to various degrees. HMA materials and cement treated materials were adjusted as well.

Zones 3 and 6 experience not significant frost penetration so the average year was divided into three periods: summer (normal) period, winter-spring (wet) period, and wet recovery period. The seasonal variation factor was required to account for the temporary increase in the subgrade water content during the wet period.

Table 2.7. Seasonal variation factors used in Idaho M-E design procedure [7].

Climate Zone	Material	Seasonal Variation Factor (R)			
		Frozen	Thaw	Summer	Fall
Zone 1	Base/Subbase	1.00	0.65	1	1
	Subgrade	11.20	0.43	1	1
Zone 2	Base/Subbase	1.00	0.65	1	1
	Subgrade	11.20	0.43	1	1
Zone 3	Base/Subbase	0.65	0.85	1	1
	Subgrade	0.35-0.81	0.68-0.90	1	1
Zone 4	Base/Subbase	1.00	0.65	1	1
	Subgrade	11.20	0.43	1	1
Zone 5	Base/Subbase	1.00	0.65	1	1
	Subgrade	11.20	0.43	1	1
Zone 6	Base/Subbase	0.65	0.85	1	1
	Subgrade	0.27-0.73	0.63-0.87	1	1

Texas

The Texas Transportation Institute with the Texas Highway Department instituted a cooperative research program called “Seasonal Variations of Pavement Deflections in Texas” [5]. Deflections produced by a Dynaflect as were used as an index of pavement strength and measurements were made over one year’s time. The geographical areas for test sections were based on temperature and precipitation.

It was concluded that seasonal variations in the deflections of Texas pavements do exist, and that they tend to vary sinusoidally, with a period of one year [5]. They used an empirical model to relate these changes to pavement performance and concluded that seasonal changes in

deflection were usually less important than spatial changes in the pavement-subgrade system, which occur in distances that were relatively short (less than one mile).

Asphalt Institute

The Asphalt Institute developed a mechanistic based design method for streets and highways [49]. For this process, charts are used to calculate a design thickness. The input are the expected number of ESALs and the design resilient modulus of the subgrade. Resilient modulus tests are performed on subgrade samples and a cumulative distribution function is created. The traffic loads, in ESALs, are used to determine the design subgrade percentile according to Table 2.8. A conservative design value for the resilient modulus of the subgrade is chosen by selecting a modulus value that falls below a certain percentile of test results for the section of the road under consideration [49]. The layer thickness is determined by charts that give layer thickness as a function of the subgrade resilient modulus and expected traffic. Three sets of mean annual air temperatures and their environmental conditions were used in this manual.

Table 2.8. Traffic ESALs and the corresponding subgrade percentile used by the Asphalt Institute [49].

Traffic, ESAL	Design Subgrade Percentile
$\leq 10^4$	60
10^4 to 10^6	75
$\geq 10^6$	87.5

From the preceding discussion of pavement design approaches, it was concluded that seasonal changes in pavement material mechanical properties do occur and there was a need for characterizing seasonal effects on pavement materials for use in a M-E pavement design procedure specific to Minnesota.

CHAPTER THREE

METHODOLOGY

Introduction

This chapter presents the methodology used to quantify seasonal variations in backcalculated layer moduli. It begins with an overview that discusses typical seasonal variations in pavement layer moduli, the process used in this report to quantify these variations, and a description of the types of pavement materials characterized in this study. Next, the process of relating climate factors at a given location to subsurface environmental conditions of a pavement structure is discussed. Then the process of relating the subsurface environmental conditions of a pavement structure to the mechanical properties of the pavement layers is discussed. Finally, these relationships are incorporated together for use in a M-E pavement design procedure.

Overview

Typical Seasonal Variations in Pavement Layer Modulus

In most of the United States, seasonal changes in temperature and precipitation greatly affect the stiffness of a pavement structure. Changes in temperature will affect the viscosity of the asphalt cement (AC) in HMA and cause the layer modulus to increase or decrease accordingly (Table 3.1). Changes in precipitation and temperature also affect the amount of moisture and the state of moisture in the aggregate base and soil subgrade layers, which cause the layer moduli to change on a seasonal basis (Table 3.1).

Table 3.1. Typical relative pavement layer moduli values per season.

Season	Relative Modulus of Elasticity		
	HMA	Aggregate Base	Soil Subgrade
Winter	High	High	High
Spring	Intermediate	Low	Low
Summer	Low	Intermediate	Low
Fall	Intermediate	Intermediate	Intermediate

While all pavement layer moduli reach a maximum value simultaneously during the winter, research has shown that the layers reach minimum values during different periods in a typical year [2, 3, 4, 5, 6, 7]. The stiffness of the HMA layer is at a minimum in the summer when higher temperature cause the AC viscosity to decrease. For an aggregate base layer, the modulus is at a minimum in the early spring due to thawing. Since thawing begins at the surface of a pavement structure, the base layer will thaw prior to the subgrade layer and moisture will be trapped between the HMA layer and the frozen subgrade layers below. The base layer modulus is at a minimum until the moisture is drained. As the subgrade layer thaws it experiences a similar decrease in moduli. However, since the fine-grained subgrade material typically has a lower permeability than the aggregate base material, it will drain slower and recover more slowly than the aggregate base. Also, the increase of precipitation events in the spring and summer can cause moisture to accumulate in the subgrade layer, and the modulus of the layer may not recover until late summer or early fall.

It is important to characterize the duration and magnitude of these changes in pavement layer moduli for design in a given region. This study was conducted to characterize these changes for Minnesota and to suggest a method useful to other areas.

Process Used to Quantify Seasonal Effects on Pavement Layer Moduli

The process used to conduct this study is shown in Figure 3.1. Essentially, the effects of temperature and precipitation fluctuations on the pavement layer temperature, moisture content and state of moisture were quantified and used to predict the seasonal changes in the pavement layer moduli. These predicted moduli were then compared to moduli backcalculated from deflections measured between 1994 and 1996.

The first step in the procedure (Figure 3.1) was to create a site-specific climate atlas (Appendix B) for each location to determine average climate factors, which included daily air temperature and precipitation levels. Next, environmental condition data were obtained from the sensors mentioned above and analyzed for trends. A sinusoidal air temperature algorithm, surface temperature algorithm and temperature profiles were used to relate daily air temperature to in situ temperature. The FI was used to relate daily air temperature to the state of moisture in the aggregate base and soil subgrade layers. Precipitation events were used to explain trends in the moisture content cycles of these unbound layers on a seasonal basis.

The second step in the process was to relate the seasonal subsurface environmental conditions to seasonal moduli. An exponential equation was developed from laboratory tests of HMA samples taken from Mn/ROAD to predict the HMA modulus at various temperatures. This equation was used with a field temperature algorithm to predict seasonal HMA layer moduli (E_{HMA}) and was compared to backcalculated moduli. Seasonal values for aggregate base (E_{AB}) and soil subgrade (E_{SG}) moduli were determined as a function of the material type, moisture content and state of moisture per season.

The final step in this process is to evaluate the trends in the pavement layer moduli and incorporate the trends into a M-E design process. To accomplish this step, a typical year is

separated into seasons in which at least one pavement layer moduli varies substantially. Next, the moduli are evaluated in terms of percent difference from the normal or design layer moduli of the material.

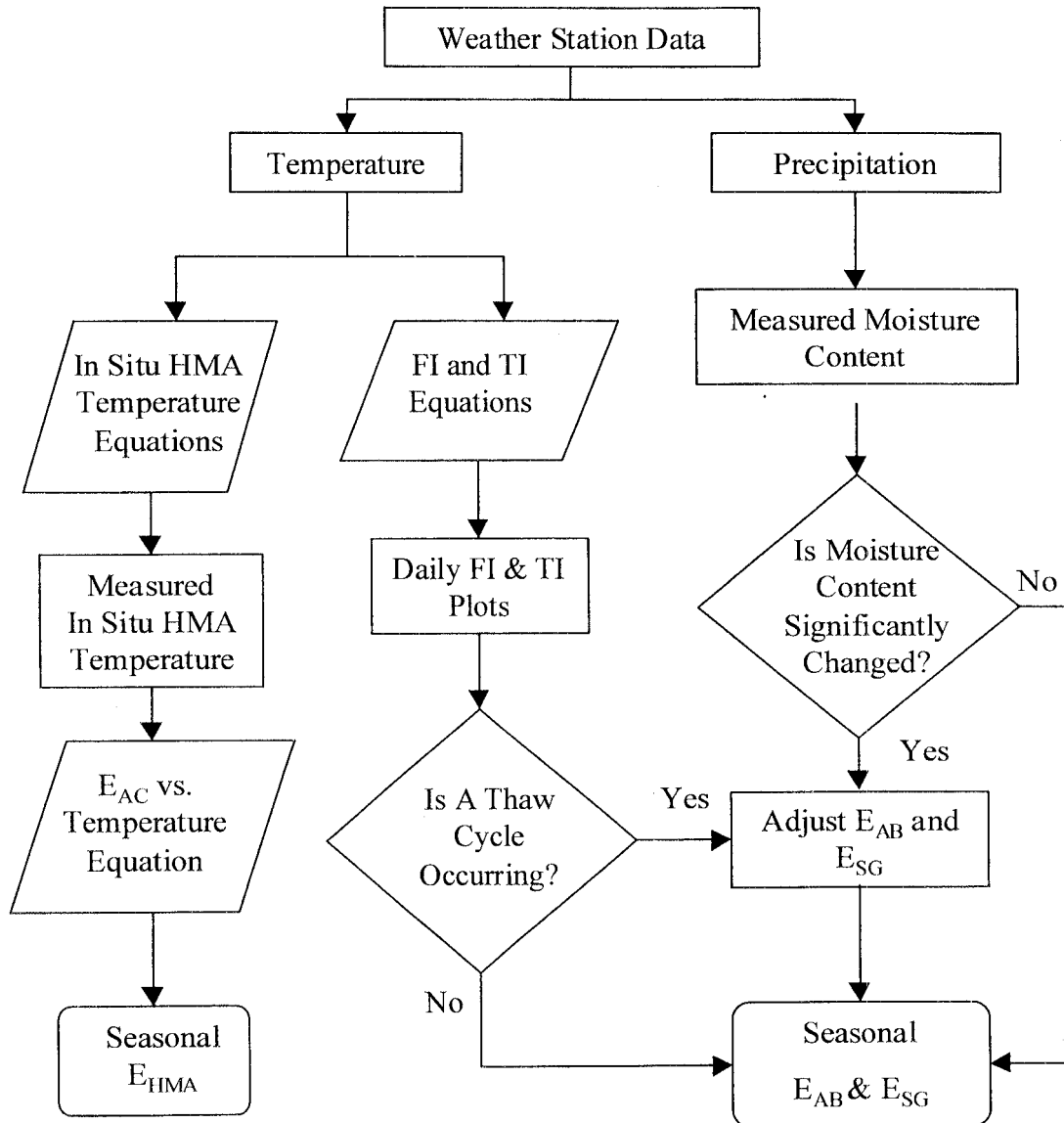


Figure 3.1. Process used to quantify the relationships between climate factors and pavement material properties for M-E design.

Materials Description

The data used in this study were obtained from Mn/ROAD and three LTPP SMP sites. On-line weather station databases supplied daily temperature and precipitation data. Field environmental conditions including temperature, moisture content and state of moisture were measured by environmental sensors, which included thermocouples and thermistors, time domain reflectometers, Watermarks and resistivity probes. Finally, laboratory and deflection test data were used to determine the pavement layer moduli. There were not enough test sections to statistically evaluate variable compositions of pavement structures by replication, however some of the data accumulated can be analyzed statistically. For example, there is enough backcalculated resilient modulus data on a seasonal basis and environmental sensor data to analyze the trends statistically.

Mn/ROAD Test Sections

The structure of the Mn/ROAD test sections used in this study are shown in Table 3.2. The AC used in the HMA layers of the Mn/ROAD test sections investigated was either 120/150 penetration grade or AC 20 viscosity grade, where the AC 20 binder has a higher viscosity than the 120/150 pen. grade. The test sections have, by design, a range of 5.4 to 6.4% asphalt content determined using Marshall mix design.

The base and subbase aggregate material used in Mn/ROAD are Class 3 Special, Class 4 Special, Class 5 Special and Class 6 Special, abbreviated as Cl. 3 Sp., Cl. 4 Sp., Cl. 5 Sp. and Cl. 6 Sp., respectively. Table 3.3 provides the gradation and plasticity specifications for the aggregates and the actual gradations are shown in Table 3.4. The term “special” indicates that the gradation limits were stricter than existing Mn/DOT specifications to increase the material

uniformity at the Mn/ROAD site; and extended the range of gradation to accentuate differences in the performance of the materials. Note that the actual gradation data for the Cl. 6 Sp. base material has 5 to 13 percent passing the 0.075 mm (No. 200) sieve with a mean value of 9 percent, which is outside of the specified range.

Cl. 3 Sp. and Cl. 4 Sp. are used primarily as subbase layers for the flexible pavement test sections. Both materials met the May 1988 Mn/DOT Specifications for Select Granular Barrow (No. 3149.2B). Cl. 5 Sp. and Cl. 6 Sp. are primarily used as higher quality base course materials for flexible pavement. The Cl. 6 Sp. aggregate base material consists of 100 percent crushed quarry material, while the other aggregate base materials are derived from glacial gravel pits.

The stress dependency determined from laboratory tests for the Cl. 5 Sp. and Cl. 6 Sp. aggregates is shown in Figure 3.2 [50]. It is shown that the modulus increased with an increase in the bulk stress for both of the materials.

The engineered subgrade material in the Mn/ROAD test sections consists of one of two general soil types. The first soil is primarily a loam with an AASHTO classification of A-6 [51] that was subcut and backfilled to a depth of 1.8 m (6 ft.) and has a design R-value of 12 (1655 kPa). For test section 24 and 25, a subcut was made to 2.1 m (7 ft.) and backfilled with a clean sand with a design R-value of 70 (1655 kPa) to evaluate the effect of a more granular subgrade material on the pavement structure.

A saturated soil layer exists at Mn/ROAD that has an effect on the backcalculated layer moduli. Newcomb et al. [52] found that the depth to the watertable is variable depending on the time of year and location along the Mn/ROAD project.

Table 3.2. Flexible pavement test cells at Mn/ROAD included in study.

Test Section	Surface Thickness, mm	AC Type	Asphalt Content %	Base Thickness, mm	Base Material	Design Subgrade Soil R - value (1655 kPa)
1	145	120/150 pen	5.8	840	Cl. 4 Sp.	12
2	145	120/150 pen	6.4	100	Cl. 6 Sp.	12
				710	Cl. 4 Sp.	
3	145	120/150 pen	6.1	100	Cl. 5 Sp.	12
				840	Cl. 3 Sp.	
4	225	120/150 pen	5.6	-	None	12
14	275	120/150 pen	5.8	-	None	12
15	275	AC 20	5.8	-	None	12
16	200	AC 20	5.6	710	Cl. 3 Sp.	12
17	200	AC 20	5.8	710	Cl. 3 Sp.	12
19	200	AC 20	6.4	710	Cl. 3 Sp.	12
20	200	120/150 pen	6.4	710	Cl. 3 Sp.	12
21	200	120/150 pen	6.1	585	Cl. 5 Sp.	12
22	200	120/150 pen	5.8	460	Cl. 6 Sp.	12
24	75	120/150 pen	6.4	100	Cl. 6 Sp.	70
25	125	120/150 pen	6.1	-	None	70
26	150	120/150 pen	6.1	-	None	12
27	75	120/150 pen	6.4	280	Cl. 6 Sp.	12
28	75	120/150 pen	6.1	330	Cl. 5 Sp.	12
30	125	120/150 pen	5.8	305	Cl. 3 Sp.	12
31	75	120/150 pen	5.8	100	Cl. 5 Sp.	12
				305	Cl. 3 Sp.	

Table 3.3. Gradation and plasticity specifications for the aggregates at Mn/ROAD [50].

Sieve Size, mm (in.)	Pavement Base/Subbase Material			
	Cl. 3 Sp.	Cl. 4 Sp.	Cl. 5 Sp.	Cl. 6 Sp.
	Percent Passing			
37.5 (1.5)	-	100	-	-
25.4 (1)	-	95/100	100	100
19 (0.75)	-	90/100	90/100	85/100
12.5 (0.5)	100	-	-	-
9.5 (0.375)	95/100	80/95	70/85	50/70
4.75 (No. 4)	85/100	70/85	55/70	30/50
2.00 (No. 10)	65/90	55/70	35/55	15/30
0.425 (No. 40)	30/50	15/30	15/30	5/15
0.075 (No. 200)	8/15	5/10	3/8	0/5
Plasticity Requirements				
LL	35 max.	35 max.	25 max.	25 max.
PI	PI<12	PI<12	PI<6	PI<6

Table 3.4. Actual percent passing for Mn/ROAD flexible pavement test sections and the specified range (Spec.).

Sieve Size, mm (in.)	Mn/ROAD Cl. 3 Sp. (6 test sections)			Mn/ROAD Cl. 4 Sp. (1 test section)		
	Mean	Actual Range	Spec.	Mean	Actual Range	Spec.
37.5 (1.5)	100	100/100		100	100/100	
25.4 (1)	100	100/100		100	100/100	
19 (0.75)	99	96/100		98	94/100	
9.5 (0.375)	92	80/100	95/100	84	60/99	80/95
4.75 (No. 4)	82	66/94	85/100	68	37/91	70/85
2.00 (No. 10)	69	52/85	65/90	55	23/80	55/70
0.425 (No. 40)	31	20/44	30/50	25	11/42	15/30
0.075 (No. 200)	9	6/12	8/15	8	5/11	5/10
Sieve Size, mm (in.)	Mn/ROAD Cl. 5 Sp. (3 test sections)			Mn/ROAD Cl. 6 Sp. (2 test sections)		
	Mean	Actual Range	Spec.	Mean	Actual Range	Spec.
37.5 (1.5)	100	100/100		100	100/100	
25.4 (1)	100	100/100		100	100/100	
19 (0.75)	98	91/100		99	95/100	
9.5 (0.375)	88	69/99	70/85	89	60/99	50/70
4.75 (No. 4)	75	42/92	55/70	77	37/92	30/50
2.00 (No. 10)	61	25/82	35/55	63	23/82	15/30
0.425 (No. 40)	27	11/42	15/30	29	11/42	5/15
0.075 (No. 200)	8	5/13	3/8	9	5/13	3/8

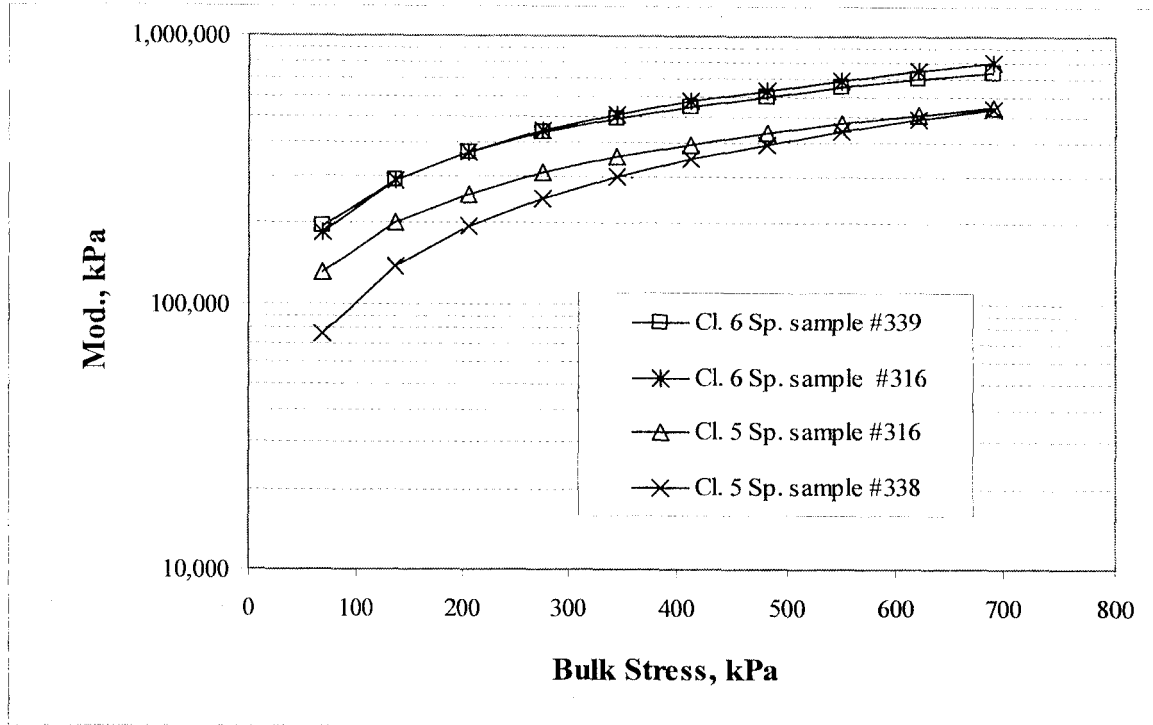


Figure 3.2. Modulus vs. bulk stress for Cl. 5 Sp. and Cl. 6 Sp. samples from Mn/ROAD [50].

Long Term Pavement Performance (LTPP) Seasonal Monitoring Program (SMP) Sites

Three LTPP SMP flexible pavement sites located in Minnesota were investigated in this study. Descriptions of the sites are given in Tables 3.5, 3.6 and 3.7. The site located in Little Falls, MN on U.S. Hwy 10 was evaluated in this study prior to the overlay that occurred in the summer of 1995.

Table 3.5. LTPP SMP sites used in study.

Site #	Location	Hwy	Layer Thickness, mm		% Pass. 75 μ m Sieve in Base Material	Subgrade Type
			HMA	Base		
27-1018	Little Falls, MN	U.S. 10	115	130	6.5 to 8	Coarse Sand*
27-1028	Detroit Lakes, MN	U.S. 10	245	No Base Layer	No Base Layer	Coarse Sand*
27-6251	Bemidji, MN	U.S. 2	190	260	8.5 to 10	Coarse Sand*

* Poorly graded sand with silt

Table 3.6. Characteristics of AC in HMA layers of the LTPP SMP sites.

Site #	Average % AC	AC Penetration	Voids, %
27-1018	5.3	135	10.8
27-1028	6.4	90 – 135	10.3
27-6251	5.5	135	6.1

Table 3.7. Traffic information for LTPP SMP sites (1991).

Site #	AADT/Lane	% Trucks	ESAL/YR
27-1018	2700	13.1	92,000
27-1028	2100	12.3	76,000
27-6251	1950	15.9	79,000

Relating Climate Factors to Subsurface Environmental Conditions

Geographic Climate Data

The first step taken to characterize the climate factors that affect pavement subsurface environmental conditions was to build a climate atlas based on weather data spanning the last 30 years. The general site description included latitude, elevation, general topography of the site and the location of nearby weather stations. Sources of weather data included the on-line Midwestern Climate Information System [53], and the U.S. Weather Bureau reports from the Department of Commerce. Weather data obtained from these sources included mean, high and low

temperatures, precipitation, and snowfall, and were evaluated for trends in the temperature and precipitation data.

Daily Air Temperature and In Situ Temperature Relationships

Existing algorithms that describe the relationships between daily air temperature and in situ temperature of the HMA layer were used for the purpose of predicting HMA modulus as a function of temperature. Equation 3.1 [54] is used in this study to predict temperatures with depth in the HMA layer and is applicable to other types of pavement materials such as unbound granular and fine-grained material.

$$T(x,t) = T_{\text{mean}} + Ae^{-x\sqrt{\frac{2\pi}{P\alpha}}} \sin\left(\frac{2\pi}{P}(t) - x\sqrt{\frac{2\pi}{P\alpha}}\right) \quad (3.1)$$

where

$T(x,t)$ = soil temperature as a function of depth and time, °C,

x = depth, m,

t = Time measured from when the surface temperature passes through T_{mean} , (days),

T_{mean} = average temperature at surface, °C,

A = Maximum temperature amplitude, $(T_{\text{max}} - T_{\text{mean}})$, °C,

$\omega = 2\pi/P = 2\pi/365$,

α = thermal diffusivity, m^2/day , and

P = Period or recurrence cycle, days.

The thermal diffusivity is a measure of the rate at which a material will undergo a change in temperature in response to external temperature changes. The thermal diffusivity of dense

graded HMA was 0.121 m²/day and was obtained from measurements by Chadbourn et al. [55].

Typical values for various materials are given in Table 3.8 [54].

Table 3.8. Thermal diffusivity of various materials [54].

Material	Thermal Diffusivity, m ² /day
Water	0.0125
Ice	0.0285
Fresh Snow	0.1030
Granite	0.1290
Limestone	0.0602
Copper Metal	9.8100

To use Equation 3.1, it is necessary to estimate the mean annual surface temperature (T_{mean}), which is typically warmer at the surface for the HMA layer due to solar radiation gain. Thermocouple values were plotted and extrapolated to find the mean annual surface temperature for the Mn/ROAD test sections. In this study, Equation 3.2 [56] was modified and used to determine the average surface temperature variable (T_{mean}) for Equation 3.1. There are other surface temperature predictors [57] that were evaluated for this report, however, modifying SHRP's equation was a useful tool:

$$T_{\text{surf}} = 0.859 \bullet T_{\text{min air}} + 1.7 \quad (3.2)$$

where $T_{\text{min air}}$ = 1-day minimum air temperature, °C.

The modified surface temperature equation is:

$$T_{\text{mean}} = 0.859 \bullet T_{\text{air}} + 7.7 \quad (3.3)$$

where T_{air} = Mean daily air temperature, °C.

Temperature and State of Moisture

Freezing and Thawing Index

The depths of frost and thaw depend in part on the magnitude and duration of the temperature differential below or above freezing at the ground surface [14]. The freezing index (FI) and thawing index (TI) can be used to quantify the intensity of a freezing or thawing season. The FI [10] is defined as the positive cumulative deviation between a reference freezing temperature and the mean daily air temperature for successive days. The TI [10] is the positive cumulative deviation between the mean daily air temperature and a reference thawing temperature for successive days. Mn/DOT computes the TI by changing the reference temperature by 0.5°C increments each week, beginning with 1.5°C on the week of February 1 to 7.5°C by the week of April 26 each year [58]. The FI and TI are calculated as follows:

$$FI = \Sigma(0^{\circ}\text{C} - T_{\text{mean}}) \quad (3.4)$$

Where T_{mean} = mean daily temperature, °C = $1/2(T_1 + T_2)$, and

T_1 = maximum daily air temperature, °C,

T_2 = minimum daily air temperature, °C.

$$TI = \Sigma(T_{\text{mean}} - T_{\text{ref}}) \quad (3.5)$$

Where T_{ref} = reference freezing temperature that varies with time, °C.

Freezing Profiles

Watermarks, resistivity probes, thermocouples, thermistors, and time domain reflectometers were used to monitor freezing in the pavement sections. These measurements were combined to estimate the freezing profiles of pavement sections with time. Watermark sensors were used because they give a clear indication of freezing once the range at which they

measure moisture is exceeded. The freezing profiles were used to determine that the freezing and thawing index models previously described are accurate.

Precipitation and Moisture Content Relationships

Many factors influence the moisture content of a given soil or aggregate material, and can influence the stiffness of the pavement layer. The gradation of the material can be an indicator of the ability of moisture to drain from the layer since more fine material (material passing the 0.075 mm sieve) will increase the surface area available for water to adhere to the particles. Also, the greater the voids in a material, the greater the ability of that material to drain moisture.

Daily precipitation events, in which the water drains out of an aggregate layer within a short period of time (days), are not as influential as the spring recovery from thaw for M-E design in Minnesota. Therefore, no quantitative criteria were developed to relate the in situ moisture content to seasonal precipitation. However, it is important to recognize that precipitation events can cause a temporary increase in the moisture content of the fine-grained subgrade, especially in areas of that are prone to flooding.

Relating Subsurface Environmental Conditions to Mechanical Properties

In this section, the subsurface environmental conditions are related to the pavement layer mechanical properties (Figure 3.1). An exponential equation is derived from laboratory data to relate HMA modulus and temperature with constants that differ according to the type of AC used in the matrix. The surface temperature equations discussed earlier may be used in place of temperature data to quantify temporal variations in the HMA modulus. The moduli of the aggregate base and soil subgrade will vary depending on stress state, material type, density, moisture content and state of moisture.

The predicted moduli for the pavement layers were compared to backcalculated layer moduli from Mn/ROAD and LTPP SMP data. Since the details concerning the input in the backcalculation program differ between the Mn/ROAD and the LTPP SMP data, they are discussed in detail in Chapters Four and Five, respectively.

HMA Modulus vs. Temperature

To develop an algorithm that relates HMA resilient modulus to temperature, the results of diametral resilient modulus tests performed on Mn/ROAD samples were used [59]. The results of the tests from behind-the-paver samples with either 120/150 penetration grade or AC 20 viscosity grade asphalt cements were used to fit an exponential equation to the data:

$$E_{\text{HMA}} = a * e^{\left[\frac{(T-b)^2}{c} \right]} \quad (3.6)$$

where

E_{HMA} = modulus as a function of temperature, MPa,

T = temperature, °C, and

a , b & c = constants depending on asphalt cement.

The constants a , b and c vary according to the AC used in the HMA matrix. The coefficients were developed from AC 20 and 120/150 penetration binders and are shown in Chapter Four. This algorithm was used with field temperature data and Equation 3.1 to estimate the seasonal variations in E_{HMA} . These predicted moduli were then compared to backcalculated moduli.

Base and Subgrade Layer Moduli

As discussed in the literature review, the modulus of an unbound material is stress dependent. Figure 3.3 shows the general stress dependency trends for a granular material and a fine-grained material. It is shown for granular materials that a higher bulk stress, θ , will result in a higher stiffness. For fine-grained materials, a high deviator stress, σ_d , will result in a lower stiffness.

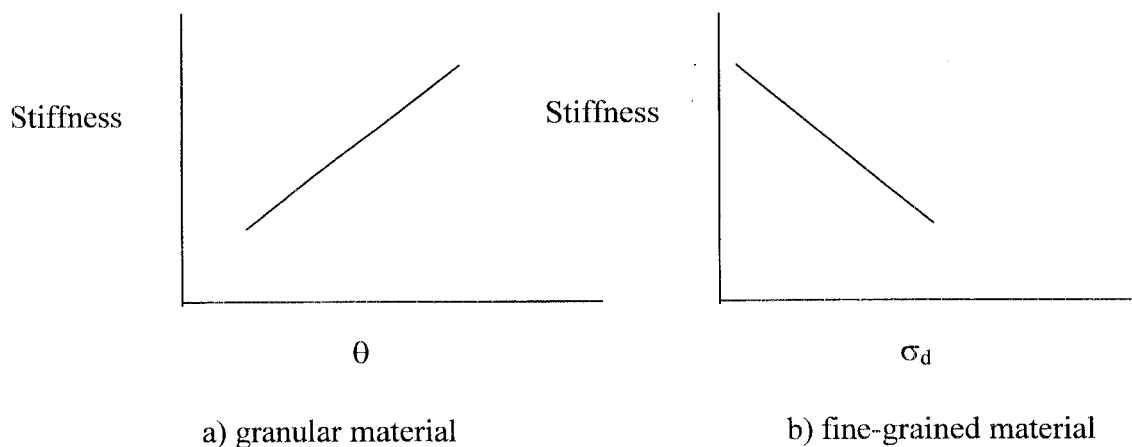


Figure 3.3. Simplified stress dependency relationships.

The magnitudes of bulk and deviator stresses depend on the whole pavement structure because they are due to layer thicknesses and load transfer. For example, consider two pavement

systems. System A has a thin HMA layer over a thin aggregate base layer, and system B has a thick HMA layer over a thick aggregate base layer. Both systems have identical HMA, aggregate base and subgrade materials. A pavement with a thin HMA layer will transfer more load to the base and subgrade layers than a pavement with a thicker HMA layer, therefore, the stresses in the base and subgrade layers will be higher and result in a stress-stiffening of the aggregate base and a stress-softening of the subgrade.

Application to Mechanistic Pavement Design

To simulate changes in layer moduli in a M-E design procedure it is necessary to divide a year into seasons [4]. This was done by graphing typical seasonal variations in the pavement layer moduli for a year and partitioning seasons where at least one of the pavement system's layer moduli had changed substantially. It was found that the variations in the backcalculated pavement layer moduli paralleled temperature cycles in a typical year, therefore, the algorithm used to define the season duration was a function of the mean daily temperature.

Table 3.9 shows the criteria for how the duration of each season is determined. Season I (winter) is when the layers are frozen and moduli are typically high. It begins when the FI exceeded 90°C-days and ended when the TI reached spring load restriction placement levels defined for Minnesota [58], which is 15°C-days. Season II (early spring) is when the base is thawing and base modulus is at a critical low. This season begins when the TI is 15°C-days and ends when the base has thawed and drained, which is typically four weeks. Season III (late spring) is the period when the base recovers to a normal value and ends when the three-day mean daily temperature rises above approximately 17°C, since this is near the temperature where the HMA layer is softer due to higher temperatures. Season IV (summer) is when maximum daily

temperatures are high and subsequently E_{HMA} is low. It ends when the three-day mean temperature remains less than 17°C. Season V (fall) is when the HMA layer regains stiffness prior to Season I. Season V is considered, for the purposes of this study, the standard value season for the layer moduli. This seasonal distribution of months was used to adjust the pavement layer moduli on a seasonal basis for the purpose of pavement design. The results of this approach are discussed in the next chapter.

Table 3.9. Seasonal distribution of a typical year for design purposes.

	Season I	Season II	Season III	Season IV	Season V
Description	Winter: <i>Layers are Frozen</i>	Early Spring: <i>Base Thaws/ SG is Frozen</i>	Late Spring: <i>Base Recovers/ SG Thaws</i>	Summer: <i>HMA Low/ SG Recovers</i>	Fall: <i>Layers are Standard</i>
Estimated duration of each season					
Beginning	FI>90°C-days	TI>15°C-days	End of Season II	3-day $T_{AVG} > 17^{\circ}C$	3-day $T_{AVG} < 17^{\circ}C$
Ending	TI>15°C-days	Approx. 28 days later	3-day $T_{AVG} > 17^{\circ}C$	3-day $T_{AVG} < 17^{\circ}C$	FI>90°C-days
Pavement layer moduli relative to fall values					
E_{HMA}	High	High	Standard	Low	Standard
E_{AB}	High	Low	Low	Standard	Standard
E_{SG}	High	High	Low	Low	Standard

Summary

This chapter described the methodology used to characterize the seasonal trends in flexible pavement layer moduli. In general, the methodology was to relate simple climate data to environmental condition data, which in turn, was related to seasonal flexible pavement layer moduli trends. Chapters 4 and 5 show the results of applying the methodology to the Mn/ROAD site and to three-LTPP SMP sites, respectively.

CHAPTER FOUR

RESULTS AND DISCUSSION OF MN/ROAD DATA

Introduction

The analysis method outlined in Chapter Three was applied to data from Mn/ROAD and the results are discussed in this chapter. The relationships between climate factors, subsurface environmental conditions and material mechanical properties are presented using weather station data, environmental sensor data, and deflection data from Mn/ROAD. These results were used to assess the seasonal variations in the stiffness of the pavement layers, which depend heavily on the environmental condition within the layer.

This chapter begins by discussing the results of the relationships between climate factors and subsurface environmental conditions, which is the first step in Figure 3.1. Climate data are discussed in terms of average daily temperature, FI, TI and precipitation events. Algorithms relating the average daily temperature to the in-situ temperature are established using thermocouple measurements. The process of using FI to estimate phase changes of the moisture in the unbound pavement layers is compared to the frost depth measurements from WMs and RPs, and unfrozen volumetric moisture content measurements from TDRs. Also evaluated are variations in the moisture content levels as measured by TDRs.

Next, the results of the relationships found at Mn/ROAD between subsurface environmental conditions and pavement material mechanical properties are discussed, which is the second step in Figure 3.1. The HMA layer moduli are predicted using the exponential model defined in Chapter Three with measured air temperature and predicted HMA temperature. TC data from 1996 are used since the accuracy of the TC data prior to this date are unreliable due to

technical problems with the sensors. The predicted HMA moduli were compared to the backcalculated moduli on days that the HMA temperatures were measured. The aggregate base and subgrade moduli are shown in terms of seasonal distributions that depend on the state of moisture and moisture content in the layers.

The last section incorporates the results into a M-E design process. The seasons were estimated to begin and end where large variations in the stiffness of the layer moduli were measured. The pavement structures at Mn/ROAD were used to determine seasonal variations in the pavement layer moduli and seasonal factors were used to quantify these changes. It is shown that it is difficult to backcalculate the pavement layer moduli when the HMA layer thickness is less than the plate radius used to in the deflection testing (in this study it was 150 mm).

Trends Between Climate Factors and Subsurface Environmental Conditions

This section discusses the results of relating climate factors to subsurface environmental conditions in a pavement structure. Average daily air temperature data are used to determine in situ temperatures, primarily in the HMA layer. Next, the state of the moisture in the base and subgrade layers is estimated from the FI and TI. Finally, typical precipitation events and their effects on the moisture content of the base and subgrade layers are discussed.

Climate Data Results

The weather stations located at Mn/ROAD have been on line since 1993 and therefore were only used for the recent climate data. The four closest weather stations to Mn/ROAD, which have data for the last several decades, are in St. Cloud, Cedar, Minneapolis-St. Paul International Airport and Buffalo. The Buffalo weather station is the closest at a distance of

about 17.7 km (11 miles) southwest of Mn/ROAD, and supplied much of the data for this study. These data were taken from numerous on-line sources including the National Climatic Data Center and National Weather Service over the years of 1960 to 1995, and missing data for the years of 1964, 1967, 1972, 1987 and 1991 were not estimated.

30 – Year Temperature Data

This region experiences wide temperature fluctuations in a typical year, as is typical for a continental climate. The mean annual temperature computed from thirty years of data is $6.8^{\circ}\text{C} \pm 1.4^{\circ}\text{C}$. The mean monthly temperature varies from a low of -11.7°C in January, to a high of 22.4°C in July, as shown in Table 4.1 and Figure 4.1.

Upon examining the temperature history at Mn/ROAD, it was evident that the mean monthly temperatures over the years of 1994 to 1996 are very similar to the thirty-year mean, as shown in Figure 4.2. The mean monthly temperatures during these years are close to the 30 - year mean monthly temperatures and fall slightly under in most cases.

Table 4.1. 30-year mean monthly temperature.

Month	30-Year Mean Monthly Temperature, °C
January	-11.7 ± 3.6
February	-8.2 ± 3.4
March	-1.2 ± 3.1
April	7.5 ± 2.2
May	14.8 ± 2.1
June	19.8 ± 1.6
July	22.4 ± 1.7
August	21.0 ± 1.5
September	15.6 ± 1.6
October	9.0 ± 1.6
November	-0.4 ± 2.1
December	-8.3 ± 3.1

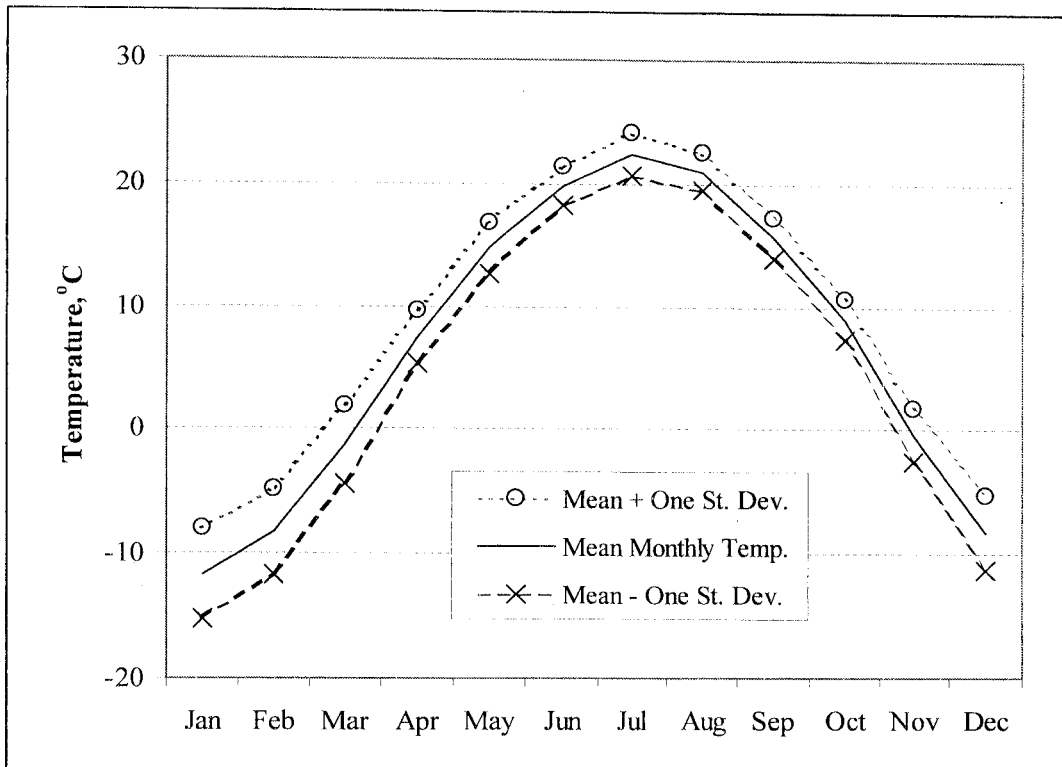


Figure 4.1. 30-year mean monthly temperature data for Buffalo (1965-1995).

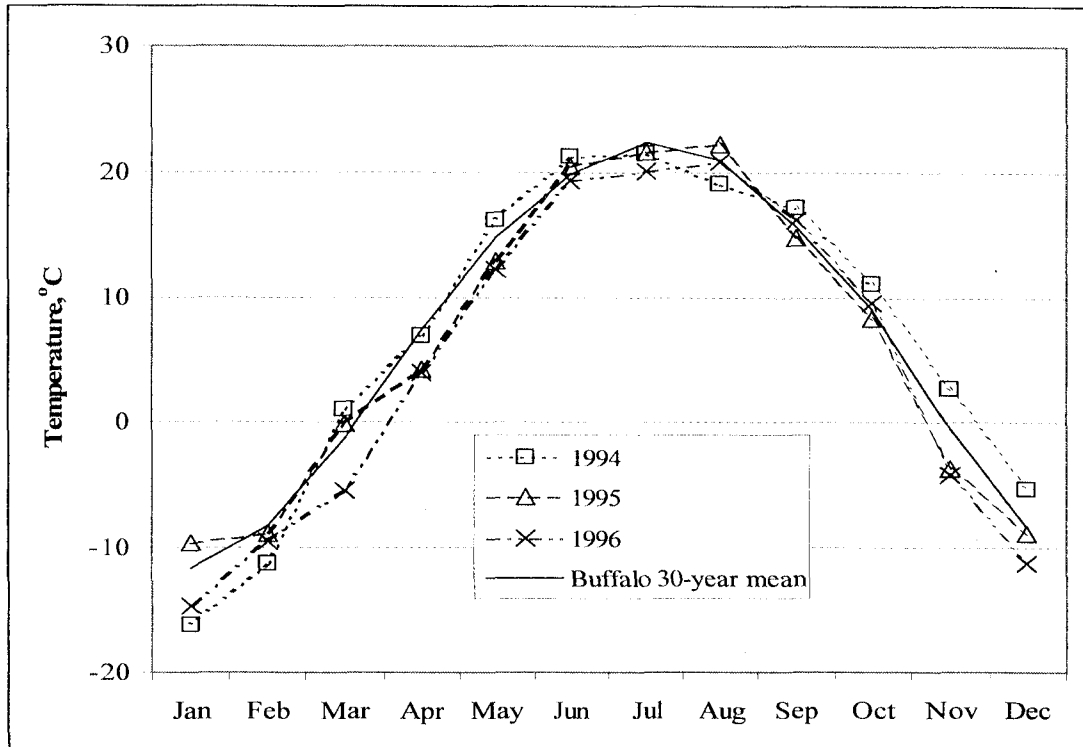


Figure 4.2. 30-year and Mn/ROAD mean monthly temperature.

30 – Year Freezing Index and Thawing Index

In this study, the start of the FI calculation is when the mean daily temperature is consistently less than 0°C, which on average, begins on November 15 for Mn/ROAD. However, it has started as early as November 1 and in some cases, as late as December 5. Similarly, the calculation of the TI begins when the mean daily temperature is greater than the thawing reference temperature. On average, thawing has begun March 20 and as early as February 27 and as late as April 9. The thirty-year distribution of the FI from the Buffalo weather station is shown in Figure 4.3 as a quartile distribution, where the FI peaks in March with a median value of 900°C-days.

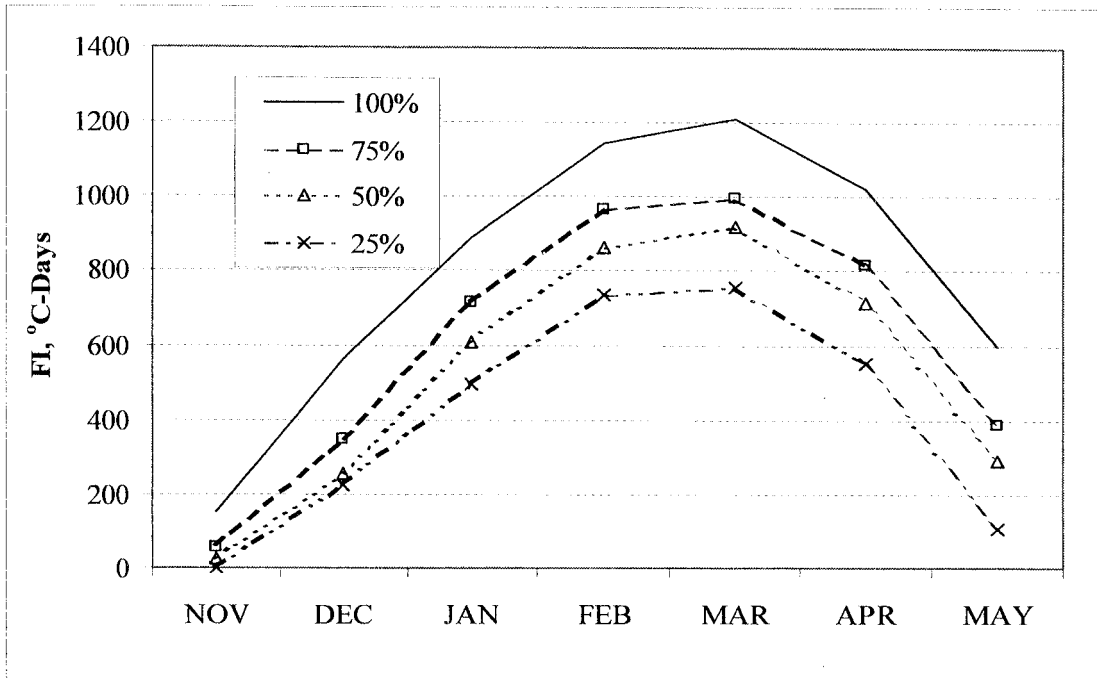


Figure 4.3. Distribution of FI over 30-years.

In this region, it is typical for the temperatures to fluctuate above and below freezing during the spring thaw period. Significant freeze-thaw cycles may occur between 1 and 10 times in a given year, based on the data between 1960 and 1995. For example, Figure 4.4 shows the daily changes in the freezing degree days during the spring of 1975.

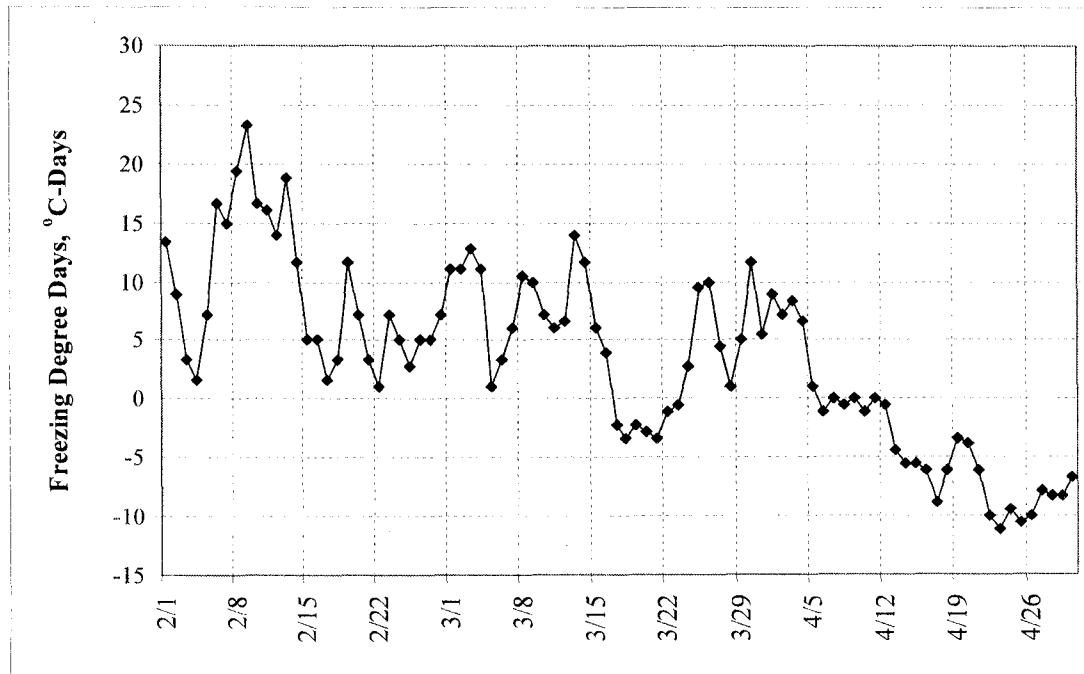


Figure 4.4. Freezing degree days beginning February 1, 1975, Buffalo.

Since Mn/ROAD was built in 1993 and through 1997, the freezing seasons determined from Buffalo weather station data have been variable compared to the 30-year average for Buffalo. Table 4.2 displays the beginning date, the date of the peak FI and the peak FI values. The 1995 – 1996 winter was the harshest thus far with a peak FI of about 1344°C-days, and the 1997 – 1998 winter was the mildest.

Table 4.2. Computed maximum FI (°C-days) at the Buffalo weather station.

Beg. FI Date	Peak FI Date	Peak FI, °C-Days
Nov. 13, 1992	Mar. 23, 1993	987
Nov. 5, 1993	Mar. 11, 1994	1167
Nov. 18, 1994	Mar. 9, 1995	901
Nov. 2, 1995	Apr. 8, 1996	1344
Nov. 9, 1996	Mar. 25, 1997	1250
Nov. 10, 1997	Mar. 20, 1998	595
Dec. 16, 1998	Mar. 14, 1999	682
30-Year Average (1960-1990)		
November 13	March 17	884

Precipitation

Between 1960 and 1995, nearly 70% of the rainfall events occurred between April and September. Figure 4.5 shows the 30-year mean monthly distribution of rainfall events. The 30-year mean annual water-equivalent precipitation for Buffalo is 740 mm with a maximum of 1000 mm and a minimum of 400 mm. The 30-year monthly distribution of snowfall is shown in Figure 4.6. Most of the snowfall occurs in the month of March (245 mm), as does the maximum monthly snowfall (1000 mm).

The precipitation events at Mn/ROAD have varied above and below the 30-year mean monthly rainfall events for the Buffalo weather station data as shown in Table 4.3 and Figure 4.7. 1993 was a high precipitation year compared to the average, especially in August.

Mn/ROAD opened to traffic in 1993, however there is little data recorded in this year due to difficulties with the weather station. It is also apparent that 1995 and 1996 were drier years.

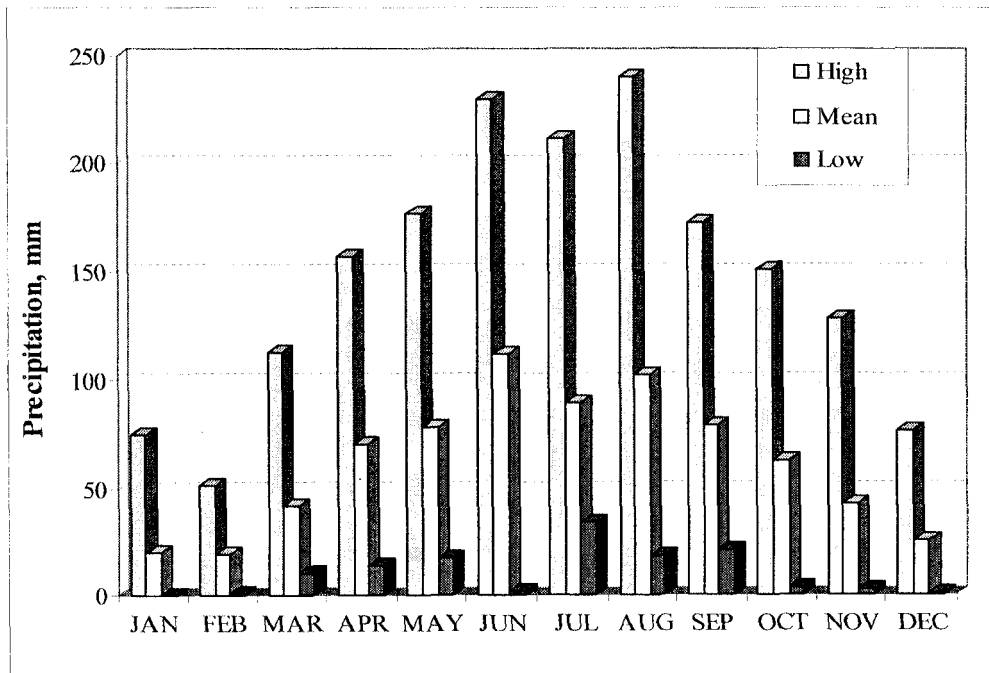


Figure 4.5. High, mean and low monthly precipitation events, 1965 - 1995, Buffalo, MN weather station.

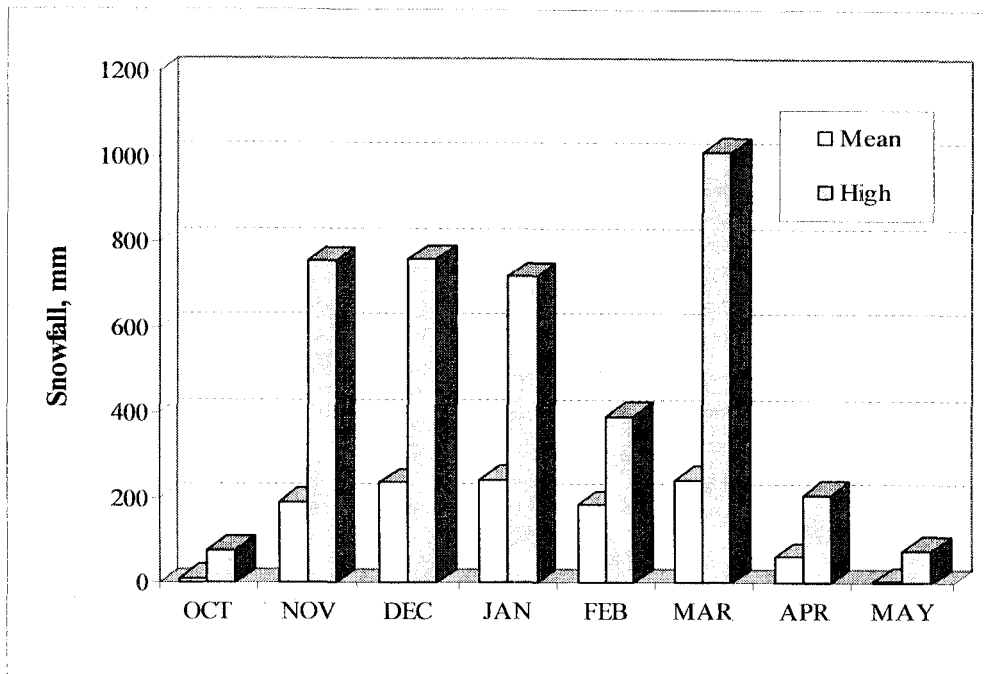


Figure 4.6. Mean and high monthly snowfall events, 1965 – 1995, Buffalo, MN weather station.

Table 4.3. 30-Year average and Mn/ROAD monthly average precipitation events, mm.

Month	1993 Avg.	Differs from Avg.	1994 Avg.	Differs from Avg.	1995 Avg.	Differs from Avg.	1996 Avg.	Differs from Avg.	30-Year Avg.
JAN	22	+2	NA	NA	9	-11	44	+24	20
FEB	7	-12	23	+4	8	-11	7	-12	19
MAR	28	-14	11	-31	54	+12	26	-16	42
APR	68	-2	139	+69	63	-7	31	-39	70
MAY	109	+31	46	-32	97	+19	92	+14	78
JUN	167	+55	83	-29	69	-43	71	-41	112
JUL	82	-7	120	+31	52	-37	80	-9	89
AUG	240	+137	125	+22	151	+48	45	-58	103
SEP	97	+18	70	-9	48	-31	22	-57	79
OCT	35	-27	55	-7	79	+17	89	+27	62
NOV	72	+30	31	-11	21	-21	125	+83	42
DEC	25	0	15	-10	28	+3	35	+10	25
TOTAL	952	+211	NA	NA	679	-62	667	-74	741

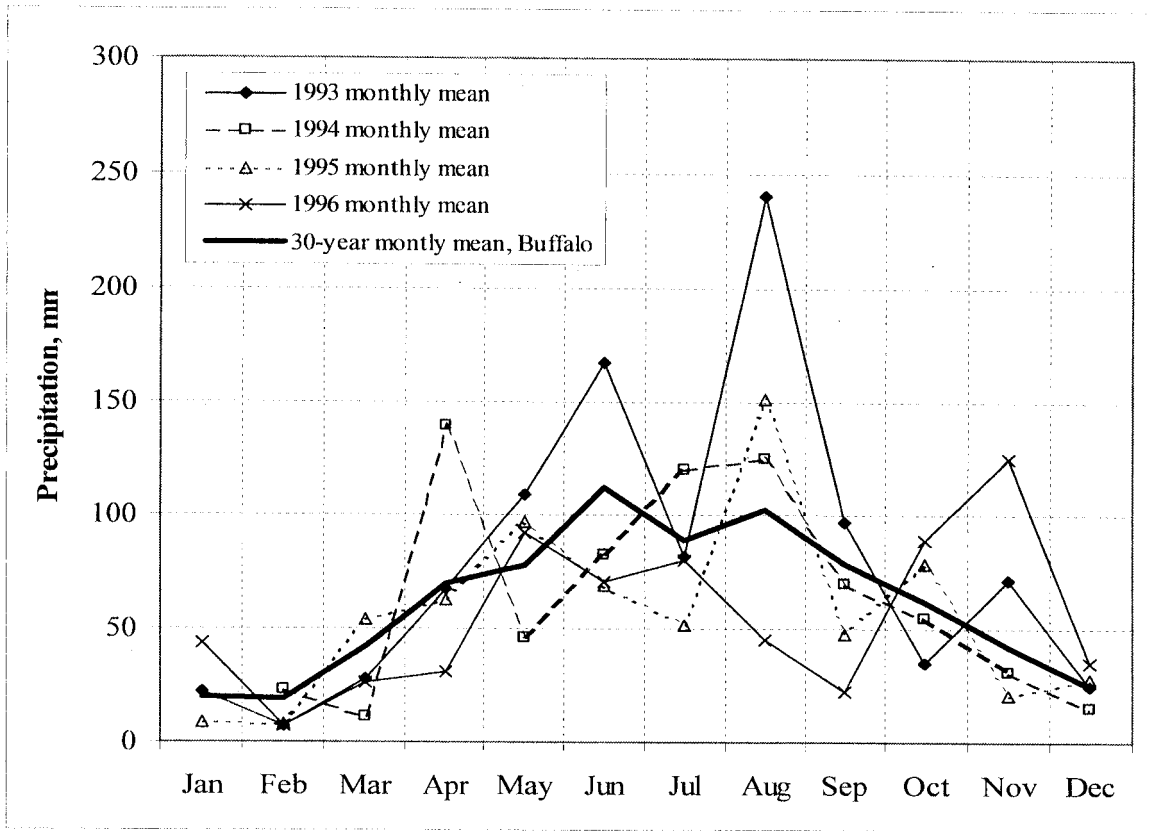


Figure 4.7. Precipitation events at Mn/ROAD between 1993 and 1996 compared to 30-year mean data from Buffalo weather station.

After researching the climate history and current climate events it was possible to quantify the relationships between climate factors and in situ environmental conditions with the use of field sensors at Mn/ROAD.

Daily Air Temperature and In Situ Temperature Results

Equation 3.1 [54] gave reasonable predicted values with R^2 values near 0.9 for the in situ temperatures at Mn/ROAD. There were a number of steps taken to determine the mean surface temperature (T_{mean}) for use in Equation 3.1. First, the mean temperature gradients were measured using thermocouple data in the HMA layer for January and July since the mean temperatures in

these months were the most extreme and are shown in Figures 4.8 and 4.9, respectively. The figures show data from test section 19, which has AC 20, and test section 20, which has 120/150 pen. The locations of the TCs in the HMA layers are near the depths of 25, 50 and 125 mm. The TC located in the top of the base layer is also used in this analysis and is located at a depth of 200 mm at test section 19 and 300 mm at test section 20.

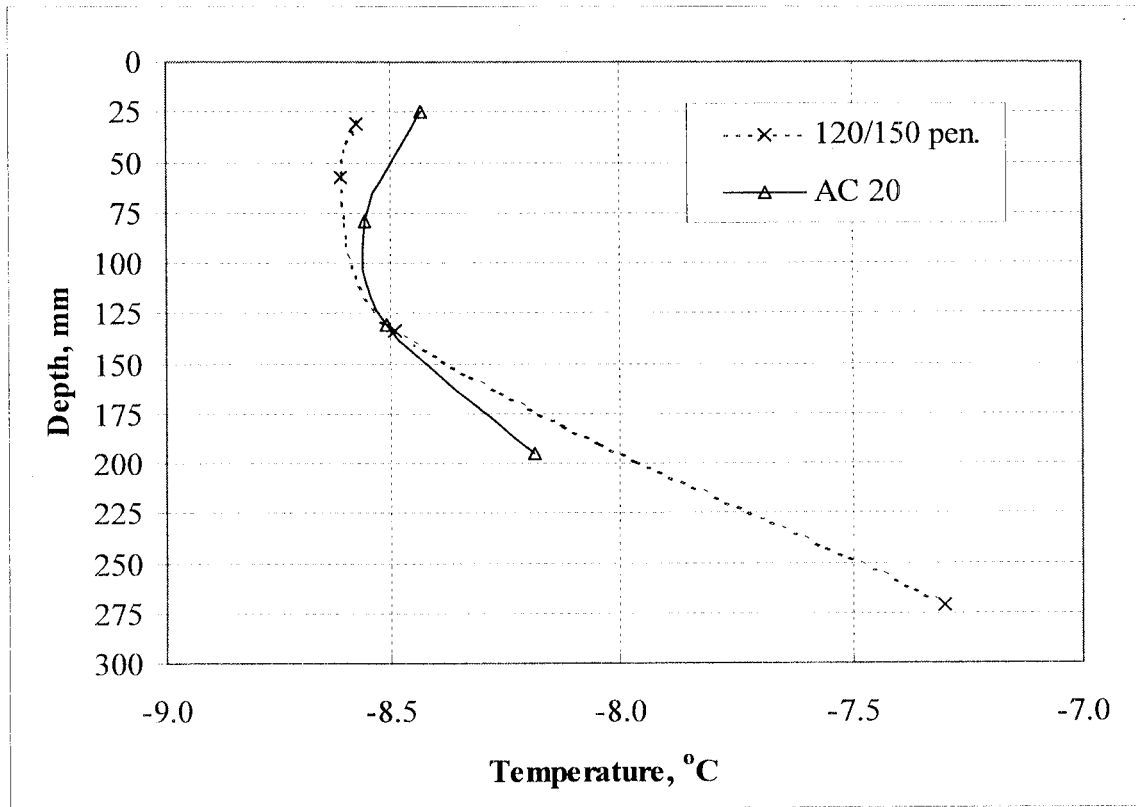


Figure 4.8. Mean monthly thermal gradient in January 1996 for test sections 19 (AC 20) and 20 (120/150 pen.).

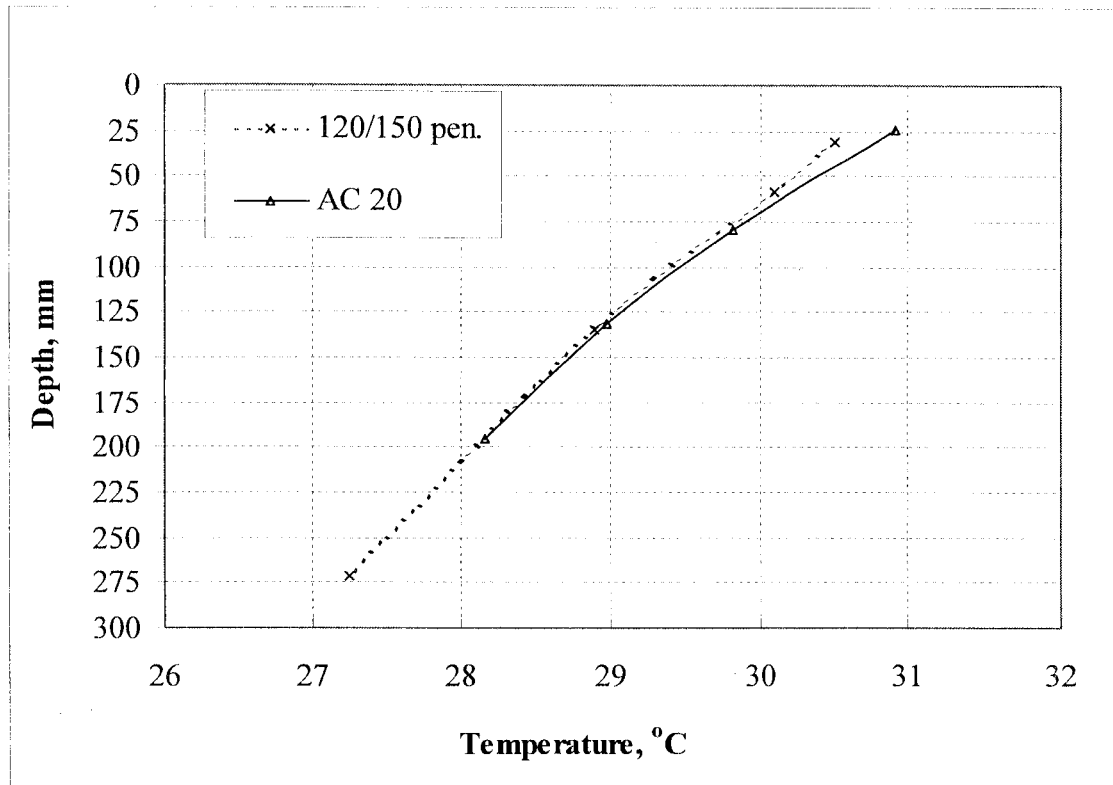


Figure 4.9. Mean monthly thermal gradient in July 1996 for test sections 19 (AC 20) and 20 (120/150 pen.).

Second, the temperature at the surface was extrapolated from these profiles. It was found that the surface temperature for these months was, on average, 0.5°C higher than the temperature measured at 25 mm in both the AC 20 and 120/150 pen HMA layers. Table 4.4 shows several predicted and measured surface temperatures for comparison. SHRP's unmodified equation underestimated the surface temperature, while the modified equation more closely estimates the surface temperature and the mean annual surface temperature.

Table 4.4. Measured and predicted mean monthly air and surface temperature, °C, 1996.

Month	Measured Monthly Air Temperature	Measured Temp. at 25 mm depth (TC)	SHRP Equation (Predicted Surface Temperature of Pavement)	Modified SHRP Equation	Extrapolated Surface Temperature
JAN	-15	-8	-11	-5	-8
FEB	-9	-1	-6	0	-1
MAR	-5	2	-3	3	3
APR	4	12	5	11	13
MAY	12	21	12	18	22
JUN	19	29	18	24	29
JUL	20	31	19	25	31
AUG	21	33	20	26	33
SEP	16	23	16	22	24
OCT	10	14	10	16	15
NOV	-4	0	-2	4	1
DEC	-11	-6	-8	-2	-6
Mean	5	13	6	12	13

As mentioned in Chapter Three, this modified equation is used to better predict the mean annual surface temperature (T_{mean}), not to predict the surface temperature from hourly or daily air temperatures. There are other surface temperature prediction tools [57] that could be used in place of the modified SHRP equation.

The third step was to use the mean annual surface temperature in Equation 3.1 to predict in situ temperature as a function of time and depth. An example is shown in Figure 4.10 for a depth of 25 mm with thermocouple data at 25 mm in 1996. This figure is representative of how well this equation fits the thermocouple data at other depths and $R^2 = 0.89$. Therefore, it appears that Equation 3.1 is an accurate estimator of mean in situ temperatures at Mn/ROAD.

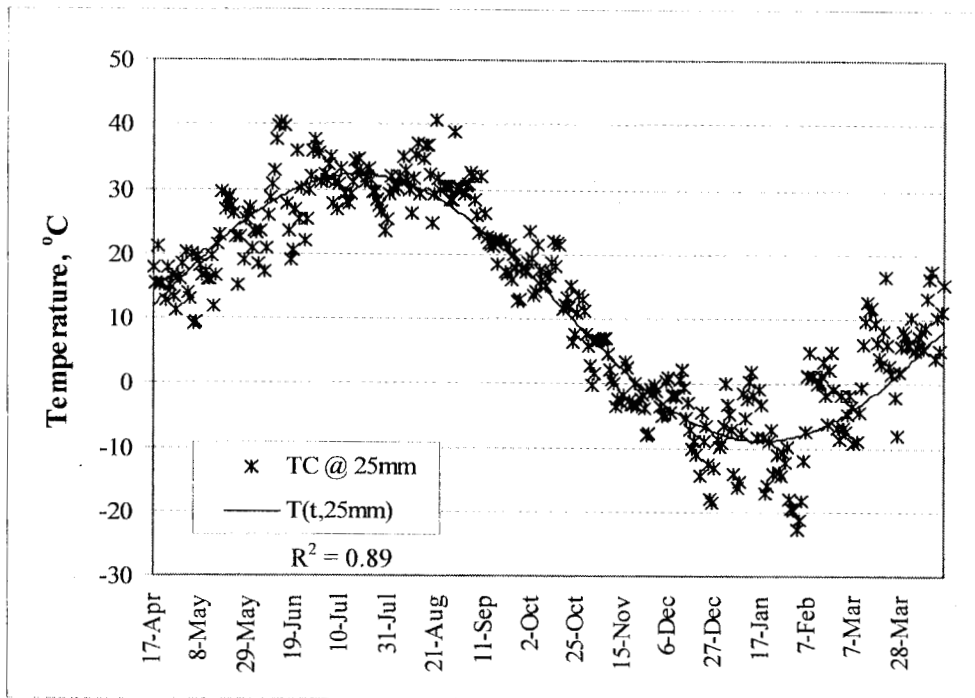


Figure 4.10. Equation 3.1 and TC values from 1996.

Precipitation and Moisture Content Variations in the Unbound Layers

Precipitation events affect the moisture content of the base and subgrade layers in a pavement structure, however the subsequent increase in the moisture content is temporary, after which the moisture content remains at a near constant level. This is evident in the time domain reflectometer data that are typically measured twice a month during the year and once a week during the thaw period.

The distributions of unfrozen volumetric moisture content measurements taken in the different base materials at various depths are shown in Tables 4.5 through 4.8. For the base materials, once the moisture has drained after the spring thaw period, the moisture contents remain close to a constant value. Typically, the less fine-grained material in the base, the lower the moisture content. The Cl. 3 Sp. base material has the greatest moisture content, while the moisture contents of the Cl. 4 Sp. and Cl. 5 Sp. base materials are close to one another, and the

Cl. 6 Sp. base material has the lowest moisture content. It is interesting to note that the moisture content increases with depth for all base materials. This is possibly due to gravitational effects drawing moisture to the bottom of the base layer, where it is unable to drain into the embankment or subgrade.

It is important to note the seasonal changes in the unfrozen volumetric moisture content measured by the TDRs. The volumetric moisture content is highest in the base material at the beginning of the thaw and returns to a near constant value shortly after the moisture has drained from the layer. It remains near a constant value in the summer and fall months and then decreases in the winter when the moisture is frozen.

Table 4.5. Unfrozen vol. m.c. distribution in percent for Cl. 3 Sp. base material, test section 17, 1994 - 1997.

Months	300 mm	COV, %	470 mm	COV, %	630 mm	COV, %
JAN	14	9	14	5	14	3
FEB	12	43	12	43	11	49
MAR	22	26	21	27	19	32
APR	24	9	24	6	24	2
MAY	24	6	25	11	25	1
JUN	25	2	25	3	27	NA
JUL	26	4	26	6	26	NA
AUG	25	7	25	7	26	8
SEP	26	10	25	10	27	5
OCT	26	6	24	3	27	2
NOV	23	7	23	3	25	3
DEC	15	15	16	24	18	24

Table 4.6. Unfrozen vol. m.c. distribution in percent for Cl. 4 Sp. base material, test section 1, 1994 - 1997.

Months	310 mm	COV, %	460 mm	COV, %	610 mm	COV, %
JAN	12	14	11	9	12	6
FEB	14	4	11	15	11	9
MAR	20	14	16	19	13	51
APR	16	77	19	2	20	3
MAY	22	4	20	7	21	5
JUN	21	3	19	4	20	1
JUL	23	5	20	8	21	7
AUG	22	5	20	4	20	4
SEP	21	5	20	6	20	7
OCT	20	2	19	2	19	5
NOV	18	8	18	5	19	3
DEC	13	2	12	2	13	2

Table 4.7. Unfrozen vol. m. c. distribution in percent for Cl. 5 Sp. base material, test section 21, 1994 - 1997.

Months	310 mm	COV, %	450 mm	COV, %	605 mm	COV, %
JAN	12	10	12	7	12	3
FEB	12	24	12	12	12	11
MAR	16	20	17	23	17	27
APR	18	8	19	5	21	5
MAY	18	2	20	3	22	4
JUN	18	4	19	4	21	5
JUL	19	5	20	5	23	6
AUG	19	2	20	1	21	1
SEP	18	5	20	3	21	1
OCT	18	4	19	1	21	1
NOV	17	3	19	1	20	NA
DEC	12	1	12	6	13	9

Table 4.8. Unfrozen vol. m.c. distribution in percent for Cl. 6 Sp. base material, test section 22, 1994 - 1997.

Months	340 mm	COV, %	490 mm	COV, %	640 mm	COV, %
JAN	8	3	8	3	11	8
FEB	8	4	7	4	9	3
MAR	12	5	12	7	19	13
APR	13	2	14	3	20	3
MAY	13	1	14	2	20	1
JUN	13	1	14	1	19	1
JUL	13	1	15	1	20	1
AUG	13	NA	14	NA	18	1
SEP	13	NA	14	1	18	1
OCT	13	1	13	2	18	1
NOV	13	2	13	2	18	1
DEC	9	3	9	5	13	5

The type of subgrade material affects the moisture content of the layer. The test sections in the low-volume road are composed of two different subgrade materials. The subgrade material in test sections 24 and 25 have a design R-value of 70 (1655 kPa), and test sections 26 and 27 subgrade material have a design R-value of 12 (1655 kPa). Figure 4.11 shows that the moisture content in the test sections with a design R-value of 12 (1655 kPa) is greater than the test sections with a design R-value of 70 (1655 kPa).

Another observation is that the subgrade soil moisture content is typically higher for full-depth HMA pavement when compared to those with an aggregate base layer. In Figure 4.11, test section 24 has a lower moisture content than 25, and 27 generally has a lower moisture content than 26. Test sections 24 and 27 both have a layer of HMA over Cl. 6 Sp. aggregate base, and test sections 25 and 26 are full-depth HMA pavements. It appears that adding an aggregate base may reduce the moisture content of the subgrade.

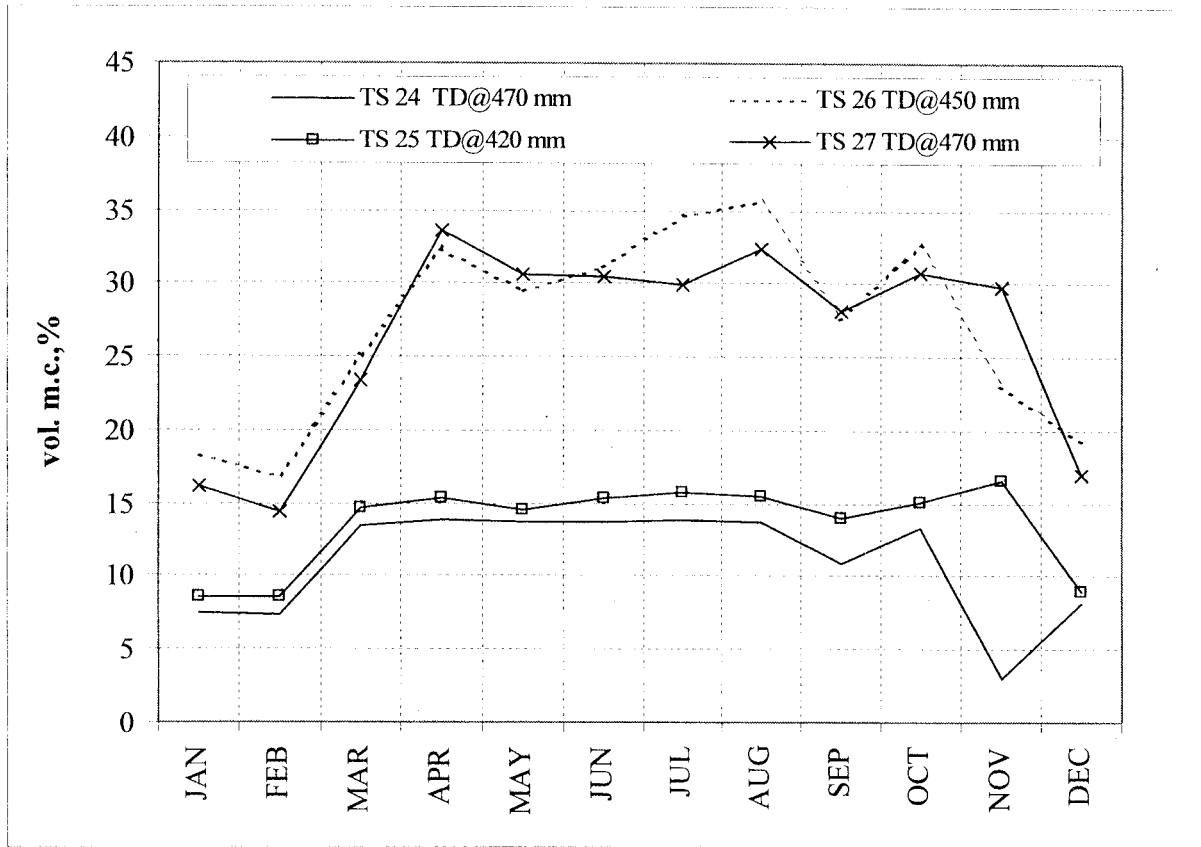


Figure 4.11. Moisture content of different subgrade materials at similar depths.

There is a slight annual increase of 1 to 2 % in the TDR measurements for all the base materials. The drift in TDR measurements in Cl. 3 Sp. and Cl. 6 Sp. base material are shown in Figure 4.12. This figure shows the TDR measurements at mid-depth of the base layer in the outer wheel path from 1993 to 1997. The drift is more apparent between 1994 and 1995 and may reflect consolidation of the material after the first year of service. Other causes of the drift may be an increase in the salinity of the water in the base layer due to de-icing agents that can alter the sensor measurements, corrosion of the sensors due to salt or moisture, or it may be that the moisture content increased from a lack of drainage.

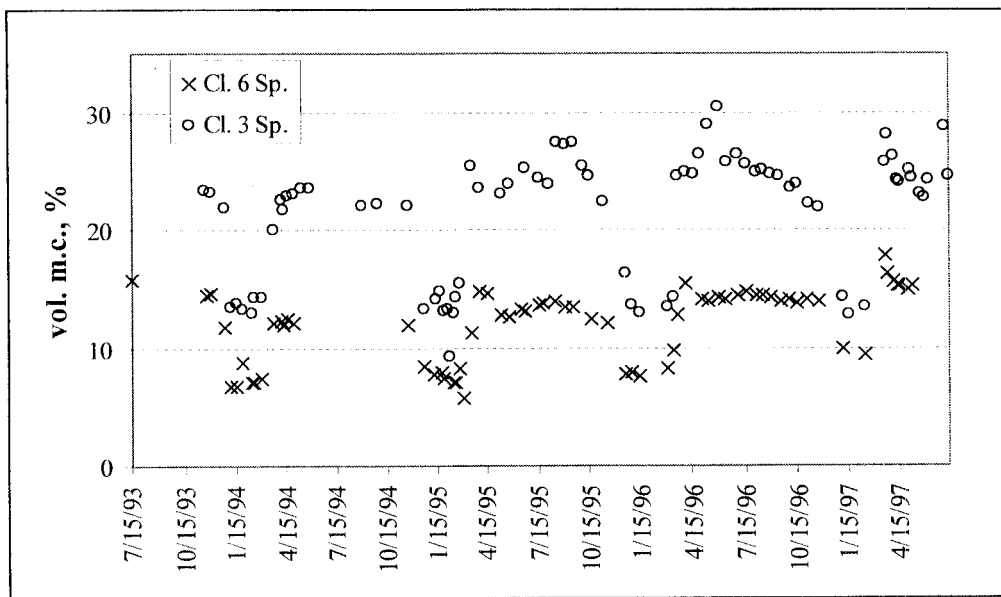


Figure 4.12. TDR data at mid-depth of Cl. 3 Sp. and Cl. 6 Sp. base materials in OWP.

Temperature and State of Moisture Results

The FI and TI were used to predict the state of moisture in the base and subgrade layers and the TC, WM and TDR sensors at Mn/ROAD were useful indicators of when and where actual thawing events occurred in the pavement structures. The TC data (Figure 4.13) shows the thermal gradient in the base layer compared to the TI for February through April 1996. The top

of the base is the first to freeze and thaw. The temperature at the top of the base (TC located at a depth of 203 mm) reaches nearly 0°C near March 11, 1996, in correlation with the TI reaching 15°C-days, which is the same date that spring load restrictions should be placed in Minnesota [58]. The data show that the criteria used to place spring load restrictions in Minnesota is a good predictor of when the base layer is thawing, and can be used in pavement design as a guideline of when the base layer stiffness is low. These dates are useful when analyzing moduli data to determine when the aggregate base moduli will be at a minimum.

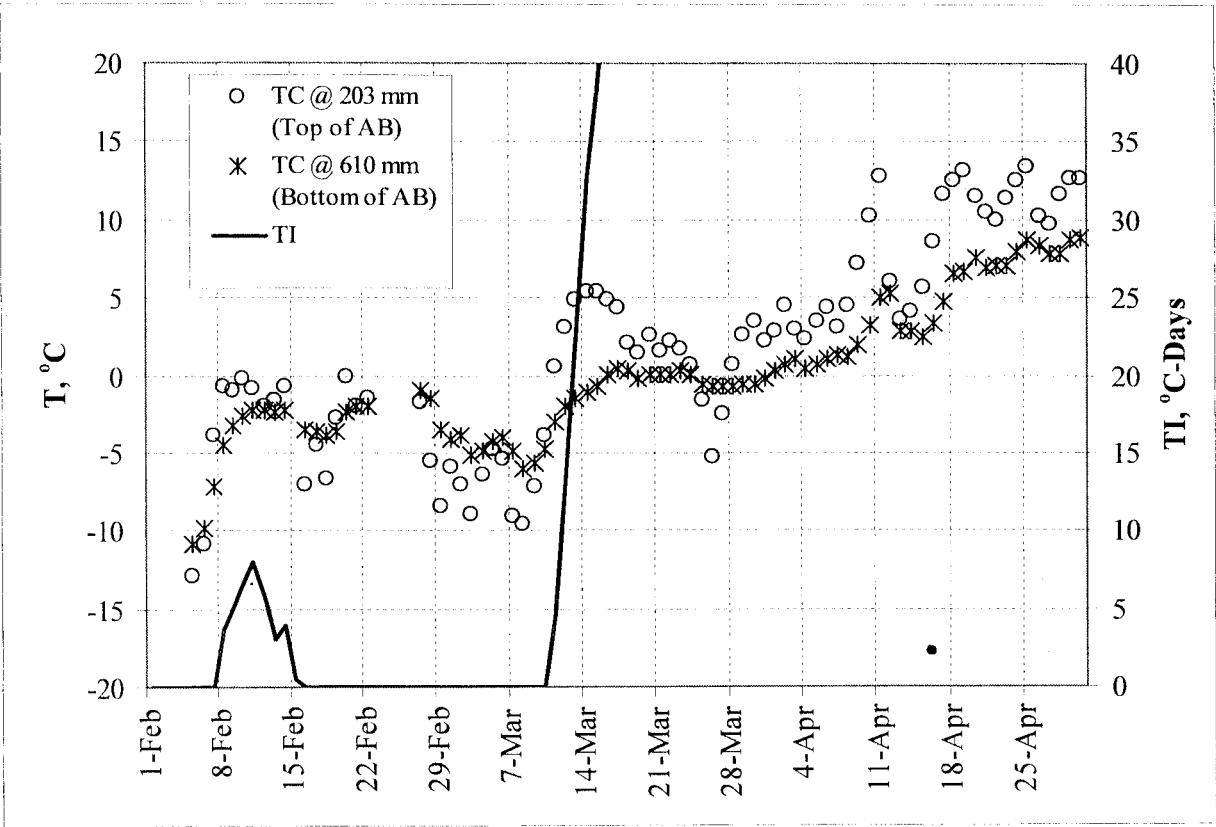


Figure 4.13. TI and TC data in test section 22, Cl. 6 Sp. base, spring 1996.

The WM sensors measure the soil pore water pressure and the data reported from these sensors are in centibars (cbar), as explained in Chapter Two. For unfrozen soil, the readings will fluctuate about some baseline value, exceeding it when the water freezes, and returning back to

the baseline after thawing. For this reason, the WM data were used as freeze/thaw indicators. Figure 4.14 shows the WM values of the sensor located in the top of the base (340 mm) returning to unfrozen values March 11, and March 14 in the bottom of the base.

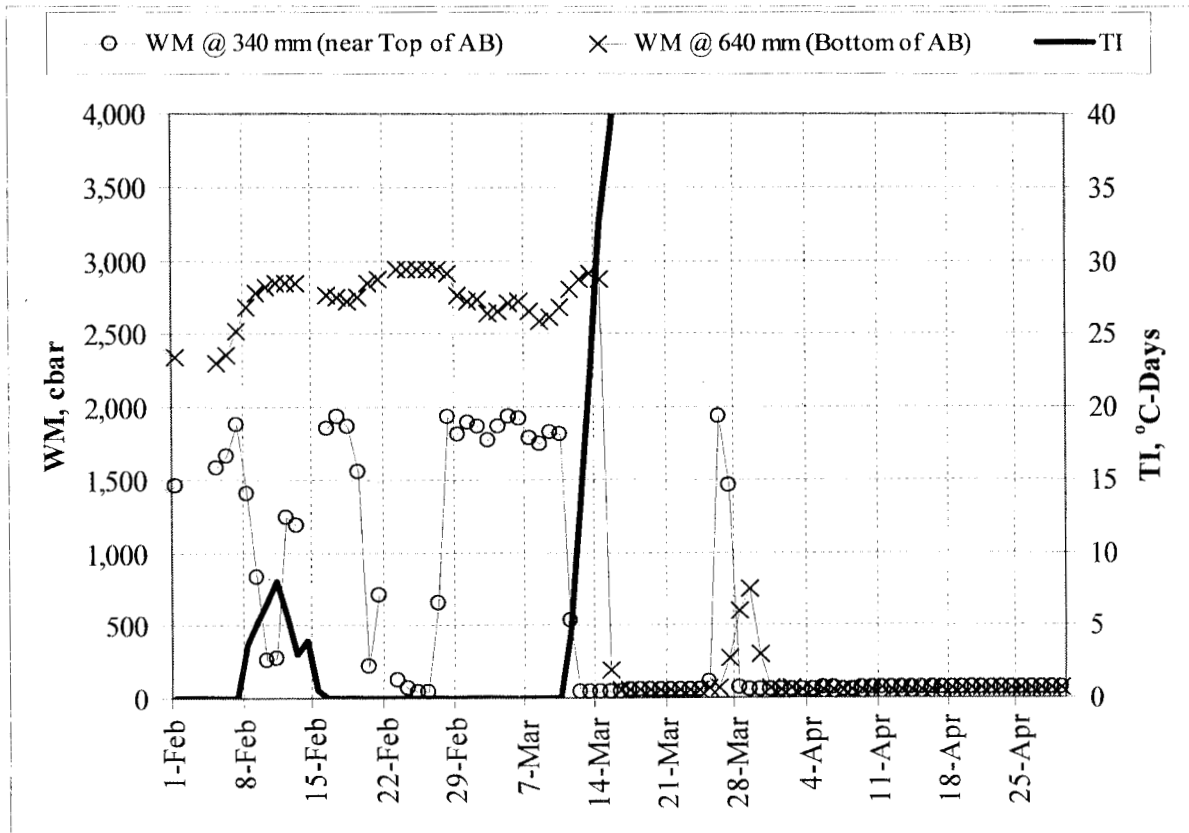


Figure 4.14. TI and WM data in test section 22, Cl. 6 Sp. base, spring 1996.

The TDR measurements taken on March 1, 12 and 20 show that the top of the base had thawed between March 1 and 12, and the bottom of the base had thawed between March 12 and 20 (Figure 4.15), similar to the TC and WM data. It is estimated that the moisture content is completely liquid by March 20.

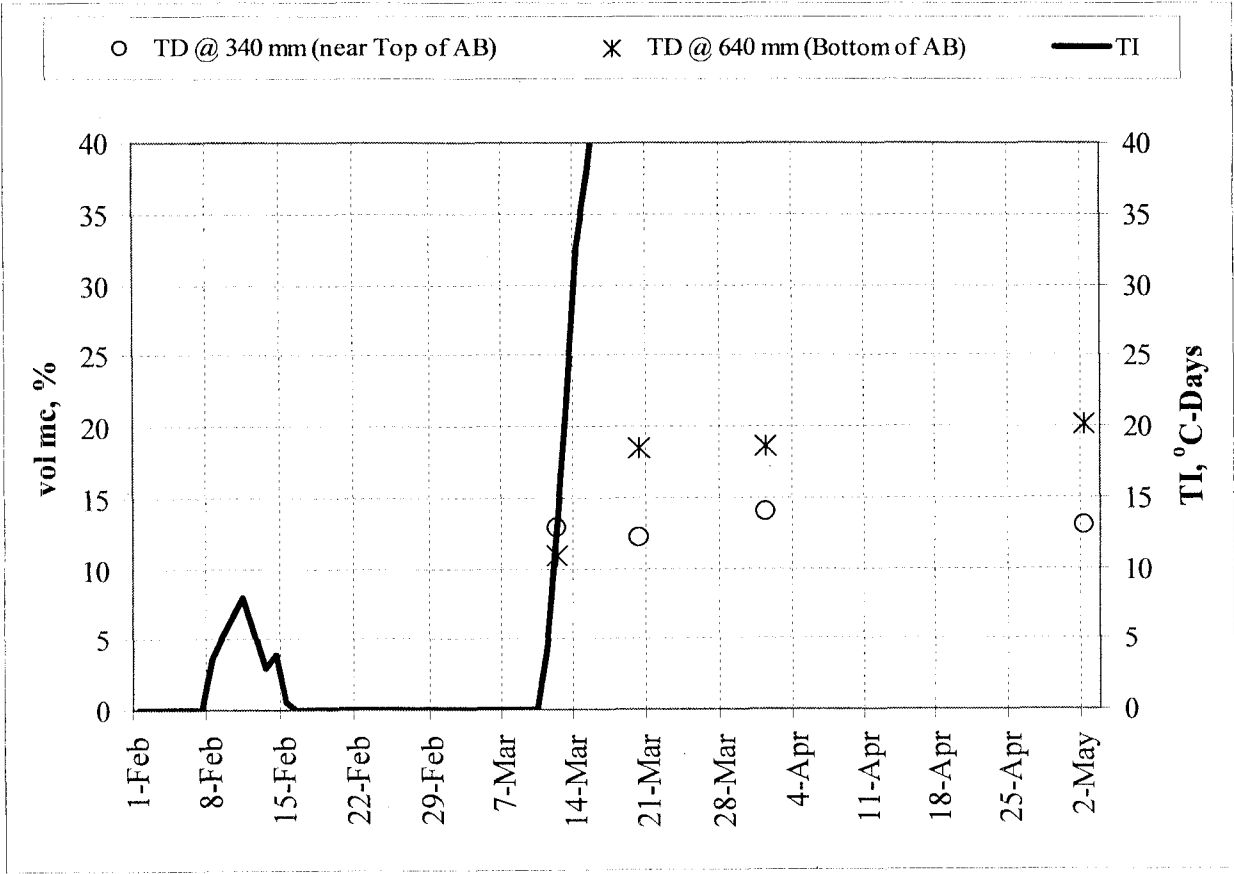


Figure 4.15. TI and TDR data for Cl. 6 Sp. base, spring 1996.

Trends Between Subsurface Environmental Conditions and Pavement Layer Stiffness

Data from Mn/ROAD were used to verify relationships between subsurface environmental conditions and pavement layer moduli. Field temperatures were used to estimate HMA moduli throughout a typical year and were compared to backcalculated moduli. The state of moisture in the base and subgrade layers is used to determine the distribution of backcalculated moduli throughout a typical year.

Predicted HMA Modulus

The seasonal trends in the HMA modulus were characterized using backcalculated HMA layer moduli. Since this data is not available to every region, the seasonal trends were also predicted using Equation 3.6. First, the coefficients for Equation 3.6 were determined for AC 20 and 120/150 pen. HMA samples from Mn/ROAD. Second, TC data were used as input in Equation 3.6 to determine the difference in the predicted HMA layer moduli at 25 mm and 195 mm, which are located at the top and bottom of the HMA layer, respectively. It was found that the predicted moduli at 25 mm were slightly lower than that at 195 mm, which was expected due to the warmer surface temperatures. Third, the predicted HMA moduli at 25 mm were compared to the backcalculated HMA layer moduli. The results showed that predicted HMA moduli was slightly higher than the backcalculated HMA layer moduli, which is important to note if the predicted HMA moduli are used in design applications. Finally, since TC data may not be available for design, Equation 3.1 was used to determine the seasonal HMA layer temperature and as input into Equation 3.6 to determine the seasonal HMA layer moduli. It was found that Equations 3.1 and 3.6 could be used to characterize seasonal changes in the HMA layer

temperature and moduli. However, these equations should be used with caution in design applications depending on the level of accuracy required.

Equation 3.6 was derived from resilient modulus laboratory tests conducted on Mn/ROAD HMA samples [59]. The coefficients shown in Table 4.9 are dependent on the AC and similar tests should be performed if HMA samples differ in composition. The modulus predicted from Equation 3.6 at different temperature values are shown in Figure 4.16 for AC 20 and 120/150 pen. HMA samples. As was expected, the AC 20 model predicts a higher modulus for the stiffer AC than the 120/150 pen asphalt (relatively softer binder), except at extremely low temperatures, in which they meet and the 120/150 function barely surpasses the AC 20 function.

Table 4.9. Coefficients of Equation 3.6 (MPa), as a function of temperature (°C).

HMA Modulus = $a * e^{((T - b)^2 / c)}$			
AC Type	a	b	c
120/150	17270	-30	-1630
AC 20	13920	-15	-1170

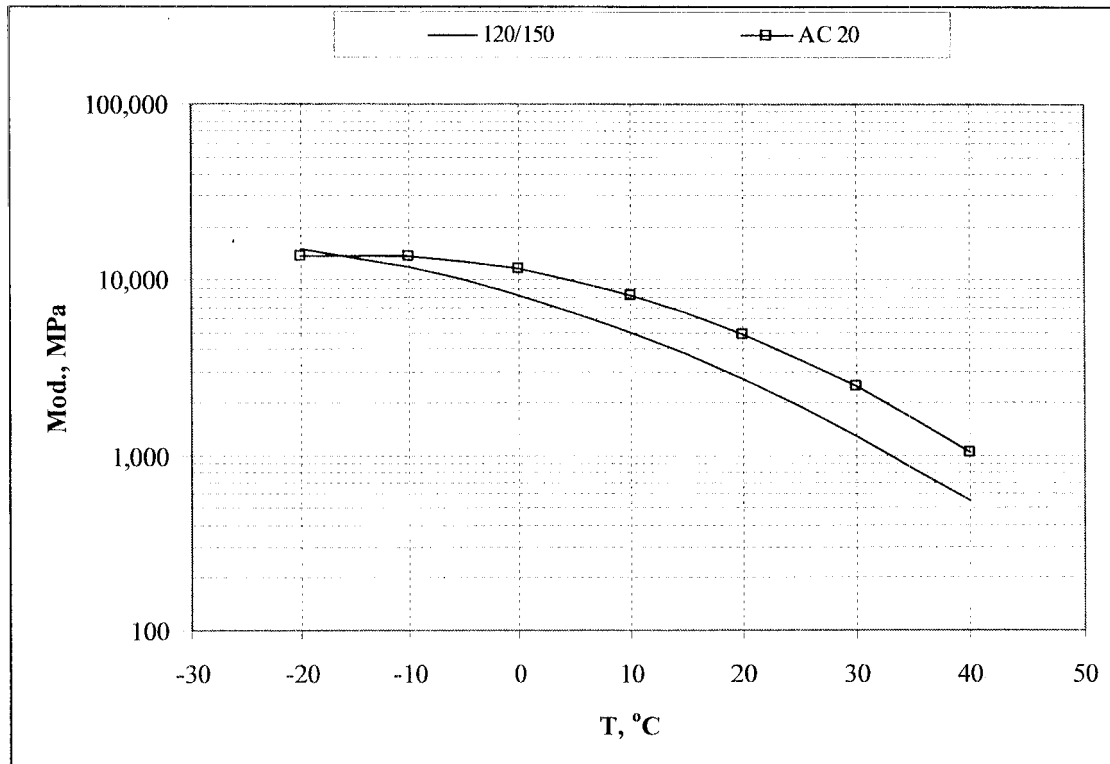


Figure 4.16. Equation 3.6 used to estimate HMA modulus from temperature data.

Using TC data in 1996, the HMA moduli calculated using Equation 3.6 were compared to backcalculated moduli. Figure 4.17 shows the predicted HMA modulus at a depth of 25 mm and at 195 mm. The modulus near the surface is predicted to be slightly lower than the bottom of the layer due to the greater temperature at the surface.

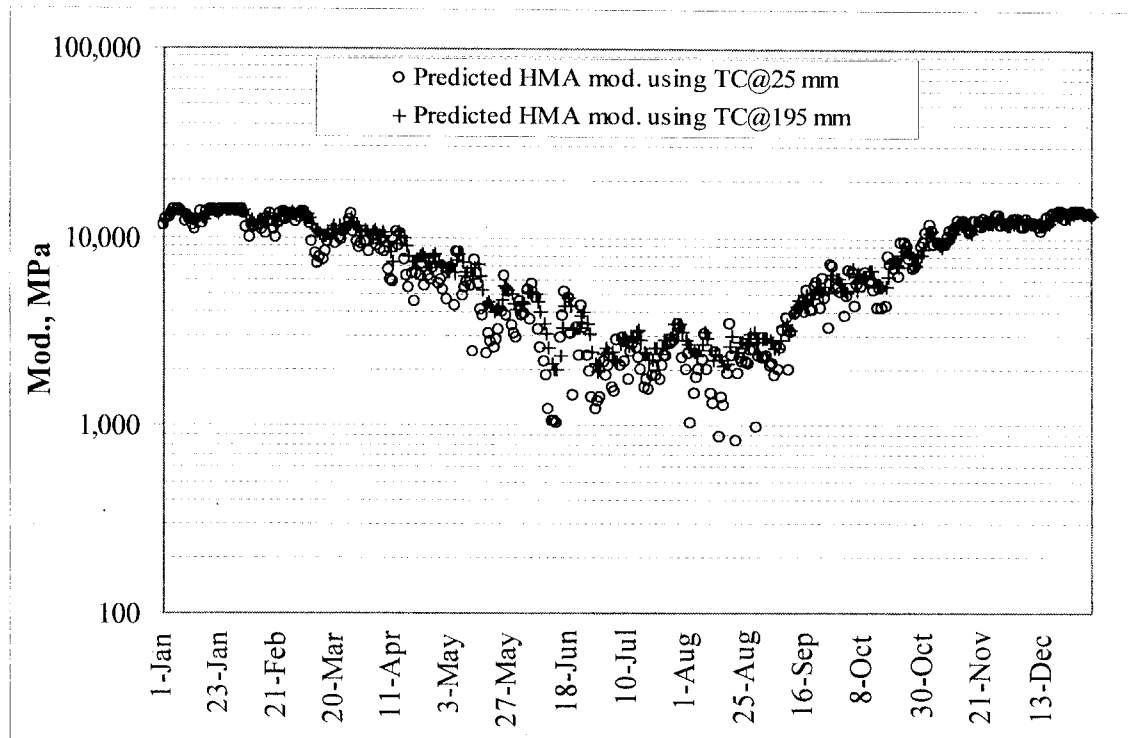


Figure 4.17. Predicted HMA modulus at 25 mm and 195 mm, in 1996.

Since backcalculated moduli are averages of the whole layer and are not computed as a function of depth, the modulus was estimated at 25 mm (Figure 4.18). The predicted modulus is slightly higher in the summer than the backcalculated modulus and therefore the prediction may need to be adjusted if used for design in another region to fit the seasonal changes.

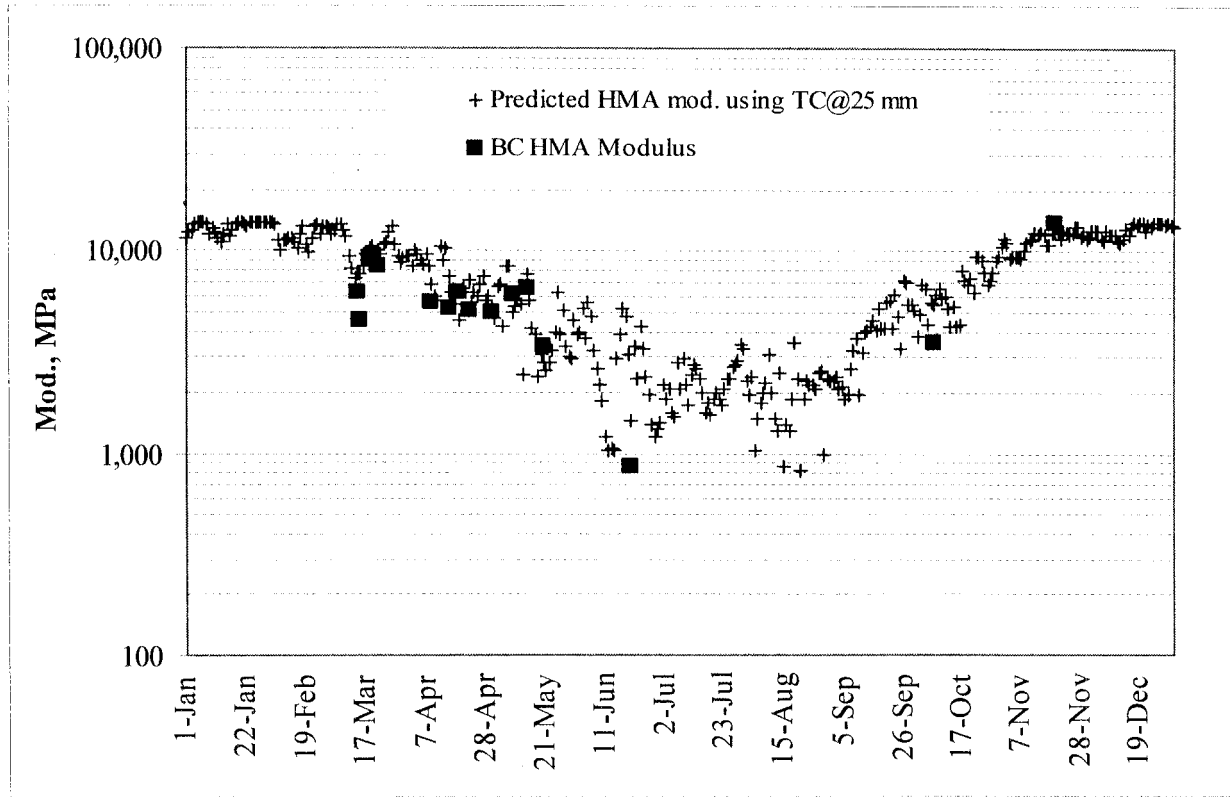


Figure 4.18. Predicted and backcalculated HMA modulus in 1996.

In Figure 4.19, the seasonal trend in HMA modulus is shown using the whiplash and the exponential model together and is compared to the backcalculated modulus. However Equation 3.1 predicts the average temperature throughout the year, and therefore can predict slightly lower summer temperatures. The net effect is a higher predicted summer modulus than the backcalculated HMA layer modulus. Therefore, the temperatures predicted using Equation 3.1 should be used with caution if they are used in place of thermocouple data in Equation 3.6.

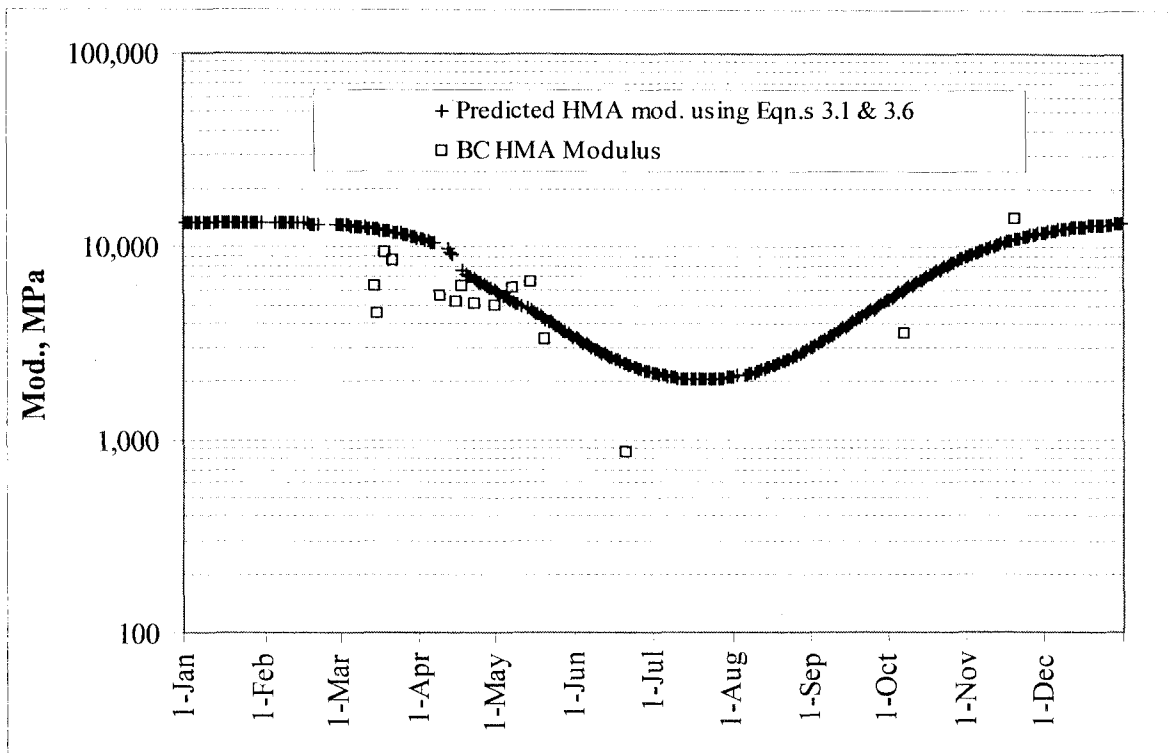


Figure 4.19. A comparison between backcalculated and predicted HMA modulus.

Predicted Base and Subgrade Layer Moduli

The seasonal variations in the backcalculated moduli of the base and subgrade layers were investigated to characterize the overall seasonal trends in the layer moduli for pavement design. Figure 4.20 shows the backcalculated layer moduli for the Cl. 6 Sp. base material and the soil subgrade for test section 22. Fewer deflection tests are performed in the late fall and winter due to weather and equipment constraints, thus the moduli are shown between March and December 1. The seasonal trend in the base layer modulus is at a minimum on March 21 at 81 MPa and returns to a baseline value near 200 MPa on May 20. This eight week recovery period is typical of the Mn/ROAD flexible pavement test sections investigated. The low modulus is a result of the spring thaw that begins at the surface layer and goes through the structure until it has completely thawed [58]. The soil subgrade modulus reaches a minimum value of 67 MPa on April 16 and returns to a baseline modulus value of 100 MPa on June 13.

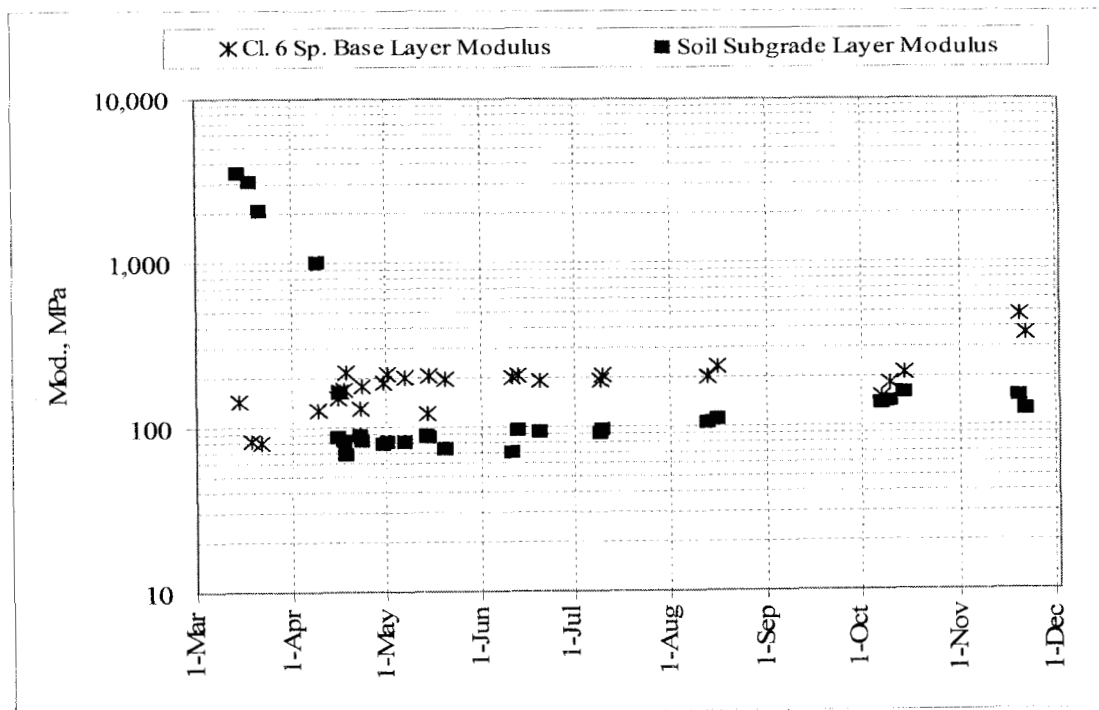


Figure 4.20. Cl. 6 Sp. aggregate base and subgrade moduli in 1996 in test section 22.

Since the data showed a direct relationship between the base and subgrade layer moduli and the state of moisture in the layer, the seasonal trends in the base and subgrade layer moduli were characterized relative to the changes in the state of moisture. Season I is when the moisture is frozen and the layers are quite stiff. Season II is the two to four week period that the base layer modulus is at a minimum. Season III is the two to four week period that the base layer modulus recovers to a baseline value, and the soil subgrade layer modulus is low. Season IV is the summer modulus values and is very close to the Season V modulus values for the base and subgrade layers.

The decrease in the stiffness of the base layer resulting from changes in the unfrozen volumetric moisture content during the spring thaw period can be seen Figure 4.21. The seasonal variations in the volumetric unfrozen moisture content are shown with the seasonal variations in the base modulus and it is evident that as the moisture thaws or increases, the base modulus decreases.

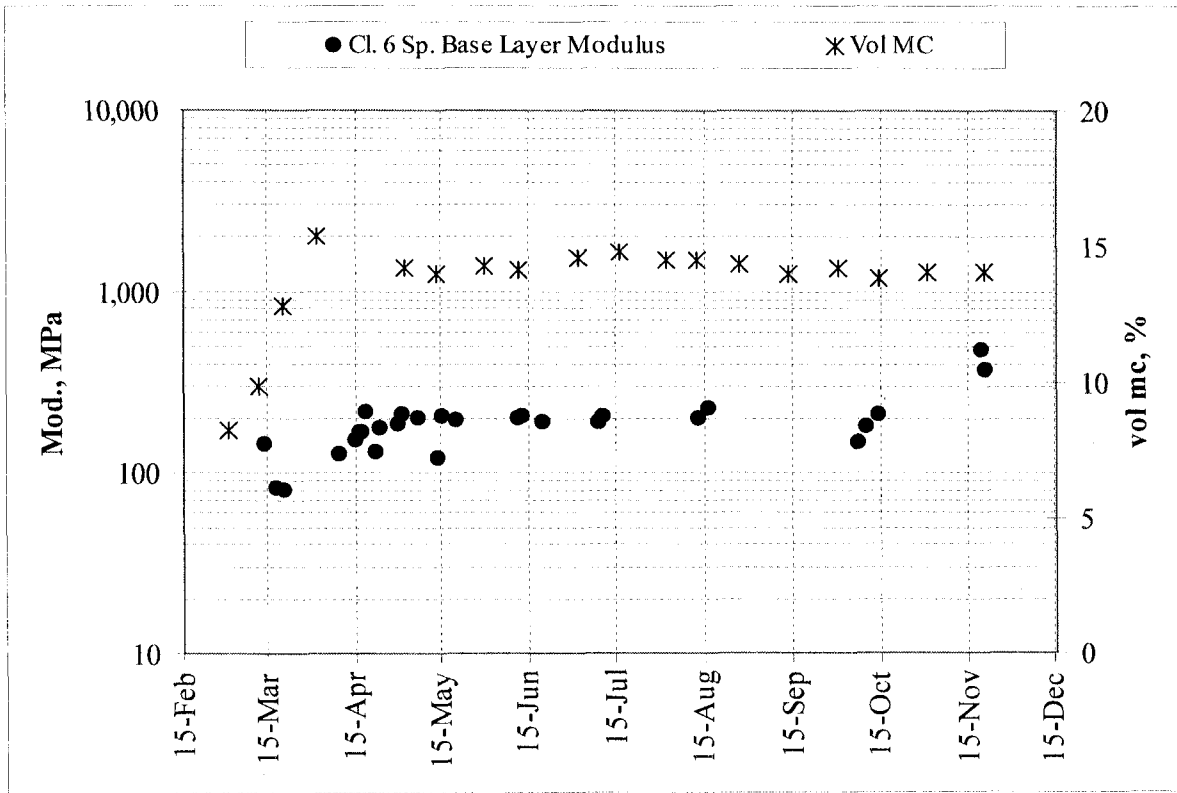


Figure 4.21. Seasonal variations in the base modulus and in the unfrozen volumetric moisture content, test section 22, 1996.

Figure 4.22 shows the base layer modulus variations in the Cl. 6 Sp. material for a thick pavement structure over a fine-grained subgrade (test section 22), a thin pavement structure with a sand subgrade (test section 24) and a thin pavement structure over a clay subgrade (test section 27). The higher moduli in test section 24 is primarily due to the clean, sand subgrade that drains moisture better than the clayey subgrade, and thus, has lower moisture content.

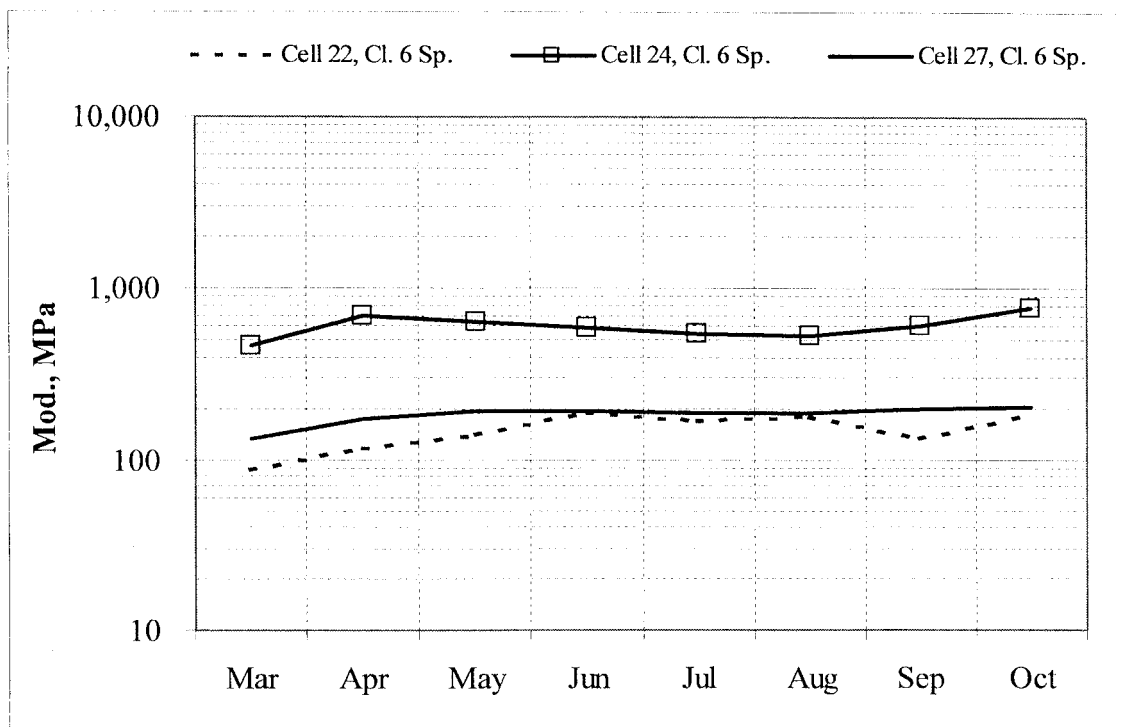


Figure 4.22. Seasonal variations in Cl. 6 Sp. moduli, 1996, test sections 22, 24 and 27.

This section discussed the relationships between field environmental conditions and the corresponding pavement layer moduli. HMA moduli were shown to vary with temperature and the base and subgrade moduli were shown to vary with moisture content and the state of moisture. The next section discusses the seasonal distribution of the pavement layer moduli and factors that can be used in design to account for these variations.

Applications in Pavement Design

The following discussion concerns the characterization of the seasonal trends in the backcalculated layer moduli for use in M-E flexible pavement design. First, the results from the HMA layer are shown and discussed. Then the aggregate base layer and subgrade layer results are shown and discussed, including the stress sensitivity of the aggregate base and subgrade layers. As a comparison to the backcalculated layer moduli, the trends in laboratory base moduli [50] are shown.

Seasonal Duration for Use in M-E Design

As discussed in Chapter Three, the typical year was divided into seasons based on changes in the layer moduli that paralleled temperature changes, and these variations shown in Table 3.9 (repeated for convenience).

Table 3.9. Seasonal distribution of a typical year for design purposes.

	Season I	Season II	Season III	Season IV	Season V
Description	Winter: <i>Layers are Frozen</i>	Early Spring: <i>Base Thaws/ SG is Frozen</i>	Late Spring: <i>Base Recovers/ SG Thaws</i>	Summer: <i>HMA Low/ SG Recovers</i>	Fall: <i>Layers are Standard</i>
Estimated Duration of Each Season					
Beginning	FI>90°C-days	TI>15°C-days	End of Season II	3-day T _{AVG} > 17°C	3-day T _{AVG} < 17°C
Ending	TI>15°C-days	Approx. 28 days later	3-day T _{AVG} > 17°C	3-day T _{AVG} < 17°C	FI>90°C-days
Pavement Layer Moduli Relative to Fall Values					
E _{HMA}	High	High	Standard	Low	Standard
E _{AB}	High	Low	Low	Standard	Standard
E _{SG}	High	High	Low	Low	Standard

It was found that the seasonal moduli values depend in part on the thickness of the layers. For example, given the same vehicle load, a thicker HMA pavement will support more load and

reduce the stress deeper in the pavement structure, whereas a thinner HMA pavement will result in higher stresses and strains in the pavement layers. Therefore, the results were divided into two groups based on layer thickness: results from thick pavements where the HMA layer thickness is greater than 150 mm, and results from thin pavements where the HMA layer thickness is equal to or less than 150 mm.

Seasonal Variations in Backcalculated HMA Modulus

In general, the backcalculated HMA layer modulus depends on the type of AC, the layer thickness and the temperature of the layer. Table 4.10 shows the variations in the backcalculated HMA modulus with seasons. As a result of a stiffer AC, the test sections with AC 20 had a higher modulus than the test sections with 120/150 pen., especially in the summer months (Season IV). This is evident in comparing the data from the full depth pavement, test sections 14 and 15. Test sections 25 and 26 are similar full-depth pavements constructed on different subgrade materials. The HMA modulus of test section 25 (with a sand subgrade) appears to be higher than test section 26 (with a fine-grained subgrade) except in the summer. However, the summer HMA modulus values for test section 26 have a COV is greater than 100%.

Table 4.10. Seasonal variations in HMA modulus, MPa (COV in %).

Test Section	AC Material	Thick., mm	Season I Winter		Season II Early Spring		Season III Late Spring		Season IV Summer		Season V Fall	
			Mod.	COV	Mod.	COV	Mod.	COV	Mod.	COV	Mod.	COV
Thin (HMA < 150 mm)												
1	120/150	145	14000	-	6231	44	3908	58	969	30	3554	31
2	120/150	145	14000	-	8339	35	5364	57	1297	32	4897	31
3	120/150	145	14000	-	8853	36	5232	55	1406	45	4807	32
Thick (HMA > 150 mm)												
4*	120/150	225	14000	-	9760	23	6390	54	1313	73	4421	31
14*	120/150	275	13878	-	10139	20	7019	48	1371	26	4582	29
15*	AC 20	275	13986	-	11662	18	8668	41	2143	43	6133	27
16	AC 20	195	14000	-	10364	24	6970	46	2091	31	5113	28
17	AC 20	195	14000	-	11451	18	6623	48	2004	44	5064	25
19	AC 20	195	14000	-	10869	25	6491	51	1964	33	5104	27
20	120/150	195	14000	-	10529	27	4885	60	1222	49	3823	29
21	120/150	195	14000	-	9859	27	5494	50	1655	45	4495	19
22	120/150	195	14000	-	10014	26	5707	54	1842	45	5686	21
Thin (HMA < 150 mm)												
24 ^c	120/150	75	11333	25	6255	44	4286	55	2191	50	4168	53
25 ^{c*}	120/150	125	6734	27	7160	42	5063	55	1677	49	4707	55
26*	120/150	150	9428	35	5150	43	3723	64	2364	106	3023	70
27	120/150	75	10769	19	7547	46	4126	63	2353	46	4299	51
28	120/150	75	9541	50	7760	48	3849	61	1967	36	4803	55
30	120/150	125	12895	20	6865	47	3307	76	1245	35	2743	56
31	120/150	75	7609	60	8737	36	4779	52	2487	33	5452	51

^c indicates design subgrade R-value = 70

* indicates full-depth pavement

- indicates maximum modulus value was reached

Table 4.11 shows the seasonal factors for each test section relative to the Season V value. It can be seen from this table that the moduli in Season I are between 1 and 5 times greater than Season V. It is evident that at higher temperatures in the summer, the moduli of the HMA layers are greatly reduced.

Table 4.11. HMA seasonal factors.

Test Section	AC	Thickness, mm	Seasonal Factor				
			Season I Winter	Season II Early Spring	Season III Late Spring	Season IV Summer	Season V Fall
Thin (HMA < 150 mm)							
1	120/150	145	3.9	1.8	1.1	0.27	1.0
2	120/150	145	2.9	1.7	1.1	0.26	1.0
3	120/150	145	2.9	1.8	1.1	0.29	1.0
Thick (HMA > 150 mm)							
4*	120/150	225	3.2	2.2	1.4	0.30	1.0
14*	120/150	275	3.0	2.2	1.5	0.30	1.0
15*	AC 20	275	2.3	1.9	1.4	0.35	1.0
16	AC 20	195	2.7	2.0	1.4	0.41	1.0
17	AC 20	195	2.8	2.3	1.3	0.40	1.0
19	AC 20	195	2.7	2.1	1.3	0.38	1.0
20	120/150	195	3.7	2.8	1.3	0.32	1.0
21	120/150	195	3.1	2.2	1.2	0.37	1.0
22	120/150	195	2.5	1.8	1.0	0.32	1.0
Thin (HMA < 150 mm)							
24 ^c	120/150	75	2.7	1.5	1.0	0.53	1.0
25 ^{c*}	120/150	125	1.4	1.5	1.1	0.36	1.0
26*	120/150	150	3.1	1.7	1.2	0.78	1.0
27	120/150	75	2.5	1.8	1.0	0.55	1.0
28	120/150	75	2.0	1.6	0.8	0.41	1.0
30	120/150	125	4.7	2.5	1.2	0.45	1.0
31	120/150	75	1.4	1.6	0.9	0.46	1.0
Average values of seasonal factors							
Thick	AC 20	>150 mm	2.6	2.1	1.4	0.39	1.0
Thick	120/150	>150 mm	2.5	2.2	1.3	0.32	1.0
Thin	120/150	<150 mm	2.8	1.8	1.1	0.44	1.0

^c indicates subgrade with design R-value = 70

* indicates full – depth pavement

Seasonal Variations in Aggregate Base Backcalculated Moduli

The backcalculated aggregate base layer modulus is at a minimum in Season II, begins to recover in Season III, and then remains at a standard value in Seasons IV and V. The backcalculated modulus is at a maximum in Season I since the measured deflections are very small at this time.

It was expected that the backcalculated base moduli would follow trends similar to laboratory modulus trends that were determined from an Illinois study [50]. Laboratory triaxial tests were conducted on the aggregate base materials used at Mn/ROAD to measure the modulus of these materials. In the Illinois study, three models were used to characterize the modulus as a function of stress. The K - θ model was selected for this study.

$$E_R = K \cdot \theta^n \quad (4.1)$$

where

E_R = resilient modulus = E_{AB} ,

K = constant,

n = stress sensitivity parameter,

θ = bulk stress, = $\sigma_1 + 2 \cdot \sigma_3$,

σ_1 = major principal stress, and

σ_3 = minor principal stress.

In general, it is expected that the base material moduli will increase as moisture content decreases, the bulk stress increases or the amount of material passing the 0.075 mm sieve decreases. The lab data shows that the Cl. 6 Sp. exhibited a higher modulus than the Cl. 5 Sp.

and Cl. 3 Sp. below a bulk stress of 70 kPa, Figure 4.23 [50]. The lab moisture content and density of the base material is given in Table 4.12. Also evident was the increase in the moduli with increasing bulk stress and higher moduli values at lower moisture contents. The dry density also affects the modulus as shown by the Cl. 6 Sp. material.

An inherent assumption when comparing base materials is that the modulus of the coarser material should not decrease as much during the thaw period and should recover more quickly due to the higher permeability. This assumption has not been well-supported in the backcalculated layer moduli.

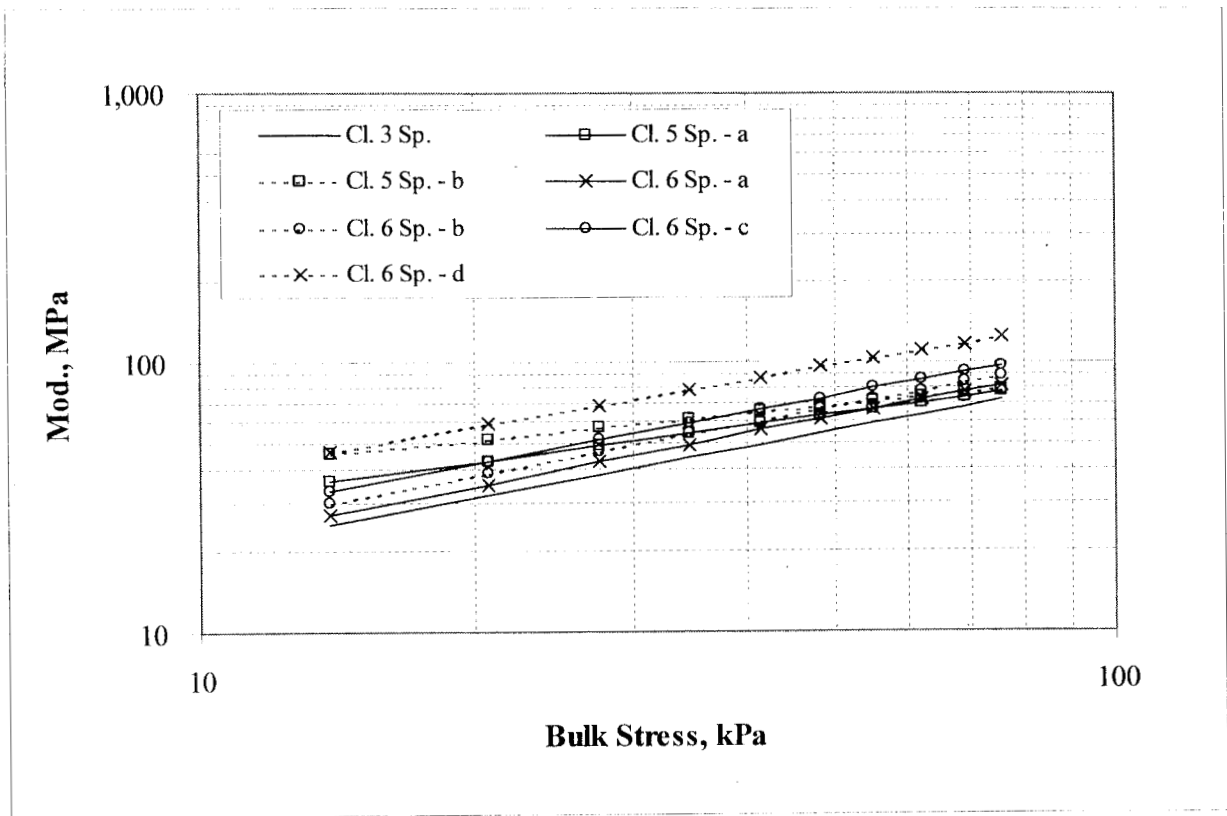


Figure 4.23. Illinois modulus models [50] for Mn/ROAD base materials.

Table 4.12. Moisture and density of materials used in Illinois study [50].

Base Material	Moisture Content, %	Density, g/cm ³
Cl. 3 Sp.	7.0	2.04
Cl. 5 Sp. – a	6.8	2.19
Cl. 5 Sp. – b	7.7	2.23
Cl. 6 Sp. – a	6.3	2.15
Cl. 6 Sp. – b	5.4	2.13
Cl. 6 Sp. – c	7.3	2.10
Cl. 6 Sp. – d	6.3	2.23

Backcalculated Base Layer Moduli

The seasonal trends in moduli for the various base materials at Mn/ROAD are similar. As was previously mentioned, the modulus values cycle from a maximum in the winter to a minimum during the early spring thaw period (Table 4.13). However, the relative magnitude of the modulus values for the different base materials are not as expected. It would seem reasonable that a crushed granite material such as the Cl. 6 Sp. found in test sections 22, 24 and 27 would have a higher modulus than Cl.3 Sp., Cl. 4 Sp. or Cl. 5 Sp. which have more fine-grained material as well as higher moisture contents. It also seems reasonable to expect that the Cl. 6 Sp. modulus would not decrease as greatly during the spring thaw since it has a lower moisture content and fewer fines. These expected results were not measured with the FWD at test section 22, as shown in Table 4.13. It is also evident from the data in Table 4.13 that for a thinner HMA pavement, the modulus of the base layer is higher than for a thicker HMA pavement. This is due to the higher bulk stress in the thinner HMA pavements.

Table 4.13. Seasonal distribution of base layer moduli at Mn/ROAD.

Test Section	Season I Winter		Season II Early Spring		Season III Late Spring		Season IV Summer		Season V Fall	
	Mod.	COV	Mod.	COV	Mod.	COV	Mod.	COV	Mod.	COV
	MPa	%	MPa	%	MPa	%	MPa	%	MPa	%
Thin (HMA < 150 mm)										
1	5500	-	151	21	156	13	171	11	177	17
2	5500	-	145	14	158	16	181	9	178	17
3	5500	-	144	26	167	17	213	14	193	16
Thick (HMA > 150 mm)										
16	5500	-	138	24	162	21	200	9	211	15
17	5500	-	119	24	146	17	189	9	191	13
19	5500	-	127	23	149	18	185	9	192	15
20	5500	-	103	28	144	14	192	11	180	10
21	5500	-	137	18	176	19	211	13	197	18
22	5500	-	88	35	132	40	183	20	157	27
Thin (HMA < 150 mm)										
24 [*]	417	198	671	92	545	34	461	26	548	31
27	416	29	126	32	177	26	190	44	195	16
28	2898	75	102	28	142	18	140	21	156	15
30	5471	4	161	41	262	21	262	22	299	19
31	4742	30	107	19	131	11	146	15	155	13

^{*} indicates subgrade with a design R-value = 70

- indicates maximum modulus value was reached

The stresses in the pavement were calculated after the modulus was estimated in EVERCALC, and from these the bulk and deviator stresses were calculated. The bulk stress in the middle of the aggregate base layers are shown in Table 4.14. Typically the bulk stress is the greatest in Season IV, due to higher stress transferred to the base layer in summer when the HMA layer stiffness is lower.

Table 4.14. Seasonal distribution of bulk stresses in aggregate base layers.

Season	Bulk Stress, kPa			
	Cl. 3 Sp. Test Section 17	NA	Cl. 5 Sp. Test Section 21	Cl. 6 Sp. Test Section 22
Thick (HMA > 150 mm)				
II	31	NA	34	48
III	26	NA	31	31
IV	32	NA	41	39
V	30	NA	31	34
Thin (HMA < 150 mm)				
Season	Cl. 3 Sp. Test Section 30	Cl. 4 Sp. Test Section 1	Cl. 5 Sp. Test Section 28	Cl. 6 Sp. Test Section 27
II	62	32	119	128
III	14	27	94	83
IV	26	34	117	108
V	21	28	104	104

Table 4.15 shows the seasonal factors used to characterize the seasonal trends in the base layer moduli. On average, the base modulus in Season II is less stiff by 65% of the Season V value, and in Season II, and by 85% in Season III. The seasonal modulus values are at a maximum value in Season I when the pavement is frozen.

Table 4.15. Seasonal factors for the aggregate base layer.

Test Section	Season I Winter	Season II Early Spring	Season III Late Spring	Season IV Summer	Season V Fall
Thin (HMA < 150 mm)					
1	31	0.85	0.85	0.97	1
2	31	0.81	0.89	1.02	1
3	28	0.75	0.87	1.10	1
Thick (HMA > 150 mm)					
16	26	0.65	0.77	0.95	1
17	29	0.62	0.76	0.99	1
19	29	0.66	0.78	0.96	1
20	31	0.57	0.80	1.07	1
21	28	0.70	0.89	1.07	1
22	35	0.56	0.84	1.17	1
Thin (HMA < 150 mm)					
24 ^c	1	1.2	1.0	0.84	1
27	2	0.65	0.91	0.97	1
28	19	0.65	0.91	0.90	1
30	18	0.54	0.88	0.88	1
31	31	0.69	0.85	0.94	1

^c indicates subgrade with design R - value = 70

It is possible that the backcalculation method may not be addressing certain issues. The method assumes the pavement layers are linear elastic, meaning that the modulus is defined by a linear relationship between the stress and strain shown by section A of the curve in Figure 4.24. It may be that the stress in the base exceeds the elastic range, shown by section B of the curve in Figure 4.24.

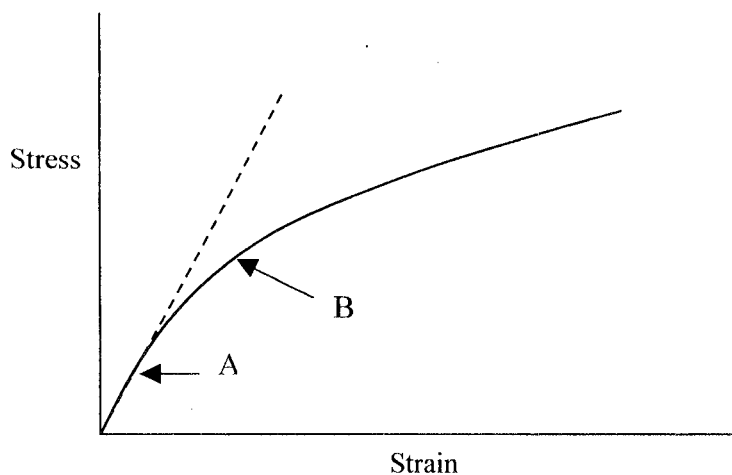


Figure 4.24. Linear (A) and non-linear (B) stress-strain relationships.

From the Illinois study [50] it was expected that the Cl. 6 Sp. base material would have the greatest modulus followed by Cl. 5 Sp., Cl. 4 Sp., and Cl. 3 Sp., respectively (Figure 4.23). It was also estimated that for the same base material, the thin pavement structures would have higher bulk stresses and therefore greater moduli (Figure 4.23). Table 4.16 shows that the backcalculated layer moduli do not always follow these expectations. The modulus of the Cl. 6 Sp. for test section 22 is lower than that of the thick and thin Cl. 5 Sp. and Cl. 3 Sp. pavement structures. Test section 24 has a much greater moduli than test section 22, possibly due to the sand subgrade. Also, the thin pavement structure with Cl. 5 Sp. (test section base material has a lower base modulus than the thick pavement structure. For the test sections in which the layer modulus backcalculated is questionable, there is a lack of other test sections for comparison.

Therefore, it can be concluded that backcalculated layer moduli may not follow the estimated trends in the modulus measured in the laboratory.

Table 4.16. Mean base layer moduli (MPa) for thick and thin pavements.

	Cl. 3 Sp.	Cl. 4 Sp.	Cl. 5 Sp.	Cl. 6 Sp.	
Thick Pavements (HMA > 150 mm)					
Test Sections	16,17,19,20	-	21	22	
HMA thickness	200 mm	-	200 mm	200 mm	
AB thickness	710 mm	-	585 mm	460 mm	
Season I	5500	-	5500	5500	
Season II	122	-	137	88	
Season III	150	-	176	132	
Seasons IV & V	193	-	204	183	
Thin Pavements (HMA < 150 mm)					
Test Sections	30	1	28	24	27
HMA thickness	125 mm	145 mm	75 mm	75 mm	75 mm
AB thickness	305 mm	840 mm	330 mm	100 mm	280 mm
Season I	5500	5500	5500	5500	5500
Season II	161	144	102	670	126
Season III	262	167	142	545	177
Seasons IV & V	299	203	148	505	193

The volumetric moisture content of the base layers was investigated for its effect on modulus. The moisture content of the aggregate base layers in the test sections show that the Cl. 6 Sp. layer has the lowest volumetric moisture content, followed by Cl. 5 Sp. and Cl. 3 Sp, (summarized in Tables 4.17 through 4.22).

Table 4.17. Volumetric moisture content (%) for test section 22 (thick) with Cl. 6 Sp.

Month	Aggregate Base Layer			Subgrade Layer			
	341, mm	488, mm	640, mm	933, mm	1237, mm	1536, mm	2240, mm
JAN	8	8	11	23	31	34	17
FEB	8	7	9	15	18	22	17
MAR	11	11	14	21	23	25	17
APR	13	13	18	30	33	31	17
MAY	13	14	20	38	40	38	19
JUN	13	14	19	34	37	35	19
JUL	13	14	20	-	-	-	19
AUG	13	14	18	36	40	36	19
SEP	13	14	18	35	39	36	19
OCT	13	13	18	33	38	35	19
NOV	12	13	18	33	34	33	18
DEC	8	8	12	29	34	36	19

Table 4.18. Volumetric moisture content (%) for test section 27 (thin) with Cl. 6 Sp.

Month	A. Base	Subgrade Layer					
	308, mm	472, mm	600, mm	930, mm	1234, mm	1515, mm	2289, mm
JAN	10	16	18	18	25	31	32
FEB	8	14	16	18	19	26	32
MAR	15	25	27	25	21	29	31
APR	17	35	36	35	28	31	32
MAY	20	34	35	32	-	34	33
JUN	18	33	38	34	34	31	34
JUL	17	30	36	36	-	34	34
AUG	17	32	36	35	-	31	34
SEP	17	31	35	34	-	34	34
OCT	19	31	33	33	-	33	34
NOV	12	28	29	29	-	31	35
DEC	9	17	20	32	-	34	31

Table 4.19. Volumetric moisture content (%) for test section 21 (thick) with Cl. 5 Sp.

Month	Aggregate Base Layer			Subgrade Layer			
	311, mm	451, mm	604, mm	896, mm	1207, mm	1518, mm	2420, mm
JAN	11	12	12	27	30	36	30
FEB	10	12	11	17	15	23	22
MAR	15	15	16	25	21	24	27
APR	17	18	21	36	35	34	26
MAY	18	20	21	-	39	39	30
JUN	18	19	21	40	33	34	26
JUL	19	21	23	-	-	-	33
AUG	19	20	21	-	38	35	28
SEP	18	20	21	40	37	35	30
OCT	18	19	21	38	35	33	29
NOV	17	19	20	36	33	36	28
DEC	12	12	13	29	31	36	29

Table 4.20. Volumetric moisture content (%) for test section 28 (thin) with Cl. 5 Sp.

Month	A. Base	Subgrade Layer					
	323, mm	469, mm	622, mm	920, mm	1256, mm	1536, mm	2490, mm
JAN	-	-	-	-	-	-	-
FEB	10	14	14	17	21	27	33
MAR	-	-	-	-	-	-	-
APR	-	-	33	-	-	-	37
MAY	22	36	35	-	-	-	36
JUN	-	-	-	-	-	-	-
JUL	23	33	33	-	-	-	32
AUG	19	-	-	-	-	-	-
SEP	20	32	31	36	31	34	31
OCT	20	32	32	-	-	-	34
NOV	17	29	29	-	-	-	33
DEC	-	-	-	-	-	-	-

Table 4.21. Volumetric moisture content (%) for test section 17 (thick) with Cl. 3 Sp.

Month	Aggregate Base Layer			Subgrade Layer			
	326, mm	472, mm	631, mm	936, mm	1234, mm	1539, mm	2460, mm
JAN	14	14	14	18	25	32	41
FEB	11	12	11	14	14	19	38
MAR	20	19	19	21	21	22	42
APR	23	24	24	33	29	30	39
MAY	24	26	25	33	33	34	40
JUN	26	25	27	35	39	39	42
JUL	26	26	26	36	40	39	43
AUG	25	25	26	35	38	39	41
SEP	26	25	27	37	-	-	-
OCT	26	24	27	35	39	38	-
NOV	23	22	24	31	35	34	40
DEC	14	14	16	23	32	34	44

Table 4.22. Volumetric moisture content (%) for test section 30 (thin) with Cl. 3 Sp.

Month	A. Base	Subgrade Layer					
	302, mm	472, mm	619, mm	924, mm	1234, mm	1533, mm	2460, mm
JAN	14	21	18	25	34	36	37
FEB	17	19	17	21	23	28	34
MAR	22	30	25	24	26	27	33
APR	27	36	34	37	37	33	34
MAY	29	35	37	39	35	32	32
JUN	35	-	35	-	36	34	37
JUL	28	-	36	-	39	36	-
AUG	27	39	36	-	39	37	-
SEP	26	36	35	-	38	37	34
OCT	26	35	34	38	36	35	-
NOV	21	32	30	-	34	32	39
DEC	15	20	20	32	32	32	35

The density of the base layer material, as determined by the sand cone test, was investigated. Table 4.23 shows that the material with the highest density was the Cl. 5 Sp. base material, followed by Cl. 6 Sp., Cl. 4 Sp. and Cl. 3 Sp. The higher density of the Cl. 5 Sp. material may cause the Cl. 5 Sp. modulus to be greater than the Cl. 6 Sp., however this cannot be confirmed with the data presented here.

Table 4.23. Mean dry density and moisture content from sand cone test data.

Test Section	Aggregate Base Material	Mean Moisture Content, %	Mean Dry Density, g/cc
1	Cl. 4 Sp.	8.06	2.068
16	Cl. 3 Sp.	8.03	2.062
17	Cl. 3 Sp.	8.06	2.068
19	Cl. 3 Sp.	8.04	2.063
20	Cl. 3 Sp.	8.10	2.078
21	Cl. 5 Sp.	8.40	2.156
22	Cl. 6 Sp.	8.18	2.100
24	Cl. 6 Sp.	8.15	2.092
27	Cl. 6 Sp.	8.30	2.129
28	Cl. 5 Sp.	8.55	2.193
30	Cl. 3 Sp.	7.96	2.042

Backcalculation Input Sensitivity Analysis

A sensitivity analysis was performed to evaluate the effect of varying the weighting factors on the sensors in the backcalculation process for a thick and a thin pavement structure. Trials were run in which the sensor data were weighted differently and in some cases, the subgrade and HMA modulus were set at a constant value. Table 4.24 and Figure 4.25 show that for a thick pavement (without setting the subgrade modulus) the aggregate base and soil subgrade modulus values will vary from 70 to 190 MPa for a day in October, depending on the weighting factors for the sensors used in the backcalculation process. Using 7 sensors gives a base modulus value of 136 MPa while the use of 9 sensors gives a base modulus value of 191 MPa. For this pavement, the aggregate base modulus (E_{AB}) is less than the subgrade modulus (E_{SG}) until 8 sensors are used.

The input into the backcalculation program with the most significant influence on the layer moduli is the number of sensors and the weighting of the sensors. Using 7 sensors instead of 6 leads to an increase in the estimate of layer moduli. This was seen using deflections in June and July for test section 28 (thin pavement with Cl. 5 Sp.), in which 6 sensors gave a base modulus of 100 MPa and 7 sensors gave a base modulus of 135 MPa.

Table 4.24. Test section 21 – thick pavement layer moduli.

Trial	Sensors	Weighting Factors	No. of Sensors	Backcalculated Modulus, MPa		
				E_{HMA}	E_{AB}	E_{SG}
A	1-3	0.33	3	6,165	111	264
B	1-4	0.25	4	6,168	90	327
C	1-5	0.2	5	6,455	70	424
D	1-6	0.17	6	5,921	105	184
E	1-7	0.14	7	5,564	124	160
F	1-8	0.125	8	4,910	156	136
G	1-9	Uniform	9	4,251	191	123
G2	1-6,8	0.14	7	5,747	136	51

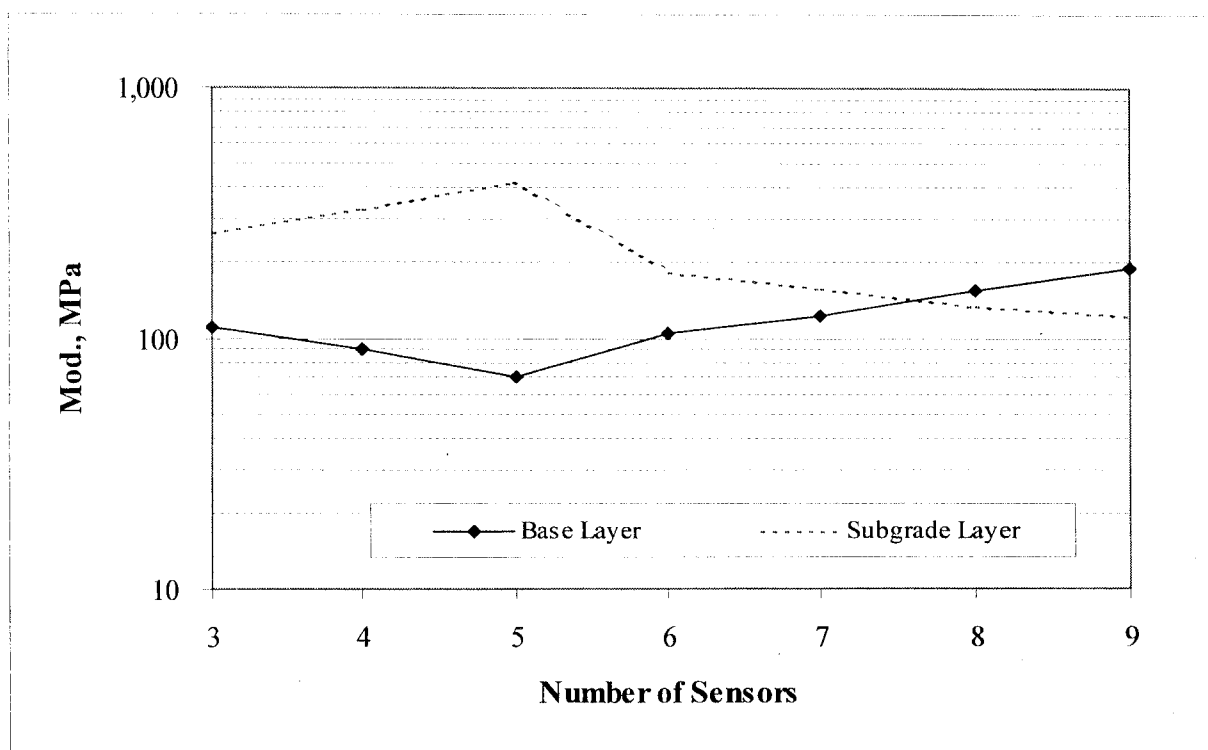


Figure 4.25. Modulus sensitivity for thick pavement, Cl. 5 Sp.

It is shown in Table 4.25 and Figure 4.26 that, for a thin pavement with the same base material (Cl. 5 Sp.), E_{GB} was calculated at 151 and 171 MPa for seven and nine sensors, respectively. Table 4.26 also shows a large variance in E_{HMA} , depending on the number of sensors used. The subgrade modulus values stay between 79 and 107 MPa as opposed to the thick pavement subgrade modulus which range from 51 and 424 MPa.

Table 4.25. Test section 28 – thin pavement layer moduli.

Trial	Sensors	Weighting Factors	No. of Sensors	Backcalculated Modulus, MPa		
				E_{HMA}	E_{AB}	E_{SG}
H	1-3	0.33	3	11,790	91	107
I	1-4	0.25	4	11,074	105	91
J	1-5	0.2	5	10,873	107	89
K	1-6	0.17	6	11,084	104	90
L	1-7	0.14	7	9,832	119	87
M	1-8	0.125	8	8,063	142	83
N	1-9	Uniform	9	6,507	171	79
N2	1-6,8	0.14	7	7,622	151	82

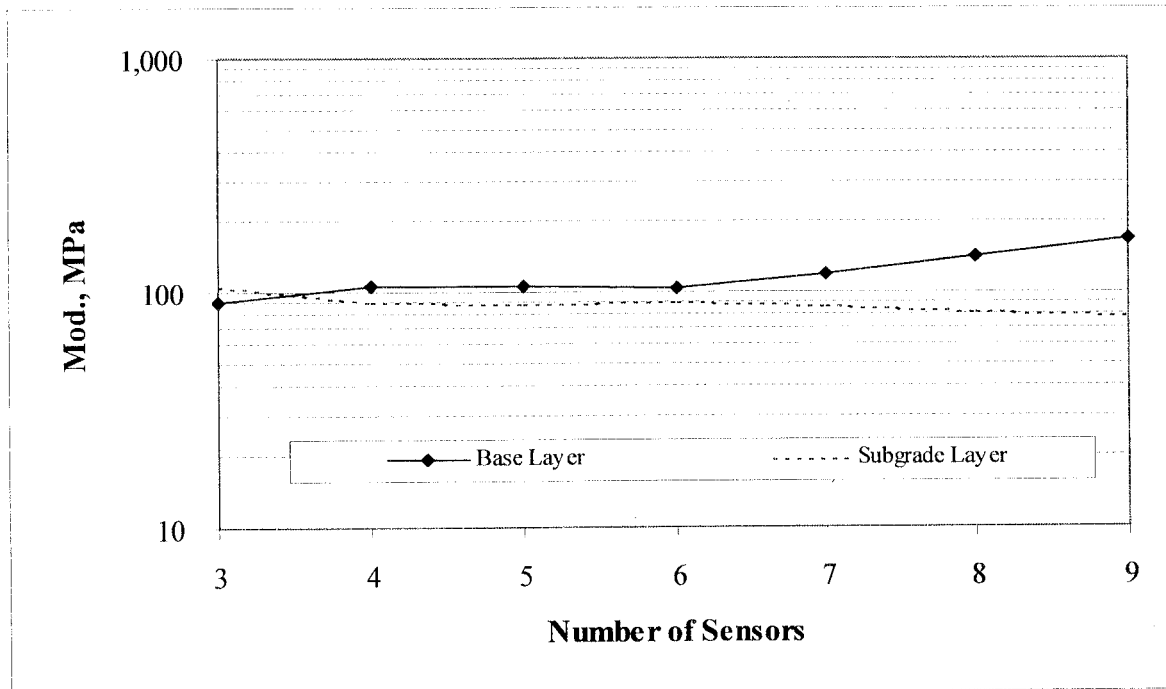


Figure 4.26. Modulus sensitivity for thin pavement, Cl. 5 Sp.

Another set of trials was conducted by estimating the HMA modulus from the exponential relationship described earlier and setting it as a constant. Table 4.26 and Figure 4.27 show that for a thin pavement with E_{HMA} set as a constant, the difference between 7 and 9 sensors is minimized. For a thick pavement, setting E_{HMA} does not have as significant an influence since the backcalculated E_{HMA} is fairly constant between 4,251 and 6,455 MPa.

Table 4.26. Test section 28 – thin pavement moduli with E_{HMA} set at 6,000 MPa.

Trial	Sensors	Weighting Factors	No. of Sensors	Backcalculated Modulus, MPa		
				E_{HMA}	E_{AB}	E_{SG}
O	1-3	0.33	3	6,000	253	60
P	1-4	0.25	4	6,000	203	70
Q	1-5	0.2	5	6,000	177	77
R	1-6	0.17	6	6,000	152	84
S	1-7	0.14	7	6,000	150	84
T	1-8	0.125	8	6,000	159	82
U	1-9	Uniform	9	6,000	173	79
U2	1-6,8	0.14	7	6,000	166	80

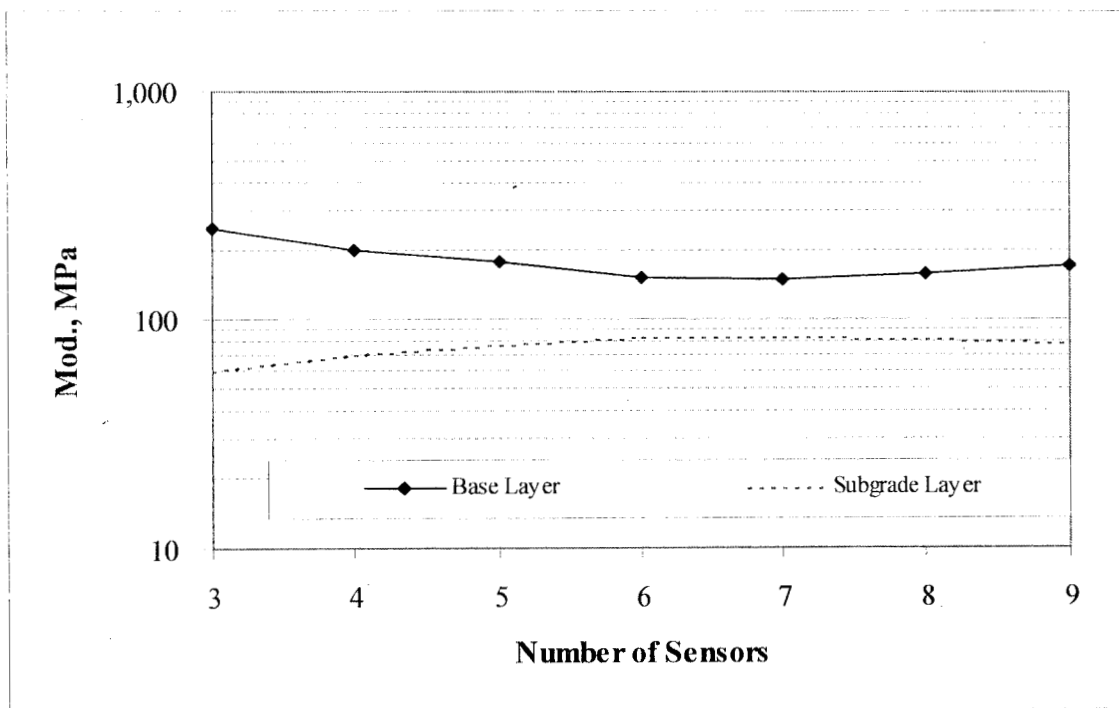


Figure 4.27. Modulus sensitivity for thin pavement, Cl. 5 Sp., $E_{HMA} = 6000$ MPa.

From this analysis, it is evident that the program used to backcalculate the layer moduli is sensitive to the number of sensors used and the non-linearities that are prevalent in the subgrade and base layers. Another issue that might influence the behavior of the pavement is the condition of the surface of the pavement structure. It may be that the moduli of the layers are affected by the presence of thermal or fatigue cracks as well as the stage of crack growth. It stands to reason that if a crack has progressed through the pavement surface, that the corresponding deflections measured will be greater than those of a sound pavement surface.

Seasonal Variations in Backcalculated Subgrade Layer Moduli

The subgrade backcalculated moduli are shown in Table 4.27 and change seasonally such that the maximum is typically reached in Seasons I and II, the minimum is in Seasons III and IV, and again, Season V is used as a baseline value that the other seasons are compared. The mean soil subgrade moduli values are shown in Table 4.28 for the thick and thin pavements. Non-linearities in the subgrade soil are apparent in the modulus values between the thick and thin pavements and between the different subgrade materials. It seems that the subgrade layer modulus is greater in the thick pavements (HMA > 150 mm) compared to the thinner pavements (HMA < 150 mm), possibly due to the stress-softening of the fine-grained subgrade soil when it is subject to greater deviator stress under higher loads. The deviator stress is calculated at the top of the subgrade layer and is higher in Season IV, Table 4.29.

In a fine-grained material, the modulus decreases when the deviator stress is increased and this is especially apparent in the full-depth test sections with a clayey subgrade. It is apparent that a sand subgrade (test section 25) is stiffer than a fine-grained subgrade (test section 26) as was expected. The full depth test sections 14 and 15 have a significantly lower modulus than the

other thick pavement subgrades, possibly due to the absence of an aggregate base layer and the consequential increase in the deviator stress in the subgrade.

The seasonal variation in the subgrade modulus for the various test sections analyzed are given in Table 4.30. In general, the average seasonal factor for the fine-grained subgrade was 75% in Season III and 70% in Season IV compared to Season V. In general, the sand subgrade did not vary in stiffness relative to Season V.

Table 4.27. Seasonal distributions of the subgrade backcalculated modulus, MPa.

Test Section	Season I Winter		Season II Early Spring		Season III Late Spring		Season IV Summer		Season V Fall	
	Mod.	COV, %	Mod.	COV, %	Mod.	COV, %	Mod.	COV, %	Mod.	COV, %
Thin (HMA < 150 mm)										
1	1773	10	162	114	55	29	30	33	67	26
2	1723	16	198	91	61	21	50	22	79	20
3	2358	12	251	94	69	25	52	30	86	19
Thick (HMA > 150 mm)										
4*	5500	-	509	-	92	-	99	-	153	-
14*	5500	-	323	-	79	-	107	-	138	-
15*	5500	-	342	-	82	-	111	-	140	-
16	1800	7	268	66	104	23	100	13	129	14
17	1992	7	353	57	102	23	94	18	130	13
19	2234	5	331	68	109	26	107	21	136	18
20	2581	4	392	60	100	26	78	36	136	13
21	2303	6	322	61	114	20	118	16	138	14
22	1834	10	314	67	103	24	102	18	140	16
Thin (HMA < 150 mm)										
24 ^c	2438	45	158	51	141	12	148	11	126	13
25 ^{**}	1041	23	216	-	170	-	173	-	165	-
26 [*]	5114	25	234	-	93	-	71	-	118	-
27	3500	-	164	100	52	22	59	31	76	22
28	2976	28	174	102	53	26	58	28	75	22
30	1541	32	144	100	47	35	43	41	56	33
31	2449	34	167	92	63	23	73	25	83	19

^c indicates subgrade with R70

* indicates full – depth pavement

- indicates maximum modulus value was reached

Table 4.28. Mean subgrade modulus, MPa, for all test sections.

Subgrade Designed R-value	Mean Subgrade Modulus, MPa				
	Season I Winter	Season II Early Spring	Season III Late Spring	Season IV Summer	Season V Fall
R-Value =12 thin HMA layer	2,993	223	65	59	88
R-Value =12 thick HMA layer	2,968	331	99	102	136
R-Value = 70 thin HMA layer	1,739	187	155	160	145

Table 4.29. Seasonal distributions of the deviator stress, kPa.

Test Section	Season I Winter		Season II Early Spring		Season III Late Spring		Season IV Summer		Season V Fall	
	σ_d	COV, %	σ_d	COV, %	σ_d	COV, %	σ_d	COV, %	σ_d	COV, %
Thin Pavements (HMA < 150 mm)										
1	19	7	13	41	10	36	8	33	11	34
2	20	10	13	41	11	41	11	33	12	35
3	18	6	12	46	9	39	8	35	10	34
Thick Pavements (HMA > 150 mm)										
4*	238	24	33	62	34	67	93	46	53	42
14*	169	29	20	62	20	75	66	38	35	42
15*	163	31	19	59	17	71	51	46	29	47
16	22	4	12	39	11	40	15	37	13	37
17	23	3	12	39	11	39	14	36	13	36
19	24	2	12	38	12	39	15	36	13	37
20	26	2	11	35	12	38	14	40	15	36
21	32	3	15	40	15	39	20	35	17	36
22	35	22	15	41	17	43	25	36	19	37
Thin Pavements (HMA < 150 mm)										
24 ^c	90	51	91	28	103	27	126	24	96	29
25 ^{c*}	170	25	76	38	90	41	150	32	92	47
26*	245	14	75	50	63	52	83	61	80	42
27	79	21	46	31	40	27	48	35	46	25
28	71	23	40	29	37	25	43	27	40	23
30	42	14	25	31	20	28	24	38	23	28
31	53	20	33	27	31	23	36	25	33	22

^c indicates subgrade with R-value = 70

* indicates full depth pavement

Table 4.30. Seasonal factors for subgrade layers.

Subgrade Designed R-value	Seasonal Design Factor				
	Season I Winter	Season II Early Spring	Season III Late Spring	Season IV Summer	Season V Fall
R-Value =12 thin HMA layer	33	2.5	0.75	0.68	1
R-Value =12 thick HMA layer	22	2.4	0.73	0.75	1
R-Value = 70 thin HMA layer	13	1.3	1.1	1.1	1

Summary

This section discussed the variations in predicted and backcalculated pavement layer moduli. Factors were used to determine seasonal trends in the stiffness of the pavement layers in each test section. In general, the HMA layer was soft during the summer months, the aggregate base layer was soft during the thaw period, and the subgrade layer was soft in the spring and summer months.

The backcalculated HMA modulus is dependent on the stiffness of the AC, the thickness of the layer and temperature. The condition of the pavement surface with respect to cracking also affects the stiffness. It was shown that it is difficult to backcalculate the pavement layer moduli when the HMA layer thickness is less than the plate radius used to in the deflection testing (in this study it was 150 mm).

The amount of fine material in the subgrade affects the backcalculated modulus. The clean sand subgrade was stiffer than the fine-grained subgrade and also behaved as a coarse-grained material by increasing in stiffness with an increase in bulk stress. It was shown that the stiffness of the similar fine-grained subgrade material used at Mn/ROAD is lower in a full-depth pavement due to higher deviator stress than in the pavements with an aggregate base layer.

Also, it was found that the method of backcalculation has a significant influence on the results of the backcalculated layer moduli. It was expected that for a base material with fewer fines, lower moisture content and a similar level of compaction would have a higher modulus than that of a base material without these characteristics. This was not always evident in the backcalculated data that were evaluated at the Mn/ROAD site, especially for the thicker test sections. For this reason it is suggested that more research is needed concerning backcalculation.

CHAPTER FIVE

RESULTS AND DISCUSSION OF GREATER MINNESOTA DATA

Introduction

It has been recognized in many flexible design procedures that seasonal fluctuations of pavement layer moduli vary with changing climatic conditions. These variations can affect the design input and output of a flexible pavement structure. One of the primary goals of the LTPP SMP sites is to monitor seasonal changes in the pavement layer moduli for design purposes [31]. The analysis method described in Chapter 3 was applied to data from the LTPP SMP [32, 33, 34] sites for the purposes of validating and extending the trends found at Mn/ROAD to the greater Minnesota area and the results are discussed in this chapter. Wherever possible, the data for all three LTPP SMP sites are shown, however, data from the Bemidji [32] site were the most complete and are shown to illustrate the main points. Figure 5.1 shows the location of the LTPP SMP sites and the location of the weather stations in Minnesota.

This chapter discusses the relationships between climate factors, subsurface environmental conditions and material mechanical properties using weather station data, environmental sensor data, and deflection data from the three LTPP sites. The results are incorporated into a M-E design process. Seasonal factors derived from Mn/ROAD were compared to those from the LTPP sites. As expected, there are differences since the majority of the Mn/ROAD cells have a clayey subgrade and the LTPP sites have a sandy subgrade.

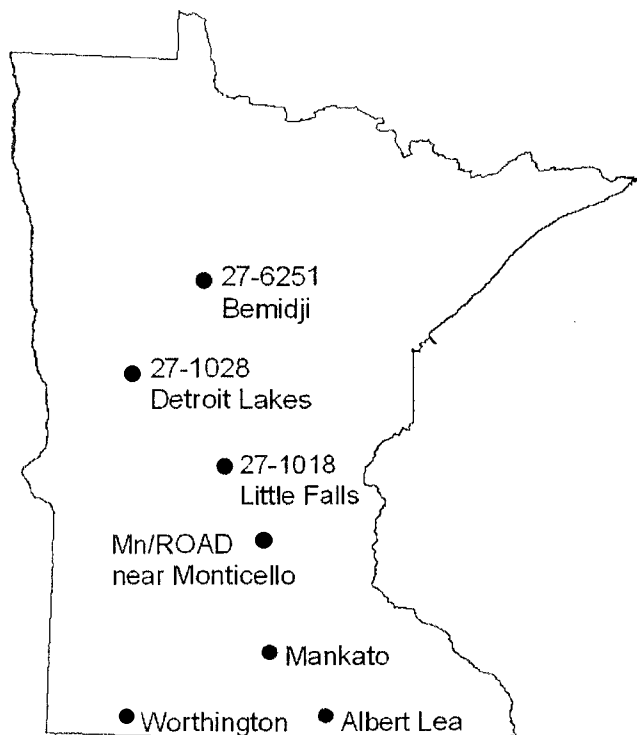


Figure 5.1. Location in Minnesota of the three LTPP SMP sites, Mn/ROAD, and the other weather stations used in this study.

Table 3.9 (in Chapter Three) shows the concept used to divide a year into five seasons based on air temperature and its affect on the stiffness of the pavement layers at the Mn/ROAD site. The same seasonal distribution is used for the analysis of the data from LTPP SMP and other Minnesota sites. The use of five seasons accounts for the weakened condition of the pavement during the spring load restriction (SLR) period, which typically begins in March in Minnesota, Table 5.1. New legislation has set the duration of the SLR at 8 weeks, unless signs are posted [58]. It is also important to note that Minnesota allows a 10% increase in the gross vehicle weight (GVW) of truck traffic during the winter months since the pavement structures

are frozen and able to carry higher loads. The increased loads are removed either March 7, or when SLR begins, whichever occurs first.

Table 5.1. Mean and standard deviation of spring load restriction placement dates in Minnesota, 1986 - 2000 [58].

	North Zone	Central Zone	Metro Zone	Southeast Zone	South Zone
Mean	Mar. 16	Mar. 12	Mar. 10	Mar. 9	Mar. 7
St. Dev., days	10	9	8	10	9

Geographic Climate Data Results

The mean temperature, precipitation and snowfall events that are measured at various weather stations throughout Minnesota were analyzed for statewide trends. Table 5.2 shows the mean monthly temperature measured from seven weather stations in Minnesota. The 30-year mean annual temperature varies from 3°C in Bemidji to 7°C in Mankato. The length and severity of the winter seasons were quantified using the FI and are shown in Table 5.3. The mean date that the FI calculation begins and the maximum value of the FI were determined from thirty years of mean daily temperature data. It can be seen in this table that the freezing season length and severity (as measured by the maximum value reached) is greatest for the north.

Precipitation and snowfall data are graphed in Figures 5.2 and 5.3, respectively, and show that the precipitation trends are similar for the three LTPP sites investigated in Minnesota. One difference is that Little Falls is slightly wetter and typically has a greater snowfall in March than the other two sites.

Table 5.2. 30-year mean monthly temperature (°C) data from weather stations in Minnesota.

Month	Bemidji	Detroit Lakes	Little Falls	Buffalo	Albert Lea	Mankato	Worthington
JAN	-16	-15	-13	-12	-11	-10	-11
FEB	-13	-11	-9	-8	-8	-7	-8
MAR	-5	-4	-2	-2	-1	0	-1
APR	4	5	7	7	7	8	7
MAY	12	13	14	14	15	15	14
JUN	17	18	19	20	20	20	20
JUL	20	20	22	22	22	22	22
AUG	18	19	21	21	21	21	20
SEP	12	14	15	16	16	16	15
OCT	6	7	8	9	9	9	8
NOV	-4	-3	-1	0	0	-1	-1
DEC	-12	-11	-9	-8	-8	-7	-8
Mean	3	4	6	7	7	7	6

Table 5.3. Duration and magnitude of winter season for cities in Minnesota, 1965-1995.

Weather station sites - ordered from north to south	Beginning Date		Maximum FI, °C-days		
	Mean	St. Dev.	Mean	St. Dev.	Date
Bemidji	8-Nov	7 Days	1508	246	28-Mar
Detroit Lakes	10-Nov	6 Days	1364	300	24-Mar
Little Falls	13-Nov	8 Days	1100	248	20-Mar
Buffalo (near Mn/ROAD)	13-Nov	8 Days	920	240	19-Mar
Albert Lea	18-Nov	8 Days	899	237	16-Mar
Mankato	18-Nov	9 Days	846	230	15-Mar
Worthington	17-Nov	7 Days	961	255	17-Mar

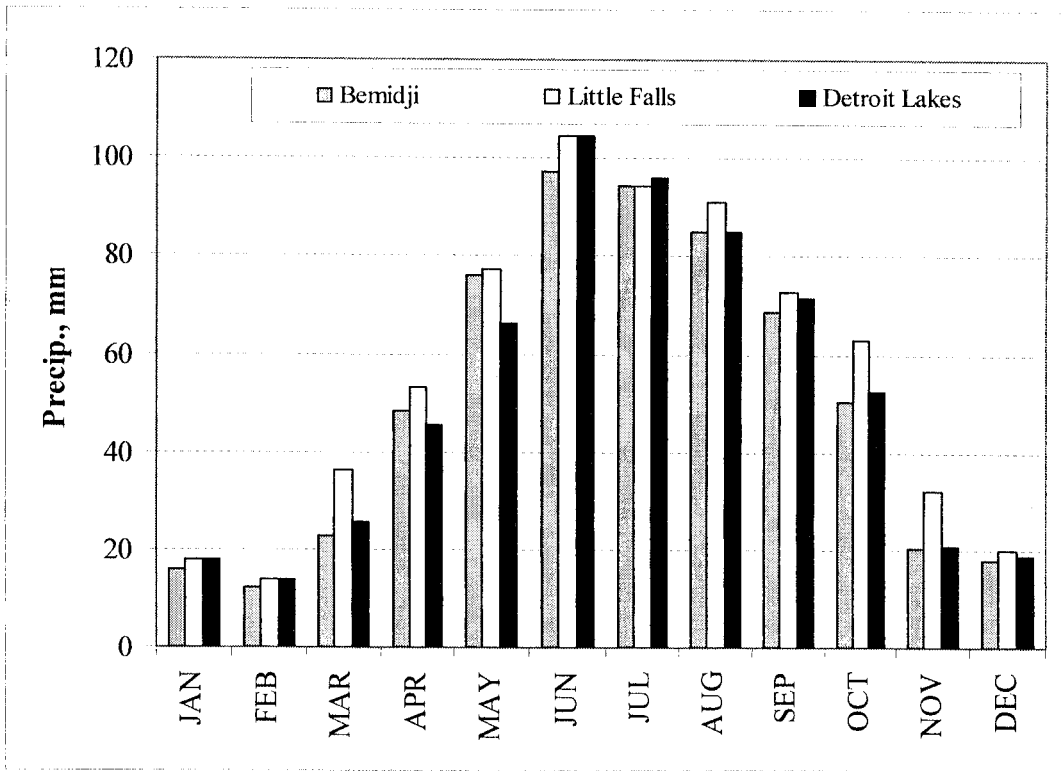


Figure 5.2. 30-year mean monthly precipitation events for the LTPP SMP sites in Minnesota.

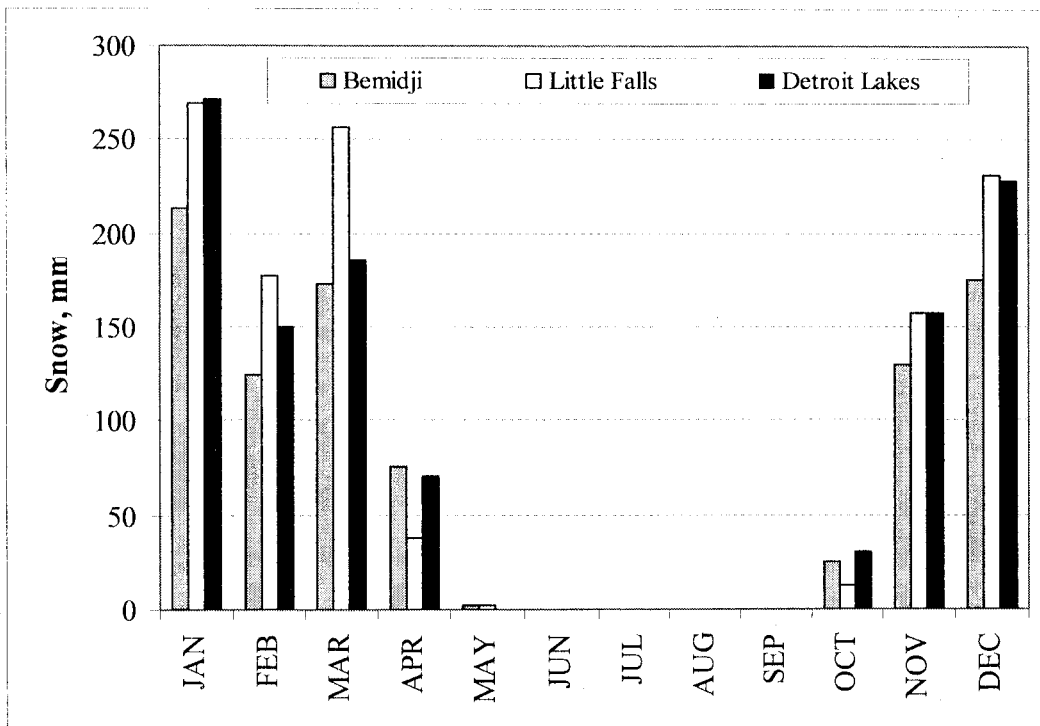


Figure 5.3. 30-year mean monthly snowfall for the LTPP SMP sites in Minnesota.

Environmental Condition Data Results

HMA Layer

As discussed previously, the temperature fluctuations in the HMA layer vary with air temperature. Equation 3.1 was used with LTPP SMP thermistor data and the results from the Bemidji site (#27-6251) for 1996 are shown in Figure 5.4. In this example, the mean surface temperature measured was 9.5°C (rather than 12°C from Mn/ROAD), however, the depth was 25 mm and the thermal diffusivity was 0.121 m²/day, similar to the Mn/ROAD analysis. It can be seen from Figure 5.4 that Equation 3.1 predicted slightly higher temperatures in the summer than the measured values, and the $R^2 = 0.89$. The sites show similar trends for 1994 through 1996.

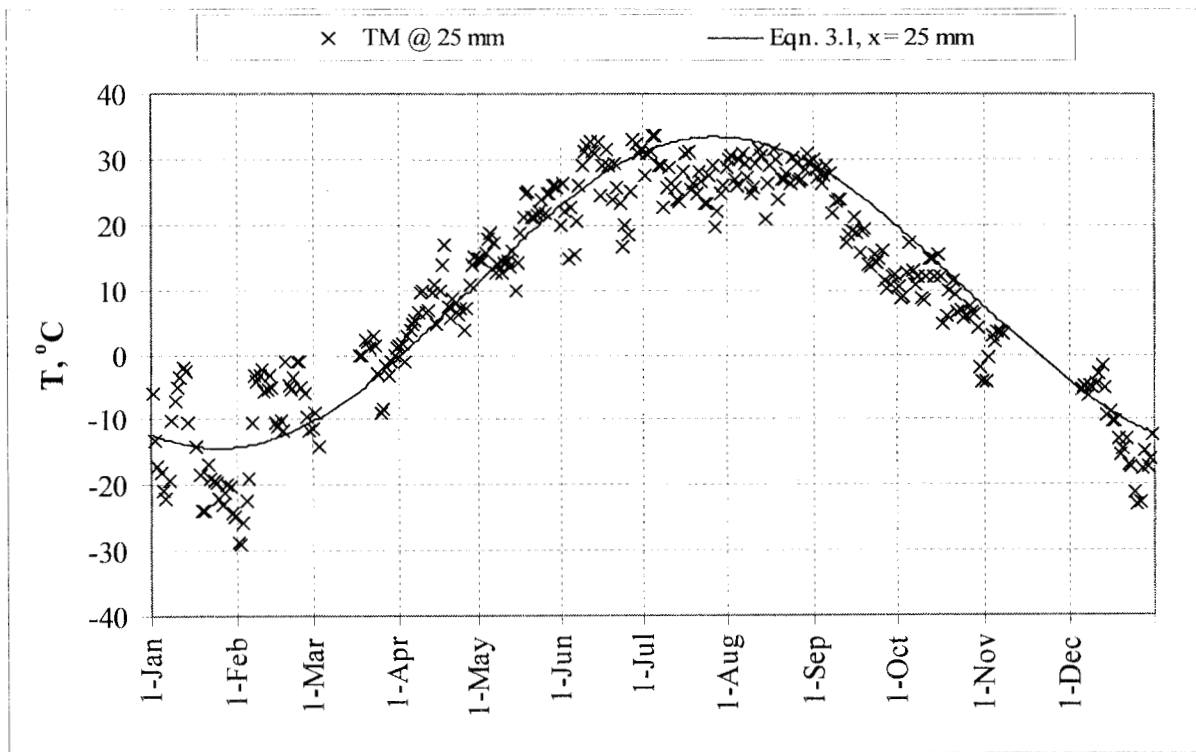


Figure 5.4. Predicted temperature using Equation 3.1 and TM temperature measured at 25 mm in the HMA layer of the Bemidji site (# 27-6251), 1996.

AB and SG Layers

Moisture Content

The LTPP SMP moisture data exhibited trends similar to those measured at Mn/ROAD. The unfrozen volumetric moisture content of the aggregate base layer decreases in the winter when the layer is frozen, increases in the early spring with thawing, and decreases slightly to a near constant level in the summer and fall. The TDR data were available between 1993 and 1995 and are shown in Tables 5.4 through 5.6. These data were measured biweekly during the thaw period, monthly throughout the remainder of the year, and were analyzed using Topp's equation [32, 33, 34]. Since the monthly moisture content measurements were fairly uniform during the summer, it was concluded that the precipitation events had little effect on the in situ moisture content.

The moisture content measured with depth of pavement varies with pavement structure and the type of material in the layers. For instance, the full-depth pavement at Detroit Lakes (#27-1028) shows a gradient in which the moisture is higher directly under the HMA layer and decreases with depth. This is in contrast with the moisture gradient found at the Little Falls (#27-1018) and Bemidji (#27-6251) structures that have an aggregate base layer, and the moisture content increases with depth of pavement. One possible explanation for this may be from the accumulation of subsurface moisture in this layer due to the impermeability of the HMA surface. Another trend noted was that in contrast to the fine-grained subgrade material at Mn/ROAD, the subgrade materials at the LTPP SMP sites are coarse-grained, sandy materials and tend to have a lower moisture content.

Table 5.4. Little Falls seasonal volumetric moisture content, %, between 8/24/93 and 6/13/95.

Layer	Depth of TD, mm	Season I: Winter	Season II: Early Spring	Season III: Late Spring	Season IV: Summer	Season V: Fall
AB	180	8	16	15	15	14
SG	330	12	12	13	12	12
	485	12	12	15	13	12
	635	14	17	20	18	15
	785	24	22	27	27	26
	940	31	18	29	32	30
	1090	25	12	25	31	30
	1245	25	22	26	25	27
	1550	27	16	21	28	27
	1855	30	24	30	30	30

Table 5.5. Detroit Lakes (full depth HMA site) seasonal volumetric moisture content, %, between 10/20/93 and 6/14/95.

Layer	Depth of TD, mm	Season I: Winter	Season II: Early Spring	Season III: Late Spring	Season IV: Summer	Season V: Fall
SG	310	NA	12	13	10	12
	460	NA	12	12	11	12
	610	NA	12	11	9	10
	760	11	15	12	9	11
	920	12	NA	12	11	12
	1085	9	NA	10	9	NA
	1220	7	NA	9	7	7

Table 5.6. Bemidji seasonal volumetric moisture content, %, between 9/15/93 and 6/15/95.

Layer	Depth of TD, mm	Season I: Winter	Season II: Early Spring	Season III: Late Spring	Season IV: Summer	Season V: Fall
AB	290	13	20	20	20	20
	445	12	17	16	17	17
SG	610	11	15	16	16	17
	750	14	13	15	15	17
	900	11	13	15	15	16
	1060	12	11	15	15	15
	1220	13	12	16	15	16
	1365	20	8	12	13	12
	1670	15	8	12	14	13
	1970	16	11	15	16	16

State of Moisture Results

The changes in the state of moisture in the unbound layers were predicted using the TI and was compared to available data measured from TMs, TDs and RPs. The following graphs use data from the Bemidji site (#27-6251) during the spring of 1995 and are representative of the trends found at each of the LTPP SMP sites. The permanent thaw period in 1995 occurred over a period of 2 to 3 days. Figure 5.5 shows that the TI value reached 15°C-days on March 10, and 30°C-days on March 11, which corresponds with the dates that the restrictions should and must be placed, respectively. Figure 5.6 shows the TM sensor values in the base layer surpassing 0°C between March 10 and March 12. Figure 5.7 and Table 5.7 show the thaw reaching a depth of 750 mm (measured from TDs) and 790 mm (measured from RPs) by March 16, and a complete thaw by April 13. The condition of the pavement structure on the days that the sensors were not read is unclear, however it is clear that the thaw occurred quickly in 1995 and this was indicated by the TI.

The thaw also occurred quickly at the Mn/ROAD site from WM sensors measurements in test section 17, Figure 5.8. This test section is composed of approximately 200 mm of HMA over 710 mm of Cl. 3 Sp aggregate base over a clayey subgrade, and is comparable to the Bemidji site that has 190 mm of HMA over 260 mm of aggregate base over a sandy subgrade. The base layer thicknesses are different, however the similar HMA layer thicknesses allow for a comparison of the thawing that occurs in the base layer. Note that the WM data were used in this study as a means to determine the depth of frost and thaw in the pavement structure, and that a decrease in the measured soil tension of an order of magnitude signaled a change in the state of moisture from a liquid to a solid state. Figure 5.7 shows thawing to a depth of 450 mm by March 12 in cell 17, similar to the Bemidji test section. It was expected that the Mn/ROAD test section would

thaw sooner since it is located further south, however it would seem that thawing at the two sites occurs almost simultaneously given the data from the spring of 1995. It is possible that the pavement at the Bemidji site thawed quickly due to the sandy subgrade and it was less susceptible to freeze-thaw cycles, however, due to the lack of data available, it is difficult to determine if this is true.

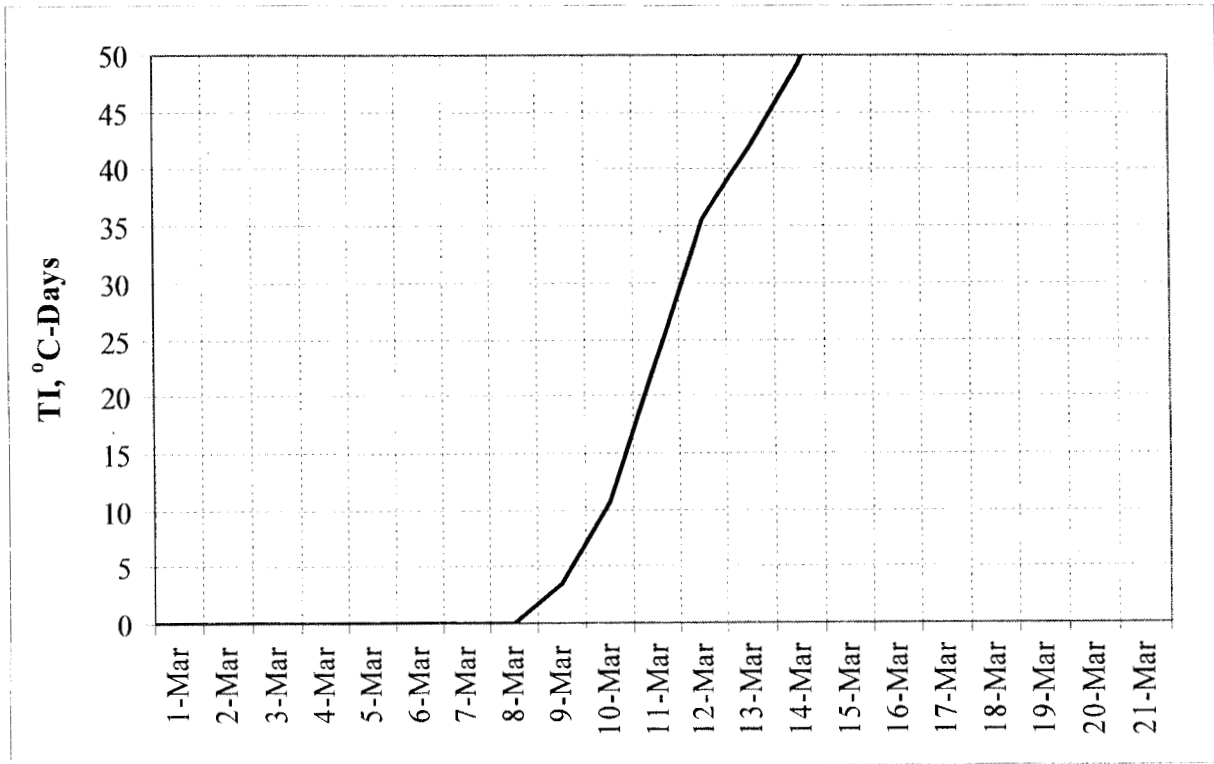


Figure 5.5. TI in Bemidji, spring 1995.

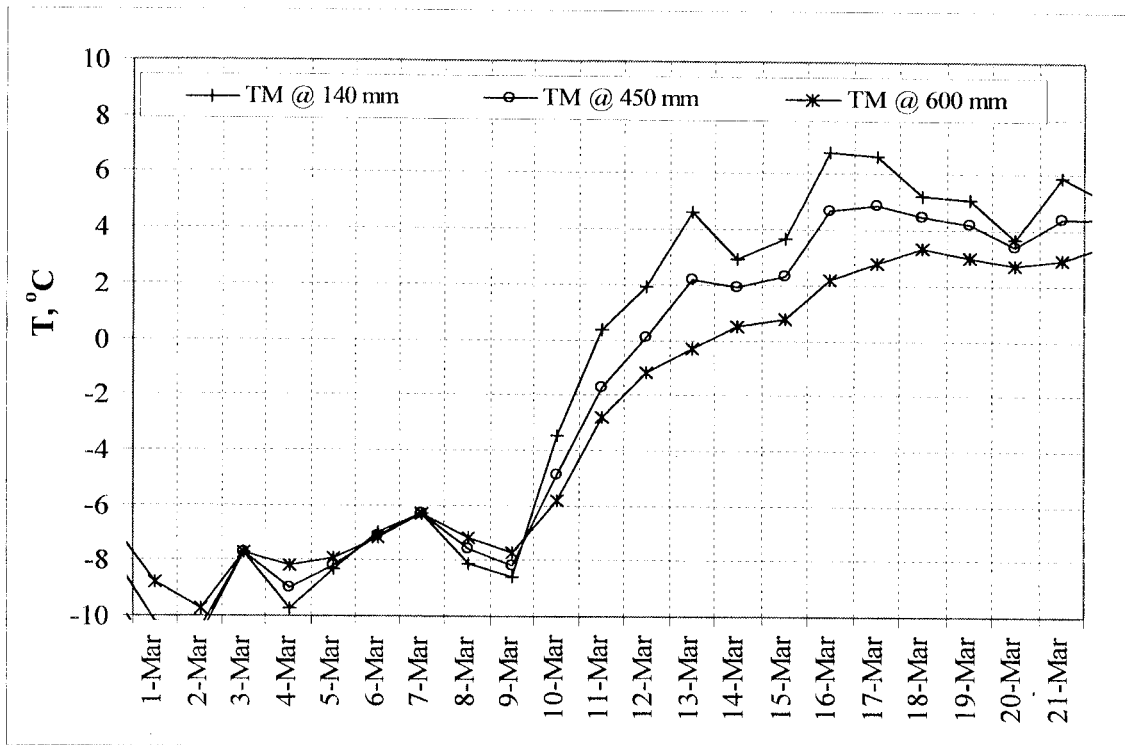


Figure 5.6. TM data from the Bemidji site (#27-6251), March 1995.

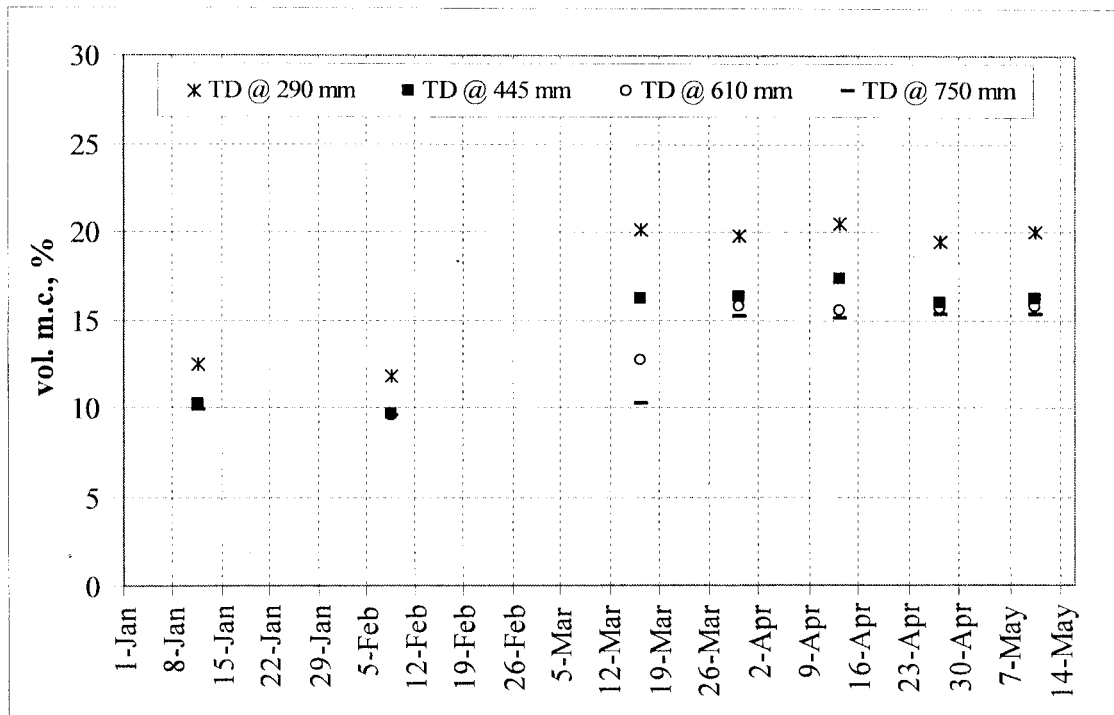


Figure 5.7. TDR data from the Bemidji site (#27-6251) beginning January 1, 1995.

Table 5.7. RP data for the three LTPP SMP sites

Site #	1994		1995	
	Date	Frozen Depth, mm	Date	Frozen Depth, mm
27-1018 Little Falls	Feb 8	0 to 1780	Not Available	
	Mar 8	Thaw is Out		
27-1028 Detroit Lakes	Feb 9	0 to 2290	Not Available	
	Mar 9	0 to 2290		
	Mar 23	1170 to 2290		
	Apr 5	1780 to 2290		
	Apr 26	Thaw is Out		
27-6251 Bemidji	Feb 16	0 to 2160	Jan 11	0 to 1780
	Mar 16	735 to 2160	Feb 8	0 to 1780
	Mar 30	1190 to 2160	Mar 16	790 to 1955
	Apr 13	1750 to 2030	Mar 30	1500 to 2030
	May 3	Thaw is Out	Apr 13	Thaw is Out

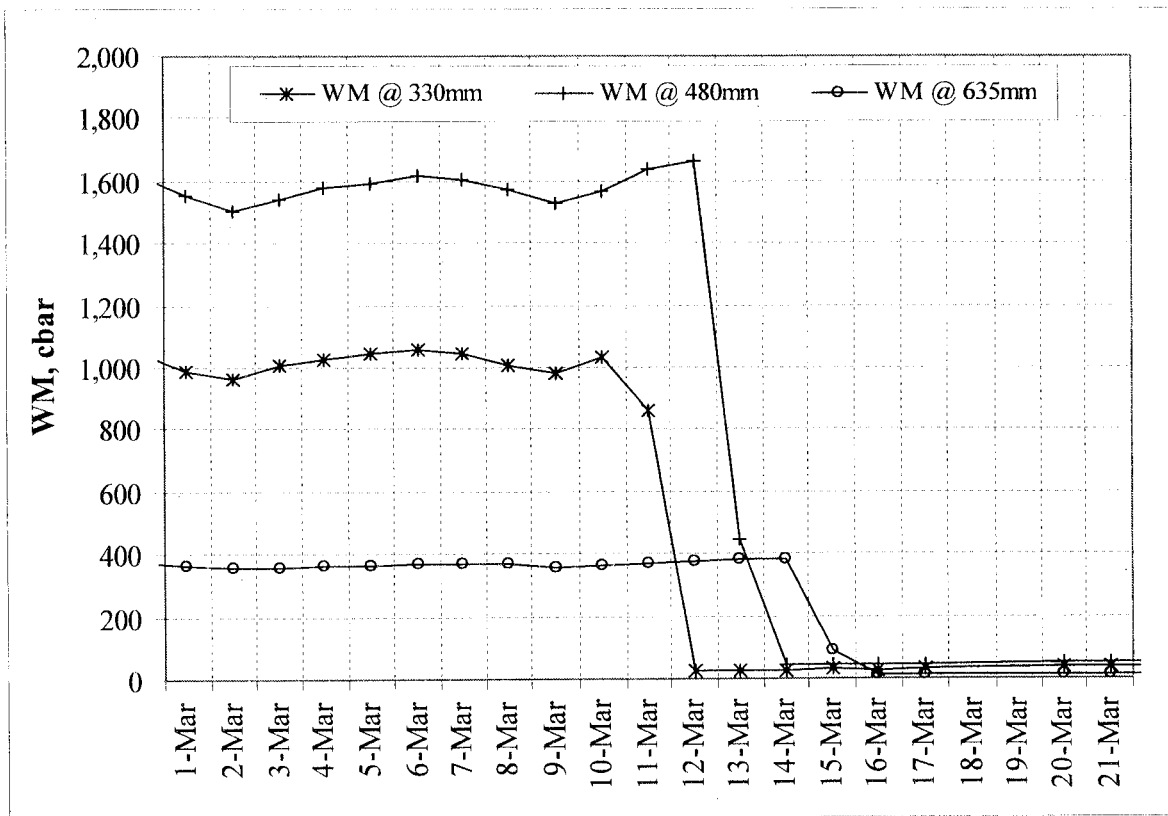


Figure 5.8. Mn/ROAD test section 17 spring 1995 frost depth data from WM sensors at 330 mm, 480 mm and 635 mm.

Pavement Layer Stiffness Results

Backcalculation Input

The pavement layer moduli were backcalculated using similar input as the Mn/ROAD data discussed in Chapter Four. Seven sensors were used to measure the deflections during the FWD testing that was performed on the three LTPP SMP sections. The pavement backcalculation program EVERCALC version 5.01 was used with the following boundaries:

- 150 mm plate radius,
- uniform sensor weighting factor,
- sensor spacing at 0, 203, 305, 457, 610, 914, and 1524 mm,
- HMA layer Poisson's ratio = 0.35, maximum modulus = 14000 MPa and minimum modulus = 700 MPa,
- aggregate base layer Poisson's ratio = 0.40, maximum modulus = 3500 MPa and minimum modulus = 35 MPa,
- subgrade layer Poisson's ratio = 0.45, maximum modulus = 3500 MPa and minimum modulus = 5 MPa, and
- rigid layer Poisson's ratio = 0.45, modulus set at 345 MPa, program allowed to determine depth.

HMA Layer Modulus

The seasonal trends in the HMA layer moduli of the three LTPP SMP sites are similar to that from the Mn/ROAD data. Figure 5.9 shows a comparison between the backcalculated HMA moduli and the predicted HMA moduli at the Bemidji site in 1994. Three trends are shown in this graph. The first trend is the HMA layer moduli predicted from Equation 3.6 with measured temperature data at 25 mm. The second trend is the HMA layer moduli predicted from Equation 3.6 with predicted temperatures at 25 mm calculated from Equation 3.1. The third trend is the backcalculated HMA layer moduli. The predicted HMA moduli capture the general seasonal trend. However, as expected, the trend was characterized better using measured in situ temperature data rather than predicted temperature data from Equation 3.1.

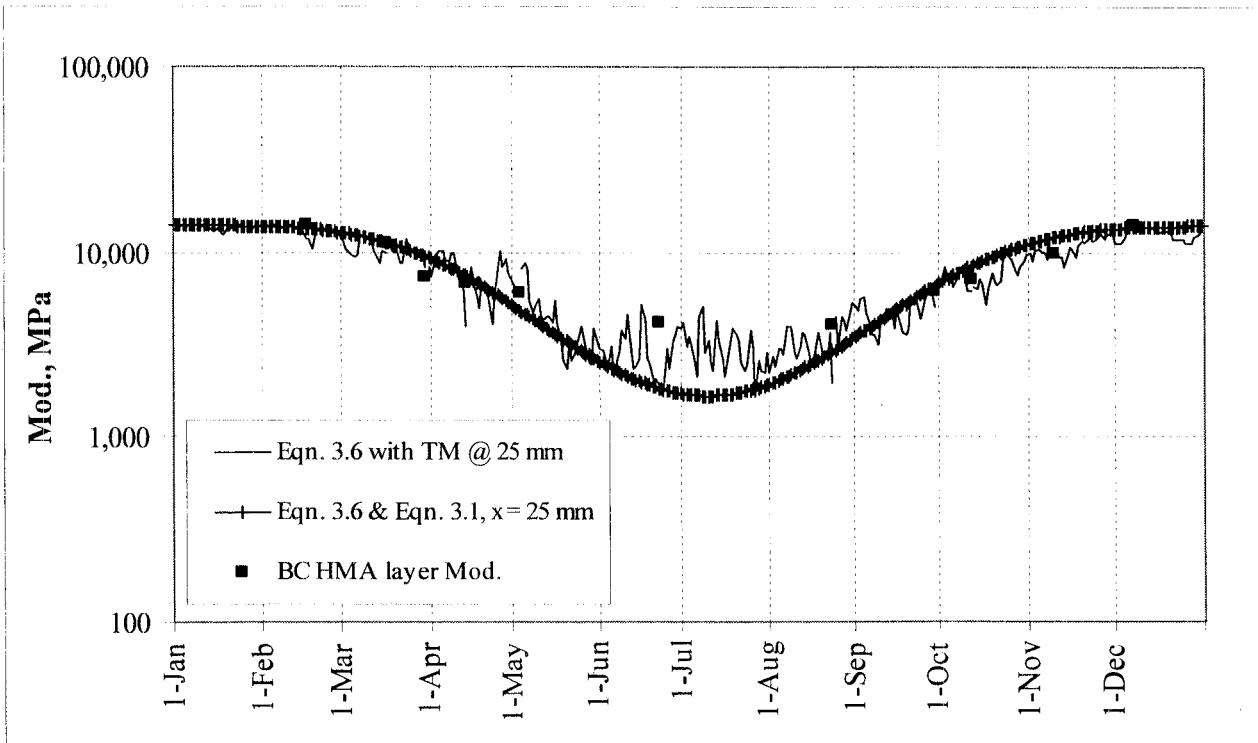


Figure 5.9. Bemidji site (#27-6251) predicted and backcalculated HMA modulus, 1994, using Equations 3.1 and 3.6.

AB and SG Layer Moduli

The backcalculated aggregate base and subgrade layer moduli show a distinct trend in the seasonal fluctuations similar to the trends seen from the data at Mn/ROAD, Figure 5.10. The base layer stiffness decreases to a minimum value when the early spring thaw occurs and rebounds to a near constant value in the summer months. The subgrade layer stiffness thaws after the base layer and stays at a minimum value through the summer. Both layers reach a maximum stiffness in the winter when the layers are frozen. Also shown in Figure 5.10 is the volumetric moisture content data measured at 290 mm in the base layer. It is apparent that as the unfrozen volumetric moisture content increases, the base modulus decreased. Thus, there exists a seasonal

trend between the base moduli and the state of moisture in the base layer that can be used to characterize the seasonal changes in the base and subgrade moduli for design purposes.

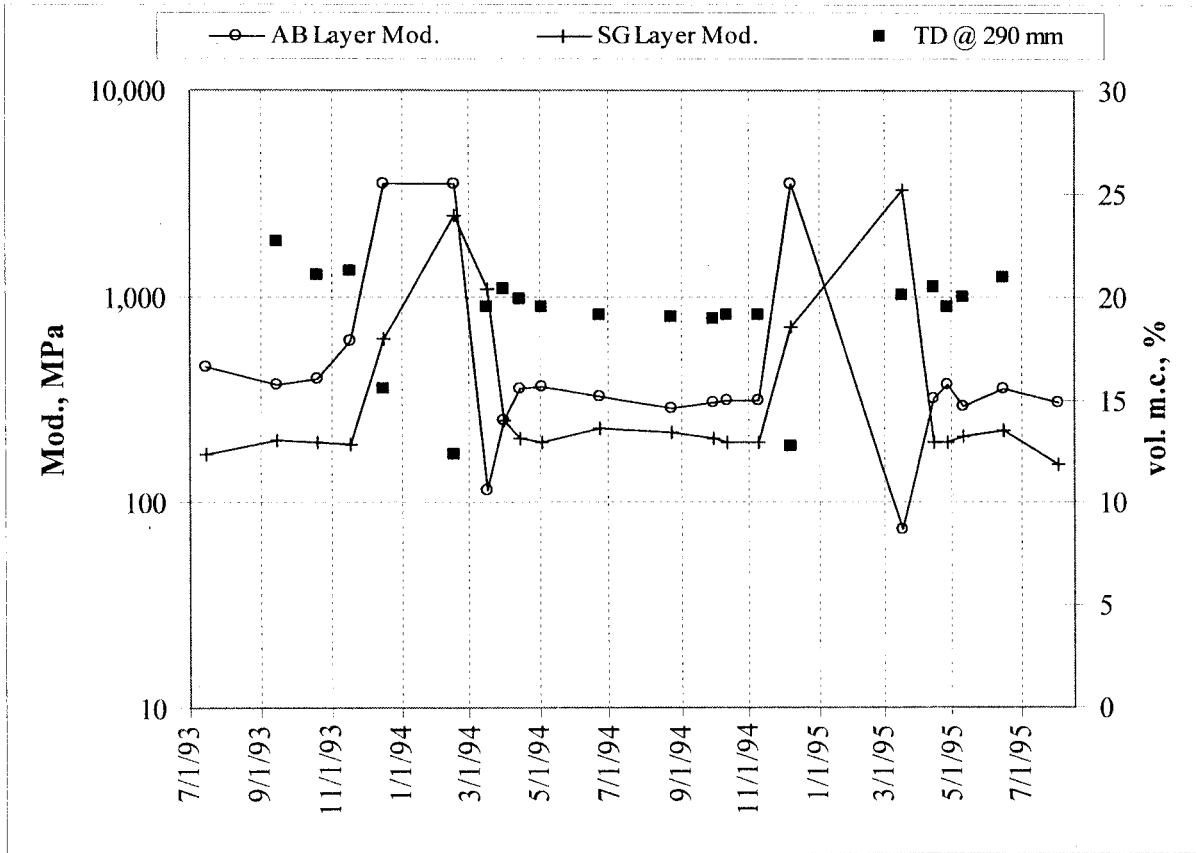


Figure 5.10. Seasonal variations in the AB and SG layer moduli compared to the volumetric moisture content at the Bemidji site.

Applications in Pavement Design

Seasonal Duration in Minnesota

The seasonal durations were defined in Chapter Three with Table 3.8. In this section, Table 3.8 is used to derive the duration of the seasons for weather station sites located in the SLR zones of Minnesota and this is shown in Table 5.8. The thawing index was computed using MnDOT's method [58] for each of the sites.

Table 5.8. Beginning date of seasons based on 30-year average temperature data.

Weather Station Location	Season I: <i>Winter</i> FI>90°C-days	Season II: <i>Early Spring</i> TI>15°C-days	Season III: <i>Late Spring</i> 4 Weeks	Season IV: <i>Summer</i> 3-day Tav>17°C	Season V: <i>Fall</i> 3-day Tav<17°C
Bemidji	28-Nov	28-Mar	25-Apr	14-Jun	31-Aug
Detroit Lakes	1-Dec	25-Mar	22-Apr	13-Jun	5-Sep
Little Falls	6-Dec	20-Mar	17-Apr	4-Jun	12-Sep
Buffalo (Mn/ROAD)	9-Dec	17-Mar	14-Apr	1-Jun	13-Sep
Albert Lea	11-Dec	17-Mar	14-Apr	30-May	13-Sep
Mankato	12-Dec	12-Mar	9-Apr	30-May	16-Sep

Seasonal Layer Moduli and Seasonal Factors

The trends in the backcalculated layer moduli are similar to those found from the Mn/ROAD data and are shown in Table 5.9. The seasonal factors were calculated by dividing the seasonal layer moduli by the Season V modulus and are shown in Table 5.10. There are some questionable backcalculated base layer moduli for the Little Falls and Bemidji sites. This may be due to the similarity between the coarse-grained material in the base and subgrade materials.

Table 5.9. Seasonal variations in the layer moduli at the LTPP SMP sites, MPa (COV in %).

Site	Season I: Winter		Season II: Early Spring		Season III: Late Spring		Season IV: Summer		Season V: Fall	
	Mod.	COV	Mod.	COV	Mod.	COV	Mod.	COV	Mod.	COV
<i>Hot Mix Asphalt Layer</i>										
Bemidji	14000	N/A*	9289	20	6791	22	4342	28	7574	20
Detroit Lakes	14000	N/A*	13140	19	11716	23	7018	22	11616	18
Little Falls	14000	N/A*	9577	44	4238	58	2762	20	3762	29
<i>Aggregate Base Layer</i>										
Bemidji	5500	N/A*	143	63	649	8	373	25	331	14
Detroit Lakes	NA									
Little Falls	5500	N/A*	82	57	859	64	606	20	780	22
<i>Subgrade Layer</i>										
Bemidji	2078	9	1532	85	204	3	191	20	196	3
Detroit Lakes	1109	22	678	72	156	14	156	5	154	6
Little Falls	2816	15	1921	85	104	38	120	14	102	20

*Only one test

Table 5.10. Seasonal factors of the LTPP SMP sites.

Site	Season I: Winter	Season II: Early Spring	Season III: Late Spring	Season IV: Summer	Season V: Fall
<i>Hot Mix Asphalt Layer</i>					
Bemidji	1.8	1.2	0.9	0.6	1.0
Detroit Lakes	1.2	1.1	1.0	0.6	1.0
Little Falls	3.7	2.5	1.1	0.7	1.0
<i>Aggregate Base Layer</i>					
Bemidji	16.6	0.4	2.0	1.1	1.0
Detroit Lakes	NA				
Little Falls	7.1	0.1	1.1	0.8	1.0
<i>Subgrade Layer</i>					
Bemidji	10.6	7.8	1.0	1.0	1.0
Detroit Lakes	7.2	4.4	1.0	1.0	1.0
Little Falls	27.6	18.8	1.0	1.2	1.0

Another resource that provides some indication of statewide moduli trends is the Subgrade Atlas created by the University of Minnesota [60]. In this study, statewide deflection test data between the years of 1983 and 1993 were used to estimate a composite moduli which were then analyzed statistically for every trunk highway in every district. It was intended to aid highway engineers in the selection of design subgrade modulus values. Table 5.11 shows the average subgrade layer moduli for each district and more detailed information can be found in the report [60].

Table 5.11. Backcalculated subgrade layer moduli for each district in Minnesota [60].

District Number	Fall Subgrade Modulus, MPa	
	Mean	St. Dev.
1	142	72
2	143	71
3	177	66
4	148	70
5	174	51
6	156	70
7	119	41
8	130	54
9	193	68
All Districts	147	67

Summary

In summary, the LTPP SMP sites show similar trends in the seasonal modulus to those observed at Mn/ROAD. Variations in the data between the three LTPP SMP sites and Mn/ROAD were in part due to the geographical locations and the type of material used. These changes could be accounted for in a M-E design process by adjusting the material property input and the duration of the seasons.

CHAPTER SIX

INTEGRATED CLIMATE MODEL

Introduction

The modeling of the load response of flexible pavements requires knowledge of traffic loading, materials, and climate. In particular, the seasonal variation of pavement material properties has been shown to heavily influence the rate and magnitude of accumulated damage in flexible pavements. Decreasing either the strength or the stiffness of the pavement can accelerate damage in pavements. The strength of the pavement denotes the largest stress that the pavement can sustain and it governs the bearing capacity of the pavement. Similarly, the pavement moduli determine the strains and displacements of the pavement system, as it is loaded and unloaded. Both of these material characteristics are strongly influenced by seasonal variations in climate. The strength and stiffness of pavement materials is dependent on temperature, moisture content, and the state of moisture. In general, the strength of a pavement system decreases with an increase in temperature and moisture content. Similarly, the pavement layer stiffness tends to increase with decreasing water content or when frozen.

The incorporation of seasonal variability of pavement material properties takes on importance in pavement design as practice evolves from considering worst case conditions to a recognition that damage needs to realistically reflect the soil conditions at various times. In particular, the advent of M-E design procedures provides a rational framework for the incorporation of the seasonal variation of pavement material properties into pavement design procedures.

The ability to predict and analytically quantify the climatic effects on pavement strength and stiffness has been investigated by numerous researchers, but few comparisons with measured field data have been completed due to the lack of pavement sites with extensive arrays of monitoring instrumentation. One such analytical prediction tool entitled “The Enhanced Integrated Climate Model (ICM)” [9] is used in this study to predict seasonal variations at the Mn/ROAD site. The climatic factors used as inputs into the model include temperature, rainfall, wind speed, and solar radiation. The ICM will then be used to model the temperature, moisture content, layer moduli, as well as advances of freezing and thawing fronts at two representative test sections at the Mn/ROAD site. Finally, comparisons will be made between the predictions from the ICM and the actual measured values of the parameters of interest. The main components of the ICM are discussed in the next section.

The Enhanced Integrated Climate Model

The ICM is a one-dimensional coupled heat and moisture flow model that is intended for use in analyzing pavement soil systems. It has the capability of generating patterns of rainfall, solar radiation, cloud cover, wind speed, and air temperature to simulate the upper boundary conditions of a pavement-soil system. The program calculates the temperature, pore pressure, moisture content, and resilient modulus for each node in the profile for the entire analysis period, as well as frost, infiltration and drainage behavior.

The ICM is composed of four major components that are shown in Figure 6.1 [9] and the components are: 1) a Precipitation Model (Precip Model), 2) an Infiltration and Drainage Model (ID Model), 3) a Climatic-Materials-Structural Model (CMS Model), and 4) the CRREL Frost Heave-Thaw Settlement Model (CRREL Model). The Precip and ID Models were developed at

Texas A&M University [61, 62]. The CMS Model was developed at the University of Illinois [63] and the CRREL Frost Heave and Thaw Settlement Model was developed at the United States Army Cold Regions Research and Engineering Laboratory [64].

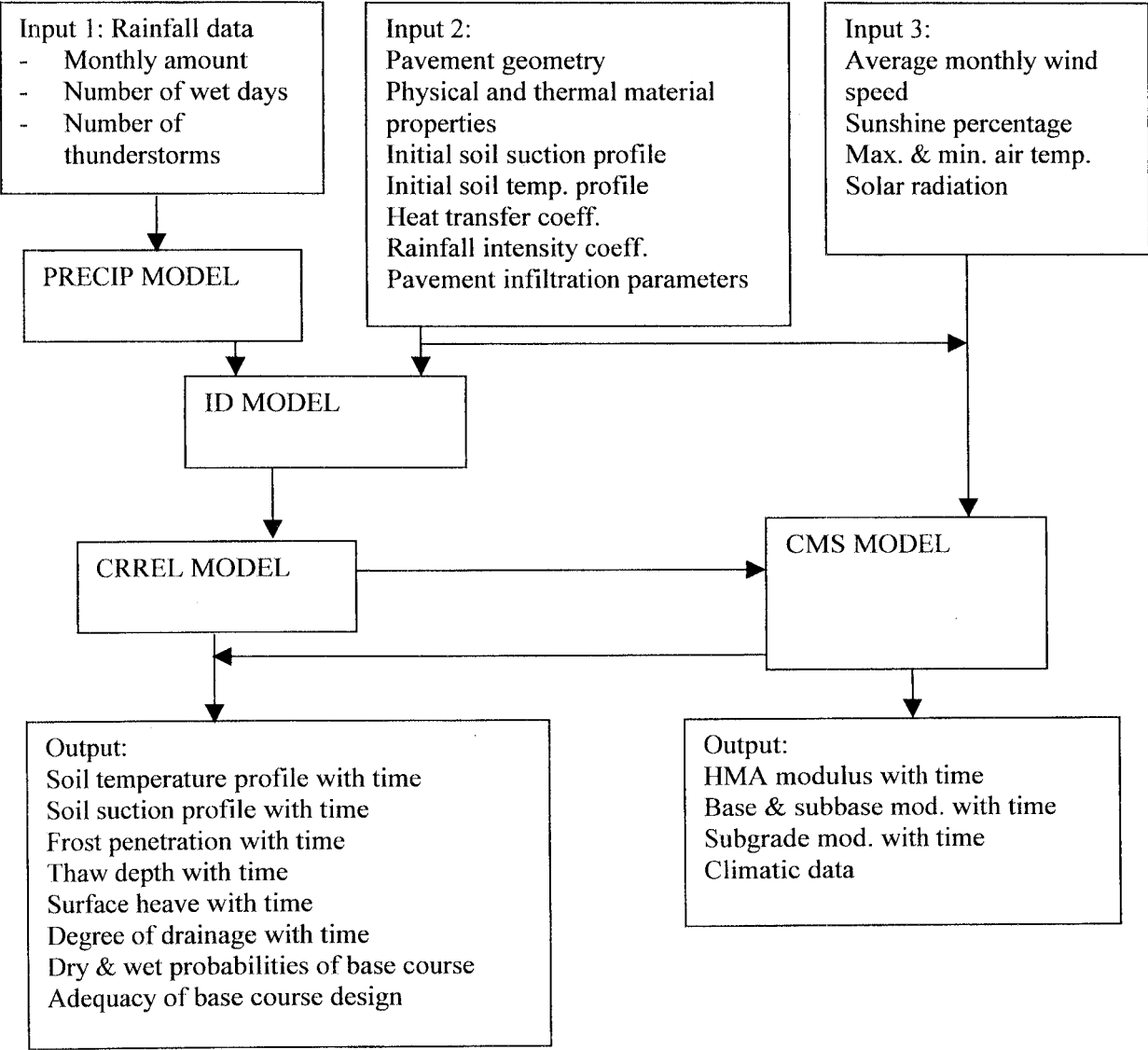


Figure 6.1. Integrated Climate Pavement Model [9].

The components of the ICM were developed independent of each other for the most part, but were combined into the ICM [9] with the purpose of performing integrated pavement structure and subgrade analysis. The details of the theory behind the ICM can be found in Lytton, et al. [9] and the use of the model is detailed by Larson and Dempsey [65]. For the purposes of this report, the four major components of the ICM are reviewed briefly.

Precipitation Model

The Precipitation Model allows the user to specify either simulated or actual rainfall data. In the simulation part of the model, average climatic data and congruential mathematical concepts are used to simulate rainfall patterns that are considered acceptable for design purposes.

Infiltration and Drainage Model

The ID Model performs drainage and infiltration analysis and pavement drainage evaluation. In terms of predicting seasonal variations in pavement material properties, the infiltration module is the most important module. It performs probabilistic analyses of rainfall amounts and patterns derived from the simulation part of the Precipitation Model or from actual rainfall amounts. The ID Model then conducts a rainfall analysis to calculate the probability of wet and dry days. This information is used to model the infiltration of water through cracks in the pavement and calculate the probability of having a wet or dry pavement profile.

Climatic-Materials-Structural Model

The CMS Model considers radiation, convection, conduction, and the effects of latent heat to generate heat flux at the pavement surface, which then is used to establish a temperature profile through the pavement surface layer. A one-dimensional, finite difference-based, heat transfer model is used to determine the temperature distribution in the pavement layers. The value for the temperature at the bottom of the pavement layer is given to the Frost Heave and Thaw Settlement Model, which determines the soil temperature conditions. The CMS model also determines the changes in HMA stiffness and the resilient modulus of the base, subbase, and subgrade with time. The CMS model does not consider transpiration, condensation, evaporation, sublimation, or heat fluxes caused by precipitation and moisture infiltration.

Frost Heave and Thaw Settlement Model

The Frost Heave and Settlement Model (CRREL Model) is a coupled heat and moisture flow mathematical model for soils. The phase change of water to ice is computed using the CRREL Model, as well as changes in soil temperature profile, and thus frost penetration and thaw settlement. The soil suction profile with time is also determined.

Description of Test Sections and Parameters Used

The Mn/ROAD test sections selected for this study were test sections 17 and 22. Both are flexible pavement test sections, consisting of 197 mm (7.75 in.) AC 20 and 120/150 pen. HMA mixtures, respectively. The aggregate base thicknesses are 710 mm (28 in.) and 457 mm (18 inches), respectively, consisting of Cl. 3 Sp. and Cl. 6 Sp. The subgrade for both test sections is an engineered fine-grained soil, classified as an A-6(7) material, with a design R-value of 12 (1655 kPa). The Ground Water Table (GWT) at both test sections fluctuates from season to season, and year to year. However, for the two years included here, namely Fall of 1995 to Fall of 1997, the GWT for test sections 17 and 22 were found on the average at depths of 2.8 m (9.2 ft.), and 4.27 m (14.0 ft.). The asphalt content for both test sections was taken as 5.8 %, and the total unit weight of the two mixtures was 22.04 kN/m³ (140.4 lb/ft³). The dry unit weights of the test section 17 and 22 bases were 20.4 kN/m³ (130 lb/ft³) and 20.6 kN/m³ (131 lb/ft³), respectively.

Summary of Other Input Parameters

The various input parameters needed for the ICM are summarized below. Details concerning the meaning of each parameter and in some cases of how to estimate them can be found in Larson and Dempsey [65]. Table 6.1(a) summarizes the baseline input required to run the ICM. This includes data such as latitude, geographic region, number of days in analysis period, as well as background information on the thermal properties associated with the site of interest. Similarly, Table 6.1(b) summarizes the input required for the infiltration and drainage calculations performed in the ICM. Tables 6.2(a), 6.2(b), and 6.2(c) summarize the input properties required for the HMA, base and subgrade layers, respectively.

Table 6.1(a). Baseline input for the Integrated Climate Model.

Integrated Climate Model Inputs		
Parameter	Test Section 17	Test Section 22
Latitude	45° 078'	
Climate Region	II-A	
Default Weather Station	Fargo, ND	
Analysis Period	9/1/1995 – 8/31/1997	
Length of Analysis Period	731 days	
First month in analysis period	September	
Time increment for output	2 hours	
Time increment for calculation	0.1 hours	
Climatic/boundary condition dialog box		
Lower boundary suction	0 kPa (0 psi) at GWT	
Thermal Properties Dialog Box		
Modifier of overburden pressure during thaw	0.5	
Emissivity factor	0.9 (slightly aged HMA)	
Cloud base factor	0.85	
Max. convection coefficient	5.19 W/m-°C (3 BTU/hr-ft-°F)	
Coefficient of variation of unsaturated permeability	1.0	
Time of day when min. air temperature occurs	04:00	
Time of day when max. air temperature occurs	15:00	
Upper temp. limit of freezing range	0°C (32°F)	
Lower temp. limit of freezing range	-1.1°C (30°F)	

Table 6.1(b). Input for the infiltration and drainage calculations.

TTI Infiltration and Drainage Box		
Parameters	Test Section 17	Test Section 22
Linear length of cracks/joints	210.6 m (691 ft)	224.0 (735 ft)
Total length surveyed for cracks and joints	1524. m (500 ft)	
Type of fines added to base course	Clay	inert mineral filler
Percentage of fines added to base course	12 %	5%
Percentage of gravel in base course	8%	54%
Percentage of sand in base course	80%	41%
One sided width of base course	6.7 m (22 ft)	
Slope ratio/base tangent value	2.0 %	
Internal boundary condition	Flux	
Evaluation period	10 years	
Constant K for intensity-duration-recurrence equation	0.25	
Power of rainfall duration, n	0.75	
Shape constant for rainfall-intensity-period curve	1.65	

Table 6.2(a). Properties of HMA layer.

HMA Material Properties		
Layer description	HMA – Test Section 17 (AC 20)	HMA – Test Section 22 (120/150 Pen)
Thickness of Layer	195 mm (7.75 inches)	
Number of elements in this layer	4	
Coarse aggregate content in asphalt	35 %	
Air content in asphalt layer	6 %	4 %
Gravimetric water content of asphalt layer	0.5 %	
Resilient modulus & temperature relationship	See Table 4.9	
Thermal conductivity of asphalt layer	Unfrozen: 1.04 W/m-°C (0.6 BTU/hr-ft-°F) Freezing: 1.04 W/m-°C (0.6 BTU/hr-ft-°F) Frozen: 1.04 W/m-°C (0.6 BTU/hr-ft-°F)	
Heat capacity of asphalt	Unfrozen: 0.92 kJ/kg-°C (0.22 BTU/lb-°F) Freezing: 5.02 kJ/kg-°C (1.2 BTU/lb-°F) Frozen: 0.92 kJ/kg-°C (0.22 BTU/lb-°F)	
Total unit weight of asphalt	Unfrozen: 2.25 g/cm ³ (140.4 lb/ft ³) Freezing: 2.25 g/cm ³ (140.4 lb/ft ³) Frozen: 2.25 g/cm ³ (140.4 lb/ft ³)	

Table 6.2(b). Properties of aggregate base course layers.

Material Properties Dialog Box – Layer 2		
Parameter	Test Section 17	Test Section 22
Thickness of layer	710 mm (28 in.)	455 mm (18 in.)
Number of elements	10	10
Porosity, n	0.238	0.248
Saturated Permeability, K_{sat}	0.00137 m/hr (0.0045 ft/hr)	0.0393 m/hr (0.129 ft/hr)
Dry unit weight, γ_{dry}	2.08 g/cm ³ (129.8 lb/ft ³)	2.10 g/cm ³ (131.1 lb/ft ³)
Dry thermal conductivity	0.519 W/m-°C (0.3 BTU/hr-ft-°F)	
Dry heat capacity	0.712 kJ/kg-°C (0.17 BTU/lb-°F)	
Coefficient of volume compressibility	0.1	
Gardner's unsaturated permeability function	Multiplier: 0.001 Exponent: 3.52	Multiplier: 1.0729x10 ⁻⁶ Exponent: 5.8979 (set at 5.0 in ICM, due to program input limitations)
Gardner's moisture content function	Multiplier: 0.02654 Exponent: 0.5933	Multiplier: 1.001 Exponent: 0.4444
Resilient Modulus	Unfrozen: 192 MPa (27,783 psi) Frozen: 5574 MPa (808,500 psi)	Unfrozen: 185 MPa (26,901 psi) Frozen: 5574 MPa (808,500 psi)
Poisson's ratio	Frozen: 0.25 Unfrozen: 0.25	Frozen: 0.25 Unfrozen: 0.25

Table 6.2(c). Properties of subgrade layer.

Material Properties Dialog Box – Layer 3		
Parameter	Test Section 17	Test Section 22
Thickness of layer	1.897 m (74.65 in.) set at GWT	3.61 m (142.25 in.) set at GWT
Number of elements	12	
Porosity, n	0.49	
Saturated Permeability, K_{sat}	0.0003048 m/hr (0.0001 ft/hr)	
Dry unit weight, γ_{dry}	1.80 g/cm ³ (112.47 lb/ft ³)	
Dry thermal conductivity	0.346 W/m-°C (0.2 BTU/hr-ft-°F)	
Dry heat capacity	0.71 kJ/kg-°C (0.17 BTU/lb-°F)	
Coefficient of volume compressibility	0.8	
Gardner's unsaturated permeability function	Multiplier: 0.001 Exponent: 2.23	
Gardner's moisture content function	Multiplier: 0.0023 Exponent: 0.6962	
Resilient Modulus	Unfrozen: 95.2 MPa (13,818 psi) Frozen: 2017.9 MPa (292,824 psi)	Unfrozen: 103.3 MPa (14,994 psi) Frozen: 1857.8 MPa (269,598 psi)
Poisson's Ratio	Frozen: 0.25 Unfrozen: 0.45	
Length of recovery period	30 days	
Factor of M_R reduction during thawing	20%	

Temperature Predictions

The procedure used to establish the temperature distribution in the ICM begins by establishing the surface temperature, followed by the calculation of temperatures throughout the pavement layers. The surface temperatures are determined through heat flux surface boundary computations, which impose an energy balance on the pavement surface [9, 66, 67]. A one-dimensional, finite difference, heat transfer model is used to determine the distribution of temperatures in the pavement layers. The model accounts for radiation, convection, conduction, and the effects of latent heat. Temperatures at nodal points throughout the pavement structure are a function of the previous temperature at the nodal point, the temperature in adjacent nodal

points and the time increment. Details of the finite difference approach used to calculate the temperature distributions can be found in Dempsey et al. [63].

Figures 6.2 and 6.3 show a comparison between the predicted and measured temperatures in the HMA layer and the base for test section 17. The trends in the predicted temperatures in the HMA layer compare very favorably to the measured values. However, the predicted temperatures in the aggregate base material are slightly lower than those of the measured temperatures. Similar results were obtained for test section 22, as shown in Figures 6.4 and 6.5.

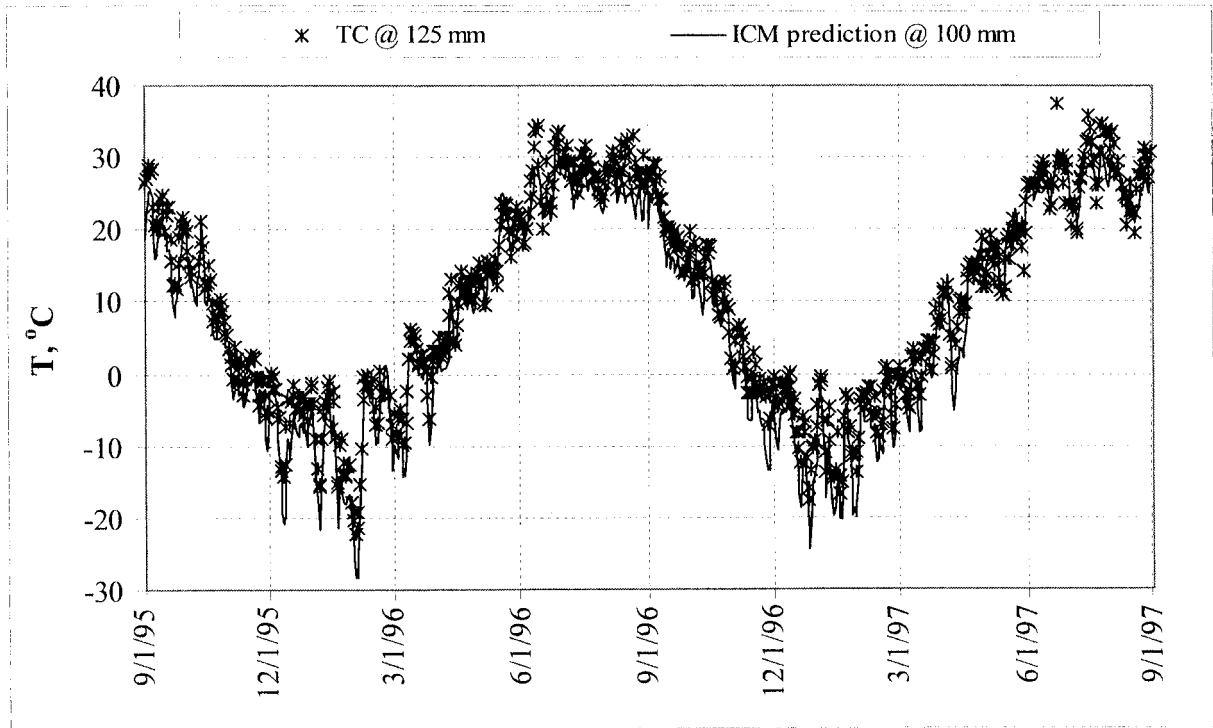


Figure 6.2. Comparison between predicted and the measured temperature in the HMA layer in test section 17.

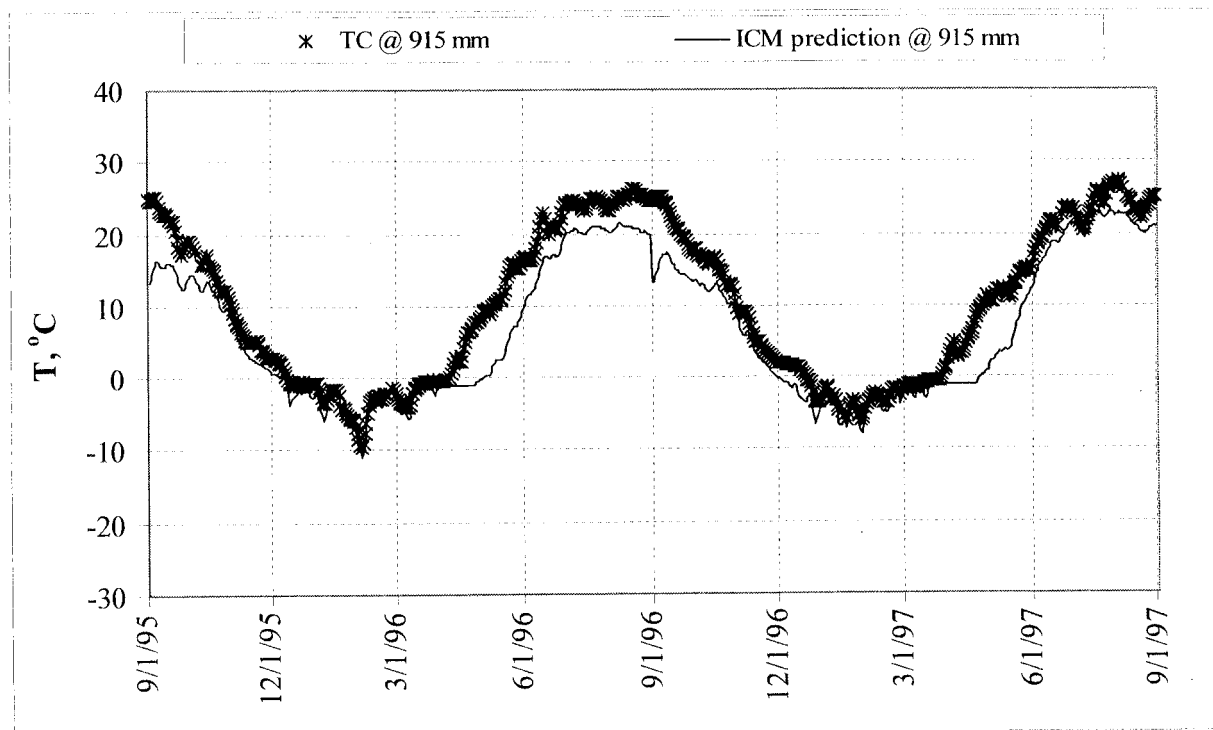


Figure 6.3. Comparison of predicted and measured temperatures in the Cl. 3 Sp. base layer in test section 17.

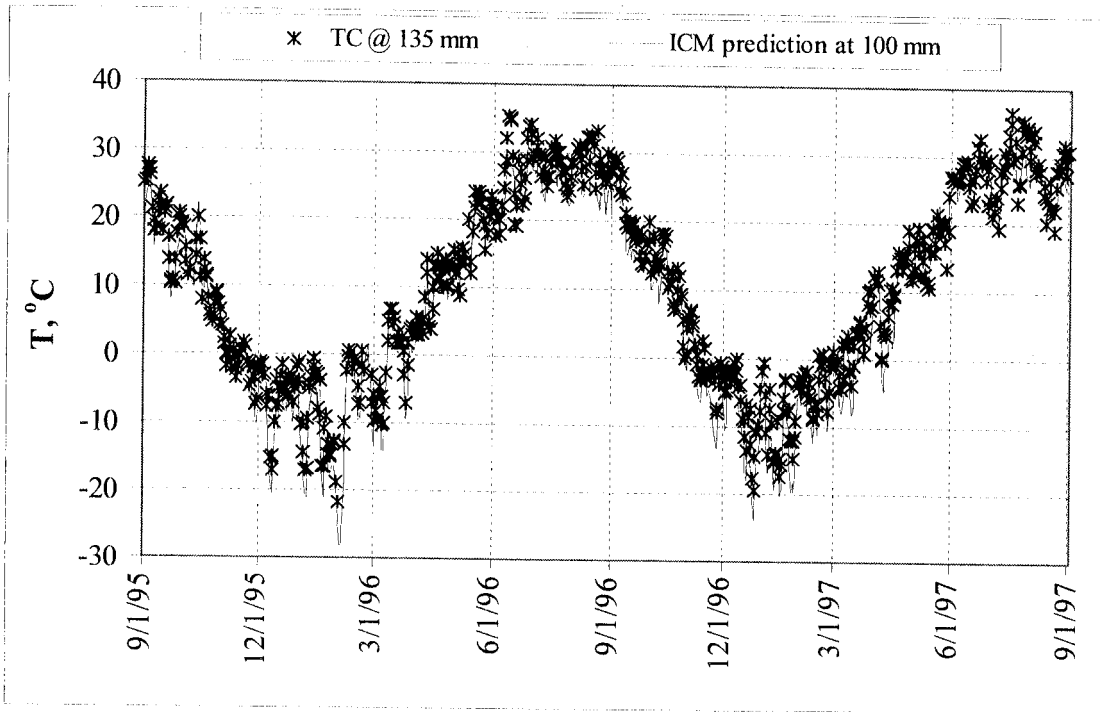


Figure 6.4. Comparison of predicted and measured temperatures in the HMA layer in test section 22.

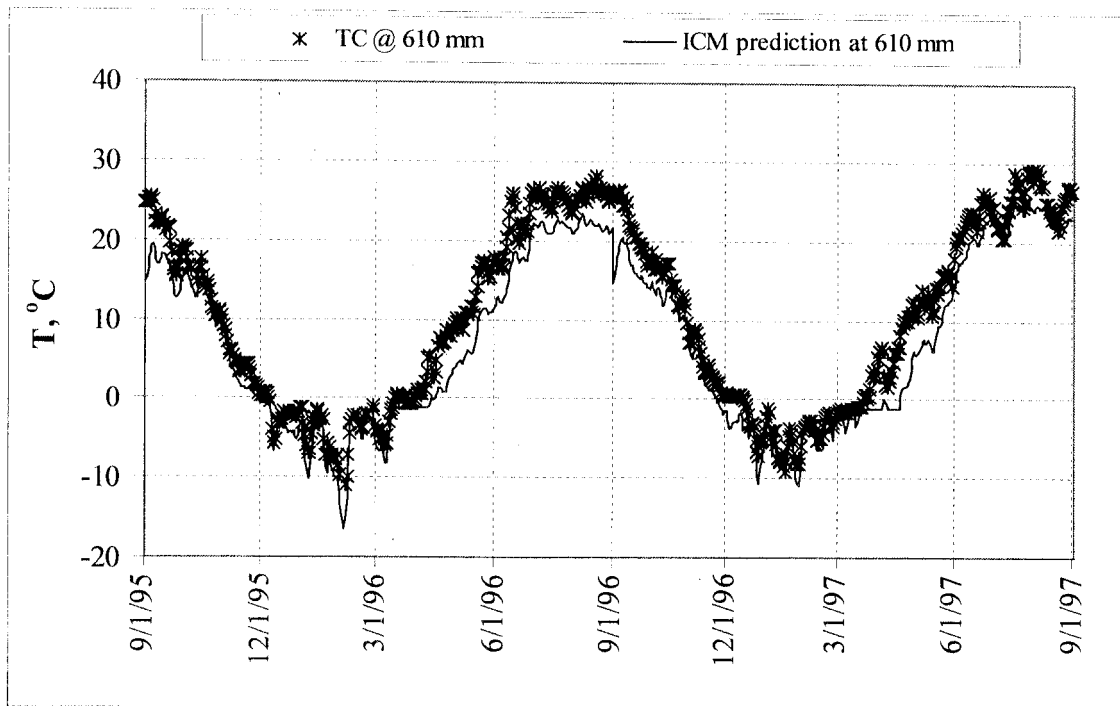


Figure 6.5. Comparison of predicted and measured temperatures in the Cl. 6 Sp. base layer in test section 22.

Moisture Content Predictions

The ICM uses a three-staged process to calculate the water contents in the base and subgrade layers. First, the equilibrium water contents are determined by assuming a static suction profile above the water table. Second, the shape of the moisture characteristic curves is established from a series of regression equations [9]. Third, the gravimetric water contents are computed from the moisture characteristic curves for the suction estimated in step one.

The results of the predicted volumetric moisture contents in the base layers of test sections 17 and 22 are shown in Figures 6.6 and 6.7, respectively. The in situ volumetric moisture contents were measured with TDRs, placed at different locations in the base material. In both cases, the predicted moisture contents agree with the measured moisture content fairly closely, except during spring thaw, when the ICM misses the critical increase in moisture content. Noticeable differences remain in the winter months, where the ICM predicts that the entire base is frozen with no unfrozen pore water. The TDR results indicate some volume of unfrozen water during the winter months. However the calibration of the TDR probes may be in error.

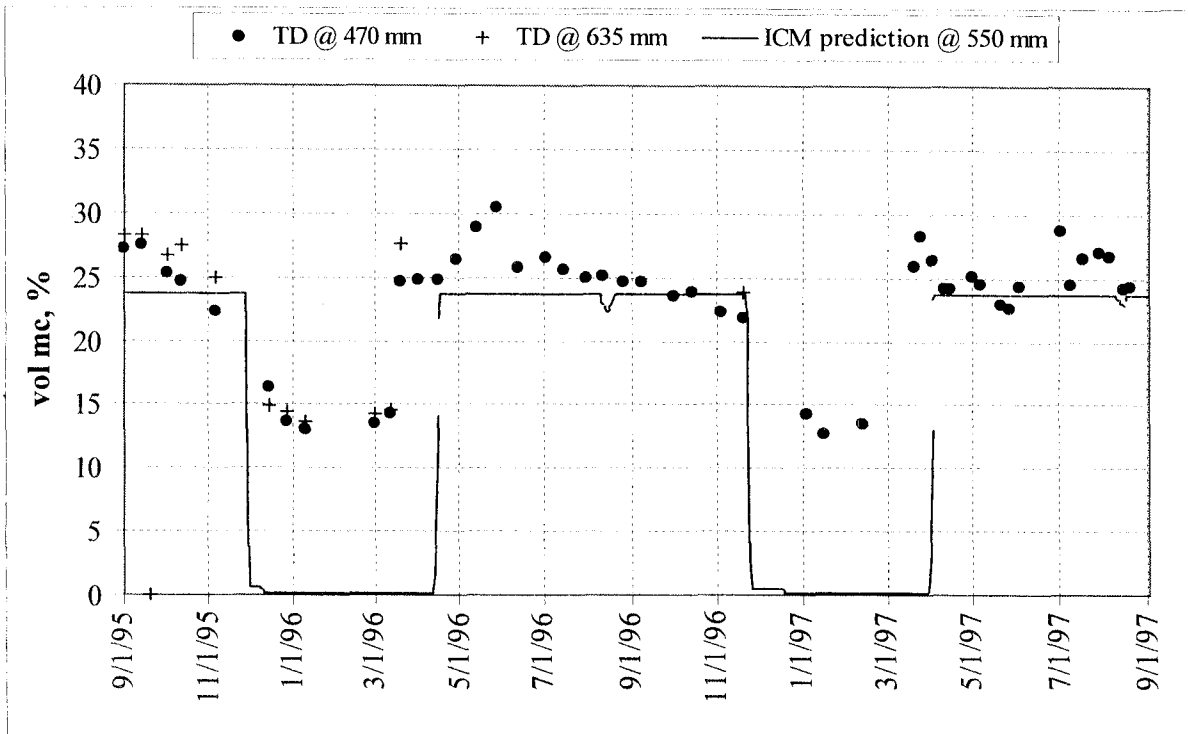


Figure 6.6. Comparison between predicted and measured volumetric moisture content in the base layer of test section 17.

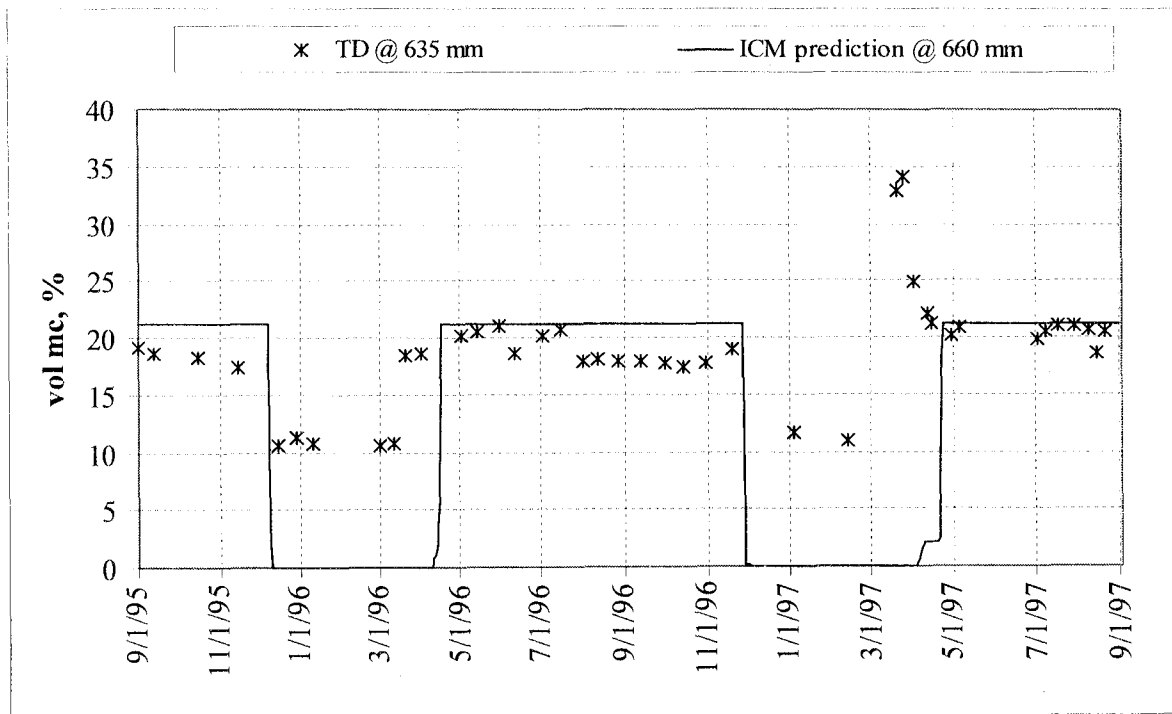


Figure 6.7. Comparison of measured and predicted volumetric moisture content in the base layer of test section 22.

Freezing and Thawing Predictions

The procedure used to calculate the depth of frost and thaw penetration in the ICM is described in detail in Lytton, et al. [9]. The calculations rely on the U.S. Army Cold Regions Research and Engineering Laboratory (CRREL) model, developed previously [64]. The main features of the model are based on a numerical solution of the coupled heat and moisture transport problem. The CRREL model attempts to simulate the process that occurs in the freezing zone.

Figures 6.8 and 6.9 show the results of the predicted thawing fronts with time for test sections 17 and 22 during the spring of 1996. The ICM predictions indicate that the bases for both test sections would not have thawed out until around the third or fourth week in April. This does not agree with measured retreat of the freezing front with WMs. The measured data indicate that the base in test section 22 has thawed out completely by the third week in March. This means that the ICM predicts thaw about one month later than what was measured, thus missing the critical spring thaw period.

It was observed by Guymon et al. [64] that under closely controlled laboratory testing conditions, the freezing and thawing fronts could be predicted fairly accurately with the CRREL model. Unfortunately, this requires good estimates of hydraulic parameters, such as unsaturated hydraulic conductivity, unfrozen water content, and porosity, as well as location of water table, all of which are difficult to determine for most roadway sections. It was also found by Guymon et al. [64] that it was almost always necessary to calibrate the model. Even though an arbitrarily selected “tuning” factor established good results, they recommended the more consistent E-factor for calibrating the model. The E-factor approach has been replaced in the ICM by the

development of an equation for vapor pressure of unfrozen water at temperatures below freezing [9]. In summary, it appears that better calibration is needed, based on the current results.

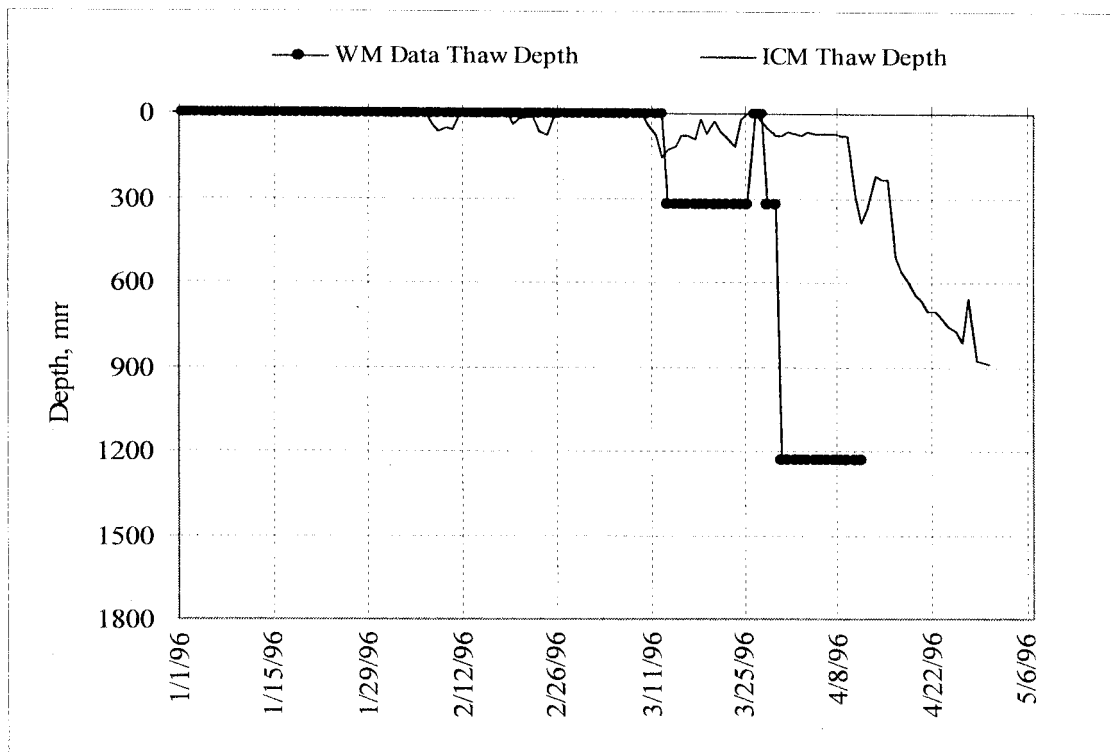


Figure 6.8. Predicted thawing front compared with WM data in test section 17, 1996.

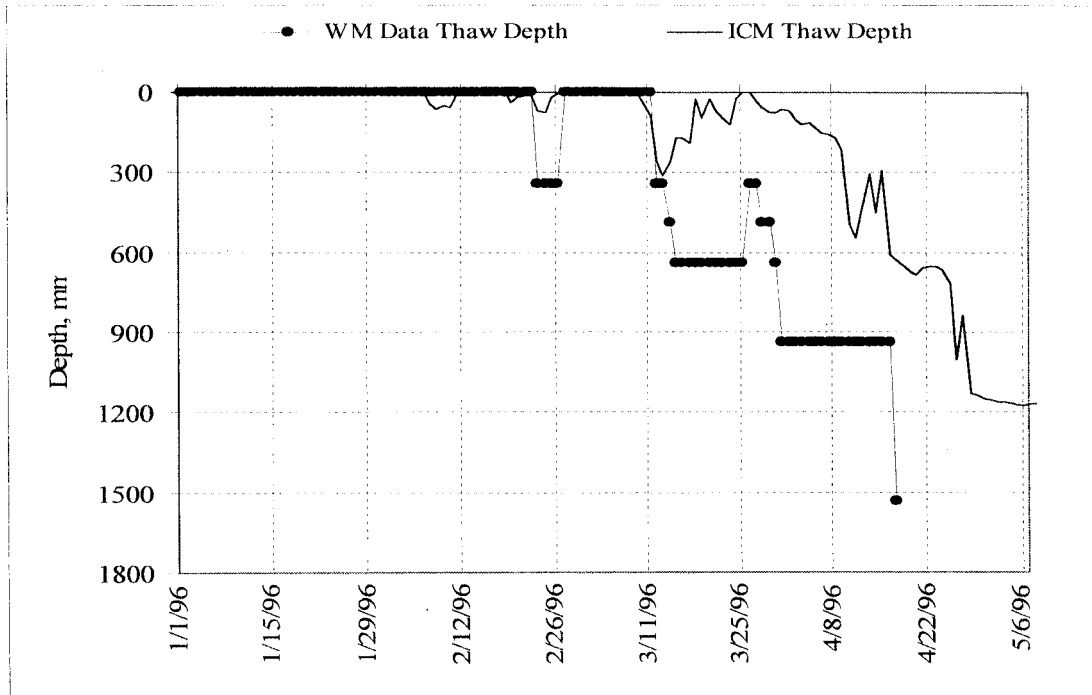


Figure 6.9. Predicted thawing front compared with WM data at test section 22, 1996.

Predictions of Layer Moduli

The ICM predicts changes in moduli of the pavement system including the HMA, base and the subgrade layers. The stiffness of the HMA layer varies with temperature, while the stiffness of the unfrozen base and subgrade depend on moisture content [9]. In the following, comparisons are made between ICM predicted and FWD backcalculated pavement layer moduli for the HMA, base and subgrade layers.

Hot Mix Asphalt Layer

The predicted stiffness of the HMA layer is determined by empirically relating the stiffness of the HMA to the stiffness of the AC and the volumetric proportion of aggregate in the HMA [10]. The ICM discretizes the pavement into a finite difference grid. Nodes are defined at the intersection of grid lines and the ICM assigns parameter values to each node in the grid. The stiffness of the AC at each node is computed for each temperature by interpolating between the values provided in the stiffness-temperature relationship. Figures 6.10 and 6.11 show the comparisons between the ICM predicted and backcalculated moduli for test sections 17 and 22, respectively. In both cases, the ICM predictions are shown to be reasonably close to the backcalculated moduli, even though the scatter in the backcalculated moduli remains higher. It should also be noted that the backcalculated moduli are significantly lower than the predicted moduli during the summer.

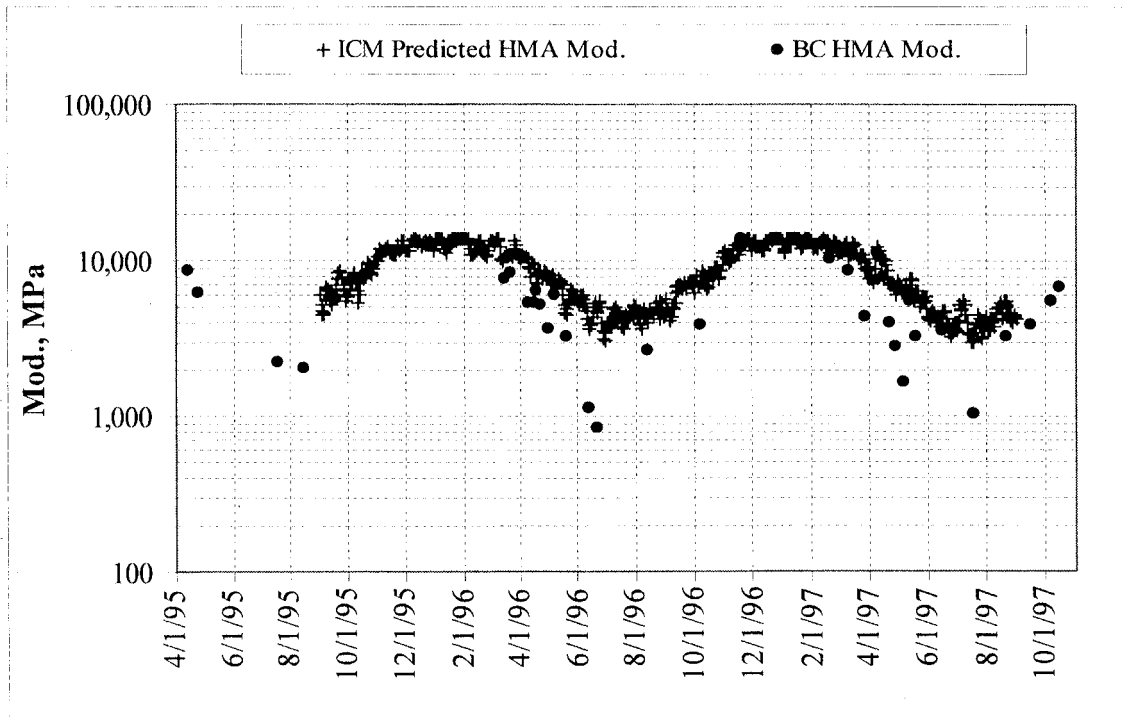


Figure 6.10. Comparison of predicted and backcalculated HMA moduli in test section 17.

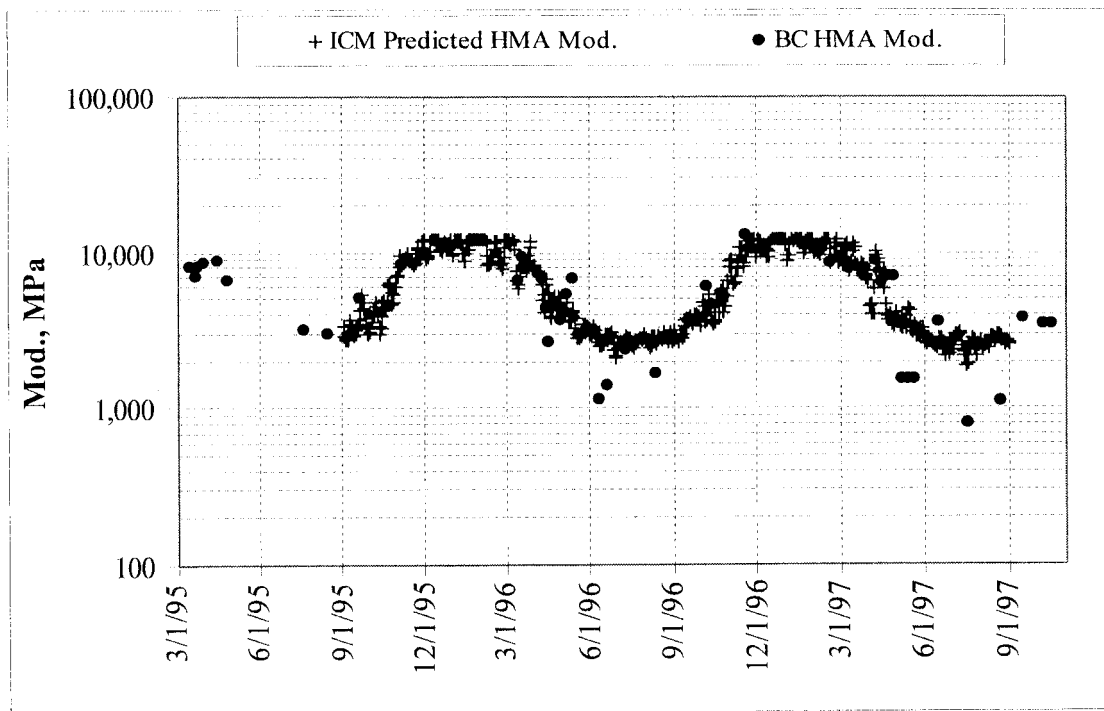


Figure 6.11. Comparison of predicted and backcalculated HMA moduli in test section 22.

Aggregate Base Layer

The ICM assumes that the modulus of the aggregate base is insensitive to moisture content when it is unfrozen [9]. To predict the variations in the base moduli, frozen and unfrozen values must be provided in the input data. The program will then select the appropriate value depending on the predicted temperature in the base. Therefore, the ICM does not really predict actual moduli values in the base. Rather, it predicts which of two user-specified values should be used based on predicted temperature. In this context, it is not surprising to see the differences between the ICM predicted and FWD backcalculated base modulus values for both test sections 17 and 22, as shown in Figures 6.12 and 6.13, respectively. It should be noted again that the ICM does not capture the critical spring thaw weakening period in the base layer because the ICM does not accurately predict temperature during this period.

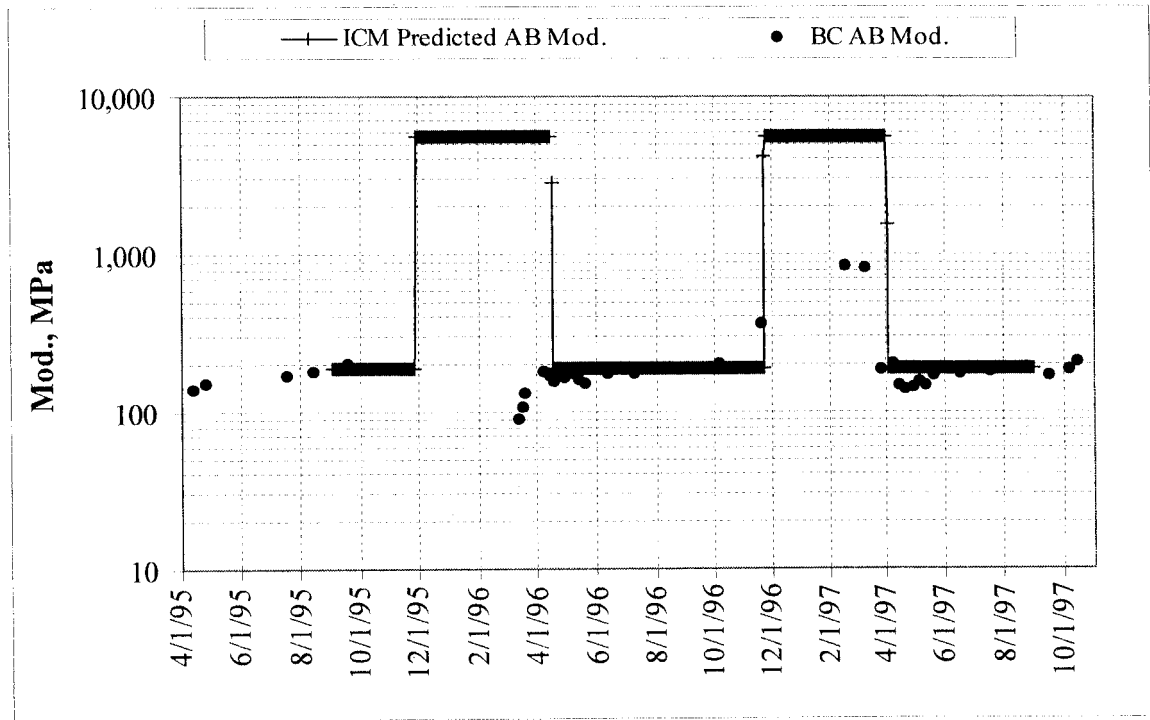


Figure 6.12. Comparison of predicted and backcalculated base layer moduli for test section 17.

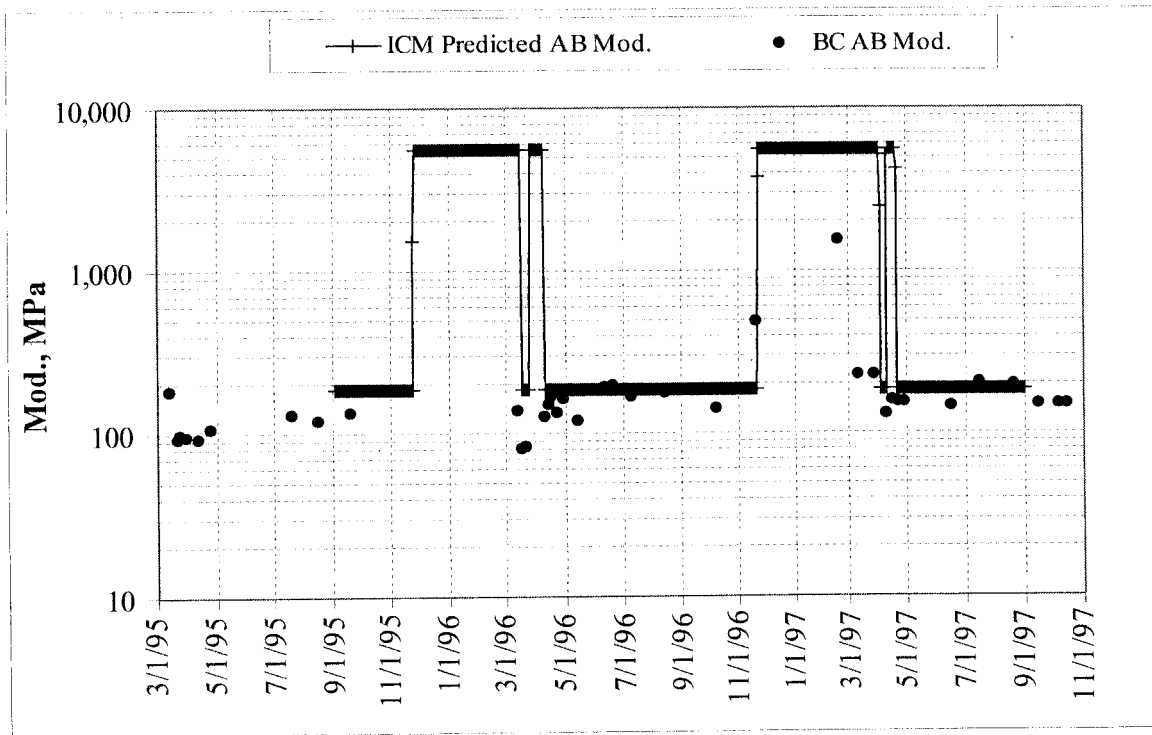


Figure 6.13. Comparison of predicted and backcalculated base layer moduli for test section 22.

Subgrade Layer

The ICM considers the subgrade modulus to have one of three possible, user-defined values of frozen, unfrozen, and thaw recovering. Figures 6.14 and 6.15 show the comparison between the “predicted” and FWD backcalculated subgrade moduli for test sections 17 and 22, respectively. Figure 6.14 shows that the initiation of thaw is not captured very well with the ICM, as discussed previously. The ICM predicts frozen modulus values until May for both years studied. This error is not as severe in test section 22, as shown in Figure 6.15, where backcalculated moduli values remain high until the end of April for both years.

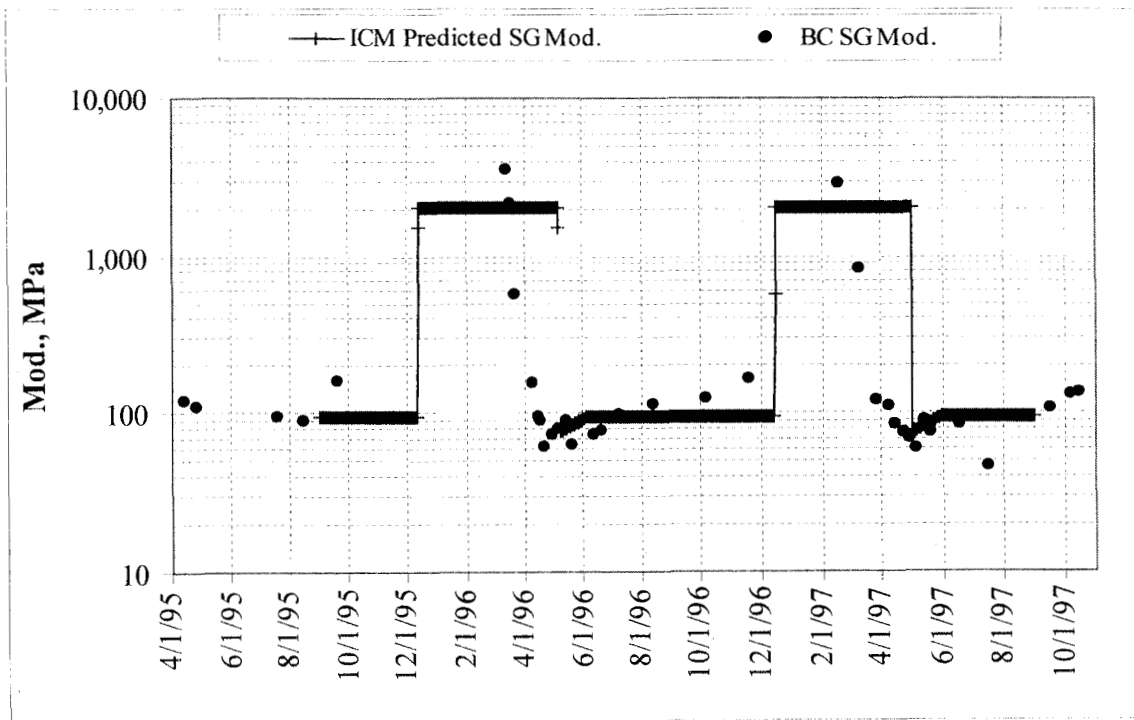


Figure 6.14. Comparison of predicted and backcalculated subgrade layer moduli for test section 17.

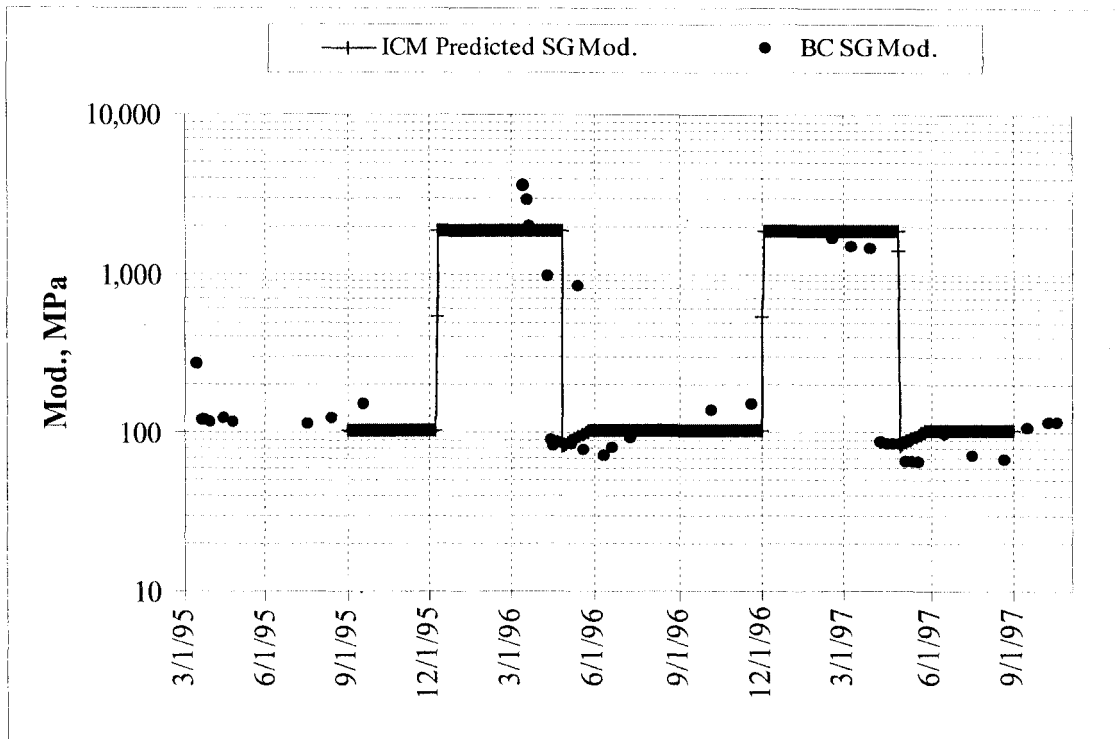


Figure 6.15. Comparison of predicted and backcalculated subgrade layer moduli for test section 22.

Other Observations on the Use of the ICM

The first significant issue is the rather extensive need for material testing to adequately use the ICM. As can be seen Tables 6.1 and 6.2, the level of detail required is significant. Even for a well-documented site like Mn/ROAD there was need to estimate a few of the parameters such as the dry thermal conductivity, dry heat capacity, and the coefficient of volume compressibility. Also, the recommended ICM default values for Gardner's unsaturated permeability and moisture content functions for the base and subgrade materials deviated significantly from the measured values. Given the sensitivity of the ICM to Gardner's functions [68], it is important to improve the accuracy of these default values in the ICM.

Another very significant issue deals with the selection of ICM default weather station data. For example, the recommended default weather station for Minnesota was located in Fargo, North Dakota. During this study, it was found that weather station data from Fargo, ND was much different than weather station data obtained at or around Mn/ROAD and could not be used to yield accurate predictions.

Finally, during this study, there were numerous instances where the ICM stalled during execution, or finished without any error messages, but did not allow the user to view results or obtain table data. In some instances, all that was required to obtain results was to re-save the file name under a different name and re-run. Similarly, importing the climatic data posed significant problems in some instances. For example, in one case, attempts to import data starting at another date because January 1 lead to garbled input data, such as negative high temperature values in July and August.

Summary

Despite some problems, the use of the ICM is advantageous. The ability to use climatic data to predict pavement temperature, moisture content, state of moisture, and variation in layer moduli with time will help in the prediction of pavement performance.

This section compared predictions of seasonal variations obtained with the ICM to measured field data from Mn/ROAD. The results indicate that it is possible to predict seasonal variations in flexible pavement layer properties using climate factors. The results presented showed that the temperature in flexible pavements could be predicted with the ICM. Similarly, the moisture contents in the various pavement layers were captured reasonably well with the ICM, as well as seasonal variations in the HMA layer modulus. In contrast, the progression of freezing and thawing fronts in flexible pavement layers were not captured adequately with the ICM, nor was the transition from frozen to unfrozen moduli for the base and the subgrade for both test sections 17 and 22.

CHAPTER SEVEN

CONCLUSIONS AND RECOMMENDATIONS

Summary

Flexible pavement design has been moving toward a more mechanistic procedure that requires knowledge of traffic loading, materials and climate to more accurately model the pavement layer behavior. One method is the mechanistic-empirical (M-E) flexible pavement design procedure that uses initial layer thicknesses, material properties, and loading conditions to model stresses, strains and deflections at critical locations in the structure to determine the optimal layer thicknesses. The empiricism of the procedure lies in the relationships between the calculated pavement responses and pavement performance. The application of an M-E design procedure allows for improved reliability in design, the ability to predict specific types of pavement distress, and the ability to reasonably predict performance from limited field and laboratory results.

A realistic approach for characterizing climate effects on the mechanical properties of the pavement layers is needed in an M-E pavement design procedure. It is important to characterize the engineering relationships between climate factors, subsurface environmental conditions and material mechanical properties with the use of instrumentation and data collection systems that monitor all these parameters. The purpose of this study was to characterize the seasonal trends in the pavement layer properties for Minnesota, and to suggest possible directions for similar studies in other regions. This study utilized the extensive work performed by other agencies for their area.

It was found that straightforward relationships exist to characterize seasonal trends in flexible pavement layer moduli based on climate and subsurface environmental condition data. More specifically, air temperature data were used to quantify seasonal fluctuations in the HMA, base and subgrade layer moduli. Mn/ROAD and three LTPP SMP sites located in Minnesota were used to provide the necessary data to characterize these trends.

It was found that for Minnesota a typical year consisted of five seasons that differed according to seasonal changes in the pavement layer stiffness. In general, the seasonal changes were governed by temperature fluctuations. Seasonal factors were used to characterize the annual changes in pavement layer moduli for the purpose of design. Using a fifth season is appropriate for areas of significant frost penetration since the base layer moduli are significantly reduced during the early spring-thaw period.

The five seasons are defined as follows:

- Winter (Season I): The layers were frozen and moduli were typically high.
- Early spring (Season II): The aggregate base layer thawed and consequently, the modulus was low.
- Late spring (Season III): The aggregate base layer recovered to a near constant modulus value. Concurrently, the subgrade layer thawed and the modulus was low.
- Summer (Season IV): The maximum daily air temperatures were high and the HMA modulus was low.
- Fall (Season V): All of the layer moduli were typically at or near a constant value. The moduli during this season were considered, for the purposes of this study, the baseline values.

Conclusions

The results of this study support the following statements.

General:

- Average daily air temperature can be used to estimate HMA temperature, as was confirmed by the use of Equation 3.1 ($R^2 = 0.89$) to predict the temperature at various depths in the HMA layer.
- The relationship between HMA temperature and moduli can be modeled exponentially, and thus, field temperature in the HMA layer can be used to estimate the HMA modulus.
- The predicted HMA modulus is slightly higher in the summer than the backcalculated modulus and therefore the prediction may need to be adjusted if used for design in another region to fit the seasonal changes.
- The TI can be used to predict moisture phase changes in the aggregate base and soil subgrade layers.
- An aggregate base or soil subgrade containing less fine-grained material will exhibit a lower overall moisture content and smaller fluctuations in the moisture content during the spring thaw period.
- The base layer modulus is at a minimum when the early spring-thaw occurs, and recovers quickly to a near constant value by late spring.
- The state of moisture in the fine-grained subgrade layer does not change from ice to liquid until late spring, at which time the layer modulus is at a minimum and remains low through much of the summer finally increasing in the fall.
- The seasonal variations in the sand subgrade modulus were similar to the aggregate base in that the layer will thaw sooner than the fine-grained subgrade, the moisture content is lower and the modulus will stay near a constant value between the spring thaw period and the fall. Also, the sand subgrade sections were fairly insensitive to thaw-weakening.

Backcalculation:

- There are non-linearities in the subgrade and base layers of a flexible pavement structure that are not adequately addressed in a linear elastic analysis tool.
- The structure of the model, the configuration of the FWD and a variety of assumptions must be considered in order to provide relative estimates.

M-E Flexible Pavement Design:

- Factors can be used to quantify seasonal variations in material properties for use in a M-E pavement design procedure.
- The duration of the seasons can be determined with the use of average daily air temperature data. The duration of the seasons varies throughout Minnesota, typically northern Minnesota has a longer winter season and a shorter summer season than southern Minnesota.
- The Subgrade Atlas [60] for Minnesota provides a useful first step in characterizing the subgrade layer moduli.

LTPP SMP Data:

- The LTPP database provides useful data to analyze seasonal variations in the stiffness of various pavement structures throughout Minnesota, however there were minimal seasonal LTPP SMP data collected during the critical spring thaw period, in particular the resistivity probe and deflection data.
- The moisture gradient in the conventional flexible pavement structures investigated were wetter near the bottom of the base, while at the full-depth HMA site near Detroit Lakes, the subgrade was wetter directly under the surface layer.

ICM:

- The ICM offers researchers the ability to use climatic data to predict pavement temperature, moisture content, state of moisture, and variation in layer moduli with time.
- The results presented showed that the temperature in flexible pavements could be predicted by the ICM. Similarly, the moisture content in the various pavement layers were captured reasonably well with the ICM, as well as seasonal variations in the HMA layer modulus.
- In contrast, the progression of freezing and thawing fronts in Mn/ROAD flexible pavement layers were not captured accurately with the ICM, nor was the transition from frozen to unfrozen moduli for the base and the subgrade layers for Mn/ROAD test sections.
- There is a need for extensive material testing to adequately make use of the ICM, where the level of detail in input may be beyond the information typically available to a highway engineer.
- The recommended ICM default values for Gardner's unsaturated permeability and moisture content functions for the base and subgrade materials deviated significantly from measured values. Given the sensitivity of the ICM to Gardner's functions [68] it is important to improve the level of accuracy of these default values in the ICM.
- In selecting the default weather station data in the ICM, it was found that weather station data from Fargo, ND was too different from weather station data obtained at or around Mn/ROAD to yield accurate predictions.

Recommendations

There are a number of avenues resulting from this research that warrant further investigation. The process used in this study could be used in other states for the design of flexible pavements, especially those affected by seasonal freeze-thaw. For instance, this study related easily attainable climate data to the seasonal variations in the flexible pavement layer stiffness. The climate data is available on-line and the pavement layer stiffness data and is available for various regions and can be retrieved from the LTPP SMP. Together this data can be used with the relationships derived in this study to characterize seasonal variations in pavement layer stiffness for a given region from climate data.

It is recommended that monitoring and data retrieval from the LTPP SMP sites be continued so that further improvements in characterizing seasonal variations in pavement layer mechanical properties and the relationships derived from this study are continually refined. It would be highly advantageous to include more fine-grained subgrade sites in the LTPP SMP sites since these are more frost susceptible.

Research is needed to address the issue of non-linear behavior in flexible pavement structures. Linear elastic analysis tools do not consider the non-linearities in the subgrade stiffness or discontinuities in the pavement surface such as cracks. These issues need to be investigated further to accurately calculate flexible pavement behavior for thin and thick pavements.

There was an annual increase of 1% in the TDR measurements between the years of 1994 and 1996. The drift in the TDR measurements could be the result of corrosion of the sensor from moisture or salinity in the moisture due to de-icing agents. Research is needed to determine the cause of this drift to validate the moisture content measurements from TDRs. The existing

equations relating measured electrical properties to predicted volumetric moisture are not adequate and further calibration is needed before accurate predictions can be made.

Also, changes in the consolidation of the pavement layers should be investigated to determine the influence on the moisture content or watertable after construction and during the first year of service. This may account for a drift in the moisture content and consequently in the modulus of the unbound layers.

To adequately use the M-E design procedure, an engineer needs to have a full understanding of the design input values including the pavement material characterization. It is recommended that further research be conducted to create a smooth transition between current flexible pavement design and the M-E design procedures. This may entail the development of correlations between modulus and R-value, CBR or other material properties.

REFERENCES

1. AASHTO, "AASHTO Guide for Design of Pavement Structures," American Association of State Highway and Transportation Officials, Washington, D.C., 1993.
2. Kersten, M.S., Skok, E.L., "Application of AASHO Road Test Results to Design of Flexible Pavements in Minnesota," Minnesota Investigation # 183, 1968.
3. Lary, J.A., Mahoney, J.P., "Seasonal Effects on the Strength of Pavement Structures," *Transportation Research Record*, No. 954, Washington, D.C., 1984.
4. Mahoney, J.P., Lee, S.W., Jackson, N.C., Newcomb, D.E., "Mechanistic-Based Overlay Design Procedure for Washington State Flexible Pavements," Washington State Transportation Center, 1988.
5. Poehl, R. and Scrivner, F.H., "Seasonal Variations of Pavement Deflections in Texas," Research Report 136-1, Study 2-8-69-136, Flexible Pavements, January 1971.
6. Watson, D.K., "Seasonal Variation in Material Properties of a Flexible Pavement," A Thesis for the Degree of Masters of Science, Department of Civil and Geological Engineering, University of Manitoba, Winnipeg, Manitoba, 1996.
7. Bayomy, F.M., Al-Kandari, F.A., and Smith, R.M., "Mechanistic-Based Flexible Overlay Design System for Idaho," *Transportation Research Record 1543*, National Research Council, Washington, D.C., 1996.
8. Van Deusen, D.A., "Selection of Flexible Backcalculation Software for the Minnesota Road Research Project," Minnesota Department of Transportation, MN/PR - 96/29, Office of Minnesota Road Research, Maplewood, MN, 1996.
9. Lytton, R.L., D.E. Pufahl, C.H. Michalak, H.S. Liang, and B.J. Dempsey. "An Integrated Model of the Climatic Effects on Pavements." Federal Highway Administration Final Report No. FHWA-RD-90-033, McLean, Virginia, 1993.
10. Yoder, E.J. and Witczak, M.W., Principles of Pavement Design, John Wiley & Sons, Inc., pp. 177-193, 221-442, 1975.
11. Newcomb, D.E. and B. Birgisson, "Measuring In Situ Mechanical Properties of Pavement Subgrade Soils," Synthesis of Highway Practice 278, National Cooperative Highway Research Program, National Research Council, Washington, D.C, 1999.
12. Mahoney, J.P., Newcomb, D.E., Jackson, N.C., Pierce, L.M., "Pavement Moduli Backcalculation Short Course," Washington State Transportation Center, 1991.

13. Li, D. and E.T. Selig, "Resilient Modulus for Fine-Grained Subgrade Soils," *Journal of Geotechnical Engineering*, ASCE Vol. 120, No. 6, PP. 939-957, 1994.
14. Hicks, R.G., and C.L. Monismith, "Factors Influencing the Resilient Response of Granular Materials," *Highway Research Record No. 345*, HRB, National Research Council, Washington, D.C., 1971.
15. Santha, B.L., "Resilient Modulus of Subgrade Soils: Comparison of Two Constitutive Equations," *Transportation Research Record* 1462, pp. 79-90, 1995.
16. May, R.W., and Witczak, M.W., "Effective Granular Modulus to Model Pavement Responses," In *Transportation Research Record No. 810*, TRB National Research Council, Washington, D.C., pp. 1-9, 1981.
17. Uzan, J., "Characterization of Granular Materials," *Transportation Research Record* 1022, National Research Council, Washington, D.C., 1985.
18. Jin, M.S., Lee, K.W., Kovacs, W.D., "Seasonal Variation of Resilient Modulus of Subgrade Soils," *Journal of Transportation Engineering*, Vol. 120, No. 4, July/August, 1994.
19. Thompson, M.R., and Q.L. Robnett, "Resilient Properties of Subgrade Soil," *Transportation Engineer Journal*, Jan. 1979, pp. 1-89.
20. Figueroa, J.L. and Thompson, M.R., "Simplified Structural Analysis of Flexible Pavements for Secondary Roads Based on ILLI-PAVE," *Transportation Research Record* 776, National Research Council, Washington, D.C., 1980.
21. Moossazadeh, J. and M. Witczak, "Prediction of Subgrade Moduli for Soil that Exhibits Nonlinear Behavior," *Transportation Research Record* 810, National Research Council, Washington, D.C., 1981.
22. Fredlund, D.G., A.T. Bergan and P.K. Wong, "Relation Between Resilient Modulus and Stress Conditions for Cohesive Subgrade Soils," *Transportation Research Record* 642, National Research Council, Washington, D.C., 1977.
23. Drumm, E.C., Y. Boateng-Poku and T.J. Pierce, "Estimation of Subgrade Resilient Modulus from Standard Tests," *Journal of Geotechnical Engineering*, 1990/05, 116(5), 1990.
24. Shackel, B., "Changes in Soil Suction in a Sand-Clay Subjected to Repeated Triaxial Loading," *Highway Research Board* 429, 1973.
25. Mehta, P.K. and Monteiro, P. J. M., Concrete Structure, Properties, and Materials, Prentice Hall, Englewood Cliffs, New Jersey, 1993.

26. Lukanen, E.O., "Automated Deflection Testing Field Operations," Proceedings, Strategic Highway Research Program Products, Specialty Conference, American Society of Civil Engineers, Denver, Colorado, April 8-10, 1991.
27. Crovetti, J.A., Shahin, M.Y., Touma, B.E., "Comparison of Two Falling Weight Deflectometer Devices, Dynatest 8000 and KUAB 2M-FWD," Nondestructive Testing of Pavements and Backcalculation of Moduli, ASTM STP 1026, American Society for Testing and Materials, Philadelphia, Pennsylvania, 1989, pp. 59-69.
28. Lytton, R.L., "Backcalculation of Pavement Layer Properties," Nondestructive Testing of Pavements and Backcalculation of Moduli, ASTM STP 1026, American Society for Testing and Materials, Philadelphia, 1989, pp. 7-38.
29. Van Cauwelaert, F.J., D.R. Alexander, T.D. White and W.R. Barker, "Multilayer Elastic Program for Backcalculating Layer Moduli in Pavement Evaluation," Nondestructive Testing of Pavements and Backcalculating of Moduli, ASTM STP 1026, American Society for Testing and Materials, 1989.
30. Washington State Department of Transportation, "WSDOT Pavement Guide," Volume 3, Pavement Analysis Computer Software and Case Studies, February, 1995.
31. Rada, G.R., A. Lopez Jr., G.E. Elkins, C.A. Richter, B. Henderson, "Long-Term Pavement Performance Seasonal Monitoring Program: Instrumentation Selection and Installation," *Transportation Research Record* No. 1432, National Research Council, Washington D.C., 1994.
32. Van Sambeek, R.J. and R.R. Urbach, "LTPP Seasonal Monitoring Program Site Installation Report for GPS Section 276251 (27C) Bemidji, Minnesota," Braun Intertec Corporation, Minneapolis, Minnesota, January 1996.
33. Van Sambeek, R.J. and R.R. Urbach, "LTPP Seasonal Monitoring Program Site Installation Report for GPS Section 271028 (27B) Detroit Falls, Minnesota," Braun Intertec Corporation, Minneapolis, Minnesota, January 1996.
34. Van Sambeek, R.J. and R.R. Urbach, "LTPP Seasonal Monitoring Program Site Installation Report for GPS Section 271018 (27A) Little Falls, Minnesota," Braun Intertec Corporation, Minneapolis, Minnesota, January 1996.
35. Sebaaly, P., N. Tabatabaee, T. Scullion, "Instrumentation for Flexible Pavements," U.S. Department of Transportation, Federal Highway Administration, Report No. FHWA-RD-89-084, August 1989.
36. Lenk, J.D., ABC's of Thermocouples, Howard W. Sams & Co., The Bobbs-Merrill Co., Inc., Indianapolis, Indiana, 1967.

37. Beer, M.G., G.D. Johnson, D.A. Van Deusen, "Performance of Mn/ROAD Load Response and Environmental Instrumentation," Not Published, Office of Minnesota Road Research, Mn/DOT, Maplewood, MN, November, 1996.
38. B. Birgisson and R. Roberson, "Drainage of Pavement Base Material: Design and Construction Issues," *Transportation Research Record*, No. 1709, Washington, D.C., 2000, pp.11-18.
39. Hillel D., Environmental Soil Physics, Academic Press, San Diego, 1998.
40. Krantz, R.J., "An Investigation Into the Validity of Using Resistance to Identify Frozen Soil," Project Presented to the Department of Civil and Geological Engineering, University of Manitoba, Winnipeg, Canada, 1996.
41. --- "Minnesota Road Research Project Proposal" Minnesota Department of Transportation, Maplewood, Minnesota 1991.
42. Timm, D.H., B. Birgisson, and D.E. Newcomb, "Variability of Mechanistic-Empirical Flexible Pavement Design Parameters," *Proc. 5th International Conference on the Bearing Capacity of Roads and Airfields*, Vol. 1, Norwegian University of Science and Technology, Trondheim, Norway, July 1998.
43. Lary, J.A., Mahoney, J.P., Ball, C.A., and Hicks, R.G., "Seasonal Environmental Effects on the Strength of Pavement Surfaces," Research Report for the U.S. Forest Service, University of Washington, Seattle, May 1983.
44. Hein, D.K. and Jung, F.W., "Seasonal Variations in Pavement Strength," Proceedings, 4th International Conference on the Bearing Capacity of Roads and Airfields, Volume 1, July 17-21, 1994, pp. 661-676
45. Classen, A.I.M. and Ditsmarsch, R., "Pavement Evaluation and Overlay Design - The Shell Method," Proceedings, 4th International Conference on the Structural Design of Asphalt Pavements, University of Michigan, Ann Arbor, 1977, pp. 39-74.
46. Edwards, J.M., and Valkering, C.P., "Structural Design of Asphalt Pavements for Road Vehicles - the Influence of High Temperatures," *Highways and Road Construction*, vol. 42, February 1974.
47. Horak, E., "The Use of Surface Deflection Basin Measurements in the Mechanistic Analysis of Flexible Pavements," Proceedings, Vol. 1, Sixth International Conference Structural Design of Asphalt Pavements, University of Michigan, Ann Arbor, Michigan, USA, 1987.
48. Hardcastle, J.H., "Subgrade Resilient Modulus for Idaho Pavements," Final Report of Research Project No., Idaho Transportation Department, Boise, ID, June 1992.

49. Asphalt Institute, Thickness Design - Asphalt Pavements for Highway and Streets, Manual Series No. 1 (MS-1), Lexington, Kentucky, September 1981.
50. Garg, N., and M.R. Thompson, "Triaxial Characterization of Minnesota Road Research Project Granular Materials," *Transportation Research Record 1577*, National Research Council, Washington, D.C., 1997.
51. Newcomb, D.E., R. Benke and G.R. Cochran, "Minnesota Road Research Project - An Overview," *Proceedings, 6th International Specialty Conference on Cold Regions Engineering*, ASCE, New York, 1991.
52. Newcomb, D.E., D.A. Van Deusen, Y. Jiang and J. P. Mahoney, "Considerations of Saturated Soil Conditions in Backcalculation of Pavement Layer Moduli," *Transportation Research Record* No. 1473, National Research Council, Washington D.C., 1995.
53. Midwestern Climate Center, Illinois State Water Survey, "Midwestern Climate Information System," On-Line Database, <http://mcc.sws.uiuc.edu/>.
54. Andersland, O.B. and D.M. Anderson, Geotechnical Engineering for Cold Regions, McGraw-Hill Book Company, New York, 1978.
55. Chadbourn, B.A., J.A. Luoma, D.E. Newcomb and V.R. Voller, "Consideration of Hot Mix Asphalt Thermal Properties During Compaction," *Quality Management of Hot Mix Asphalt, ASTM STP 1299*, Dale S. Decker, Ed., American Society for Testing and Materials, 1996.
56. Asphalt Institute, "Performance Graded Asphalt Binder Specification and Testing," Superpave Series No. 1, SP-1, Kentucky, 1994.
57. Lukanen, E.O., R. Stubstad and R. Briggs, "Temperature Predictions and Adjustment Factors for Asphalt Pavement," Federal Highway Administration Final Report No. FHWA-RD-98-085, June 2000.
58. Ovik, J.M., J.A. Siekmeier and D.A. Van Deusen, "Improved Spring Load Restriction Guidelines Using Mechanistic Analysis," *Mn/DOT Draft Report*, July 2000.
59. Stroup-Gardiner, M. and D.E. Newcomb, "Investigation of Hot Mix Asphalt Mixtures at Mn/ROAD, Final Report," University of Minnesota, Department of Civil Engineering, February, 1997.
60. Barnes, R.J., I. Jankovic and D. Colom, "Statewide Statistical Subgrade Characterization," Minnesota Department of Transportation Report Number 95-16A, June 1995.

61. Liang, H.S. and R.L. Lytton. "Rainfall Estimation for Pavement Analysis and Design." Presented at 88th Annual Meeting of the Transportation Research Board, Washington, D.C., Jan. 1989.
62. Liu, S.J. and Lytton. "Environmental Effects on Pavement-Drainage." Volume IV, Federal Highway Administration, Washington, D.C., FHWA Report, FHWA-DTFH-61-87-C-00057, 1985.
63. Dempsey, B.J., W.A. Herlach, and A.J. Patel. "The Climatic-Materials-Structural Pavement Analysis Program." Final Report, Federal Highway Administration, Washington, D.C., FHWA/RD-84/115, Vol. 3, February, 1985.
64. Guymon, G.L. R.L. Berg, and T.C. Johnston. "Mathematical Model of Frost Heave and Thaw Settlement in Pavements." Report: U.S. Army cold Regions research and Engineering Laboratory, Dartmouth, N.H., 1986.
65. Larson, G. and B.J. Dempsey. "Enhanced Integrated Climatic Model, Version 2.0." Report No. DTFA Mn/DOT 72114, Final Report, 1997.
66. Scott, R.F., "Heat Exchange at the Ground Surface," U.S. Army Material command, Cold Regions Research and Engineering Laboratory, Hanover, N.H., 1964.
67. Berg, R.L., Energy Balance on a Paved Surface, U.S. Army Terrestrial Sciences Center, Hanover, N.H., 1968.
68. Simonsen, E. *Prediction of Climatic Effects and Pavement Response in Frost Sensitive Roads*. Licentiate Thesis, Department of Infrastructure and Planning, Royal Institute of Technology, Stockholm, Sweden, 1996.
69. Kersten, M., "Historic Climatic Summary, Mn/DOT I-94 Cold Regions Pavement Research Test Facility," Cold Regions Pavement Research Test Facility, Minnesota Department of Transportation, March 1989.

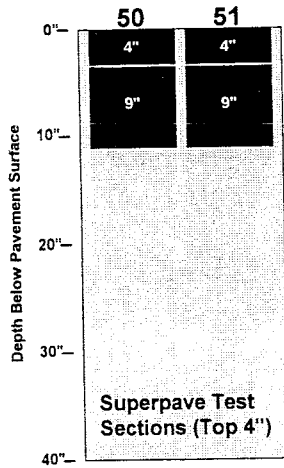
BIBLIOGRAPHY

- "Moduli from FWD Data," Research Report No. 1123-1, Texas Transportation Institute, College Station, Texas, September 1988.
- "Recommended CRPRTF Base and Road Surface Aggregate Classes," Mn/DOT I-94 Cold Regions Pavement Research Test Facility (CRPRTF), Version No. 1, Dama, Inc., May 1988.
- State of California Department of Transportation, Planning Manual, Part 7, Sacramento, California, 1978.
- "User's Guide to the BOUSDEF Program," Civil Engineering Department, Oregon State University, Corvallis.
- Andrei, R., R.A. Raab, and D.E., Esch, "Evaluation of a Time Domain Reflectometry Technique for Seasonal Monitoring of Soil Moisture Content Under Road Pavement Test Sections," Strategic Highway Research Program, Report No. SHRP-P-689, National Research Council, Washington D.C., 1994.
- Bigl, S.R., and R.L. Berg, "Modeling of Mn/DOT Test Sections with the CRREL Mechanistic Pavement Design Procedure," Draft, U.S. Army Cold Regions Research and Engineering Laboratory, Agreement Number 64632, December 1991.
- Brown, S.F. and Pappin, J.W., "Analysis of Pavement with Granular Bases, Layered Pavement System," *Transportation Research Record* 810, TRB, National Research Council, Washington, D.C., 1981.
- Chou, Y.J., Uzan, J., and Lytton, R.L., "Backcalculation of Layer Moduli from Nondestructive Pavement Deflection Data Using the Expert System Approach," Nondestructive Testing of Pavements and Backcalculation of Moduli, ASTM STP 1026, American Society for Testing and Materials, Philadelphia, 1989, pp. 341 - 354.
- Chow, V.T., Handbook of Applied Hydrology, McGraw-Hill Book Company, New York, 1964.
- Darter, M.I., Elliott, R.P., and Hall, K.T., "Revision of AASHTO Pavement Overlay Design Procedures," Preliminary Draft Final Report, Project 20-7/39, National Cooperative Highway Research Program, Transportation Research Board, Washington, D.C., June 1991.
- Darter, M.I., Smith, K.D., Hall, K.T., "Concrete Pavement Backcalculation Results from Field Studies," *Transportation Research Record* 1377, National Research Council, Washington D.C., 1991.

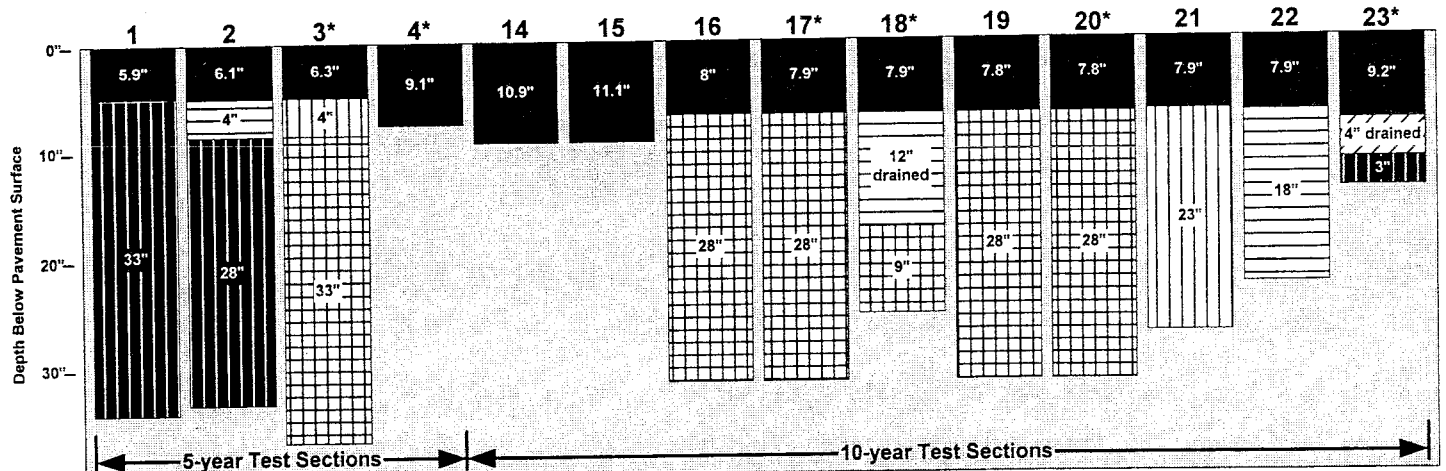
- Finn, F.N., et al., "The Use of Distress Prediction Subsystems for the Design of Pavement Structures," Proceedings, 4th International Conference on the Structural Design of Asphalt Pavements, University of Michigan, Ann Arbor, 1997.
- Finn, F., et al., "Development of Pavement Structural Subsystems," NCHRP Report 291, National Cooperative Highway Research Program, Transportation Research Board, 1986.
- Hadley, W.O., "Laboratory Techniques for Resilient Modulus Testing," Proceedings, Strategic Highway Research Program Products Specialty Conference, American Society of Civil Engineers, Denver, Colorado, April 8-10, 1991.
- Haiping, Z., Hicks, R.G., and Bell, C.A., "BOUSDEF: A Backcalculation Program for Determining Moduli of a Pavement Structure," *Transportation Research Board*, Washington, D.C., 1990.
- Huang, Y.H., Pavement Analysis and Design, Prentice Hall, Englewood Cliffs, New Jersey, 1993.
- Ioannides, A.M., Barenberg, E.J., and Lary, J.A., "Interpretation of Falling Weight Deflectometer Results Using Principles of Dimensional Analysis," Proceedings, 4th International conference on Concrete Pavement Design and Rehabilitation, Purdue University, West Lafayette, Ind., 1989.
- "ILLI-PAVE User's Manual", Transportation Facilities Group. Department of Civil Engineering, University of Illinois, Urbana-Champaign, May 1982.
- Johnson, G., Internal Memorandum at Maplewood Mn/DOT, Minnesota, 1997.
- Lade, P.V., and R.B. Nelson, "Modeling the Elastic Behavior of Granular Materials," *International Journal for Numerical and Analytical Methods in Geomechanics*, Vol. 11, No. 5, Sept.-Oct. 1987, pp. 521-542.
- Lee, S.W., "Backcalculation of Pavement Moduli by Use of Pavement Surface Deflections," Ph.D. Dissertation, University of Washington, Seattle, 1988.
- Lytton, R.L., Germann, F.P., Chou, Y.J., and Stoffels, S.M., "Determining Asphaltic Concrete Pavement Structural Properties by Nondestructive Testing," Report No. 327, National Cooperative Highway Research Program, Washington, D.C., June 1990.
- Newcomb, D.E., "Development and Evaluation of Regression Methods to Interpret Dynamic Pavement Deflections," Ph.D. Dissertation, Department of Civil Engineering, University of Washington, Seattle, Washington, 1986.
- Raad, L. and J.L. Figueroa, "Load Response of Transportation Support Systems," *Transportation Engineering Journal*, ASCE, Vol. 106, No. TE1, pp. 111-128, 1980.

- Roberts, F. L., P.S. Kandhal, D.Y. Lee and T.W. Kennedy, Hot Mix Asphalt Materials, Mixture Design, and Construction, Second Edition, NAPA Research and Education Foundation Lanham, Maryland, 1996.
- SHRP, "Low-Temperature Cracking: Test Selection," SHRP-A-400, Strategic Highway Research Program, National Research Council, Washington, D.C., 1994.
- SHRP, "Permanent Deformation Response of Asphalt Aggregate Mixes," SHRP-A-415, Strategic Highway Research Program, National Research Council, Washington, D.C., 1994.
- SHRP, "Water Sensitivity of Asphalt-Aggregate Mixes: Test Selection," SHRP-A-403, Strategic Highway Research Program, National Research Council, Washington, D.C., 1994.
- Smith, B.E. and Witzak, M.W., "Equivalent Granular Base Moduli: Prediction," *Journal of Transportation Engineering*, Vol. 107, TE6, American Society of Civil Engineering, Nov. 1981.
- Terrel, R.L., and Shute, J.W., "Summary Report on Water Sensitivity," SHRP-A/IR-89-003, Strategic Highway Research Program, National Research Council, Washington, D.C., 1989.
- Thompson, M.R., and E.J. Barenberg et al., "Calibrated Mechanistic Structural Analysis Procedures for Pavements," NCHRP 1-26, National Cooperative Highway Research Program, Transportation Research Board, March, 1990.
- Timm, D.H., B. Birgisson and D.E. Newcomb, "Development of Mechanistic-Empirical Pavement Design in Minnesota," Preprint, *Transportation Research Record*, Washington, D.C., 1998.
- Uzan, J., et al., "A Microcomputer Based Procedure for Backcalculating Layer Moduli from FWD Data," Research Report No. 1123-1, Texas Transportation Institution, College Station, Texas, September 1988.
- Van der Loo, P.J., "Creep Testing, a Simple Tool to Judge Asphalt Mix Stability," Proceedings, The Association of Asphalt Paving Technologies, Vol. 43, pp. 253-284, 1974.
- Van Deusen, D.A. and D.E. Newcomb, "Strains Due to Load in Frozen and Thawed Flexible Pavements," Proceedings, 4th International Conference in the Bearing Capacity of Roads and Airfields, Vol. 1. 1994.
- Zhang, W., *Viscoelastic Analysis of Diametral Compression Test on Asphalt Concrete*, Ph.D. Thesis, University of Minnesota, 1996.

APPENDIX A
MN/ROAD LAYOUT



Mix Gradation	Restricted Zone	Coarse
Construction Date	Jul 97	Jul 97



Asphalt Binder	AC120/150	AC120/150	AC120/150	AC120/150	AC120/150	AC 20	AC 20	AC 20	AC 20	AC 20	AC120/150	AC120/150	AC120/150	AC120/150
Marshall Design	75	35	50	Gyratory	75	75	Gyratory	75	50	35	35	50	75	50
Subgrade "R" Value	12	12	12	12	12	12	12	12	12	12	12	12	12	12
Construction Date	Sep 92	Sep 92	Sep 92	Sep 92	Jul 93	Jul 93	Jul 93	Jul 93	Jul 93	Jul 93	Jul 93	Jul 93	Jul 93	Sep 93

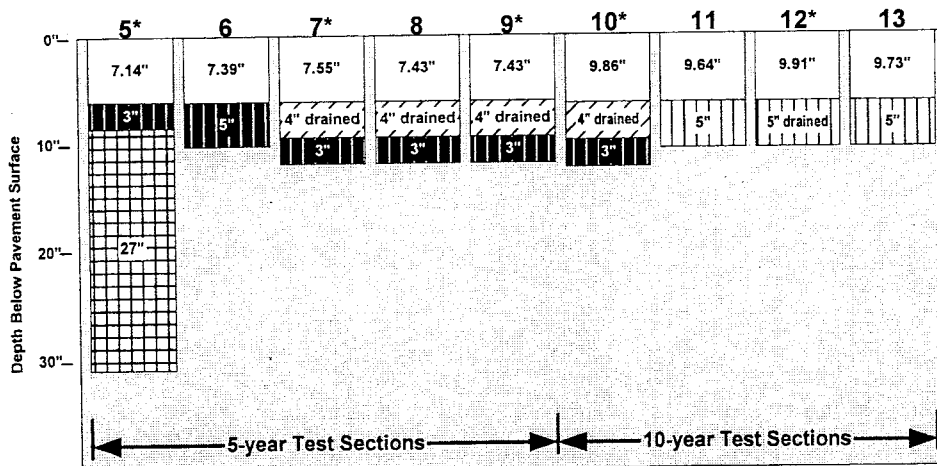
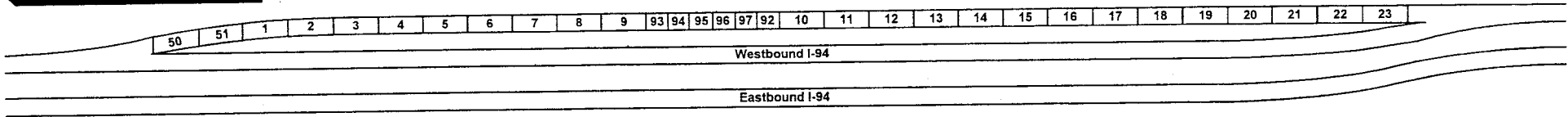
Legend

- Hot Mix Asphalt
- ▨ Concrete
- ▧ Class 3 Sp.
- ▩ Permeable Asphalt Stabilized Base
- ▤ Class 4 Sp.
- ▥ Class 5 Sp.
- ▦ Class 6 Sp.

Mainline Test Road

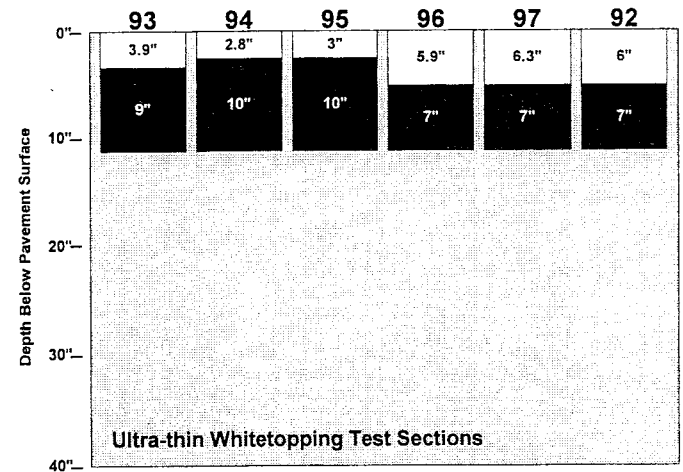
Date Revised: 02/03/00
 Filename: mnroad_bw.vsd
 * Cells that are LTP Sections - GPS Database

I - V

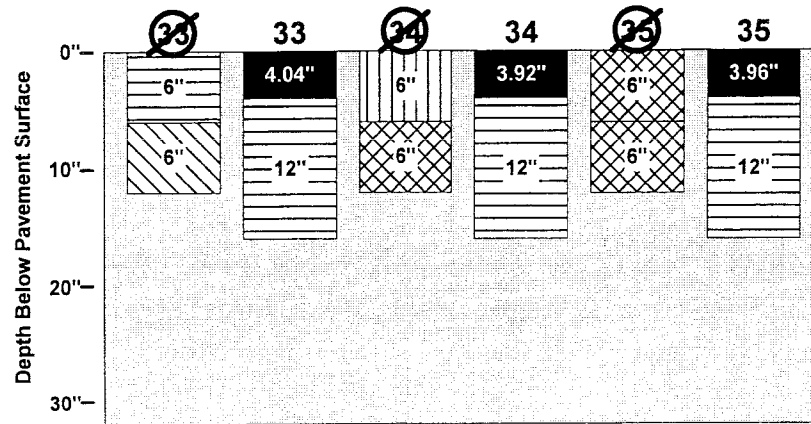


Panel Width**	13' / 14'	13' / 14'	13' / 14'	13' / 13' / 14'	13' / 13' / 14'	12' / 12'	12' / 12'	12' / 12'	12' / 12'
Panel Length	20'	15'	20'	15'	15'	20'	24'	15'	20'
Dowel Diameter	1"	1"	1"	1"	1"	1 1/4"	1 1/4"	1 1/4"	1 1/2"
Subgrade "R" Value	12	12	12	12	12	12	12	12	12
Construction Date	Sep 92	Sep 92	Sep 92	Sep 92	Sep 92	Jun 93	Jun 93	Jun 93	Jun 93

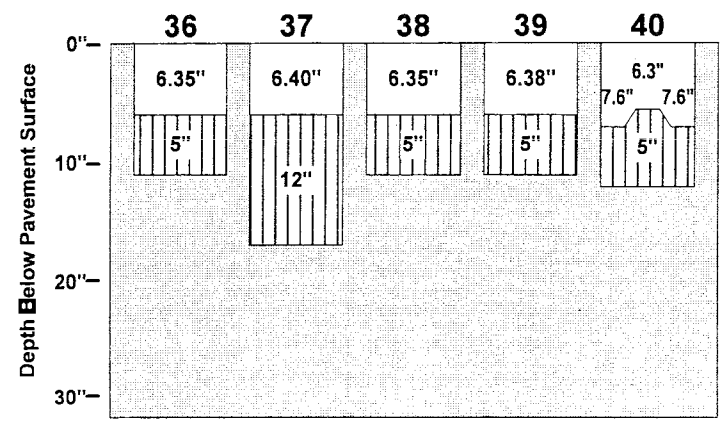
** Passing/Driving or Shoulder/Passing/Driving Suppl. Steel



Longitudinal Joint Spacing	4'	4'	6'	6'	12'	12'
Transverse Joint Spacing	4'	4'	5'	5'	10'	10'
Fibers	Polypropylene	Polypropylene	Polyolefin	Polypropylene	Polypropylene	Polypropylene
Dowels	No	No	No	No	No	Yes
Construction Date	Oct 97	Oct 97	Oct 97	Oct 97	Oct 97	Oct 97



Asphalt Binder	12	PG 58-28	12	PG 58-34	12	PG 58-40
Subgrade "R" Value	12	12	12	12	12	12
Construction Date	Sep 96	Aug 99	Sep 96	Aug 99	Sep 96	Aug 99



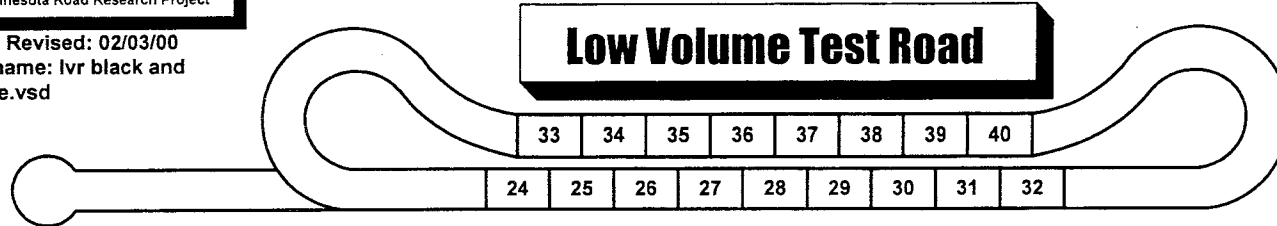
Panel Width**	12' / 12'	12' / 12'	12' / 12'	12' / 12'	12' / 12'
Panel Length	15'	12'	15'	20'	15'
Dowel Diameter	1"	None	1"	1"	None
Subgrade "R" Value	70	70	12	12	12
Construction Date	Jul 93				

Cells that have been re-constructed with new materials

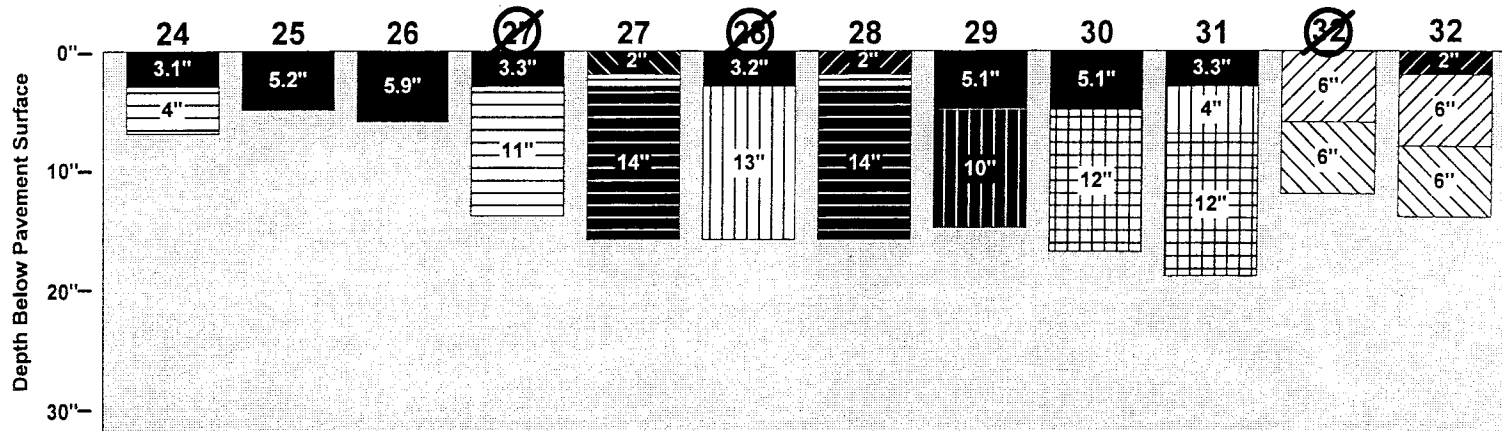


Date Revised: 02/03/00
 Filename: lvr black and white.vsd

Low Volume Test Road



Legend			
	Hot Mix Asphalt		Class 3 Sp.
	Concrete		Class 4 Sp.
	Crushed Stone Base		Class 5 Sp.
	Class 1		Class 6 Sp.
	Class 1c		Oil / Gravel
	Class 1f		Double Chip Seal



Asphalt Binder	AC 120/150	AC 120/150	AC 120/150	AC 120/150		AC 120/150		AC 120/150	AC 120/150	AC 120/150		
Marshall Design	35	50	50	35		50		50	75	75		
Subgrade "R" Value	70	70	12	12	12	12	12	12	12	12	12	12
Construction Date	Aug 93	Aug 93	Aug 93	Aug 93	Aug 99	Aug 93	Aug 99	Aug 93	Aug 93	Aug 93	Sep 96	Aug 99

APPENDIX B

PROCEDURE FOR CREATING THE CLIMATIC ATLAS

Certain steps were adhered to in the creation of this climatic atlas for Mn/ROAD. First, a general site description was made concerning latitude, elevation, general topography of the site and a search for nearby weather stations was made, similar to Kersten's research [69]. This information gave a picture of the type of climate expected at the site, such as the large temperature fluctuations in a year for a typical site located 45° latitude north of the equator, a typically non-arid environment, possible wetland areas, and a somewhat flat and uniform surface elevation as opposed to a mountainous region.

Next, possible sources for weather data were investigated. One on-line source is the Midwestern Climate Center, Illinois State Water Survey [53] at <http://mcc.sws.uiuc.edu/>. It is available by subscription and has weather station data available in a spreadsheet format. This same information can be found in the U.S. Weather Bureau reports from the Department of Commerce. Weather data obtained from these sources are daily high, low, and average temperatures, monthly high, low and average precipitation events and monthly high and average snowfall data. Thirty years of data were used for a normal distribution of temperature and precipitation data. The Buffalo weather station only provides temperature data over the years of 1958 to 1997 and precipitation data over the years of 1948 to 1997

The last step is to evaluate the climatic data. Climatic conditions of concern are temperature fluctuations, precipitation events, snowfall, freezing and thawing indices. These conditions can help determine the temperature, moisture content and moisture state of the pavement structure. Freezing, thawing and evaporation data can be calculated using daily and monthly average temperature data. Final data is presented in graphs to illustrate monthly variations in the climatic conditions.

APPENDIX C

DATABASE TABLES AND QUERIES

Table C.1. “Sensor” table column headings.

<u>Name</u>	<u>Type</u>
CELL	NUMBER(2)
MODEL	CHAR(2)
SEQ	NUMBER(3)
ACCESS_IND	CHAR(1)
DEPTH	NUMBER(6,2)
OFFSET	NUMBER(7,2)
SPEED	CHAR(1)
STATION	NUMBER(8,2)
TERMINATION	CHAR(1)
DEPTH_END	NUMBER(6,2)
SERIAL_NUMBER	CHAR(20)
ORIENTATION	CHAR(1)
PLACEMENT	CHAR(1)
FAIL_DATE	DATE
PAVE_ELEV	NUMBER(6,3)
NORTHING	NUMBER(10,3)
EASTING	NUMBER(10,3)
CHAIR_POSITION	CHAR(7)
RDWY_ORIENTATION	CHAR(13)
FAIL_PERSON	VARCHAR2(3)
FAIL_REASON	VARCHAR2(60)

Table C.2. “Cells” table column headings.

<u>Name</u>	<u>Type</u>
CELL	NUMBER(2)
CELL_DESC	VARCHAR2(20)
START_GRADE	NUMBER(5,3)
START_STATION	NUMBER(8,2)
START_ELEVATION	NUMBER(6,2)
END_GRADE	NUMBER(5,3)
END_STATION	NUMBER(8,2)
END_ELEVATION	NUMBER(6,2)
DRAINAGE_TYPE	VARCHAR2(4)
CABINET	VARCHAR2(4)
DRAIN_ID	NUMBER(2)
AGG_FACTOR_CELL_NUMBER	NUMBER(2)
PCC_FACTOR_CELL_NUMBER	NUMBER(2)
AC_FACTOR_CELL_NUMBER	NUMBER(2)
START_STATION_NO_CORE	NUMBER(8,2)
END_STATION_NO_CORE	NUMBER(8,2)

Table C.3. “FWD_Tests” table column headings.

<u>Name</u>	<u>Type</u>
TEST_FILENAME	VARCHAR2(8)
TEST_SERIAL_NUMBER	VARCHAR2(8)
TEST_SEQUENCE	NUMBER(6)
TEST_STATION	NUMBER(8,2)
TEST_TIME_BASE	DATE
TEST_OFFSET	NUMBER(7,2)
TEST_LAYE_LAYER_NUMBER	NUMBER(2)
TEST_CELL_CELL_NUMBER	NUMBER(2)
TEST_SURFACE_TEMP	NUMBER(6,2)
TEST_OFFSET_SOURCE	VARCHAR2(8)

Table C.4. “FWD_Backcalc_Results_v50” table column headings.

<u>Name</u>	<u>Type</u>
FWD_FILENAME	VARCHAR2(8)
FWD_SERIAL_NUMBER	VARCHAR2(8)
TEST_SEQ	NUMBER(6)
PEAK_SEQ	NUMBER(6)
BACKCALC_PROGRAM	VARCHAR2(20)
BACKCALC_MODEL	VARCHAR2(1)
BACKCALC_STATION	VARCHAR2(10)
FWD_LOAD	NUMBER
RMS_ERROR_PCT	NUMBER
LAYER_NUMBER	NUMBER(2)
MODULUS	NUMBER
LOCATION	NUMBER
H_STRESS	NUMBER
H_STRAIN	NUMBER
V_STRESS	NUMBER
V_STRAIN	NUMBER
STIFF_LAYER_DEPTH	NUMBER

Table C.5. “Weather” table column headings

<u>Name</u>	<u>Type</u>
DAY	DATE
HOUR	NUMBER(2)
QHR	NUMBER(2)
AIR_TEMP	NUMBER(8,4)
ATMOS_PRES	NUMBER(8,4)
PRECIP_NW	NUMBER(8,4)
PRECIP_SE	NUMBER(8,4)
REL_HUMIDITY	NUMBER(8,4)
SOLAR_RAD_IN	NUMBER(8,4)
SOLAR_RAD_OUT	NUMBER(10,4)
WIND_DIRECTION	NUMBER(8,4)
WIND_GUST	NUMBER(8,4)
WIND_SPEED	NUMBER(8,4)

Figure C.1. Example TC query.

```
set pagesize 20000
set feedback on
spool 95tc21.txt
select
  cell, day, seq, AVG(value)
from
  tc_1995
where
  cell = 21
group by cell, seq, day
order by cell, day, seq;
spool off
```

Figure C.2. Example TDR query.

```
set pagesize 20000
set feedback on
spool 95td21.txt
select
  v.day, v.cell, v.seq, v.value*100,
  a.depth*12
from
  td_values v, sensors a
where
  a.cell = v.cell
  and a.seq = v.seq
  and a.cell = 21
  and a.model = 'TD'
  and v.day between '01-JAN-95' and '31-DEC-95'
order by day, cell, seq;
spool off
```

Figure C.3. Example WM query.

```
set pagesize 20000
set feedback on
spool WM2297.txt
select
  day, seq, AVG(value)
from
  wm_1997
where
  cell = 22
  and seq between 8 and 14
group by day, seq;
spool off
```

Figure C.4. Example sensor location query.

```
set pagesize 20000
set feedback on
spool wmloc.txt
select
  cell, seq, station, offset*12, asbdepth*12
from
  asbuilt_sensor_locations
where
  model = 'WM'
  and cell = 1
order by cell, seq;
spool off
```

Figure C.5. Example RP query.

```
set pagesize 20000
set feedback on
spool 96RP1.txt
select
  day, cell, seq, avg_value
from
  rp
where
  cell = 1
order by cell, seq;
spool off
```

Figure C.6. Example weather query.

```
set pagesize 25000
set feedback on
spool avT9397.txt
select
  day, AVG(air_temp)
from
  weather
where
  day between '01-jan-93' and '30-nov-97'
group by day;
spool off
```

Figure C.7. Example FWD query.

```
set pagesize 25000
set feedback on
spool Mr20B.txt
select
  t.test_time_base, v.modulus,
  v.backcalc_station, v.layer_number
from
  fwd_backcalc_results_v50 v, fwd_tests t
where
  t.test_cell_cell_number = 20
  and v.fwd_filename = t.test_filename
  and v.fwd_serial_number = t.test_serial_number
  and v.test_seq = t.test_sequence
  and t.test_time_base between '01-JAN-96' and '31-DEC-96'
  and v.backcalc_model = 'B'
order by test_time_base, v.layer_number;
spool off
```




Office of Research Services
395 John Ireland Blvd., Mail Stop 330
Saint Paul, Minnesota 55155



(651) 282-2274